UNIVERSITY OF BIRMINGHAM

PROPERTIES OF CONCRETE WITH RECYCLED AGGREGATES AS COARSE AGGREGATE AND AS-RECEIVED/SURFACE-MODIFIED RUBBER PARTICLES AS FINE AGGREGATE

by

Haolin Su

A thesis submitted to University of Birmingham

for the degree of

DOCTOR OF PHILOSOPHY in Civil Engineering

April, 2015

ACKNOWLEDGEMENT

The author would like to express his sincere gratitude to Prof. Jian Yang who supervised this research for his valuable time and patient guidance. Thanks to the co-supervisors Dr. Gurmel Ghataora and Dr. Samir Dirar for their useful suggestions and comments. Appreciations are also given to Dr. Min An, Prof. Tung-Chai Ling and Prof. Felix Schmid for their helpful information.

Thanks to Mr Dave Cope in the Civil Engineering Laboratory for his assistance in carrying out the experimental phase of this project and the author's friend Mr Shunde Qin for his help during the casting and testing. In addition, Shanghai Jiao Tong University and China Building Materials Academy are also appreciated for the utilization of their advanced testing devices.

Last but not least, much gratitude is given to the author's parents and Michelle Jin for their support and understanding. Meanwhile, thanks to all of the author's mentors and friends who gave positive help on the way of accomplishing the research work. Your trust and encouragement make this thesis successfully completed.

TABLE OF CONTENTS

ABSTRACT

Cement-based rubber concrete has been researched for over twenty years. Rubber aggregate, mainly from over one billion discarded end-of-life tyres every year worldwide, is usually used to substitute aggregates in concrete mixture. A general consensus is that the ductility, resilience, impact resistance and dynamic energy dissipation capacity of rubber concrete increase and strength decreases with a rising proportion of rubber phase in concrete due to the elastic and soft nature of rubber material. How to reduce the significant loss of strength has remained unresolved. Therefore, this thesis explores some approaches by studying the effect of rubber aggregate size and rubber surface modification on performance of rubber concrete. Meanwhile, influence of substitution ratio of recycled aggregate and rubber aggregate on compressive strength of the concrete designed by the author was also investigated.

Three groups of singly-sized rubber particles and one sample of continuous size grading (prepared by blending the three singly-sized samples to form the same particle size distribution of sand) were used to replace 20% of fine aggregate by volume. According to the experiment results, it was demonstrated that rubber particle size affects concrete workability and water permeability to a greater extent than fresh density and strength. Concrete with rubber particles of larger size tends to have a higher workability and fresh density than that with smaller particle sizes. However, rubber aggregates with smaller or continuously graded particle sizes are shown to have higher strengths and water permeability resistance.

The influence of recycled aggregate content within the range of 0-100% as the substitution for coarse aggregate and rubber content within the range of 0-40% as the substitution for fine

aggregate on cube compressive strength of the designed concrete with recycled aggregate and rubber particles as aggregates simultaneously was investigated from both analyses of experiment results and inspections of microstructure aspects. Based on the experimental work, four equations with recycled aggregate and rubber replacement ratio as independent variables were proposed to predict the cube compressive strength of this designed concrete material.

Surface of rubber aggregate was modified by soaking in saturated sodium hydroxide solution (NaOH) or silane coupling agent (SCA) before using. It is experimentally shown that SCA has a positive effect on reducing the loss of strength of rubber concrete, especially when concrete is weak. This effect becomes more significant with the increase of mass fraction of SCA solution because SCA plays an enhanced role in developing adhesion between organic rubber particles and inorganic concrete cement paste to increase the bond strength of interface, leading to an improvement in interfacial transition zone. Experiment results also show a higher deformability, Young's modulus, water permeability resistance, and better fatigue performance such as a longer fatigue life, higher ductility and damping capacity of the concrete samples with SCA-treated rubber than with as-received or NaOH-treated rubber. A brief cost analysis suggests that this method of surface modification is economically viable. Referring to a provided fatigue load spectrum and fatigue failure mechanism, this method is potentially to be used for rubber concrete in high-cycle fatigue condition.

Keywords: analysis and prediction, compressive strength, fatigue performance, flexural properties, interfacial transition zone, loss of strength, mercury intrusion porosimetry, particle size distribution, recycled aggregate, rubber concrete, scrap tyre, silane coupling agent, surface modification, water permeability.

ABBREVIATIONS

BS	British Standard
CCSR20	concrete with combined-size rubber, 20% replacement of fine aggregate by volume
CCSR-AR	concrete mixture with as-received combined size rubber particles
CCSR-N2h	concrete mixture with combined size rubber particles which were soaked in sodium hydroxide saturated aqueous solution for 2 hours
CCSR-N24h	concrete mixture with combined size rubber particles which were soaked in sodium hydroxide saturated aqueous solution for 24 hours
CCSR-SCA	concrete mixture with combined size rubber particles which were coated with silane coupling agent
CRA20	concrete with rubber sample A, 20% replacement of fine aggregate by volume
CRB20	concrete with rubber sample B, 20% replacement of fine aggregate by volume
CRC20	concrete with rubber sample C, 20% replacement of fine aggregate by volume
CSR	combined-size rubber
DoE	Department of Environment
EN	European Norm
GGBS	ground granulated blast furnace slag
ISAT	Initial Surface Absorption Test
NaOH	sodium hydroxide
NMPS	nominal maximum particle size
PFA	pulverized fuel ash
PSD	particle size distribution
RA	rubber sample A

RAC	recycled aggregate concrete
RB	rubber sample B
RC	rubber sample C
REF	reference mix without rubber
RRC	recycled rubber concrete
RSRAC	steel fibre reinforced recycled aggregate concrete
SCA	silane coupling agent
SSD	saturated surface dry
w/c	water cement ratio
XRD	X-ray diffraction
1dCCS	1 day cube compressive strength
3D	three-dimensional
7dCCS	7 days cube compressive strength
28dCCS	28 days cube compressive strength

LIST OF FIGURES

LIST OF TABLES

CHAPTER 1

INTRODUCTION

1.1 Overview

Concrete is one of the primary materials used in construction, due to its excellent features such as high compressive strength, good durability properties, versatility and availability, cost effectiveness, as well as the ability to produce complex geometrical shapes to fit different requirements. So far, there are many types of concrete used for different purposes. For example, self-compacting concrete can flow and compact by its own gravity, favourable for the situation where vibration is not able to apply. Recycled aggregate concrete is a kind of concrete which uses recycled materials, usually referred to aggregate from demolished buildings, to replace natural aggregate for cost effectiveness and environment sustainability. Early strength concrete has a relative high strength in the early age after casting, which is suitable for emergent repairs, especially in cold condition. Corrosion resistant concrete is usually adopted in marine environment where a lot of chloride ions and sulphate ions exist.

Over the last 20 years, extensive research has been undertaken into the effects of using recycled rubber as an aggregate replacement of concrete. As is known to all, concrete is of high compressive strength but weak in tension or ductility. Therefore, the addition of rubber aggregate helps improve the inherently poor ductility, tensile and dynamic properties but reduces the strength of concrete due to the nature of rubber material. Rubber concrete is often proposed for applications such as highway crash barriers and other impact loading scenarios. However, practical projects to date which have been carried out for a specific use are still scarce.

1.2 Background

1.2.1 Scrap tyre

The rapid development of vehicle industry has rendered a huge growth in scrap tyre (Figure 1-1), and this has created a pressing problem, which has been called as ‘black pollution’. Landfill has not been permitted in some countries since several years ago, e.g. since July 2006 in the UK. Up to 2000, only five states in US had no restrictions on disposal of waste tyre, not only because of the limited land, but also due to its non-biodegradation, which may pose a potential environment concern. So reusing scrap tire is a rather urgent need for sustainable development. Several ways have been proposed, to name a few, being used in asphalt pavement, burning for energy, or as feedstock for cement kiln. However, limited demand or high capital cost or environment pollution by incineration has significantly restricted its current use. Concrete is the second most widely used material in the world which can consume large amount of scrap tyres if the tyres are used to replace natural aggregate of concrete. In addition, without incineration or burying, the environment is well protected for sustainability. Hence, reusing scrap tyre in concrete could be a potential solution.

1.2.2 Recycled aggregate

As mentioned above, concrete is the second most widely used material in the world because of its favourable properties. However, an important ingredient in concrete, natural aggregates, are greatly used. This is disappointing for sustainable development because sand and gravels

are non-renewable materials. Meanwhile, with the development of society, more and more new buildings have been constructed, especially in developing counties. Correspondingly, many old buildings are or will be demolished, which causes a large amount of construction wastes generated (Figure 1-2). In the last few decades, a variety of recycling methods for construction and demolition wastes have been explored and well developed. Recycled aggregates can be treated into different size to replace fine or coarse aggregate respectively. Many conclusions and recommendations have been drawn. However, the study of using recycled aggregate in concrete with scrap tyre rubber together has not been researched. Therefore, this will be studied in the present research.

Figure 1-1. Scrap tyres.

Figure 1-2. Building in demolition.

1.2.3 Benefits of recycled materials

The use of waste and recycled materials in the construction could have both economic and environmental benefits. There are several materials used in the construction that could be

recyclable, such as fine aggregate, coarse aggregate, and additions. The use of such materials would not only reduce the initial costs, but also create a far more sustainable approach to the construction, which is a clear selling point to a lot of investors. By cutting and grinding the tyres down into small particles, they can effectively be used in several concrete applications. Besides, a more traditional approach to reduce costs and environmental impact of concrete is to use industrial wastes such as pulverized fuel ash and ground granulated blast furnace slag to substitute part of cement. It has been confirmed that PFA and GGBS have a positive effect on the performance of concrete. Therefore, this method is also a sustainable option as it is taking the waste from one industrial process, and using it in another.

1.3 Research gaps

Through the literature review in Chapter 2, some main research gaps are found as follows:

- Rubber aggregate acts as void in concrete structure. Stress concentration usually arises at the interface between rubber particles and concrete matrix. The size of rubber aggregate affects the occurrence of stress concentration. In other words, size of rubber particles influences the strength of concrete. However, reports on the effect of rubber particles size on the properties of concrete are limited.

- Studies have been widely reported on replacement of coarse aggregate by recycled aggregate and replacement of fine aggregate by waste tyre rubber in separate concrete. But investigation on replacing aggregates by both recycled aggregate and rubber simultaneously in concrete is rather scarce in the literature.

- How to reduce the loss of strength caused by the addition of rubber aggregate is being investigated. Some approaches were reported to have achieved varying degrees of success. Nonetheless, none of the surface modification on rubber aggregate has shown significant effect on reducing the strength loss.

1.4 Aims and objectives

The aims of this study are to present a new concrete material containing recycled aggregate, scrap tyre rubber, and PFA simultaneously for cost effectiveness and environment sustainability and; to reduce the loss of strength of rubber concrete for more application areas.

The main objectives include:

- To find out the influence of different replacement ratios of recycled materials on the strength of the designed concrete and determine the optimum substitution ratio.

- To propose some equations to predict the compressive strength of the designed concrete.

- To clarify that the effect of rubber particle size on the properties of rubber concrete.

- To explore the feasibility of using SCA or NaOH to pre-treat rubber aggregate so as to reduce the loss of strength of rubber concrete.

- To identify the influence of mass fraction of SCA on the reduction of strength loss of rubber concrete.

- To confirm the effect of surface modified rubber aggregate by SCA on some other properties of rubber concrete such as fatigue performance, water permeability, Young's modulus.

1.5 Methodologies

Most of the conclusions derive from experimental work and data analysis. To achieve the above mentioned aims and objectives, a large amount of experiments were carried out according to relative BS EN. It includes the property tests of raw materials, laboratory work of mixing, casting, sampling and curing. Besides, the property tests of the resulting concrete samples such as workability, compressive strength, and flexural strength were also tested in compliance with BS EN. The results were used to compare with each other and statistical methods were used to get the tendency. Then conclusions or recommendations were summarised based on the experimental and analytical work.

1.6 Outline of thesis

CHAPTER 1 gives an introduction of this thesis, including the overview and background of rubber concrete and benefits of recycled materials. Some research gaps, aims and objectives, and outline of this thesis are listed.

CHAPTER 2 reviewed the literature which closely relates to the scope of this thesis, covering the state-of-the-art research on rubber concrete. Some recommendations are given at the end of this chapter.

CHAPTER 3 studies the effect of rubber particle size on the properties of concrete. Concretes containing uniform size and varying size rubber aggregate were compared in terms of workability, fresh density, compressive strength, splitting tensile strength, flexural strength and water permeability. The results can be potentially beneficial to the tyre recycling industry in designing the particle size distribution of rubber particles used as recycled aggregate.

CHAPTER 4 presents an innovative concrete material containing recycled aggregate, scrap tyre rubber, and PFA simultaneously designed by the author. Effect of recycled aggregate and rubber replacement ratio on the 28 days cube compressive strength was studied based on both the analyses of experimental results and on inspection of the microstructure. Four equations were proposed to predict the cube compressive strength of this innovative concrete material. Some notes needing attention and application range of the equations were given at last.

CHAPTER 5 investigates the effect of surface modified tyre rubber aggregate on the performance of recycled aggregate concrete. NaOH and SCA were used to modify the surface of rubber aggregate and workability, compressive strength, Young's modulus, water permeability of different mixes were compared. Mass fraction of SCA was proved to influence the effect of SCA on the reduction of loss of concrete strength. Finally, a brief cost analysis indicates that it is economically viable.

CHAPTER 6 details the effect of surface modified waste tyre rubber aggregate on flexural properties and fatigue performance of recycled aggregate concrete with PFA. It includes flexural strength, deformation, fatigue life, ductility, damping capacity and damage analysis of fatigue fracture. Mechanism of strength enhancement and microstructure were also analyzed. A promising application of this concrete material was suggested referring to a provided fatigue load spectrum.

CHAPTER 7 summarises the achievements and finding in this research work, as well as renders future work in the field of rubber concrete.

CHAPTER 2

LITERATURE REVIEW

2.1 Introduction

Rubber concrete has been researched for over twenty years. Rubber aggregate is mainly sourced from the increasingly discarded end-of-life tyres, which is known as black pollution because they are not readily degradable, posing a potential fire hazards to the environment and providing breeding grounds for mosquitoes [2.1], [2.2]. They are usually used to substitute part of natural aggregates or as additive of concrete mixture. A general consensus is that the ductility, impact resistance and dynamic energy dissipation capacity increase and compressive strength decreases with a rising proportion of rubber phase in concrete due to the elastic and soft nature of rubber material. However, conclusions on some other properties such as workability, flexural strength, freeze-thaw resistance do not come to an agreement and even the same property reported by different researchers varies significantly. From the aspect of rubber aggregate itself, this is attributed to the various rubber aggregate used by different researchers. It is stated that research is required to optimise the size, shape, grading, density, amount, and methods of pre-treatment of rubber particles on the properties of rubber concrete [2.3]. In addition, manner of introducing rubber aggregate (incorporating directly, by weight, by volume), which is specified in the section of Review considerations, also affect the characteristic of concrete significantly. It is lack of reasonability to mash and compare them together, and this is probably the cause of contradictory conclusions from different researchers. Therefore, this literature review aims to examine the properties of rubber concrete, and highlights the aggregate is substituted with rubber aggregate by volume.

2.2 Review considerations

A systematic search of published papers regarding the properties of cement-based rubber concrete by means of databases of ScienceDirect, Web of Science, Google Scholar up to January 2015 was conducted. To focus on our study, we did not consider other kinds of rubber mixtures such as rubber mortar or asphalt rubber concrete. We excluded conference papers, publications which are local rather than international, and written in non-English language. We used broad keywords such as rubber, concrete, rubber concrete, rubcrete, rubberized concrete to ensure that there were no omissions, and many of the studies not relevant were then omitted. We also examined the reference list of each cited paper for other pertinent literature. Finally, a total of 92 relevant research articles [2.4]-[2.95] were found.

From a preliminary review, it was found that there are three manners to introduce rubber aggregate to concrete, namely incorporating rubber aggregate in proportion of weight or volume of concrete directly, substituting aggregates of concrete by weight and by volume. In the literature, 8 publications [2.4]-[2.11] adopted the manner of incorporating directly, 20 publications [2.12]-[2.31] adopted substituting aggregates of concrete by weight, 61 publications [2.32]-[2.90] by volume using absolute volume method, and 3 publications [2.93]-[2.95] did not specify the details. It should be noted that unlike fibre, admixture and other modifiers which occupy a low portion (< 5%) of the total volume of concrete mixture [2.74], addition of extra rubber aggregate or replacing natural aggregate of concrete with rubber by weight will cause significant issue of mixture proportioning due to the distinction of the densities of different materials. The density of natural aggregate in concrete is around 2.5 times as much as that of rubber material [2.80]. It means that if the aggregates are

replaced by rubber in the manner of weight substitution, the volume of resulting mixture would be much higher compared with the original one. Consequently, content of other aggregates and cement paste in unit volume would be decreased, resulting in severe strength reduction of concrete. It would probably cause safety problem when it is used in structural engineering applications. Besides, the changing volume would lead to incorrect concrete demand in the mix design. This is also applicable to industrial situations, as a change in volume of a mixture would cause either quantity issues for the purchaser, or cost issues for the supplier. Therefore, from the viewpoint of practical application, the manner of substituting natural aggregate of concrete with rubber aggregate by volume is preferred.

Besides, for a better comparability, research of rubber concrete for special use such as self-compacting rubber concrete [2.32]-[2.38] which has been reviewed by Najim and Hall [2.96], high-strength rubber concrete [2.39], [2.40], porous rubber concrete [2.41], and roller-compact concrete [2.42], [2.43] were not considered. Eventually, 49 papers [2.44]-[2.92] relevant to the theme of this study were reviewed and the analyses and discussions below were based on this literature.

2.3 Properties of rubber concrete

2.3.1 Slump

Results of slump from relevant references [2.44], [2.45], [2.49], [2.52], [2.53], [2.55], [2.58], [2.63], [2.65], [2.66], [2.68], [2.77], [2.79], [2.80], [2.85], [2.87], [2.90], [2.91] were converted to increment of slump and plotted in Figure 2-1. It can be seen that most of the

researchers [2.45], [2.49], [2.52], [2.53], [2.55], [2.58], [2.66], [2.79], [2.80], [2.85], [2.87], [2.90], [2.91] agree that the addition of rubber aggregate has a negative effect on the slump of fresh concrete. The reduction of the slump is mainly attributed to the rough surface of rubber aggregate compared to the smooth surface of natural aggregates. It will cause an increasing friction between fresh concrete ingredients which leads to a relatively slow movement of rubber aggregate in concrete matrix, resulting in an incompatible mix and reduction of slump.

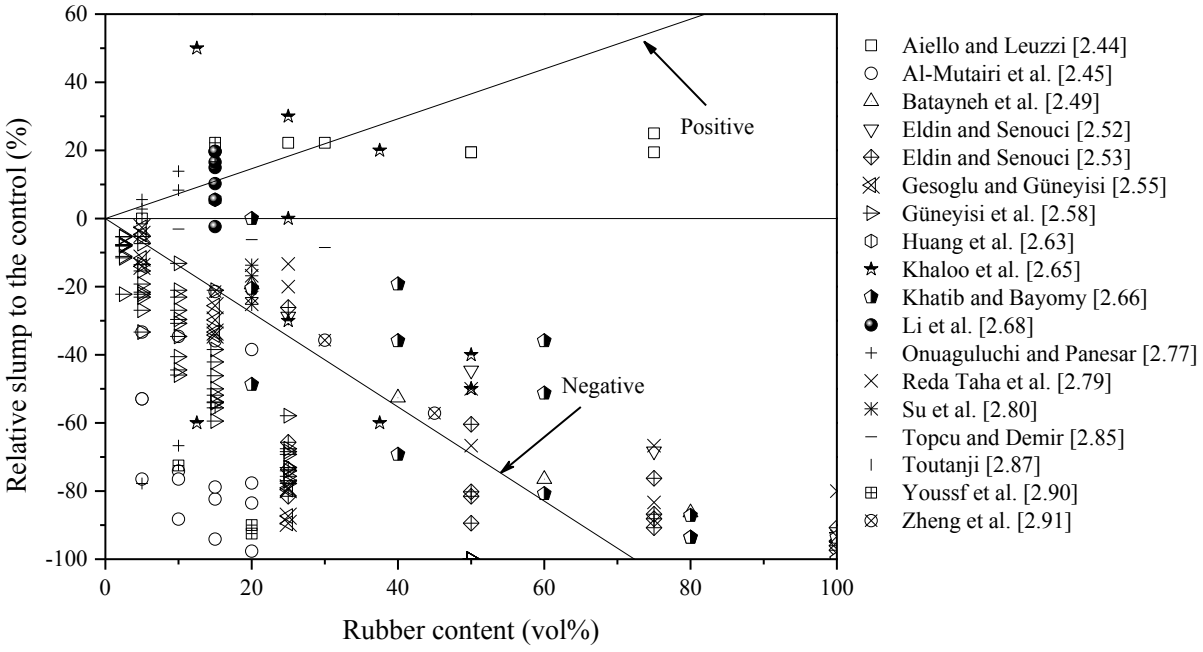

Figure 2-1. Converted relative slump to control mix.

Figure 2-2 shows some typical micrographs of surface of rubber particles. On the contrary, results from some researchers [2.44], [2.63], [2.77] show that the addition of rubber aggregate improves the slump of fresh concrete. Li et al. [2.67], [2.68] stated that the effect of rubber aggregate on the workability of concrete is minimal. Khaloo et al. [2.65] pointed out that the rubberized concrete has acceptable workability in terms of ease of handling, placement, and finishing. However, the traditional procedure of measuring the slump of fresh rubber concrete

does not support the actual state of the mix workability and another method needs to be developed to evaluate the slump of rubberized concrete [2.52], [2.53]. The above conclusions were based on the experimental results and no reasons or explanations were given. More studies are needed to explain this inconsistent conclusion.

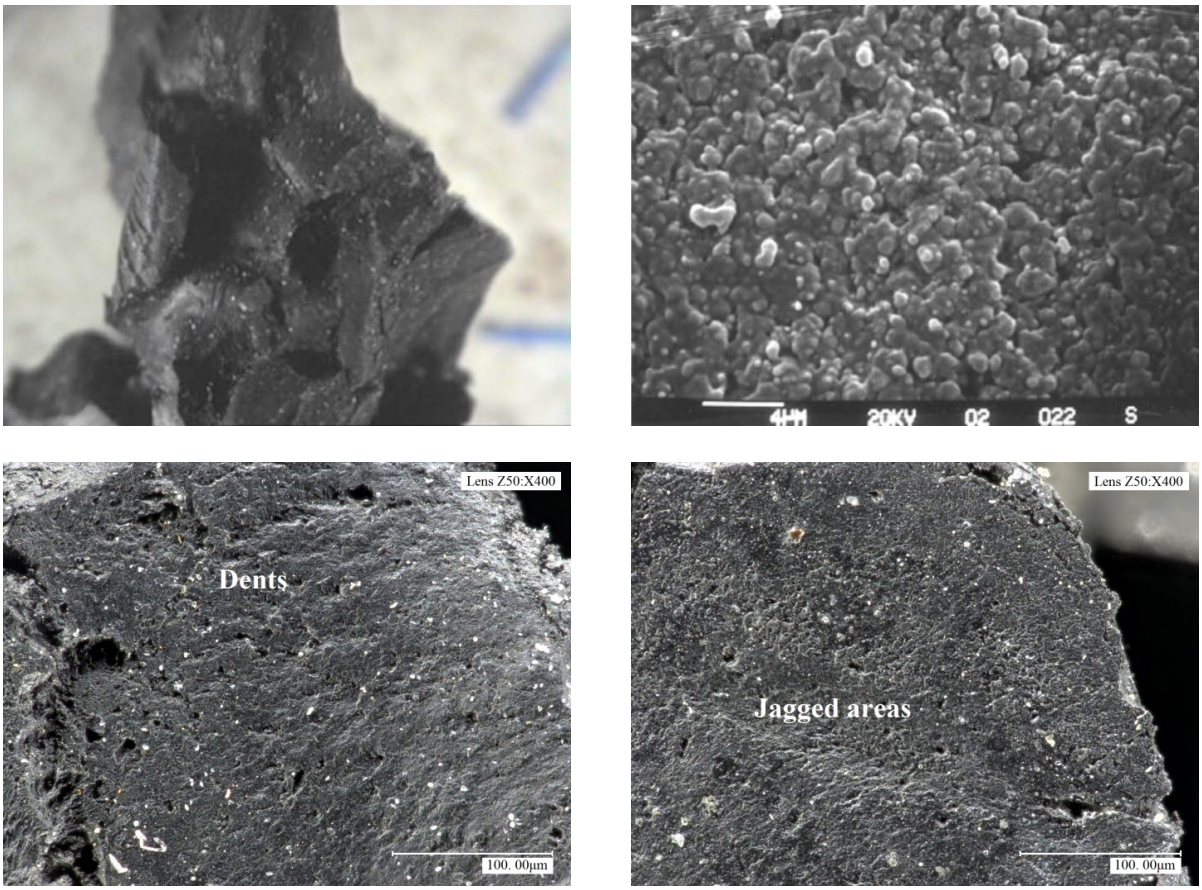

Figure 2-2. Micrographs of surface of rubber particles [2.79], [2.81].

2.3.2 Air content

Results of air content from relevant references [2.51], [2.63], [2.66]-[2.68], [2.74], [2.79] were converted to the increment and plotted in Figure 2-3. A unanimous conclusion is that the addition of rubber aggregate will cause more air content in concrete. The higher air

content of rubber concrete may be due to the non-polar nature and texture of rubber particles and their capability to entrap air on their jagged surfaces [2.97].

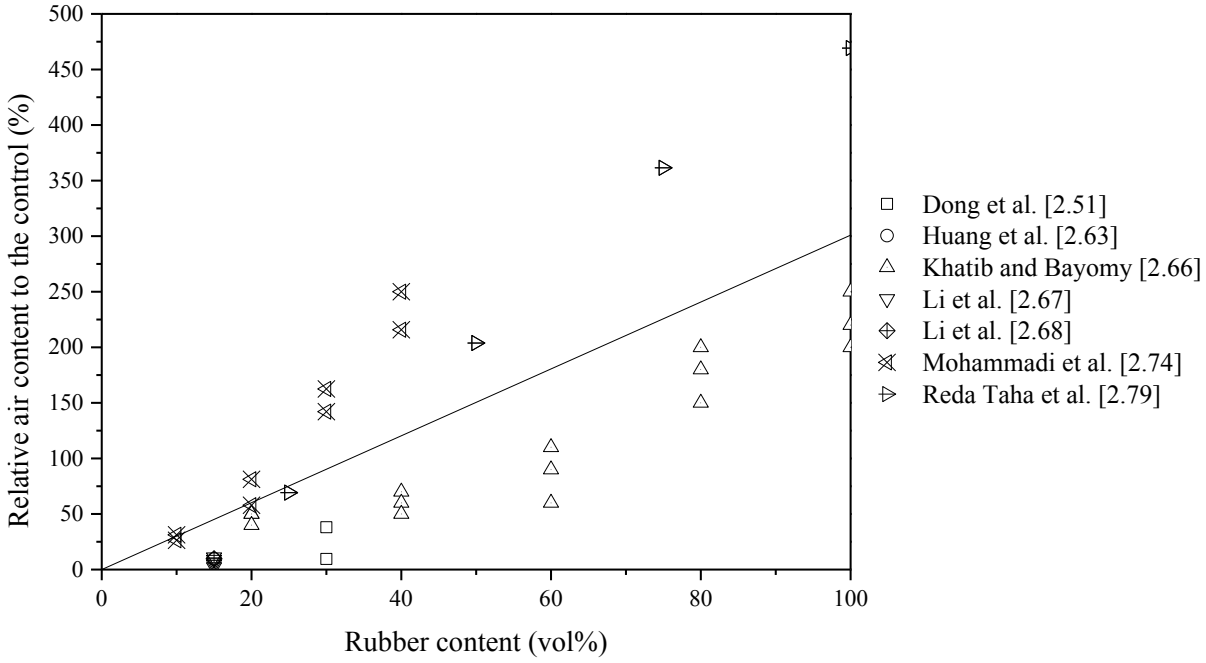

Figure 2-3. Converted relative air content to the control.

Figure 2-4 show the state of rubber particles submerged in water. It is difficult for crumb rubber to sink or be coated by water because it is hydrophobic. There are obvious air bubbles around the surface of rubber particle. When rubber is added to a concrete mixture, the rubber particles attract air due to their tendency to repel water, with the amount depending on the internal pressure in the mixture [2.65]. Air then adheres to the surface of rubber aggregate, resulting in higher air content in rubber concrete mixture [2.3].

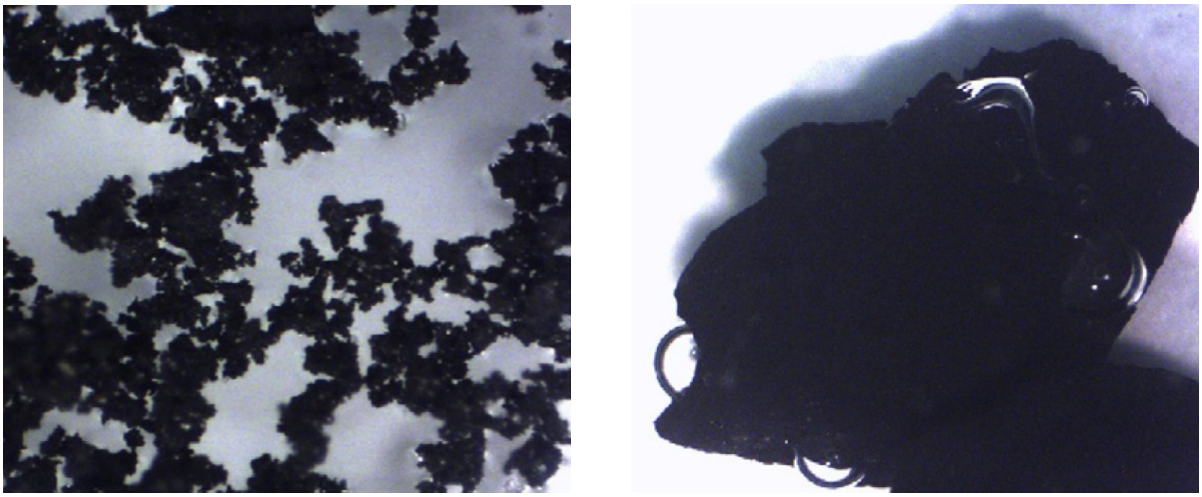

Figure 2-4. Trapped air bubbles at crumb rubber submerged in water [2.82].

2.3.3 Density

Results of density from relevant references [2.44], [2.48]-[2.53], [2.55], [2.58], [2.61], [2.65], [2.66], [2.70], [2.71], [2.73], [2.74], [2.76]-[2.79], [2.81]-[2.84], [2.86], [2.89], [2.91], [2.92] were converted to the increment and plotted in Figure 2-5. As expected, the addition of rubber aggregate reduces the density of concrete mixture. It is clear that the density of rubber concrete decreases with the increase of rubber content and the level of decrease depends on the amount of substitution. This is understandable in view of different unit weight of natural aggregate and rubber aggregate. As mentioned above, the density of natural aggregate in concrete is around 2.5 times as much as that of rubber aggregate [2.80]. Therefore, when natural aggregate is replaced by rubber aggregate by volume, the weight in the unit volume will be decreased. Most researchers stated that density of concrete decreased uniformly with the increase of proportion of rubber aggregate in the mixture. However, Benazzouk et al. [2.98] pointed out that the variation in density versus rubber content is not linear due to the

increase in the level of air-entrainment with rubber volume, which contributes to lightening the material.

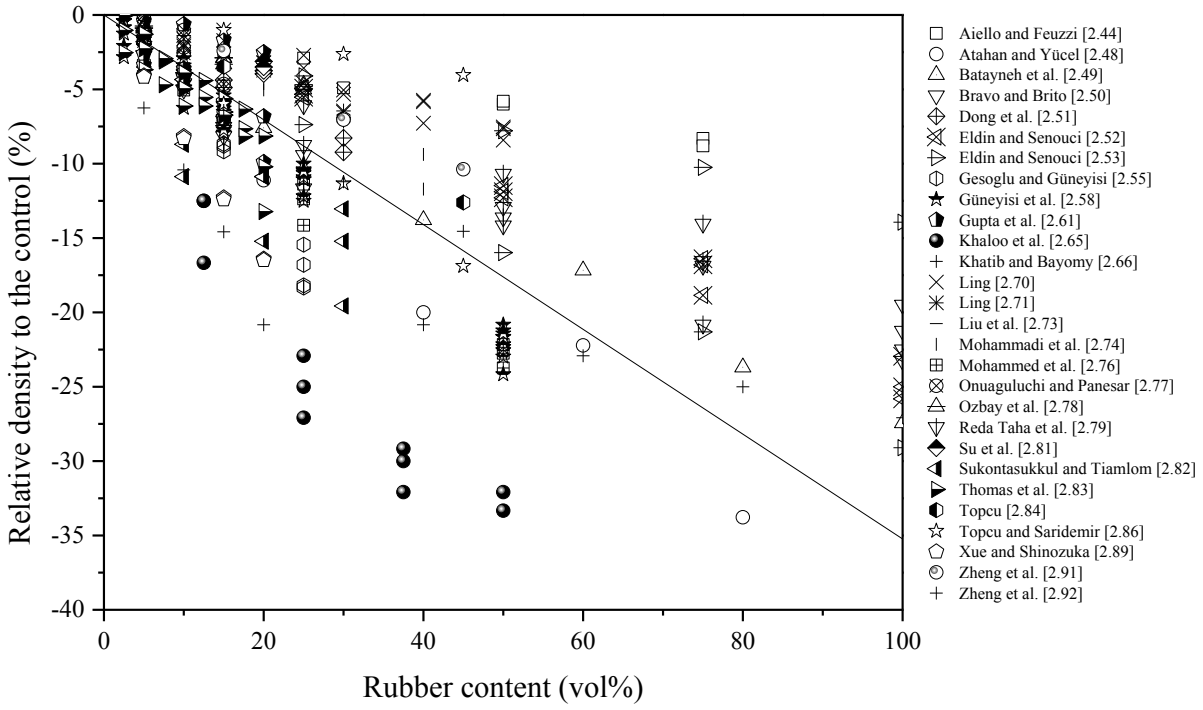

Figure 2-5. Converted relative density to the control.

2.3.4 Compressive strength

Tests on the compressive strength of rubber concrete have been conducted and reported by a large number of researchers in the literature [2.44]-[2.49], [2.51]-[2.57], [2.59]-[2.61], [2.63]-[2.75], [2.77]-[2.79], [2.81]-[2.84], [2.87]-[2.91]. Figure 2-6 shows the converted increment of compressive strength from the above references. The unanimous conclusion is that the addition of rubber aggregate results in the reduction of compressive strength of concrete and with the increase of proportion of rubber aggregate in the mixture, the loss of strength of rubber concrete becomes more significant. The main reasons can be summarized as the

following points. Firstly, rubber aggregate is much softer than natural aggregate. If natural aggregate is replaced by rubber aggregate, the load carrying material in the mixture is reduced, resulting in a loss of compressive strength. Besides, due to the low stiffness of rubber aggregate compared to natural aggregate, rubber particles can be deemed as voids in the concrete mixture. Stress concentration usually arises at the interface between rubber particles and concrete matrix. Cracks are initialised around rubber aggregate because of the elastic mismatch, which propagates to cause the failure of concrete. Last but not the least, the non-polar nature makes rubber particles entrap air on their surfaces, causing much inconsistency between rubber aggregate and the surrounding cement paste, as shown in Figures 2-7 [2.76] and 2-8 [2.61]. Therefore, the bonding of them is rather weak, resulting in

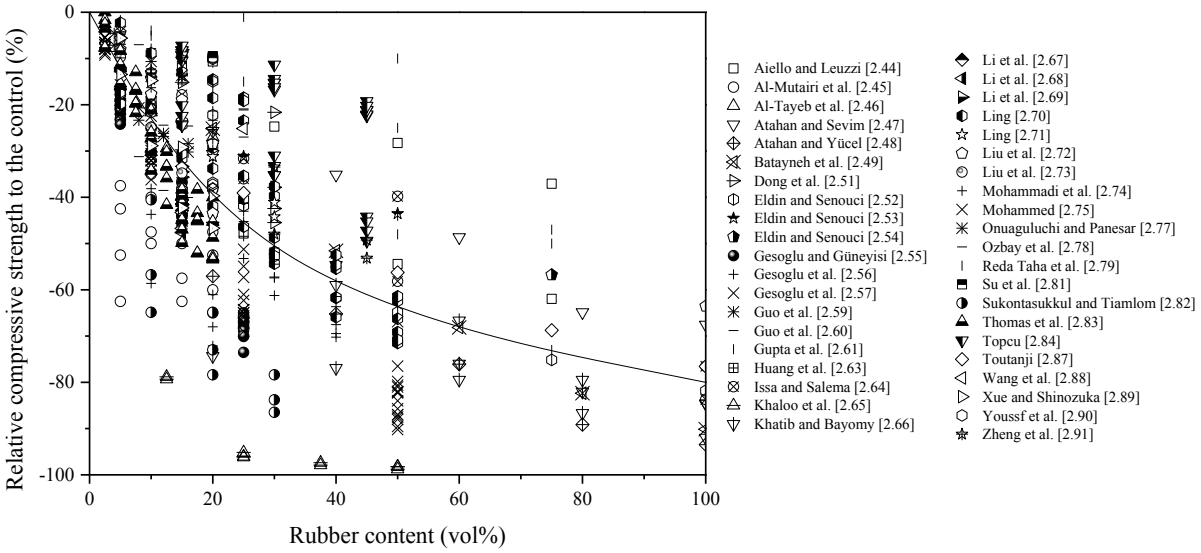

Figure 2-6. Converted relative compressive strength to the control.

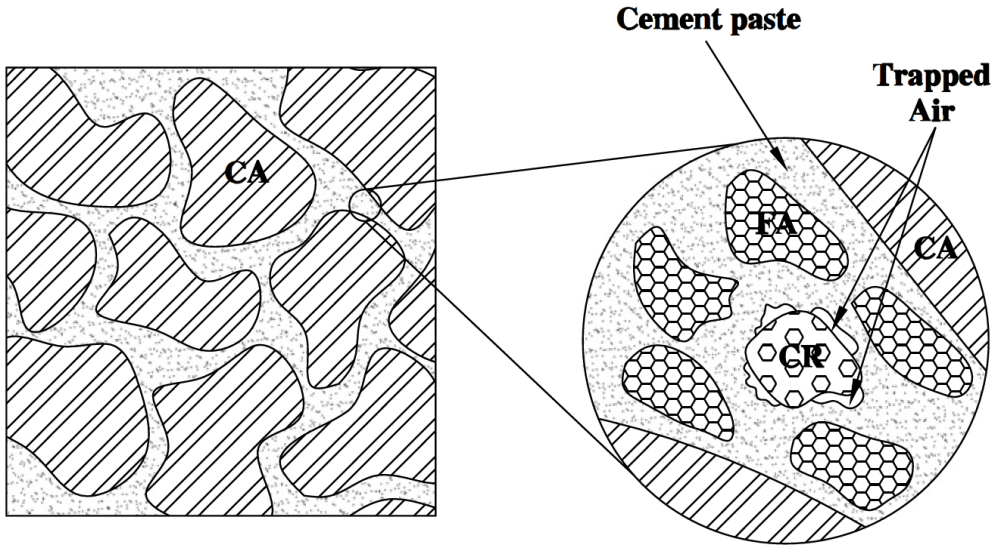

Figure 2-7. Diagrammatic drawing of microstructure of crumb rubber concrete, CA represents coarse aggregate; CR represents crumb rubber; FA represents fine aggregate [2.76].

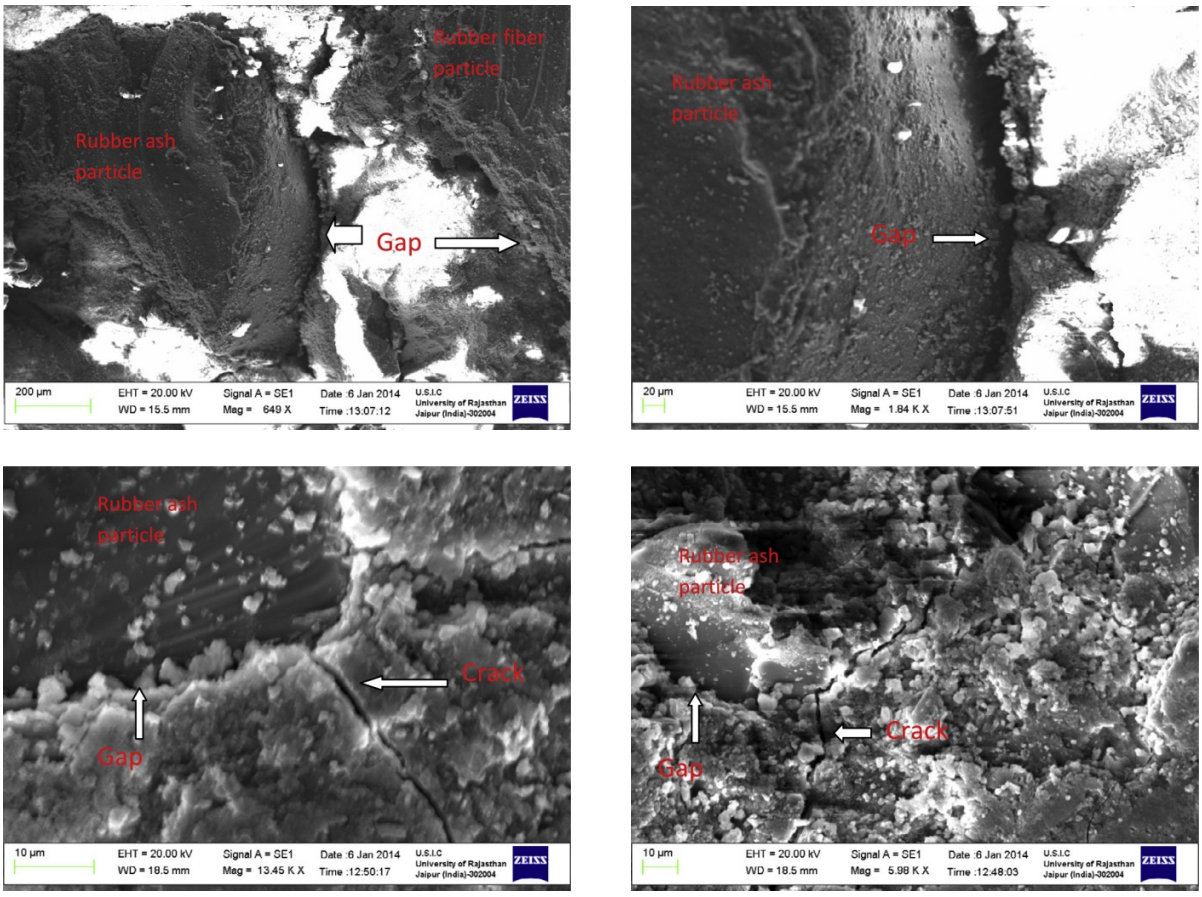

Figure 2-8. Microstructure of crumb rubber concrete [2.61].

Compressive strength is one of the most important mechanical properties of concrete, especially for structural applications. In recent years, some researchers tried different approaches to improve the bonding strength of rubber aggregate and cement paste. Some methods reported to have achieved varying degrees of success for reducing the loss of strength of rubber concrete will be particularly reviewed in the Section 2.4 of this chapter.

2.3.5 Young's modulus

Young's modulus of rubber concrete, including static Young's modulus and dynamic Young's modulus were tested by different researchers in the literature. Figure 2-9 shows the converted increment of static Young's modulus [2.46]-[2.48], [2.51], [2.53], [2.57], [2.58], [2.60], [2.61], [2.63], [2.65], [2.67]-[2.69], [2.74], [2.77], [2.82], [2.89], [2.90] and dynamic Young's modulus [2.53], [2.61], [2.85], [2.91], [2.92]. It can be seen clearly that the addition of rubber reduces Young's modulus of concrete. This effect becomes more significant when the rubber content is higher. This is understandable in view of the low stiffness of rubber material compared with natural aggregate and cement paste. The higher the proportion of rubber aggregate, the lower the Young's modulus of concrete. Moreover, it can also be found that the loss of dynamic Young's modulus is less than that of static Young's modulus from Figure 2-9. With the increase of rubber content, ratio of dynamic Young's modulus to static Young's modulus becomes higher. This is in line with the conclusion of Goulias and Ali [2.99].

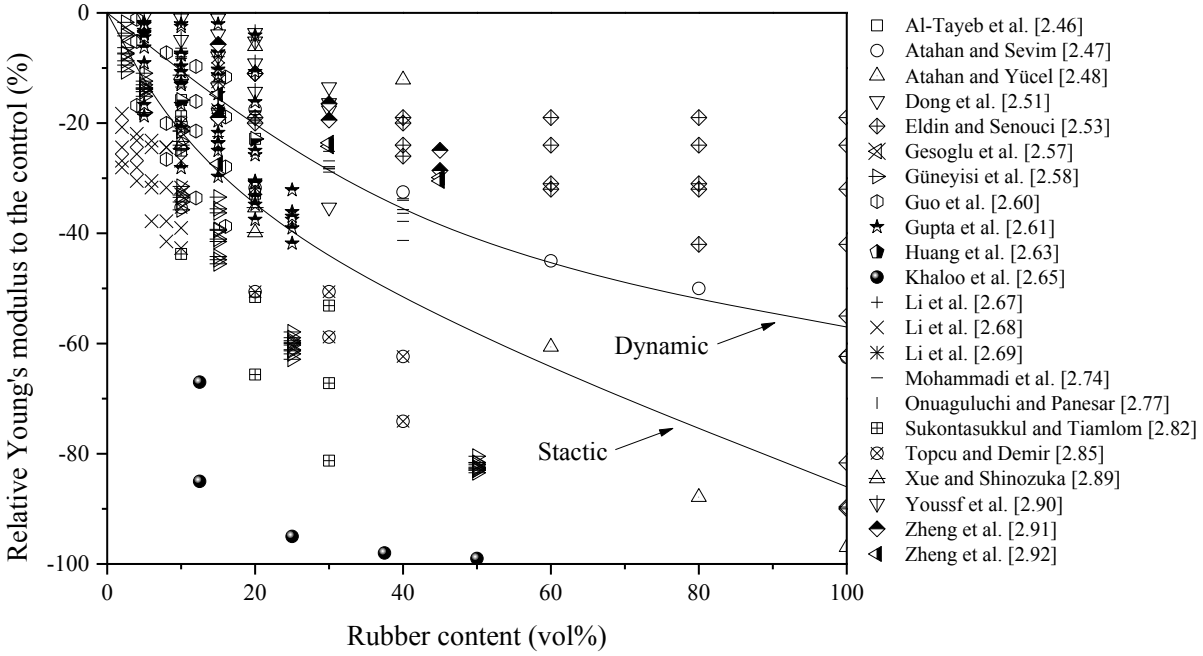

Figure 2-9. Converted relative Young's modulus to the control.

2.3.6 Splitting tensile strength and flexural strength

Figure 2-10 shows the increment of splitting tensile strength [2.46], [2.49], [2.51], [2.53], [2.54], [2.57], [2.58], [2.63], [2.68], [2.77], [2.81] and flexural strength [2.44], [2.49], [2.56], [2.61], [2.70], [2.73], [2.74], [2.81], [2.83], [2.87] based on the results of different researchers. As expected, the addition of rubber aggregate reduces splitting tensile strength and flexural strength of concrete. With the increase of rubber content, both splitting tensile strength and flexural strength decrease and the level of their reduction are quite close. The reasons of the loss of splitting tensile strength and flexural strength are similar to those affecting the compressive strength. However, from the report of Youssf et al. [2.90], when poorly-graded rubber particles were used below 3.5%, tensile strength and even compressive strength were not significantly affected. Their data showed that there were some positive increments when rubber content was less than 3.5%, but no reason was given for this.

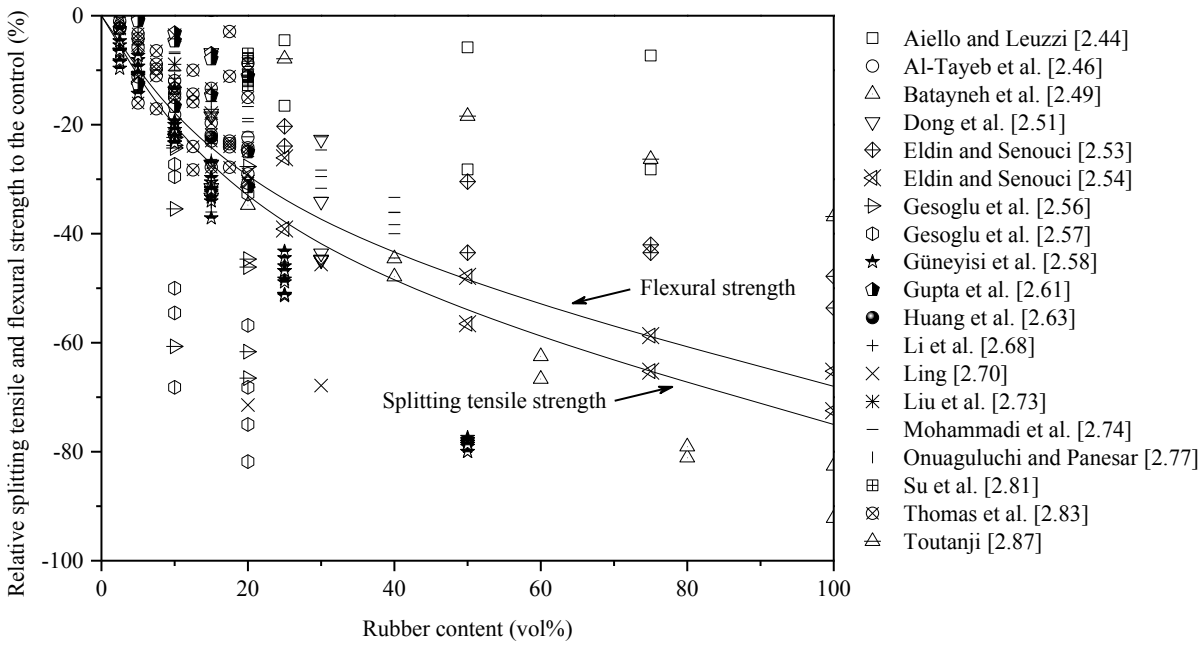

Figure 2-10. Converted relative splitting tensile and flexural strength to the control.

2.3.7 Failure mode and toughness

Figures 2-11, 2-12 and 2-13 show the failure pattern of rubber concrete under different loading conditions. It can be seen that rubber concrete tends to fail gradually. Concrete becomes ductile to some extent because of the addition of rubber materials. Therefore, the failure mode of rubber concrete is ductile rather than brittle [2.53]. In Figure 2-13(a), gradual crack propagation without a sharp tip of the crack in the case of rubber concrete was found. However, in Figure 2-13(b), a typical cracking propagation pattern of plain concrete sample with a sharp crack tip was found. These phenomenalistic observations mean that the toughness of rubber concrete is improved. Figure 2-14 shows the load-deflection curves of different researchers. It is obvious that the ultimate strength of rubber concrete was lower than normal concrete without rubber. But they can experience more deformation prior to ultimate failure and the ductility of rubber concrete is more than that of normal concrete. Due

to this performance, rubber concrete has the potential to be used in crash barriers near bridges and similar structures because of its high toughness (high-plastic energy absorption) [2.53].

(a). Rubber content is 0.

(b). Rubber content is 5%.

(c). Rubber content is 10%.

(d). Rubber content is 15%.

Figure 2-11. Failure patterns of rubber concrete cubes in compressive strength test [2.73].

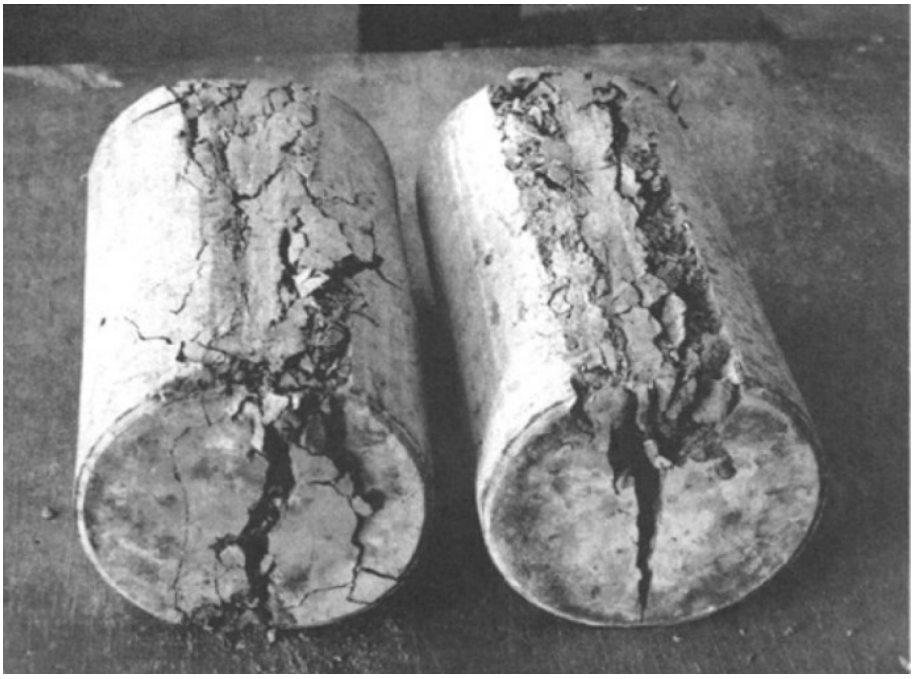

Figure 2-12. Failure pattern of rubber concrete in splitting tensile strength test [2.53].

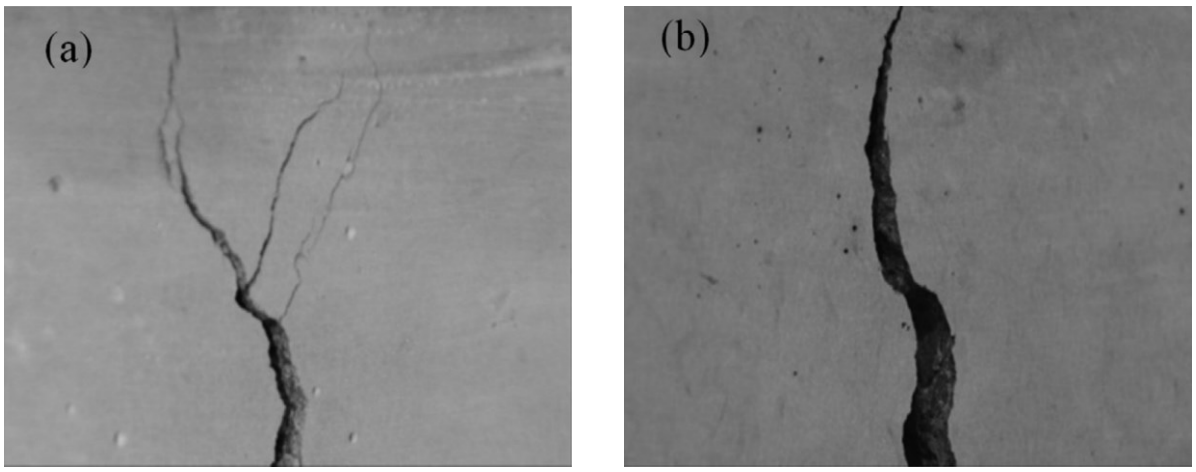

(a). Rubber concrete. (b). Normal concrete.

Figure 2-13. Failure patterns of rubber concrete prisms in flexural strength test [2.74].

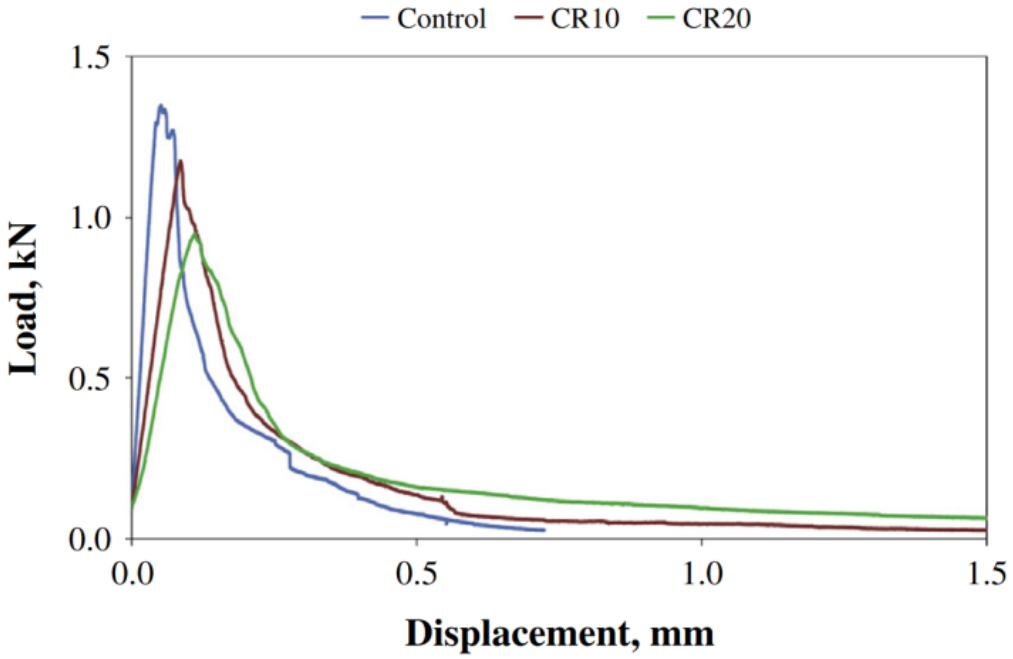

(a). Control represents rubber content of 0; CR10 represents rubber content of 10%; CR20 represents rubber content of 20% [2.57].

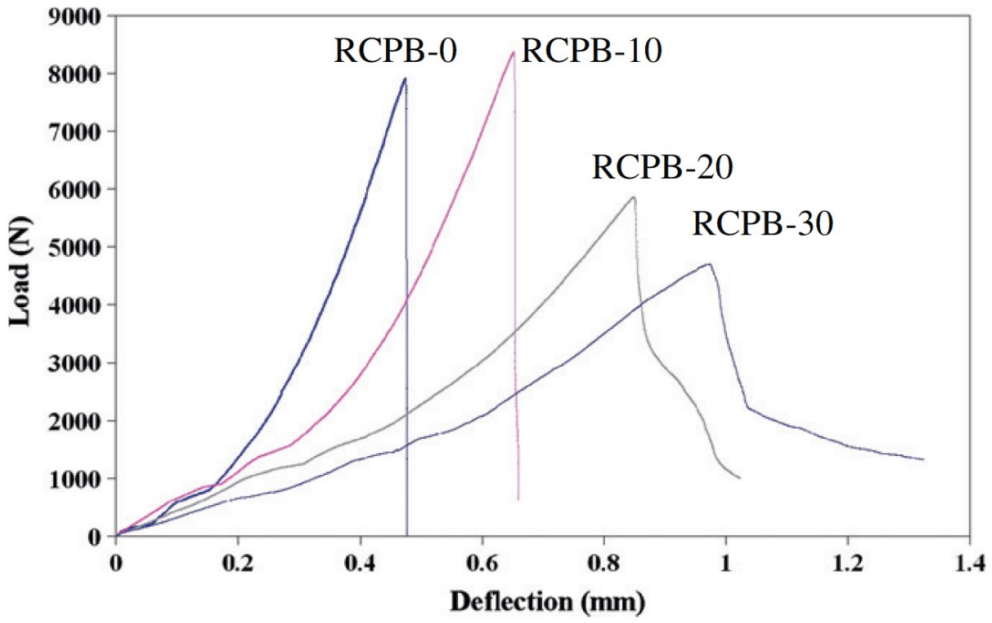

(b). RCPB-0 represents rubber content of 0; RCPB-10 represents rubber content of 10%; RCPB-20 represents rubber content of 20%; RCPB-30 represents rubber content of 30% [2.70].

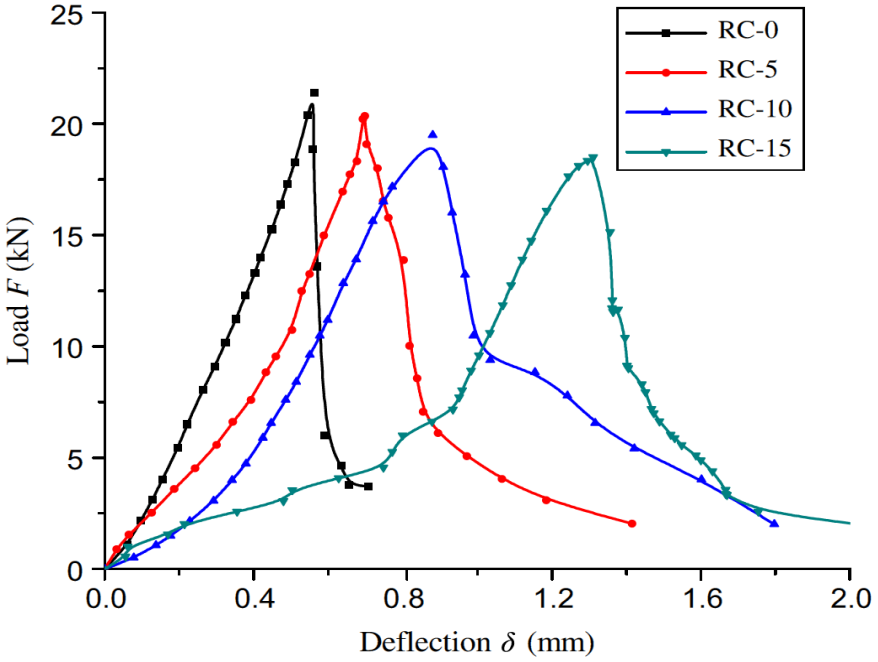

(c). RC-0 represents rubber content of 0; RC-5 represents rubber content of 5%; RC-10 represents rubber content of 10%; RC-15 represents rubber content of 15% [2.73].

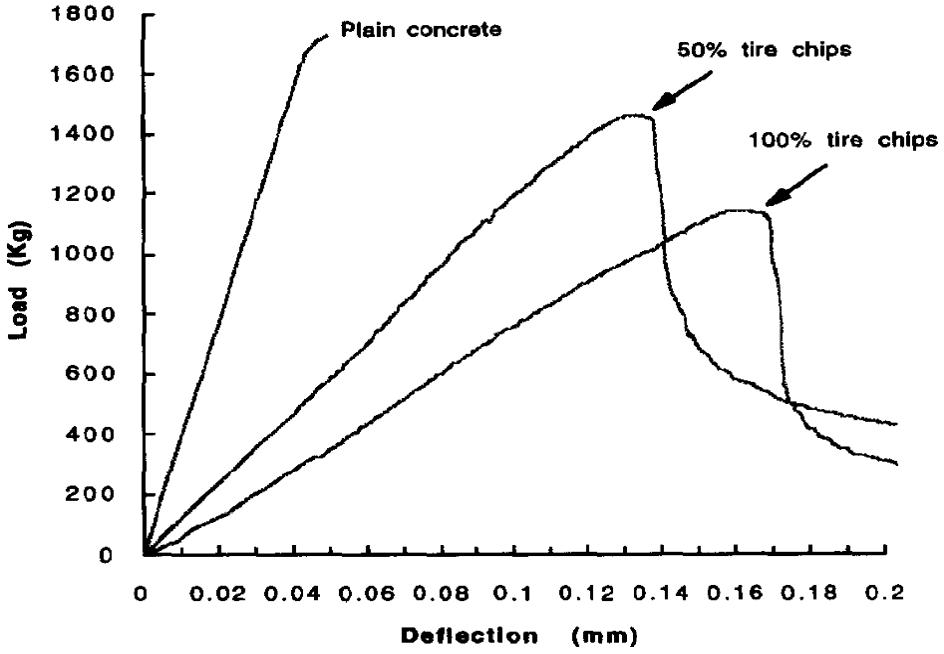

(d). Plain concrete represents rubber content of 0; 50% tire chips represents rubber content of 50%; 100% tire chips represents rubber content of 100% [2.87].

Figure 2-14. Load-deflection curves of rubber concrete [2.57], [2.70], [2.73], [2.87].

2.3.8 Energy absorption capability

Energy absorption capability of rubber concrete was evaluated by some researchers [2.48], [2.51], [2.72], [2.78], [2.91] using impact test. Their results showed that the addition of rubber aggregate enhanced energy absorption of rubber concrete compared to normal concrete. Figure 2-15 shows the relationship of average dissipating energy versus rubber replacement [2.48]. It is clear that with the increase of rubber content in concrete, the average dissipated energy increases. Besides, from Figure 2-16 [2.48], it can also be seen that the energy absorption capability of rubber concrete is better than that of normal concrete. The duration of impact increased more than 6 times between normal concrete and 100% rubber replacement samples. This is mainly because of the natural property of rubber material which has a much lower stiffness than concrete. Therefore, when rubber aggregate is used to replace natural aggregate, concrete becomes more ductile, which has been discussed in previous sections. Ozbay et al. [2.78] also reported similar conclusions that the greater the percentage of rubber aggregate, the higher energy absorption capability of rubber concrete. Based on these conclusions, rubber concrete has a high potential for applications such as safety barriers because they lead to smaller deceleration forces and hence less damage [2.48].

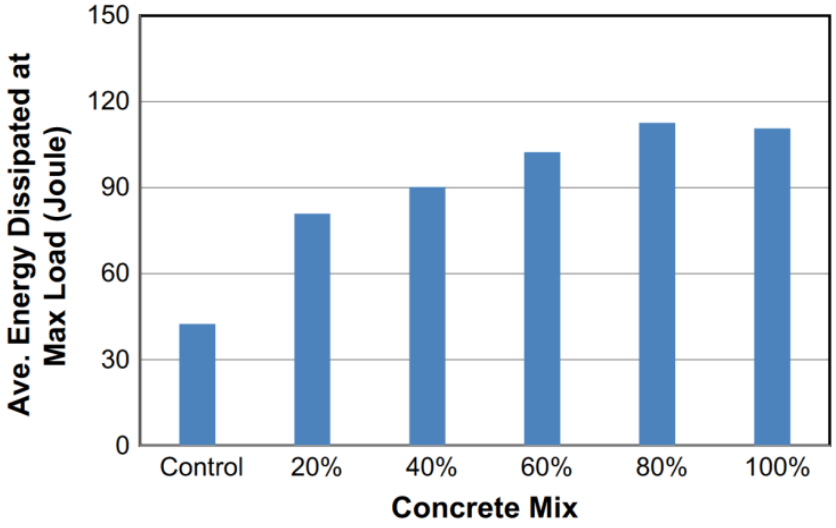

Figure 2-15. Dynamic impact test results of average energy transferred at maximum load [2.48].

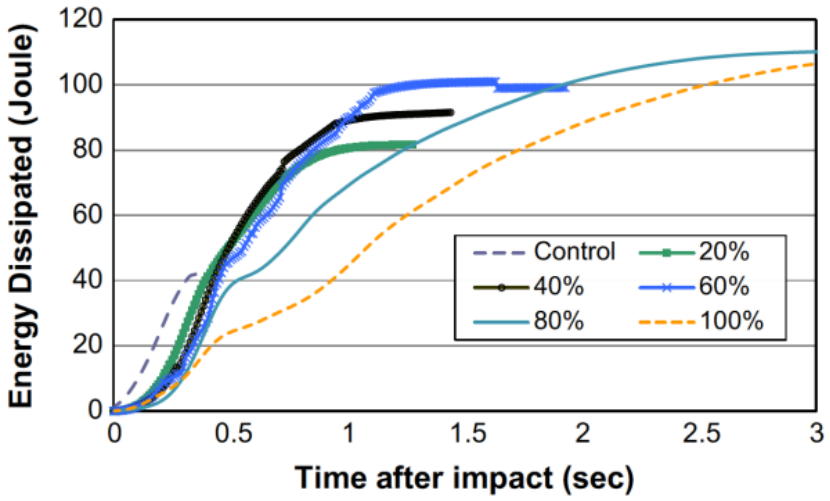

Figure 2-16. Load and energy dissipated versus time [2.48].

2.3.9 Fatigue performance

Fatigue life of rubber concrete is prolonged in accordance to the conclusions of Liu et al. [2.73], Mohammadi et al. [2.74] and Wang et al. [2.88]. Figure 2-17 shows the hit and energy-cycle curves of normal concrete and rubber concrete. The cumulated hit number produced in the testing of rubber concrete is much less than that of normal concrete. It means that less acoustic emission signals recorded in rubber concrete indicates that less damage

occurred during the fatigue process because rubber concrete has higher attenuation and better toughness owing to the inclusion of rubber aggregate. Figure 2-18 shows the S-N curves of normal concrete and rubber concrete. With the increase of rubber content, fatigue life increases. This is due to the higher energy absorption capability of rubber material which makes rubber concrete absorbing more energy before failure. Mohammadi et al. [2.74] also stated that rubber material has a positive effect on fatigue performance of concrete. However, he pointed out that less than 10% of rubber aggregate has a negative effect on fatigue behaviour. According to his results shown in Figure 2-19, other amounts more than 10% will improve the resistance of concrete against cyclic loading.

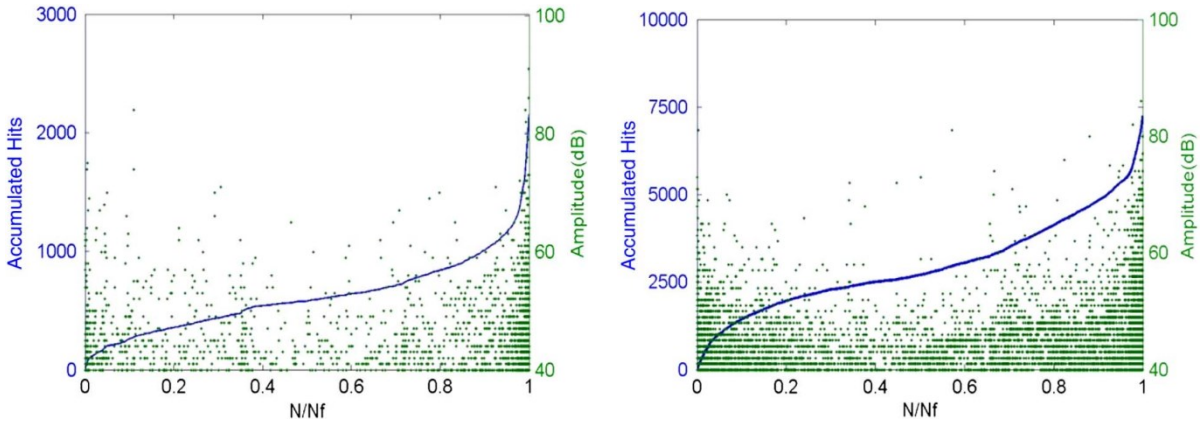

(a). Rubber concrete. (b). Normal concrete.

Figure 2-17. Hit and energy-cycle curve of rubber concrete [2.88].

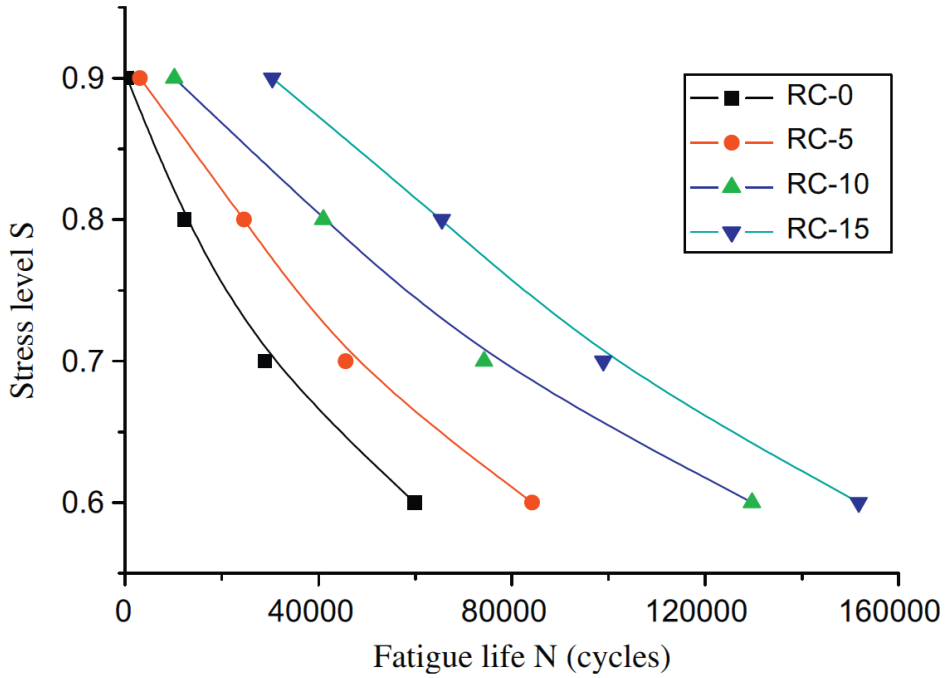

Figure 2-18. S-N curves of concrete samples.

RC-0 represents rubber content of 0; RC-5 represents rubber content of 5%;

RC-10 represents rubber content of 10%; RC-15 represents rubber content of 15% [2.73].

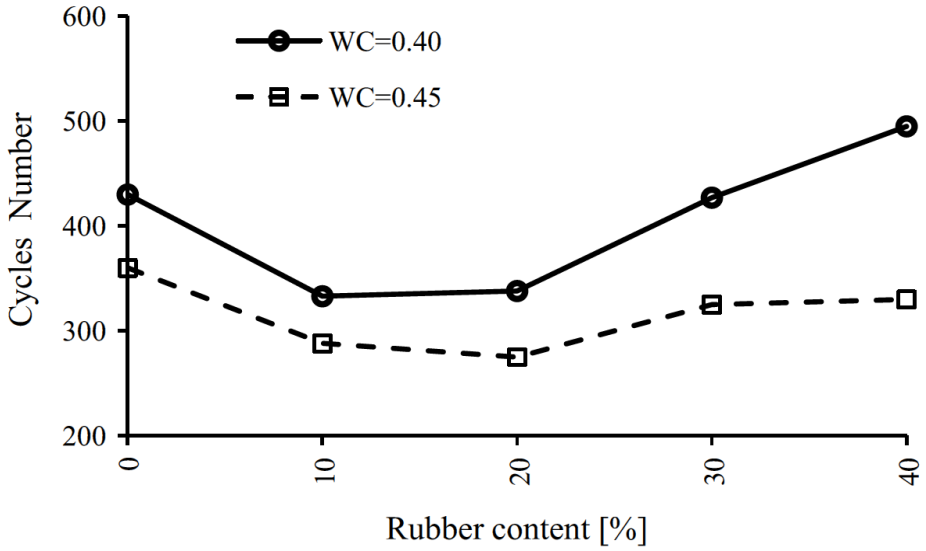

Figure 2-19. Number of cycle of rubber concrete samples before failure [2.74].

2.3.10 Abrasion resistance

When rubber concrete is used for pavement, abrasion resistance is one of the most important properties. Deterioration of concrete could happen because of the abrasion which is caused by different exposures on the surface of concrete. A typical abrasion test, as shown in Figure 2-20, is adopted by some researchers [2.56], [2.61], [2.78], [2.83] to measure the resistance of rubber concrete to wear. The conclusion drawn by Thomas et al. [2.83] is that abrasion resistance of rubber concrete is better than that of normal concrete. Rubber aggregate in concrete restrict the grinding of concrete surface, which is attributed that some rubber particles are beyond the smooth surface of concrete and act like brush, reducing the rubbing of concrete surface [2.83]. Therefore, rubber concrete has a better abrasion resistance than compared to normal concrete. Gupta et al. [2.61] also reported a similar conclusion, namely that the depth of wear of rubber concrete decreases with the increase of content of rubber fibre (shown in Figure 2-21). However, they also pointed out that when only rubber ash was used, the conclusion is opposite, as shown in Figure 2-22. With the increase of content of rubber ash, the depth of wear for rubber concrete increase. They attributed this to the lower compressive strength of rubber ash concrete [2.61]. On the contrary, Ozbay et al. [2.78] stated that the addition of rubber aggregate decreased the abrasion resistance of rubber concrete and a higher replacement of rubber material increased the mass loss and wear depth of concrete. They cited some reasons from other researchers to support their conclusions. They pointed out that the addition of rubber aggregate increased concrete porosity, which decreases the contact area of concrete with the abrasive rotating disc, causing rapid abrasion. This is completely opposite from explanations of Thomas et al. [2.83]. More research is needed to clarify this property of rubber concrete.

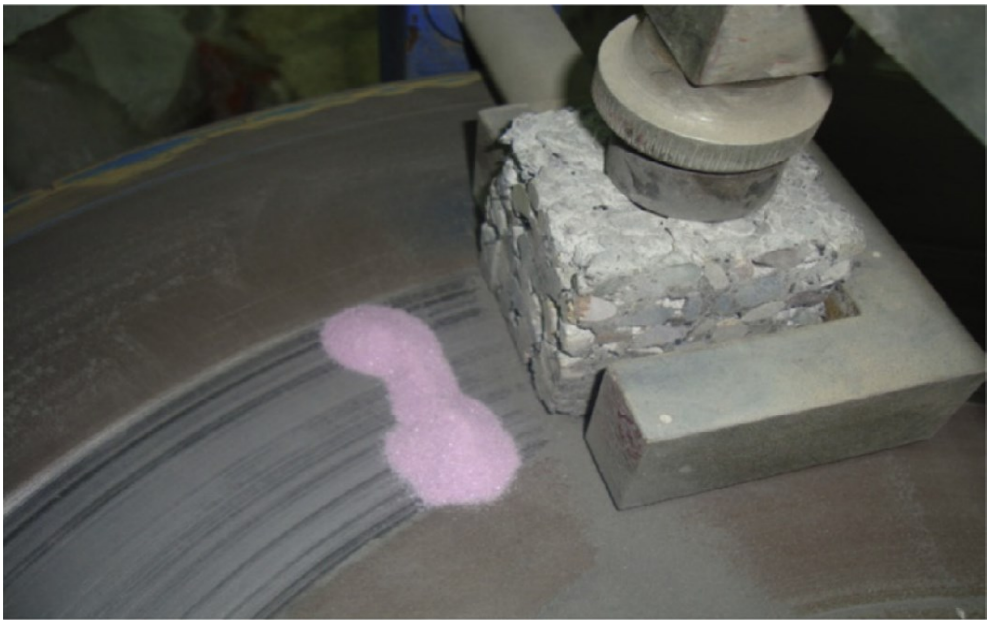

Figure 2-20. Abrasion test of rubber concrete [2.56], [2.74].

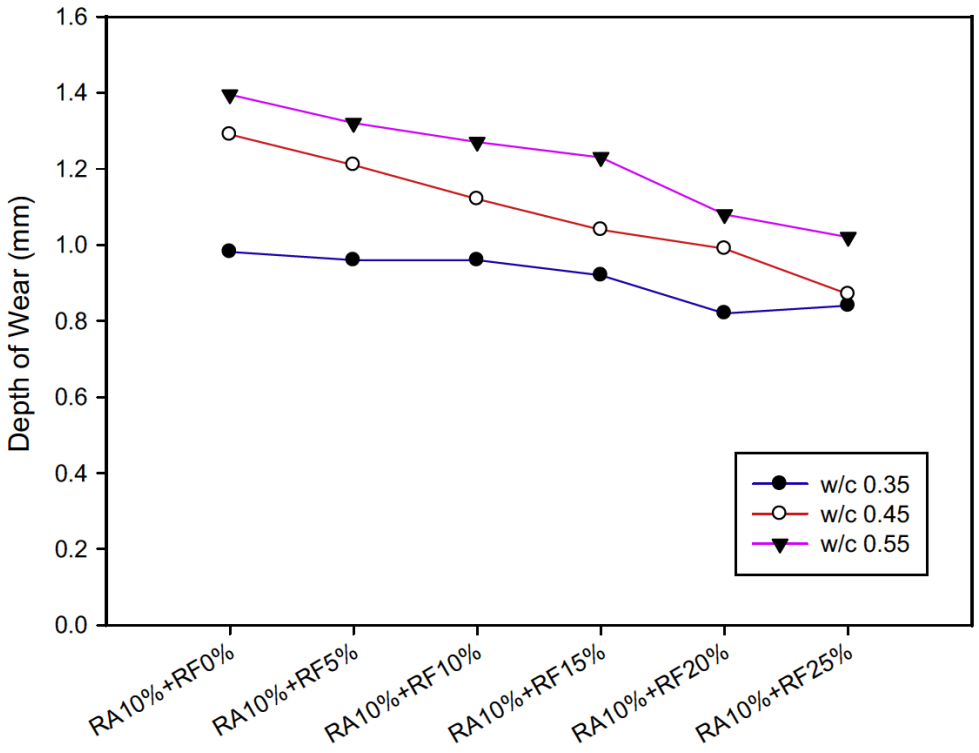

Figure 2-21. Wear depth of rubber ash and rubber fibre concrete, RA represents rubber ash; RF represents rubber fibre [2.61], [2.74].

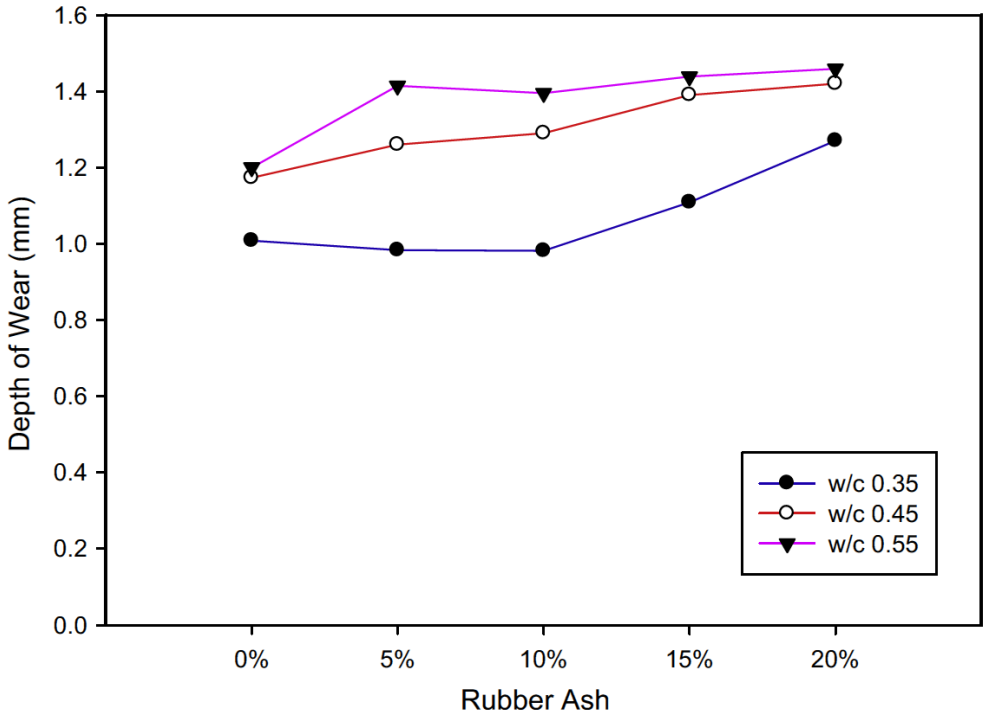

Figure 2-22. Wear depth of rubber ash concrete [2.61], [2.74].

2.3.11 Thermal conductivity

Mohammed et al. [2.76] tested the thermal conductivity of crumb rubber hollow concrete block. Their results showed that thermal conductivity of rubber concrete decreases with the increase of rubber content (Figure 2-23). This is mainly attributed to the microstructure of rubber concrete. As discussed in Section 2.3.2, air is entrapped on the surface of rubber particles, resulting in an increase of air content in hardened rubber concrete. Thermal conductivity of air which is 0.025 W/(m·k) is lower than that of concrete 1.7 W/(m·k). Besides, thermal conductivity of rubber material 0.16 W/(m·k) is also lower than that of sand 1.5 W/(m·k). Thus, both air and rubber aggregate retain the thermal flow, decreasing the thermal conductivity of rubber concrete. This enhanced performance makes rubber concrete potential to be used where thermal insulation is required.

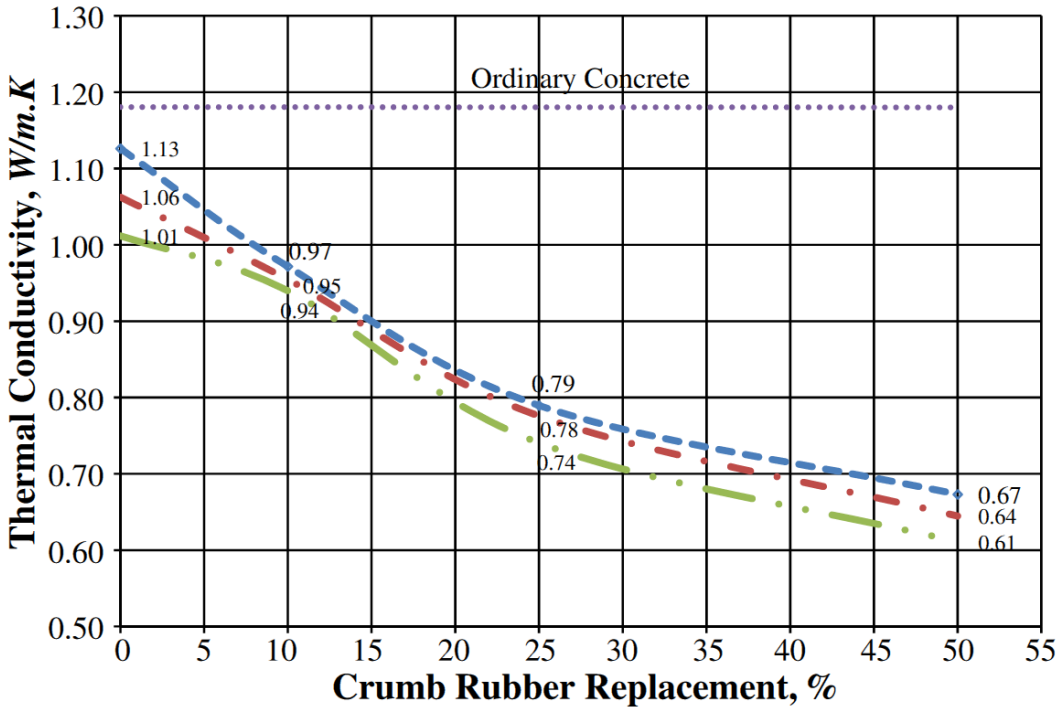

Figure 2-23. Thermal conductivity versus crumb rubber replacement [2.76].

2.3.12 Sound absorption

Results of sound absorption test on rubber concrete from Mohammed et al. [2.76] and Khaloo et al. [2.65] showed that rubber concrete has a better sound absorption than normal concrete. Figure 2-24 illustrates that noise reduction coefficient increases with the increase of rubber content. This can be explained as the sound could be easily absorbed through the entrapped air on the surface of rubber aggregates [2.76]. With the amount of rubber aggregate increases, air content increases due to the entrapped air on rubber surface, leading to a higher porosity of rubber concrete. Consequently, sound energy is absorbed more easily during the process of reflection in the air voids. Khaloo et al. [2.65] also got the similar conclusion. His results, shown in Figure 2-25 indicates that the velocity of ultrasonic waves reduce significantly with the increase of rubber content. Therefore, rubber concrete is potentially a suitable material for

the dampening of sound and other shaking energies, and can be used in noisy conditions to serve as sound insulation. He also pointed out that because of the significant reduction of ultrasonic moduli, a porous composition is needed for further analysis.

In 2014, Onuaguluchi and Panesar [2.77] conducted the test of porosity on rubber concrete. They stated that the porosity of rubber concrete, which is between 13.7% and 15.0% increases with the rubber content increases. They attributed the increased void content of rubber concrete to the tendency of rubber material to float in the mixtures and the elastic behaviour of the composite under an external loading, which made the compaction difficult and inefficient. Thus, the amount of void in rubber concrete increased with the increase of rubber content.

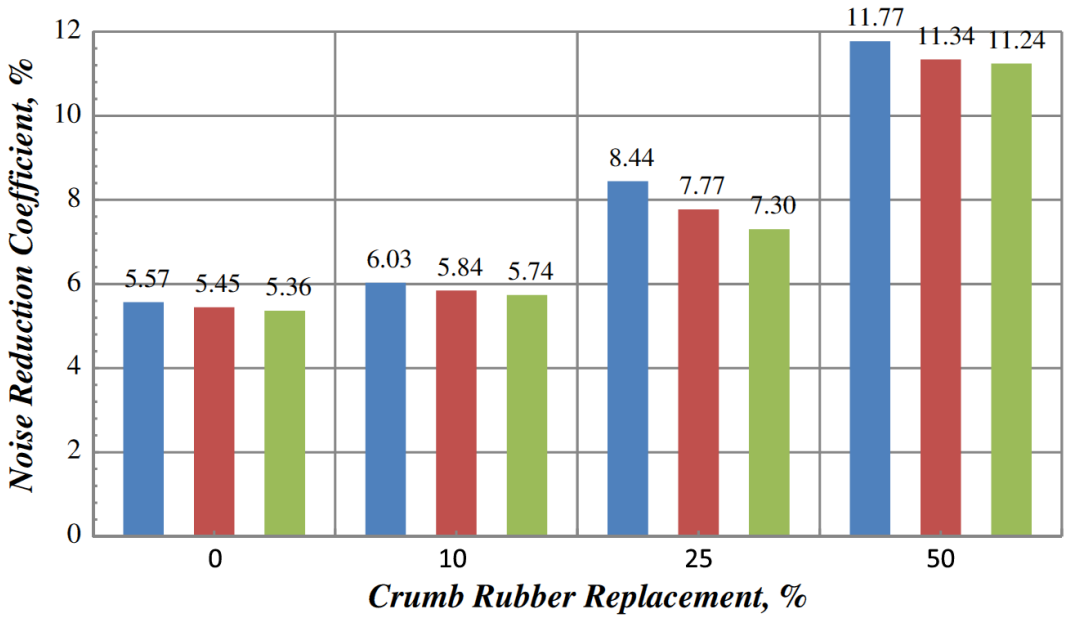

Figure 2-24. Noise reduction coefficients [2.76].

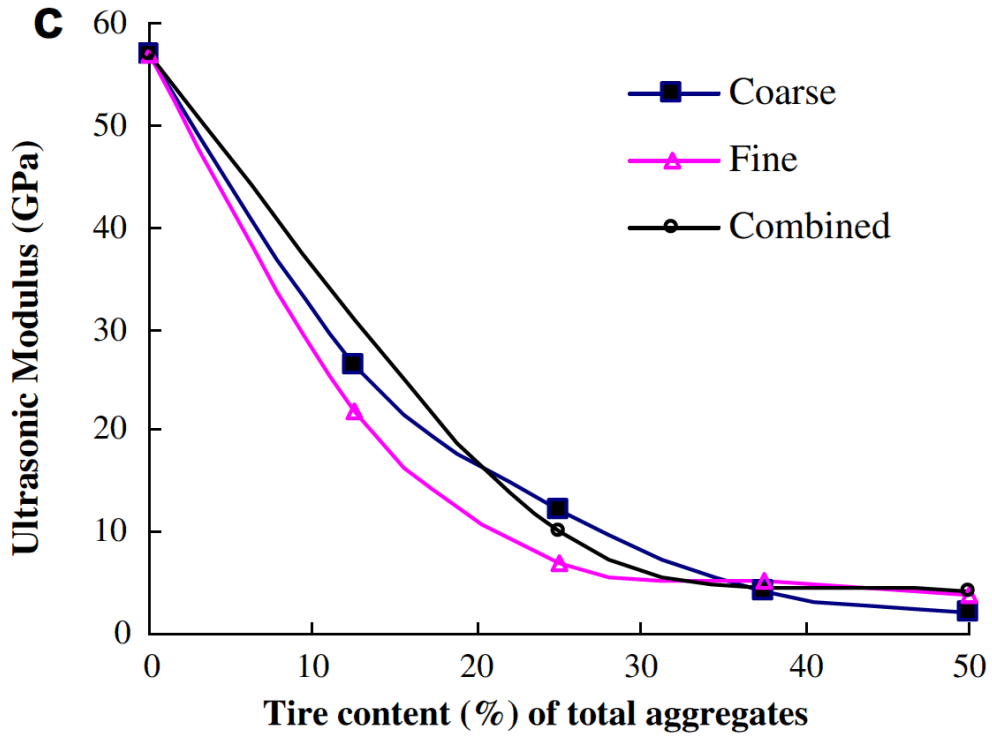

Figure 2-25. Values of the ultrasonic moduli for rubber concrete, Coarse represents natural coarse aggregate was replaced by rubber aggregate; Fine represents natural fine aggregate was replaced by rubber aggregate; Combined represents both natural coarse and fine aggregate were replaced by rubber aggregate [2.65].

2.3.13 Electrical resistivity

Electrical resistivity performance of rubber concrete was compared with that of normal concrete by Mohammed et al. [2.76] and Onuaguluchi and Panesar [2.77]. Mohammed et al. pointed out that the electrical resistivity of rubber concrete increases with the increase of rubber replacement, as can be seen in Figure 2-26. It is attributed to the nature of rubber materials which is being used as an insulator in electrical industry and function as dielectric material [2.100]. Rubber aggregate behaves as a blocking pathway for electrical transfer between the two measure electrodes. Onuaguluchi and Panesar stated that some factors such

as binder type, concrete microstructure, test age, moisture content and addition of conductive or insulating additives to mixtures can affect the surface resistivity of concrete. Their results show that the electrical resistivity of rubber concrete was higher than that of normal concrete, which is due to the electrical insulation property of rubber material. However, it should be noted that when beyond 10% rubber replacement as fine aggregate, the electrical resistivity starts to decrease as a result of the interplay of factors such as specimen microstructure and moisture content [2.77].

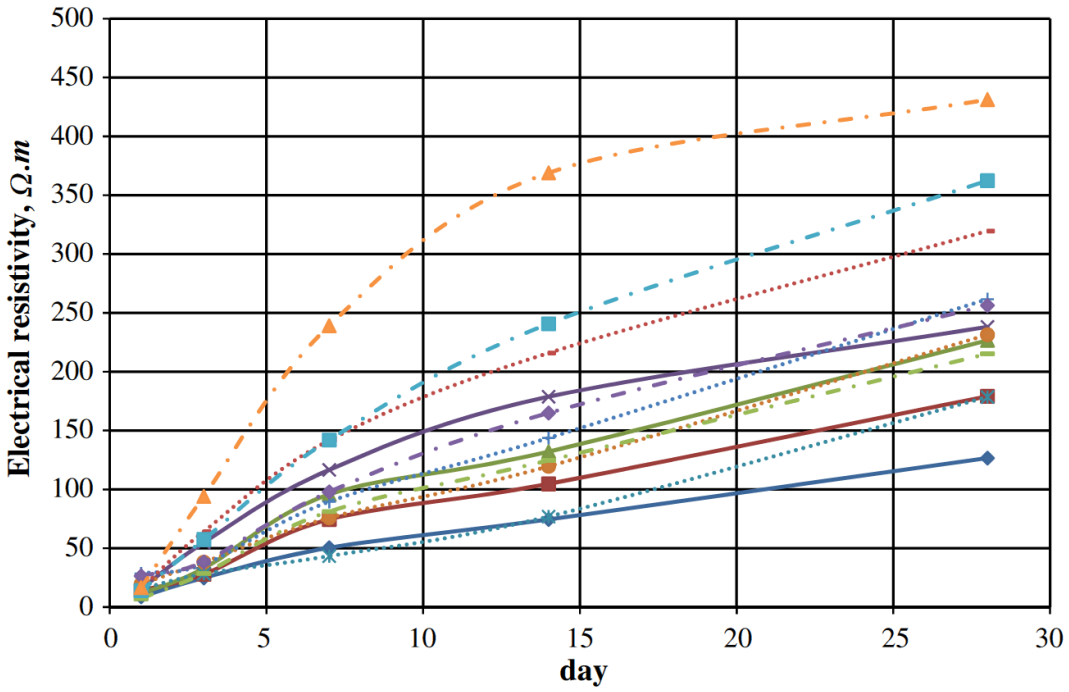

Figure 2-26. Electrical resistivity of rubber concrete [2.76].

2.3.14 Permeability

Permeability to the ingress of water and other potentially harmful substances is a very important characteristic that influences concrete durability. On the one hand, water permeability test on rubber concrete was carried out by several researchers [2.50], [2.61],

[2.76], [2.77], [2.82], [2.83]. The unanimous conclusion is that with the increase of rubber content in mixture, waster permeability resistance of rubber concrete decreases (Figure 2-27). The main reason is due to the non-polar nature of rubber materials which tends to repel water and entrap air on the surface. Voids are formed between rubber particles and matrix when the mixtures harden. Microstructure of normal concrete is changed and the porosity increases because of the extra air content. Therefore, more conduits are formed for water to transport, increasing the water permeability of rubber concrete. On the other hand, chloride ion permeability test was performed [2.50], [2.51], [2.55], [2.61], [2.77]. However, two conclusions are presented by different researchers. Gesoğlu and Güneyisi [2.55] pointed out that the penetration depth of chloride ion increased with the increase of rubber content in the concrete. As the replacement increased from 0 to 25%, the chloride ion permeability of rubber concrete was around 6-40% at 0.60 water/cement ratio and about 27-59% at 0.40 water/cement ratio greater than the reference mix. Conclusions from Dong et al. [2.51] are in line with Gesoğlu and Güneyisi. They stated that rubber concrete exhibited chloride ion penetration resistance approximately 20-40% higher than normal concrete, as can be seen in Figure 2-28. The reduced performance is due to the increased voids in the interfacial transition zone between cement matrix and rubber particles. Results of chloride ion penetration resistance test by Bravo and Brito [2.50] show that when rubber replacement was below 5%, the chloride diffusion coefficient of rubber concrete was lower than that of normal concrete. As rubber content went from 5% to 15%, the chloride diffusion coefficient increased, indicating a worse chloride ion penetration resistance. But Onuaguluchi and Panesar [2.77] and Gupta et al. [2.61] indicated that the addition of rubber materials decreased the charge transmitted in the mixture, enhancing the property of chloride ion permeability resistance. They attributed this to the high resistivity of rubber materials,

decreasing the amount of charge which can pass through the matrix. More research is needed to clarify the chloride ion permeability of rubber concrete.

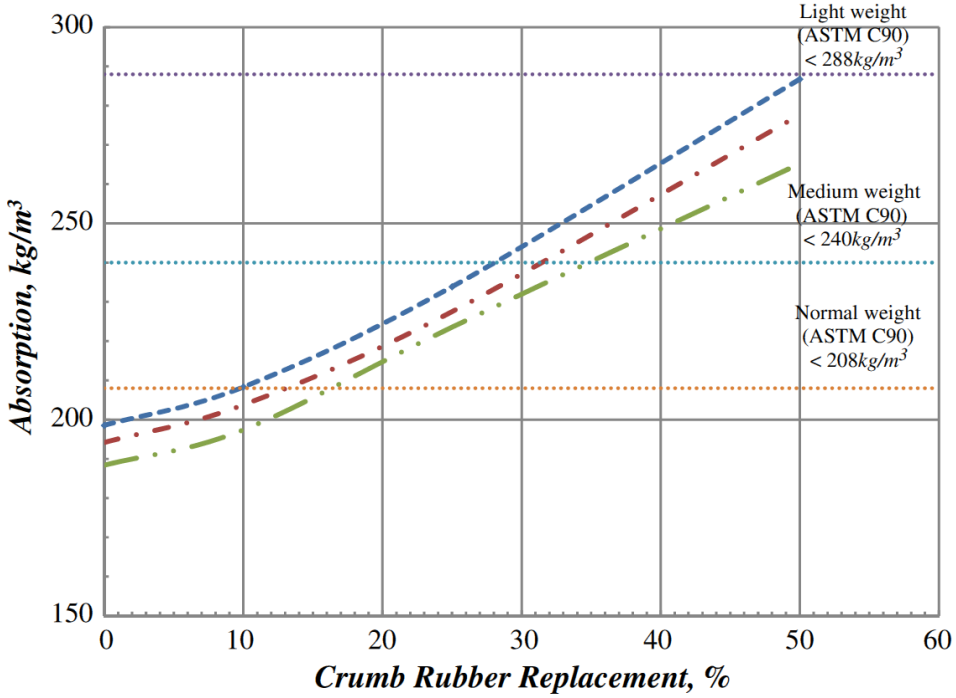

Figure 2-27. Rubber concrete absorption versus rubber replacement at the age of 28 days [2.76].

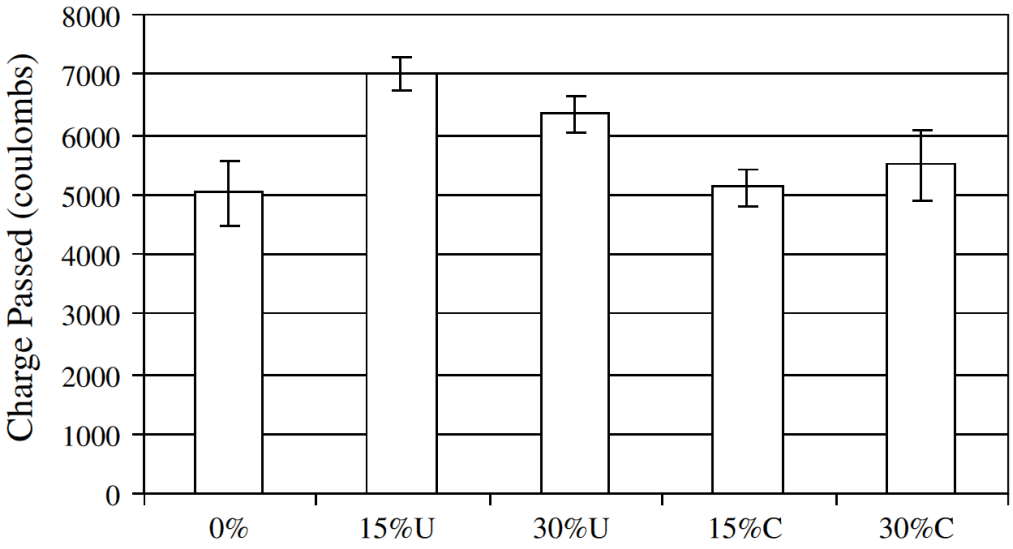

Figure 2-28. Chloride ion resistance test results [2.51].

2.3.15 Freeze-thaw characteristic

Freeze-thaw characteristic is another very important factor of concrete durability. Topçu and Demir [2.85] tested compressive strength, dynamic elasticity modulus and weight of concrete after freeze-thaw cycle. They demonstrated that there was an increase in durability against freeze-thaw when rubber content was 10%. Gesoğlu et al. [2.56] demonstrates the performance of concrete against freeze-thaw in term of mass loss. There was no obvious difference between normal concrete and rubber concrete when the cycles are below 240. However, after 300 cycles the degradation of normal concrete is severer than that of rubber concrete which can be easily seen in Figure 2-29. Rubber aggregate plays a positive role in freeze-thaw resistance of rubber concrete. On the contrary, Eldin and Senouci [2.53] argued that rubber concrete experienced more reduction in dynamic modulus of elasticity than normal concrete. The conclusion is based on the experimental results but no explanation was given.

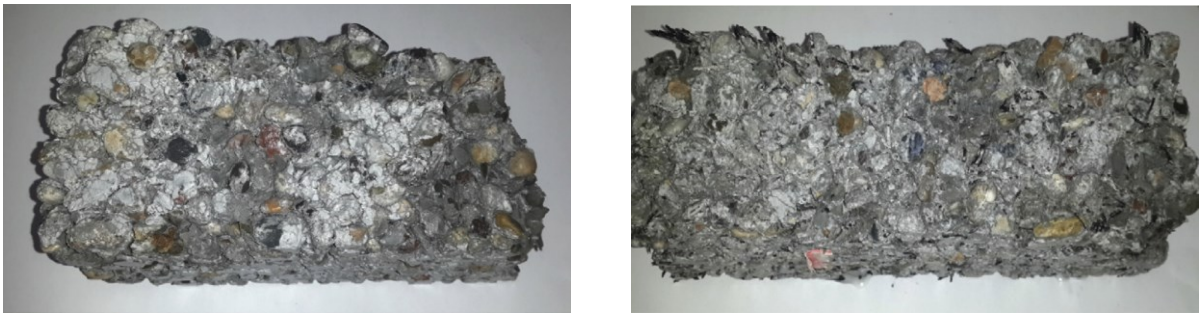

(a). Reference. (b). Rubber concrete.

Figure 2-29. Photographic view of the freeze-thaw samples after 300 cycles [2.56].

2.3.16 Shrinkage

Bravo and Brito [2.50] and Sukontasukkul and Tiamlom [2.82] stated that shrinkage of rubber concrete is higher than normal concrete and it increases with the increase of rubber content, shown in Figure 2-30. This is easy to understand as natural aggregate is replaced by rubber aggregate which is much flexible to act like spring. The loss of compressive strength and elastic modulus of aggregate causes the reduction of internal restraints and leads to higher shrinkage. Overall, large shrinkage might come from two combined effects: the lower capacity to restrict shrinkage of the matrix and the increase of more flexible materials.

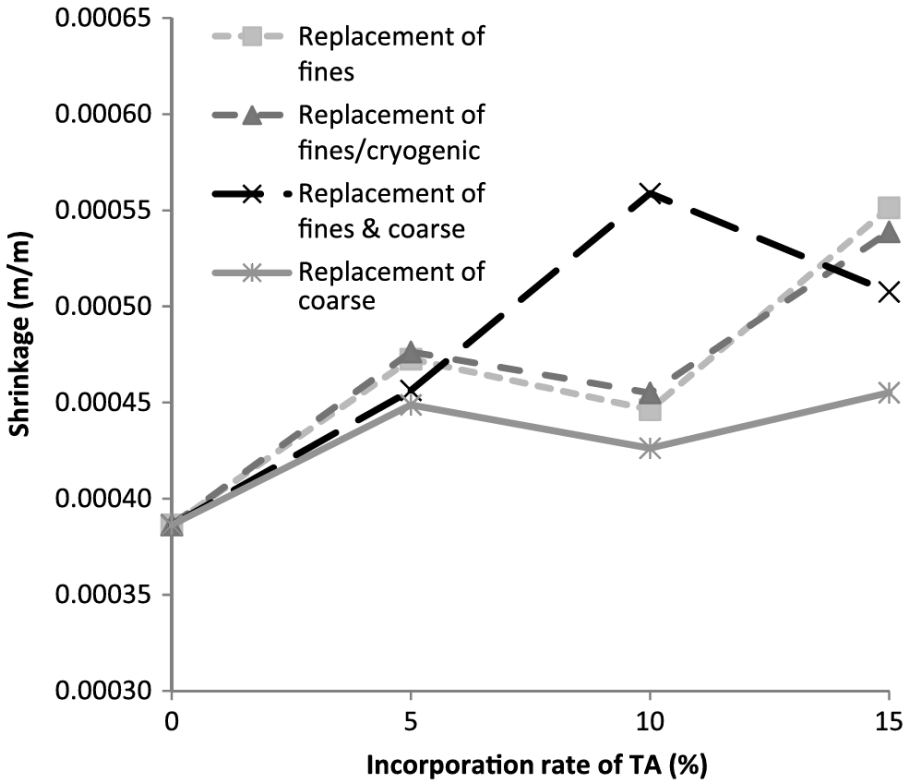

Figure 2-30. 90 days hardened-state shrinkage of concrete, TA represents tyre aggregate [2.50].

2.3.17 Carbonation

Carbonation depth of rubber concrete is higher than normal concrete and increases with the increase of rubber replacement ratio [2.50], [2.61]. This variation was predictable because when water permeability was analyzed in Section 2.3.14, the same trend was found. The property of carbonation is influenced by the same factor. The increased air content results in more voids, hence higher porosity. Therefore, the carbonation depth of concrete increased with the addition of rubber aggregate.

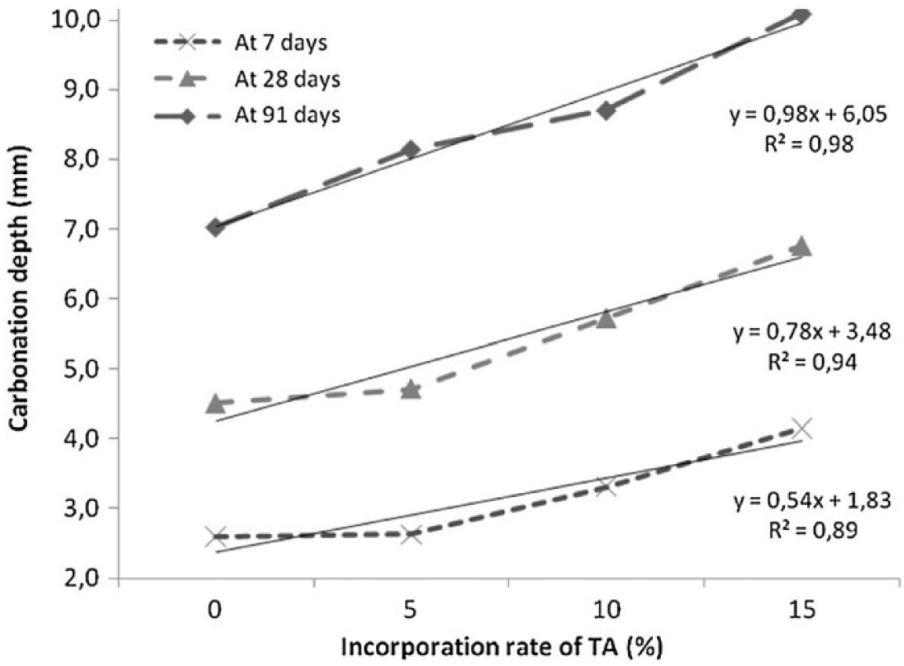

Figure 2-31. Carbonation depth versus rubber replacement ratio, TA represents tyre aggregate [2.50].

2.4 State-of-the-art research on rubber concrete

Rubber concrete has been used in some non-bearing structures such as exterior wall materials [2.101], pedestrian block [2.29], flowable fill [2.102]. Potential uses of rubber concrete have

also been reported for crash barrier, highway sound wall, garage floors, and residential drive ways [2.103]. The advantages of rubber concrete, in addition to environment benefits, are excellent energy absorbing characteristic and light weight. However, the significant loss of strength restricts their applications in structure engineering. In the above literature review, the greatest concern for using rubber aggregate in concrete is the reduction of strength since strength is one of the most important properties of concrete. How to reduce the loss of strength for more applications is constantly being researched in recent years.

One approach is to reduce the size of rubber particles. As discussed above, rubber aggregate can be deemed as voids in the concrete which easily cause stress concentration. The reduction of rubber size (to about 20 μm comparable to cement particles) will effectively reduce stress concentration and the loss of strength of concrete will be decreased. However, the cost of processing very fine rubber powder will be inevitably increased [2.103]. Yang et al. [2.10] pointed out that production of rubber particles finer than 1.5 mm significantly increased manufacturing cost. Huang et al. [2.63] also stated that the cost of crumb rubber is around ten times more than rubber chips. Therefore, it should be taken into account along with the benefit of improved performance of rubber concrete.

Another advanced method is surface-modifying the rubber aggregates to improve the bond strength between rubber aggregates and cement paste. Since the bonding along interfacial transition zone is poor, treatment on rubber particles will change its surface property and will potentially improve the bonding. Surface modification of rubber particles includes water rinse [2.8], [2.22], sodium hydroxide treatment [2.22], [2.24] [2.43], [2.90], [2.104], organic sulphur compounds treatment [2.105], pre-coating by cement paste [2.22], mortar [2.22], and

limestone powder [2.77] towards rubber aggregate. Besides, Li et al. [2.68] applied physical anchorage by drilling holes in rubber chips. Some methods were reported to have achieved varying degrees of success. However, none of them showed significant ability to prevent the sever loss of strength due to the addition of rubber aggregate. Therefore, more research is needed to be carried out to improve the bond strength in the interfacial transition zone.

2.5 Summary and recommendations

Rubber concrete has a great potential to be used in practice because it is environmentally beneficial, commercially competitive, technically sound, and supportive of a more sustainable society. However, the incompatibility issue due to chemical composition and the low stiffness of rubber materials restrict the application of rubber concrete, especially in structural engineering applications. Although many researchers have tried to reduce the loss of strength of rubber concrete, more studies are still needed to significantly improve the performance of rubber concrete. Some recommendations are listed below:

- Reduce the size of rubber particles. Since rubber aggregates can be deemed as voids in concrete, the reduction of size of rubber particles will effectively decrease stress concentration under compression so as to reduce to loss of strength of rubber concrete. Meanwhile, the cost of producing fine rubber aggregates should be considered along with the benefit of improved performance of rubber concrete.

- Improve the interfacial transition zone between rubber aggregates and cement paste. The non-polar property of rubber material makes the interfacial transition zone very poor. The

improvement of interfacial transition zone will increase their bond strength, reducing the strength loss of rubber concrete.

- Replacing natural coarse aggregate by rubber aggregate should be adopted with care. The strength of concrete depends greatly on the density, size, and hardness of coarse aggregate [2.106]. The use of soft rubber material as coarse aggregate will inevitably reduce much of concrete strength.

- From the viewpoint of practical application, the manner of substituting natural aggregate of concrete with rubber aggregate by volume is preferred.

References

[2.1] M. Nehdi, A. Khan, Cementitious composites containing recycled tire rubber: an overview of engineering properties and potential application, Cem. Concr. Aggr. 23 (2001) 3-10.

[2.2] M.W. Tantala, J.A. Lepore, I. Zandi, Quasi-elastic behavior of rubber included concrete (RIC) using waste rubber tires, Proceedings of the 12th International Conference on Solid Waste Technology and Management, Philadelphia, USA, 1996.

[2.3] R. Siddique, T.R. Naik, Properties of concrete containing scrap-tire rubber – an overview, Waste Manage. 24 (2004) 563-569.

[2.4] F. Hernández-Olivares, G. Barluenga, Fire performance of recycled rubber-filled high-strength concrete, Cem. Concr. Res. 34 (2004) 109-117.

[2.5] F. Hernández-Olivares, G. Barluenga, M. Bollati, B. Witoszek, Static and dynamic behaviour of recycled tyre rubber-filled concrete, Cem. Concr. Res. 32 (2002) 1587-1596.

[2.6] F. Hernández-Olivares, G. Barluenga, B. Parga-Landa, M. Bollati, B. Witoszek, Fatigue behaviour of recycled tyre rubber-filled concrete and its implications in the design of rigid pavement, Constr. Build. Mater. 21 (2007) 1918-1927.

[2.7] L. Li, Z. Chen, W. Xie, F. Liu, Experimental study of recycled rubber-filled high-strength concrete, Mag. Concr. Res. 61 (2009) 549-556.

[2.8] A.E. Richardson, K.A. Coventry, G. Ward, Freeze/thaw protection of concrete with optimum rubber crumb content, J. Clean. Prod. 23 (2012) 96-103.

[2.9] K.S. Son, I. Hajirasouliha, K. Pilakoutas, Strength and deformability of waste tyre rubber-filled reinforced concrete columns, Constr. Build. Mater. 25 (2011) 218-226.

[2.10] L. Yang, Z. Han, C. Li, Strength and flexural strain of CRC specimens at low temperature, Constr. Build. Mater. 25 (2011) 906-910.

[2.11] B. Yesilata, Y. Isıker, P. Turgut, Thermal insulation enhancement in concretes by adding waste PET and rubber pieces, Constr. Build. Mater. 23 (2009) 1878-1882.

[2.12] C. Albano, N. Camacho, J. Reyes, J.L. Feliu, M. Hernández, Influence of scrap rubber addition to Portland I concrete composites: destructive and non-destructive testing, Compos. Struct. 71 (2005) 439-446.

[2.13] F. Azevedo, F. Pacheco-Torgal, C. Jesus, J.L. Barroso de Aguiar, A.F. Camões, Properties and durability of HPC with tyre rubber wastes, Constr. Build. Mater. 34 (2012) 186-191.

[2.14] M. Elchalakani, High strength rubberized concrete containing silica fume for the construction of sustainable road side barriers, Structures 1 (2015) 20-38.

[2.15] N.I. Fattuhi, L.A. Clark, Cement-based materials containing shredded scrap truck tyre rubber, Constr. Build. Mater. 10 (1996) 229-236.

[2.16] E. Ganjian, M. Khorami, A.A. Maghsoudi, Scrap-tyre-rubber replacement for aggregate and filler in concrete, Constr. Build. Mater. 23 (2009) 1828-1836.

[2.17] M. R. Hall, K.B. Najim, Structural behaviour and durability of steel-reinforced structural Plain/Compacting Rubberized Concrete (PRC/SCRC), Constr. Build. Mater. 73 (2014) 490-497.

[2.18] N. Holmes, A. Browne, C. Montague, Acoustic properties of concrete panels with crumb rubber as fine aggregate replacement, Constr. Build. Mater. 73 (2014) 195-204.

[2.19] H.S. Lee, H. Lee, J.S. Moon, H.W. Jung, Development of tire-added latex concrete, ACI Mater. J. 95 (1998) 356-364.

[2.20] M. Mavroulidou, J. Figueiredo, Discarded tyre rubber as concrete aggregate: a possible outlet for used tyres, Global Nest J. 12 (2010) 359-367.

[2.21] B.S. Mohammed, N.J. Azmi, M. Abdullahi, Evaluation of rubbercrete based on ultrasonic pulse velocity and rebound hammer tests, Constr. Build. Mater. 25 (2011) 1388-1397.

[2.22] K.B. Najim, M.R. Hall, Crumb rubber aggregate coatings/pre-treatments and their effects on interfacial bonding, air entrapment and fracture toughness in self-compacting rubberised concrete (SCRC), Mater. Struct. 46 (2013) 2029-2043.

[2.23] K.B. Najim, M.R. Hall, Mechanical and dynamic properties of self-compacting crumb rubber modified concrete, Constr. Build. Mater. 27 (2012) 521-530.

[2.24] F. Pelisser, N. Zavarise, T.A. Longo, A.M. Bernardin, Concrete made with recycled tire rubber: effect of alkaline activation and silica fume addition, J. Clean. Prod. 19 (2011) 757-763.

[2.25] G. Skripkiūnas, A. Grinys, B. Černius, Deformation properties of concrete with rubber waste additives, Mater. Sci.-Medzg. 13 (2007) 219-223.

[2.26] G. Skripkiūnas, A. Grinys, K. Miškinis, Damping properties of concrete with rubber waste additives, Mater. Sci.-Medzg. 15 (2009) 266-272.

[2.27] D.G. Snelson, J.M. Kinuthia, P.A. Davies, S.R. Chang, Sustainable construction: composite use of tyres and ash in concrete, Waste Manage. 29 (2009) 360-367.

[2.28] P. Sukontasukkul, Use of crumb rubber to improve thermal and sound properties of pre-cast concrete panel, Constr. Build. Mater. 23 (2009) 1084-1092.

[2.29] P. Sukontasukkul, C. Chaikaew, Properties of concrete pedestrian block mixed with crumb rubber, Constr. Build. Mater. 20 (2006) 450-457.

[2.30] İ.B. Topçu, Assessment of the brittleness index of rubberized concretes, Cem. Concr. Res. 27 (1997) 177-183.

[2.31] İ.B. Topçu, T. Bilir, Experimental investigation of some fresh and hardened properties of rubberized self-compacting concrete, Mater. Design 30 (2009) 3056-3065.

[2.32] M.C. Bignozzi, F. Sandrolini, Tyre rubber waste recycling in self-compacting concrete, Cem. Concr. Res. 36 (2006) 735-736.

[2.33] N. Ganesan, J. Bharati Raj, A.P. Shashikala, Flexural fatigue behavior of self compacting rubberized concrete, Constr. Build. Mater. 44 (2013) 7-14.

[2.34] M. Gesoğlu, E. Güneyisi, Permeability properties of self-compacting rubberized concretes, Constr. Build. Mater. 25 (2011) 3319-3326.

[2.35] E. Güneyisi, Fresh properties of self-compacting rubberized concrete incorporated with fly ash, Mater. Struct. 43 (2010) 1037-1048.

[2.36] M.M. Rahman, M. Usman, A.A. Al-Ghalib, Fundamental properties of rubber modified self-compacting concrete (RMSCC), Constr. Build. Mater. 36 (2012) 630-637.

[2.37] A. Turatsinze, M. Garros, On the modulus of elasticity and strain capacity of self-compacting concrete incorporating rubber aggregates, Resour. Conserv. Recy. 52 (2008) 1209-1215.

[2.38] W.H. Yung, L.C. Yung, L.H. Hua, A study of the durability properties of waste tire rubber applied to self-compacting concrete, Constr. Build. Mater. 41 (2013) 665-672.

[2.39] L. Li, W. Xie, F. Liu, Y. Guo, J. Deng, Fire performance of high-strength concrete reinforced with recycled rubber particles, Mag. Concr. Res. 63 (2011) 187-195.

[2.40] S. Wong, S. Ting, Use of recycled rubber tires in normal- and high-strength concretes, ACI Mater. J. 106 (2009) 325-332.

[2.41] W. Shen, L. Shan, T. Zhang, H. Ma, Z. Cai, H. Shi, Investigation on polymer-rubber aggregate modified porous concrete, Constr. Build. Mater. 38 (2013) 667-674.

[2.42] K. Jingfu, H. Chuncui, Z. Zhenli, Strength and shrinkage behaviors of roller-compacted concrete with rubber additives, Mater. Struct. 42 (2009) 1117-1124.

[2.43] A. Meddah, M. Beddar, A. Bali, Use of shredded rubber tire aggregates for roller compacted concrete pavement, J. Clean. Prod. 72 (2014) 187-192.

[2.44] M.A. Aiello, F. Leuzzi, Waste tyre rubberized concrete: properties at fresh and hardened state, Waste Manage. 30 (2010) 1696-1704.

[2.45] N. Al-Mutairi, F. Al-Rukaibi, A. Bufarsan, Effect of microsilica addition on compressive strength of rubberized concrete at elevated temperatures, J. Mater. Cycles Waste Manage. 12 (2010) 41-49.

[2.46] M.M. Al-Tayeb, B.H. Abu Bakar, H. Ismail, H.M. Akil, Effect of partial replacement of sand by recycled fine crumb rubber on the performance of hybrid rubberized-normal concrete under impact load: experiment and simulation, J. Clean. Prod. 59 (2013) 284-289.

[2.47] A.O. Atahan, U.K. Sevim, Testing and comparison of concrete barriers containing shredded waste tire chips, Mater. Lett. 62 (2008) 3754-3757.

[2.48] A.O. Atahan, A.Ö. Yücel, Crumb rubber in concrete: static and dynamic evaluation, Constr. Build. Mater. 36 (2012) 617-622.

[2.49] M.K. Batayneh, I. Marie, I. Asi, Promoting the use of crumb rubber concrete in developing countries, Waste Manage. 28 (2008) 2171-2176.

[2.50] M. Bravo, J. Brito, Concrete made with used tyre aggregate: durability-related performance, J. Clean. Prod. 25 (2012) 42-50.

[2.51] Q. Dong, B. Huang, X. Shu, Rubber modified concrete improved by chemically active coating and silane coupling agent, Constr. Build. Mater. 48 (2013) 116-123.

[2.52] N.N. Eldin, A.B. Senouci, Measurement and prediction of the strength of rubberized concrete, Cem. Concr. Comp. 16 (1994) 287-298.

[2.53] N.N. Eldin, A.B. Senouci, Observations on rubberized concrete behavior, Cem. Concr. Aggr. 15 (1993) 74-84.

[2.54] N.N. Eldin, A.B. Senouci, Rubber-tire particles as concrete aggregate, J. Mater. Civil Eng. 5 (1993) 478-496.

[2.55] M. Gesoğlu, E. Güneyisi, Strength development and chloride penetration in rubberized concretes with and without silica fume, Mater. Struct. 40 (2007) 953-964.

[2.56] M. Gesoğlu, E. Güneyisi, G. Khoshnaw, S. İpek, Abrasion and freezeing-thawing resistance of previous concretes containing waste rubbers, Constr. Build. Mater. 73 (2014) 19-24.

[2.57] M. Gesoğlu, E. Güneyisi, G. Khoshnaw, S. İpek, Investigating properties of previous concretes containing waste tire rubber, Constr. Build. Mater. 63 (2014) 206-213.

[2.58] E. Güneyisi, M. Gesoğlu, T. Özturan, Properties of rubberized concretes containing silica fume, Cem. Concr. Res. 34 (2004) 2309-2317.

[2.59] Y.C. Guo, J.H. Zhang, G. Chen, G.M. Chen, Z.H. Xie, Fracture behaviors of a new steel fiber reinforced recycled aggregate concrete with crumb rubber, Constr. Build. Mater. 53 (2014) 32-39.

[2.60] Y. Guo, J. Zhang, G. Chen, Z. Xie, Compressive behaviour of concrete structures incorporating recycled aggregates, rubber crumb and reinforced with steel fibre, subjected to elevated temperatures, J. Clean. Prod. 72 (2014) 193-203.

[2.61] T. Gupta, S. Chaudhary, R.K. Sharma, Assessment of mechanical and durability properties of concrete containing waste rubber tire as fine aggregate, Constr. Build. Mater. 73 (2014) 562-574.

[2.62] A.C. Ho, A. Turatsinze, R. Hameed, D.C. Vu, Effects of rubber aggregates from grinded used tyres on the concrete resistance to cracking, J. Clean. Prod. 23 (2012) 209-215.

[2.63] B. Huang, G. Li, S. Pang, J. Eggers, Investigation into waste tire rubber-filled concrete, J. Mater. Civil Eng. 16 (2004) 187-194.

[2.64] C.A. Issa, G. Salem, Utilization of recycled crumb rubber as fine aggregates in concrete mix design, Constr. Build. Mater. 42 (2013) 48-52.

[2.65] A.R. Khaloo, M. Dehestani, P. Rahmatabadi, Mechanical properties of concrete containing a high volume of tire-rubber particles, Waste Manage. 28 (2008) 2472-2482.

[2.66] Z.K. Khatib, F.M. Bayomy, Rubberized Portland cement concrete, J. Mater. Civil Eng. 11 (1999) 206-213.

[2.67] G. Li, G. Garrick, J. Eggers, C. Abadie, M.A. Stubblefield, S. Pang, Waste tire fibre modified concrete, Compos. Part B-Eng. 35 (2004) 305-312.

[2.68] G. Li, M.A. Stubblefield, G. Garrick, J. Eggers, C. Abadie, B. Huang, Development of waste tire modified concrete, Cem. Concr. Res. 34 (2004) 2283-2289.

[2.69] L. Li, S. Ruan, L. Zeng, Mechanical properties and constitutive equations of concrete containing a low volume of tire rubber particles, Constr. Build. Mater. 70 (2014) 291-308.

[2.70] T. Ling, Effects of compaction method and rubber content on the properties of concrete paving blocks, Constr. Build. Mater. 28 (2012) 164-175.

[2.71] T. Ling, Prediction of density and compressive strength for rubberized concrete blocks, Constr. Build. Mater. 25 (2011) 4303-4306.

[2.72] F. Liu, G. Chen, L. Li, Y. Guo, Study of impact performance of rubber reinforced concrete, Constr. Build. Mater. 36 (2012) 604-616.

[2.73] F. Liu, W. Zheng, L. Li, W. Feng, G. Ning, Mechanical and fatigue performance of rubber concrete, Constr. Build. Mater. 47 (2013) 711-719.

[2.74] I. Mohammadi, H. Khabbaz, K. Vessalas, In-depth assessment of crumb rubber concrete (CRC) prepared by water-soaking treatment method for rigid pavements, Constr. Build. Mater. 71 (2014) 456-471.

[2.75] B.S. Mohammed, Structural behavior and *m-k* value of composite slab utilizing concrete containing crumb rubber, Constr. Build. Mater. 24 (2010) 1214-1221.

[2.76] B.S. Mohammed, K.M. Anwar Hossain, J.T.E. Swee, G. Wong, M. Abdullahi, Properties of crumb rubber hollow concrete block, J. Clean. Prod. 23 (2012) 57-67.

[2.77] O. Onuaguluchi, D.K. Panesar, Hardened properties of concrete mixtures containing pre-coated crumb rubber and silica fume, J. Clean. Prod. 82 (2014) 125-131.

[2.78] E. Ozbay, M. Lachemi, U.K. Sevim, Compressive strength, abrasion resistance and energy absorption capacity of rubberized concretes with and without slag, Mater. Struct. 44 (2011) 1297-1307.

[2.79] M.M. Reda Taha, A.S. El-Diab, M.A. Abd El-Wahab, M.E. Abdel-Hameed, Mechanical, fracture, and microstructure investigations of rubber concrete, J. Mater. Civil Eng. 20 (2008) 640-649.

[2.80] H. Su, J. Yang, G.S. Ghataora, S. Dirar, Surface modified used rubber tyre aggregates: effect on recycled concrete performance, Mag. Concr. Res. 67 (2015) 680-691.

[2.81] H. Su, J. Yang, T. Ling, G.S. Ghataora, S. Dirar, Properties of concrete prepared with waste tyre rubber particles of uniform and varying sized, J. Clean. Prod. 91 (2015) 288-296.

[2.82] P. Sukontasukkul, K. Tiamlom, Expansion under water and drying shrinkage of rubberized concrete mixed with crumb rubber with different size, Constr. Build. Mater. 29 (2012) 520-526.

[2.83] B.S. Thomas, R.C. Gupta, P. Kalla, L. Cseteneyi, Strength, abrasion and permeation characteristics of cement concrete containing discarded rubber fine aggregates, Constr. Build. Mater. 59 (2014) 204-212.

[2.84] İ.B. Topçu, The properties of rubberized concretes, Cem. Concr. Res. 25 (1995) 304-310.

[2.85] İ.B. Topçu, A. Demir, Durability of rubberized mortar and concrete, J. Mater. Civil Eng. 19 (2007) 173-178.

[2.86] İ.B. Topçu, M. Sarıdemir, Prediction of rubberized concrete properties using artificial neural network and fuzzy logic, Constr. Build. Mater. 22 (2008) 532-540.

[2.87] H.A. Toutanji, The use of rubber tire particles in concrete to replace mineral aggregates, Cem. Concr. Comp. 18 (1996) 135-139.

[2.88] C. Wang, Y. Zhang, A. Ma, Investigation into the fatigue damage process of rubberized concrete and plain concrete by AE analysis, J. Mater. Civil Eng. 23 (2011) 953-960.

[2.89] J. Xue, M. Shinozuka, Rubberized concrete: a green structural material with enhanced energy-dissipation capability, Constr. Build. Mater. 42 (2013) 196-204.

[2.90] O. Youssf, M.A. ElGawady, J.E. Mills, X. Ma, An experimental investigation of crumb rubber concrete confined by fibre reinforced polymer tubes, Constr. Build. Mater. 53 (2014) 522-532.

[2.91] L. Zheng, X.S. Huo, Y.Yuan, Experimental investigation on dynamic properties of rubberized concrete, Constr. Build. Mater. 22 (2008) 939-947.

[2.92] L. Zheng, X.S. Huo, Y.Yuan, Strength, modulus of elasticity, and brittleness index of rubberized concrete, J. Mater. Civil Eng. 20 (2008) 692-699.

[2.93] N. Holmes, K. Dunne, J. O'Donnell, Longitudinal shear resistance of composite slabs containing crumb rubber in concrete toppings, Constr. Build. Mater. 55 (2014) 365-378.

[2.94] İ.B. Topçu, N. Avcular, Analysis of rubberized concrete as a composite material, Cem. Concr. Res. 27 (1997) 1135-1139.

[2.95] İ.B. Topçu, N. Avcular, Collision behaviours of rubberized concrete, Cem. Concr. Res. 27 (1997) 1893-1898.

[2.96] K.B. Najim, M.R. Hall, A review of the fresh/hardened properties and applications for plain- (PRC) and self-compacting rubberised concrete (SCRC), Constr. Build. Mater. 24 (2010) 2043-2051.

[2.97] B.Z. Savas, S. Ahmad, D. Fedroff, Freeze-thaw durability of concrete with ground waste tire rubber, Transport. Res. Rec. 1574 (1997) 80-88.

[2.98] A. Benazzouk, O. Douzane, T. Langlet, K. Mezreb, J.M. Roucoult, M. Quéneudec, Physico-mechanical properties and water absorption of cement composite containing shredded rubber wastes, Cem. Concr. Comp. 29 (2007) 732-740.

[2.99] D.G. Goulias, A.H. Ali, Non-destructive evaluation of rubber modified concrete, Proceedings of a special conference, ASCE, New York, USA, 1997, pp. 111-120.

[2.100] N.H. Malik, A.A.Al-Arainy, M.I. Qureshi, Electrical Insulation in Power System, CRC Press, Florida, USA, 1997.

[2.101] H. Zhu, N. Thong-On, X. Zhang, Adding crumb rubber into exterior wall materials, Waste Manage. Res. 20 (2002) 407-413.

[2.102] C.E. Pierce, M.C. Blackwell, Potential of scrap tire rubber as lightweight aggregate in flowable fill, Waste Manage. 23 (2003) 197-208.

[2.103] X. Shu, B. Huang, Recycling of waste tire rubber in asphalt and portland cement concrete: An overview, Constr. Build. Mater. 67 (2014) 217-224.

[2.104] N. Segre, I. Joekes, Use of tire rubber particles as addition to cement paste, Cem. Concr. Res. 30 (2000) 1421-1425.

[2.105] L.H. Chou, C.N. Lin, C.K. Lu, C.H. Lee, M.T. Lee, Improving rubber concrete by waste organic sulphur compounds, Waste Manage. Res. 28 (2010) 29-35.

[2.106] P.K. Mehta, P.J.M. Monteiro, Microstructures, Properties, and Materials. McGraw-Hill, USA, 2013.

CHAPTER 3

PROPERTIES OF CONCRETE PREPARED WITH WASTE TYRE RUBBER PARTICLES OF UNIFORM AND VARYING SIZESD

3.1 Introduction

Waste tyres have presented a pressing global issue for the environment, as a result of a growing use of road transport vehicles. Discarded waste tyres often create 'black pollution' because they are not readily biodegradable and pose a potential threat to the environment [3.1]. Several means of reusing or recycling tyre rubber have been proposed, including the use of lightweight fill in the asphalt pavement, fuel for cement kilns, the feedstock for making carbon black, and the artificial reefs in marine environments [3.2], [3.3]. However, some of these proposals are economically or environmentally unviable.

In the past twenty years, many attempts have been made to utilise recycled waste tyre rubber as an aggregate substitute in concrete. Together with other recycled aggregates, such as recycled concrete [3.4], [3.5], and recycled glass [3.6], [3.7], the recycling of scrap tyres has become a viable option for sustainable construction. A great number of applications have been reported on the use of waste rubber aggregate since an early study [3.8]. Most researchers have confirmed that there is a decrease in compressive strength and an increase in ductility with an increasing proportion of rubber phase in the mixture [3.9]. To the authors' best knowledge, limited research work studies the effect of the size of rubber particles as fine aggregate on the properties of resulting concrete, such as workability, strength and durability,

as indicated by the literature review [3.8], [3.10]-[3.15]. Furthermore, the conclusions from the reported studies are quite inconsistent due to the wide variations in the reported results.

In an early study, Eldin and Senouci [3.8] reported that there was around 85% reduction in compressive strength and a 50% reduction in tensile strength when the coarse aggregates were fully replaced by coarse rubber chips. On the other hand, when fine aggregates were fully replaced by fine rubber, specimens lost up to 65% and 50% of their compressive strength and tensile strength respectively. Topçu [3.15] reported the decrease of about 50% in the cylinder and cube compressive strength, and of 64% in the tensile strength in the concrete mixed with fine rubber particles. Introducing coarse rubber particles reduced the cylinder and cube compressive strengths by nearly 60% to 80%, and the tensile strength by nearly 74%. These results indicate that the coarse rubber aggregates have a more significant negative effect than the fine rubber aggregates. However, the results of tests carried out by Fattuhi and Clark [3.12] indicated the opposite trend. They found that adding graded fine rubber granules lowered the compressive strength of concrete more than the graded coarse granules. This was in agreement with Goulias and Ali [3.11], but not with the findings of Eldin and Senouci [3.8] or Topçu [3.15].

In a recent study, Li et al. [3.14] reported that using rubber particle sizes between 0.25 and 1 mm has less effect on the splitting tensile strength than on the compressive strength, and finer rubber was particularly beneficial for reducing the splitting tensile strength loss. These results partially disagree with the findings of Albano et al. [3.10] who found that a decrease in the rubber particle size from 0.59 mm to 0.29 mm resulted in a lower workability and density at the fresh stage, as well as the weaker compressive and splitting tensile strengths at the dry

stage. It is difficult to directly compare the results from various resources, as the nature of the raw materials, test specimens and test methods were different. Hence, there remains a need to carry out further studies.

The aim of this study is to further the understanding of the effects of rubber particle size on the properties of concrete. To this end, three types of rubber particle samples with singly-sized rubber particles (3 mm, 0.5 mm and 0.3 mm), and a fourth with rubber particles of varying sizes were used as part of the fine aggregate in concrete. A series of tests, including workability and density at the fresh stage, the cube compressive strength, the splitting tensile strength, the flexural strength and water permeability at the hardened stage were conducted according to relevant standards. Test results were analyzed and discussed, leading to the conclusions informing the tyre recycling industry to rationally design the PSD of rubber particles as the recycled aggregates.

3.2 Preparation of concrete

3.2.1 Materials

The materials used for preparing the test specimens comprised cement, water, coarse aggregate, fine aggregate and different sizes of rubber particles.

3.2.1.1 Cement

Ordinary Portland cement with a characteristic strength of 42.5 MPa was used in accordance with BS EN 197-1 [3.16]. This cement contains 30% of pulverised fly ash which was taken

into account in the mix design process and 70% of pure cement by mass. It was stored in airtight packages before use.

3.2.1.2 Water

Tap water that is reasonably free from contamination in the laboratory was used to hydrate the cement in the mixtures.

3.2.1.3 Coarse aggregate

Crushed gravels with a nominal maximum size of 10 mm were used as the coarse aggregate. Water absorption of the coarse aggregates used in this study under SSD condition was measured by immersion in water for 24 hours, followed by removing excess surface water with wet cloth after they were moved out of water. At the time when there was no free water on the surface, aggregates were assumed to be under the SSD condition. The sampled aggregates with saturated water under the surface-dried condition were weighed and recorded as m_{SSD}. After 24 hours oven-drying at a temperature of 105ºC, aggregates were weighed and recorded as m_{OD}. The SSD water absorption was calculated by the formula of (m_{SSD} - m_{OD})/m_{OD}. The volume of the sampled aggregates under the SSD condition was measured by using the water displacement method and recorded as v_{SSD}. The SSD density of gravels was calculated by the formula of m_{SSD}/v_{SSD}. The results of SSD water absorption and SSD density of gravels are presented in Table 3-1.

Table 3-1. SSD density and SSD water absorption of natural and rubber aggregates.

Item	Sand	Gravel	RA	RB	RC	CSR
SSD density (kg/m^3)	2512	2581	1111	909	909	973
SSD water absorption (%)	1.37	1.26	4.49	10.70	10.09	8.46

3.2.1.4 Fine aggregates

Natural river sand with a maximum particle size of 5 mm was used as the fine aggregate. The procedures for measuring the sand's SSD water absorption and SSD density were the same as those for gravels, and results are presented in Table 3-1. A sieve analysis test was carried out in accordance with BS EN 933-1 [3.17]. As shown in Figure 3-1, the sand used in this study presented continuous grading.

Three different granular samples of waste tyre rubber particles, RA (cut to 3 mm), RB (ground to 0.5 mm) and RC (ground to 0.3 mm) without any treatment or contaminants, sourced from a local recycling plant, were used to replace part of the fine aggregate. CSR with continuous grading was achieved by blending RA, RB and RC manually. Sieve analysis tests were carried out and the grading curve of each sample is shown in Figure 3-1. RA, RB and RC were of relatively singly-sized, while the PSD of CSR was similar to sand with varying sizes. SSD water absorption and SSD density of rubber particles were also measured. However, rubber particles were found to float in water. To overcome this problem, a tightly woven fabric was used to wrap rubber particles. The wrapped rubber particles were submerged in a water filled bucket, followed by gentle shaking within the water to release as much trapped air as possible until it easily sank to the bottom of the bucket. Other procedures

for measurements were the same as those for measuring coarse and fine aggregates. The results of SSD water absorption and SSD density of rubber particles are shown in Table 3-1.

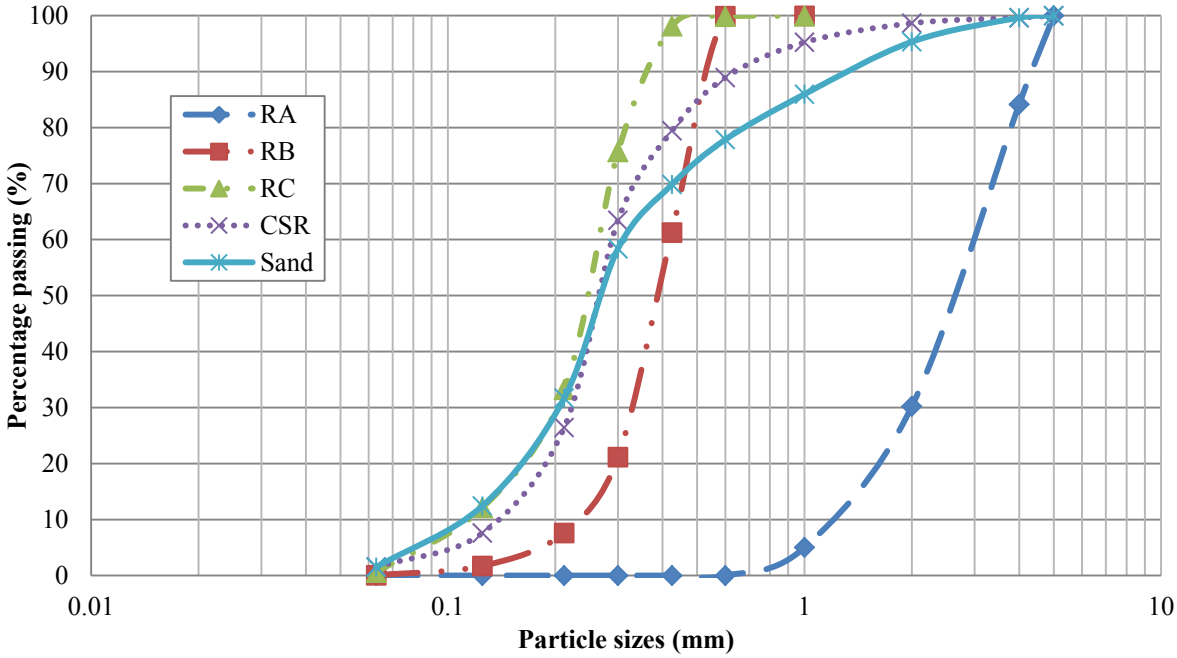

Figure 3-1. Grading curves of sand and rubber particles.

3.2.2 Mix design

Concrete mix design was undertaken by using the method documented in the 'Design of Normal Concrete Mixes' [3.18] published by the Building Research Establishment. This design method is based on the determination of the material proportions. The mix design of the reference concrete in this chapter aimed to achieve a target mean strength of 53 MPa (often referred to grade C40/50) at 28 days with a slump value of 60 – 180 mm. A w/c ratio of 0.37 was determined according to the target mean strength, the cement strength class and the type of aggregates. The amount of free water used to achieve the designed w/c ratio was determined according to the desired slump, the maximum size and the type of aggregate.

Cement content was calculated by the values of w/c ratio and the amount of free water. Different sizes of rubber aggregates were used to replace 20% of the fine aggregates by volume. The amount of coarse, fine and rubber aggregates of each concrete mixture were calculated. Five concrete mixtures were produced to study the effect of rubber particle sizes and their distribution: REF, CRA20, CRB20, CRC20 and CCSR20. All mix design parameters were kept constant throughout the experimental programme except for the fine aggregate constituent. The mixture proportions are presented in Table 3-2.

Table 3-2. Mix proportions of concrete.

Notation	Water	Cement	Sand	Gravel	Rubber
REF	234	632	519	1013	0
CRA20	232	627	416	1005	46
CRB20	230	621	410	996	37
CRC20	230	621	410	996	37
CCSR20	232	627	414	1002	40

* The values of sand, gravel and rubber are under SSD condition and the unit is kg/m^3.

3.2.3 Preparation of test specimens

3.2.3.1 Mixing

All types of aggregates were prepared under the SSD condition before mixing. The desired quantities of each item was accurately measured out and added in the following order: coarse aggregate, fine aggregate, cement and rubber aggregate in a mechanical mixer which had been inter-surface wetted. Prior to the addition of water, mixer was turned on and materials

were blended for 5 min to achieve a thorough mix. Then half of water was added into the mixer for another 5 min blending. It was then followed by the other half of water. The mechanical mixer was stopped when the mixture of ingredients appeared consistent.

3.2.3.2 Sampling

The mould shape and dimensions were: 100 mm cube, cylinder 100 mm in diameter and 200 mm in length, and 100 × 100 × 500 mm prism. Prior to pouring, the inner surfaces of the moulds were coated with a thin film of oil to prevent the concrete from adhering to the mould. All moulds were filled with fresh concrete in two equal layers, each of which was compacted using the vibrating table to remove as much air as possible. Vibration was continued for 30 s to ensure a smooth and even surface film, followed by trowelling the exposed surface to a clean finish.

3.2.3.3 Curing

Polythene sheeting was placed over the samples after casting to prevent moisture loss. After 24 h at the ambient laboratory temperature of 20ºC, the samples were carefully removed from the moulds, labelled with their IDs. The samples were then transferred to the water tank with a temperature of 20ºC, where they will cure until test age.

3.3 Experimental tests, results and discussion

3.3.1 Workability

To evaluate workability of fresh concrete, slump was measured according to BS EN 12350-2 [3.19]. The slump cone and the base plate were dampened before being placed on a horizontal surface. The mould was filled with a fresh concrete mixture in three layers, each approximately one-third of the height of mould when compacted. Each layer was compacted with 25 strokes of the tamping rod. After the top layer was compacted, the surface of the fresh concrete was struck off by means of a sawing and rolling motion with the compacting rod. Then the mould was removed from the concrete by a steady upward lift in a vertical direction with no lateral or torsional motion being imparted to the concrete. Immediately after removal of the slump cone, slump was measured and recorded by determining the difference between the height of the mould and that of the highest point of the mixture (Figure 3-2).

Figure 3-2. Typical slumped test mixture.

All the concrete mixtures were observed by visual inspection to be cohesive with no segregation or bleeding during the mixing, placing or compaction. Figure 3-3 shows the slump values obtained for all the concrete mixtures with and without the inclusion of rubber particles. The highest slump value of 95 mm was recorded for REF. The CRA20, CRB20, CRC20 and CCSR20 mixtures had slump values of 16.8% (16 mm), 23.2% (22 mm), 25.2% (24 mm) and 13.7% (13 mm) lower than that of REF. It can be implied from this result that there was a general reduction in slump values when rubber particles were used to replace sand, regardless of their particle size. This is mainly ascribed to the higher water absorption by the rubber particles compared to that of sand (see Table 3-1), which reduces the free water, thus making the overall concrete mixture less workable.

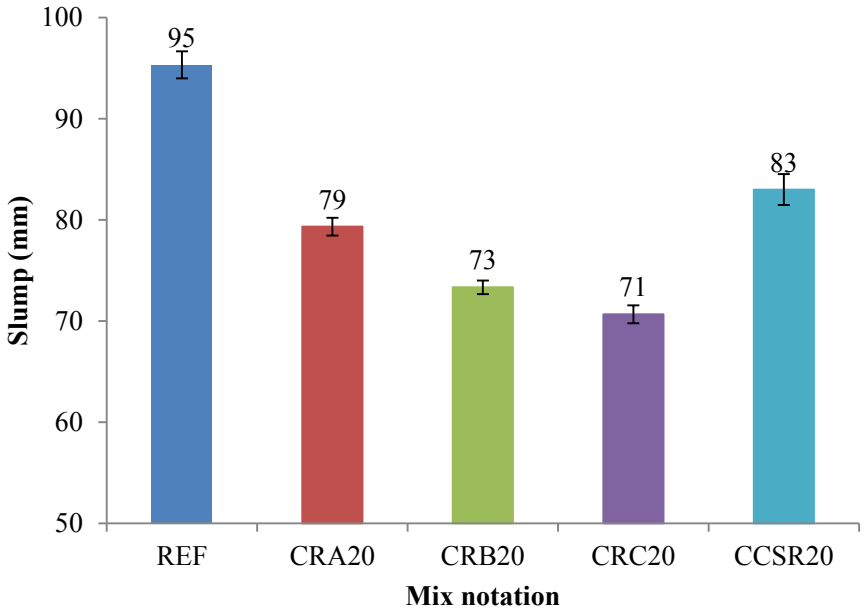

Figure 3-3. Slump of all the mixes.

Also, it was observed that there was a decrease in slump as the rubber particle size was decreased. The slump of CRA20 with the largest rubber particle size was recorded as 79 mm. When the rubber particle size decreased from 3 mm (RA) to 0.5 mm (RB), the slump of

CRB20 was 73 mm. When the rubber particle size was further reduced to 0.3 mm (RC), the slump of CRC20 continued to drop to 71 mm, which is the lowest of all the samples. This is due to the higher surface area and water absorption of the finer rubber particles. From Table 3-1, it can be seen that the SSD water absorption of the finer rubber particles, RB and RC, are 10.70% and 10.09%, which is higher than the larger rubber particles RA (4.49%). This means that during the mixing, the finer rubber particles will absorb more free water than the larger rubber particles to achieve the SSD condition. Therefore, the slump of CRB20 and CRC20 with less free water is lower than that of CRA20. Another reason may be that the surface of the finer rubber particle is rougher than the larger one. During the waste tyre treatment process, tyres are cut into small pieces before being thrown into a grinding mill. The grinding process is then carried out for a certain length of time before the different sized rubber particles are sieved and packed. Figure 3-4 show the surface of the different sized rubber particles. It can be seen clearly that there are some dents and jagged areas on the surfaces of the RB and RC samples. The surface of RA is much smoother than that of RB and RC. Moreover, the larger surface area of the finer particles produces more frictional resistance to the flowing movement of fresh concrete. Figure 3-3 also shows that the drop of slump for the CCSR20 mixture (13 mm) is lower than those of the other rubber concrete samples. This is due to the fact that the grading of the rubber particles affects the packing density of aggregates. The cement paste required to fill in the voids in the aggregate skeleton is reduced for the better packed aggregates and hence more cement paste can provide lubrication and hence increase the workability. In this case, the combined rubber particles (CCSR20) have a better packing density than those singly-sized samples, and hence show a better workability. Aggregates that do not have a large deficiency or excess of any particular size produce the most workable and economical concrete mixtures [3.20].

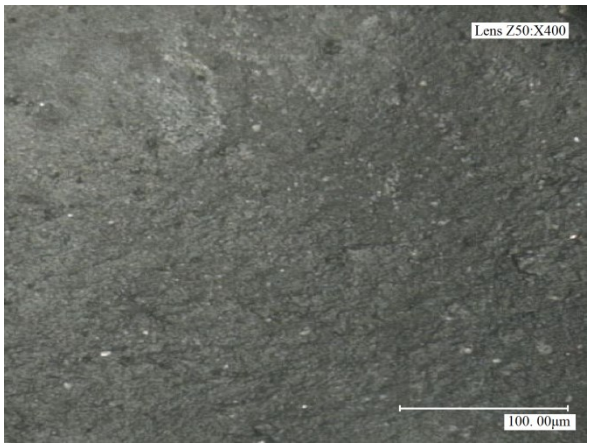

(a). Surface of RA.

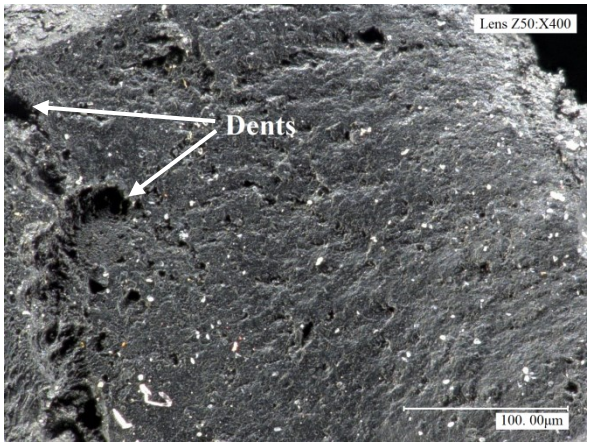

(b). Surface of RB.

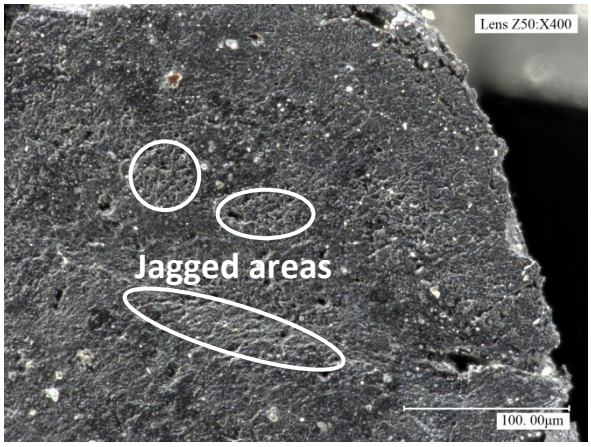

(c). Surface of RC.

Figure 3-4. Surfaces of different sizes of rubber particles.

3.3.2 Fresh density

The density test for fresh concrete was carried out in accordance with BS EN 12350-6 [3.21]. A container of known volume v_c was weighed to determine its mass and the value was recorded as m_{ec}. The container was then filled with fresh concrete in two layers, each approximately half of the height of the container. Each layer was then compacted immediately after placing it in the container by applying vibration by a vibrating table for the

minimum duration necessary to achieve full compaction of the concrete with neither excessive segregation nor laitance. After the top layer was compacted, the surface was skimmed to be smooth using a trowel and the outside of the container was wiped clean. The container with its contents was re-weighed to determine its mass and the value was recorded as m_{fc}. The fresh density was calculated using the formula of $(m_{fc} - m_{ec})/v_c$.

The fresh density test results for all the samples are shown in Figure 3-5. Irrespective of the rubber particle size used, a clear reduction in the concrete fresh density was observed with the incorporation of rubber aggregates. This is mainly due to the differences in the density of rubber aggregates. However, the rubber particles with different sizes have resulted in differing reductions in the concrete fresh density. The percentage decrease in density for CRA20, CRB20, CRC20 and CCSR20 were 3.1%, 3.9%, 3.8%, and 3.5%, as compared to REF. The reduction in the fresh density of the concrete with the RA aggregate was the smallest, while the CSR, RB and RC aggregates showed a slightly higher level of reduction. This is in agreement with the original density values of the rubber aggregates, where RA possesses a relatively higher density (1111 kg/m^3) than CSR (973 kg/m^3), RB and RC (909 kg/m^3). A similar observation on the density of rubber concrete was reported by Siddique and Naik [3.22]. They suggested that the non-polar nature of rubber particles may result in the ability to repel water and entrap air on the rubber surface, which would subsequently increase the number of air voids and thus decrease the concrete density. As the rubber content was limited to 20% in this study, the extent of differences among the concrete mixes was not significant.

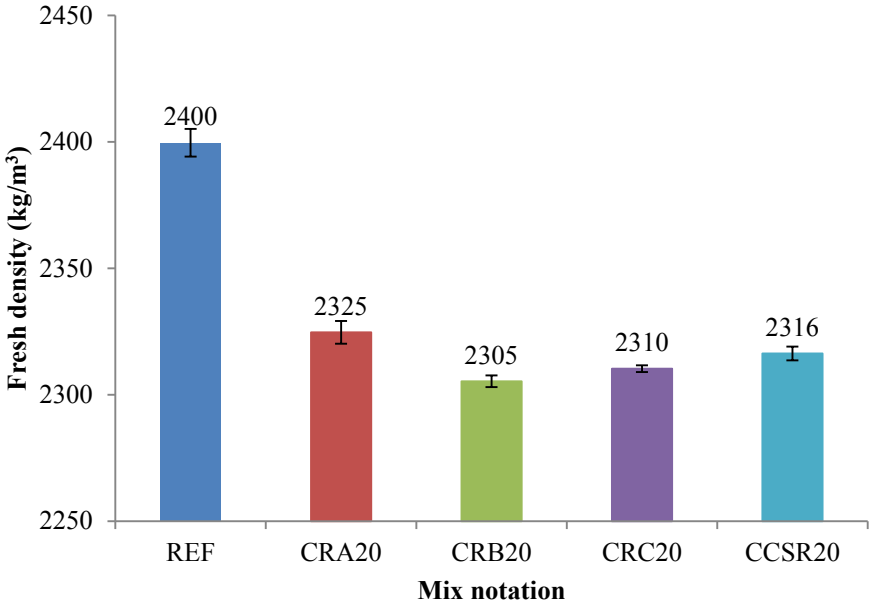

Figure 3-5. Fresh density of all the mixes.

3.3.3 Compressive strength

The 28 days compressive strength of hardened concrete was tested according to BS EN 12390-3 [3.23]. The excess moisture from the surface of the cube specimens was wiped before testing. Specimens were then positioned at the centre of the loading plate in a Denison testing machine, with two non-trowelled surfaces contacted with the loading platens so that a uniform loading can be achieved. Once the test was started, uniaxial compression was applied continuously at a constant rate of 0.6 MPa/s. When the sample failed, the value indicated was recorded, and the mean of three samples was taken as the final result.

Replacing the natural river sand with the relatively soft rubber aggregate is expected to reduce the concrete compressive strength. This was confirmed by the test results of the 28 days cube compressive strength test results, as shown in Figure 3-6. The compressive

strength of CRA20, CRB20, CRC20 and CCSR20 decreased by approximately 10.6%, 9.6%, 9.5% and 9.8% as compared to that of the REF (61.1 MPa). This can be attributed to the low stiffness and poor surface texture of the rubber particles that resulted in an inconsistency of the concrete mix, and the lack of bonding between the rubber particles and the surrounding cement paste, leading to a loss of compressive strength [3.8]. A similar decrease in strength with the use of rubber particles in concrete was reported by Guo et al. [3.24] and Li et al. [3.14]. However, all the rubber concretes investigated in this study had a compressive strength higher than the target mean strength of 53 MPa.

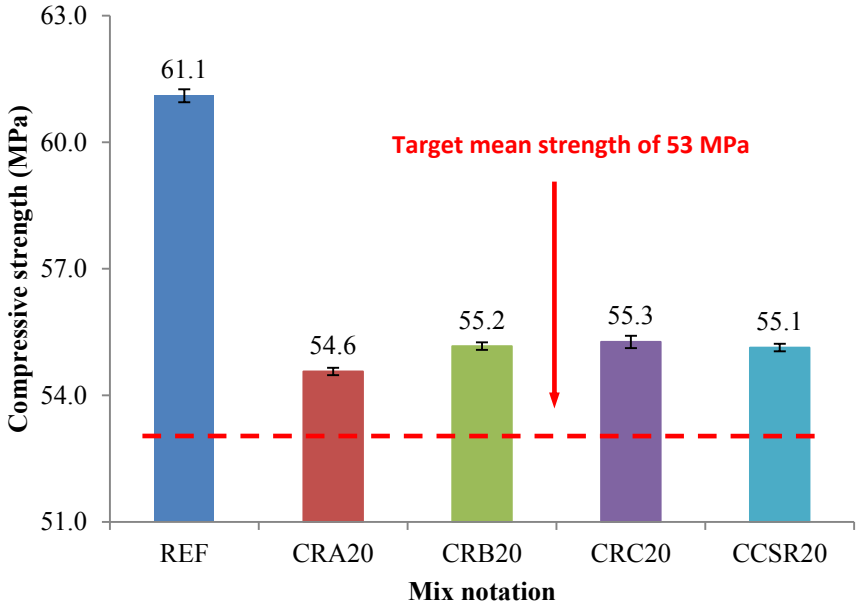

Figure 3-6. 28 days compressive strength of all the mixes.

Figure 3-6 shows that the 28 day cube compressive strengths of CRA20, CRB20 and CRC20 were 54.6 MPa, 55.2 MPa and 55.3 MPa. This indicates that the compressive strength of the concrete increased modestly with a decrease in the rubber particle size. This is because the finer rubber particles have a better voids-filling ability, resulting in low void space and leading to higher compressive strength. Also, because the failure of concrete samples is

primarily caused by debonding between the aggregates and the cement paste, the bond plays a significant role in determining the concrete strength. As reported in Section 3.3.1, RA presents a smoother surface than RB or RC, which results into a weaker bond between the rubber aggregates and the surrounding cement paste. To support this argument, a series of microscopic inspections of the crushed samples were carried out using scanning optical microscopy. The rubber-matrix interfaces were inspected in 10 crushed concrete particles from each sample. To demonstrate the difference in the interfacial behaviour, the micrographs of the fracture surfaces of CRA20 and CRC20 are presented in Figure 3-7. As shown in Figure 3-7(a) and 3-7(b), a clear discontinuity can be found along boundary lines I and II. There is a distinct groove along line II, which indicates that the adhesion between the rubber particle and the concrete matrix is poor, leading to a lower compressive strength of CRA20. In contrast, in the micrograph of CRC20 (see Figure 3-7(c)), a well-developed adhesive interfacial zone is observed between the fine rubber particle and the concrete matrix. From its 3D image shown in Figure 3-7(d), it can be seen that the transition zone between the rubber particle and the concrete matrix is smooth; whereas for CRA20 a clear trough can be observed along line II, as shown in Figure 3-7(b). This observation suggests that there is a relatively stronger bond at the interface between the finer rubber particles and the concrete matrix. Owing to the continuous grading, the CSR aggregate should have a filler effect to improve particle packing in concrete, thereby reducing the strength loss. However, the results shown in Figure 3-6 reveal that CCSR20 gained a similar strength to those of CRB20 and CRC20, which was slightly higher than that of CRA20. This observation suggests that the negative effect of the rubber surface on the compressive strength overweighs the positive filler effect of PSD, but to a minor extent.

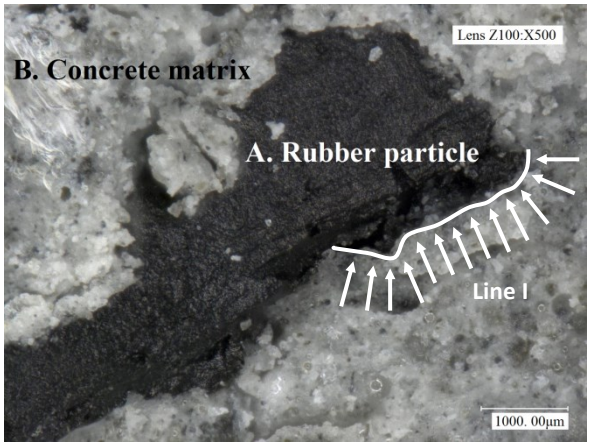

(a). Rubber-matrix interface of CRA20 (I).

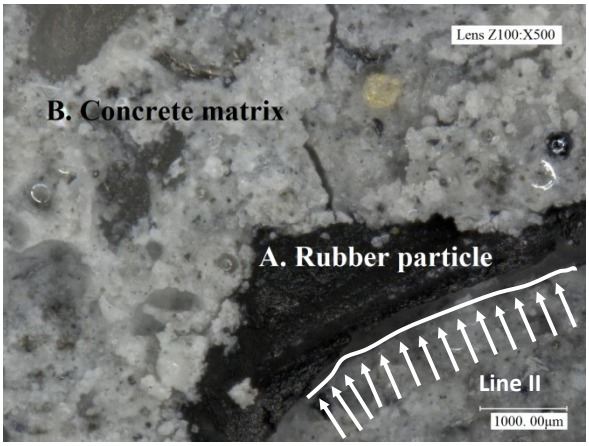

(b). Rubber-matrix interface of CRA20 (II).

(c). Rubber-matrix interface of CRC20.

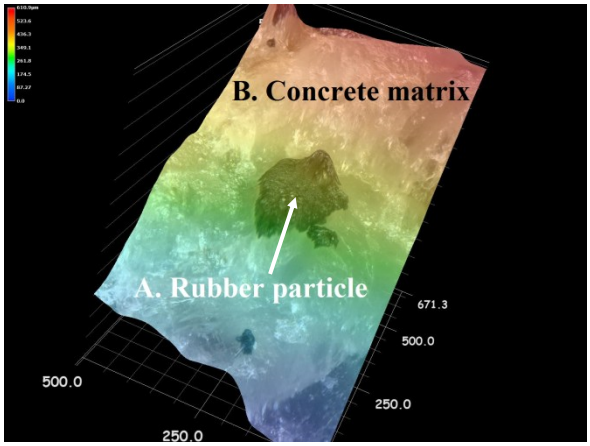

(d). 3D image of rubber-matrix interface of CRC20.

Figure 3-7. Micrographs of rubber-matrix interface.

3.3.4 Splitting tensile and flexural strength

Tests on the splitting tensile strength and the flexural strength of hardened concrete at 28 days after casting were conducted in conformity with BS EN 12390-6 [3.25] and BS EN 12390-5 [3.26], respectively. The excess moisture from the surface of the specimen was wiped before testing in a Denison strength testing machine. In the splitting tensile strength test, the concrete cylinder specimen was placed horizontally in a frame with two hardboard packing

strips positioned along the top and bottom of the specimen between the metal plate and the concrete. Continuous loading was applied by a compression platen to a narrow region of the cylinder along its length at a constant rate of 0.05 MPa/s. When the sample failed, the loading value was recorded and the mean of three samples was calculated. In measuring the flexural strength, the concrete beam specimen was positioned so that it would be simply supported on two lower rollers at a spacing of 300 mm. Continuous loading was applied by two upper rollers (at a spacing of 100 mm) to the centre of a non-trowelled specimen face at a constant rate of 0.05 MPa/s. When the sample failed, the loading value was recorded and the mean of three samples was calculated.

The results of the 28 days splitting tensile and flexural strengths tests are shown in Figure 3-8. As in the case of compressive strength, the inclusion of rubber particles decreases both the splitting tensile and the flexural strengths. These results are in line with the work reported by Toutanji [3.27] on the influence of rubber particles on the properties of concrete, which showed that there was a decrease of about 7.9% in the flexural strength with the inclusion of 25% rubber aggregate as the natural aggregate replacement. The current investigation shows that when 20% of the fine aggregate was substituted with the rubber aggregate, there was a decrease in flexural strength of approximately 12.8%, 11.3% and 10.9% for CRA20, CRB20 and CRC20. In a similar trend, there were reductions of 11.1%, 8.3% and 6.9% in the tensile-splitting strength for CRA20, CRB20 and CRC20. It can be further deduced that the smaller the size of the rubber particles, the less the strength loss. The reason for this is similar to that for the compressive strength, as the smaller rubber particles may have a filler effect to increase the compactness of the concrete, and to reduce the level of stress singularity arising at the internal voids, and consequently reduce the likelihood of fracture. This also explains

the fact that the particle size has a greater effect on reducing the splitting tensile strength and the flexural strength than on the compressive strength. Splitting tensile and flexural strengths of 3.32 MPa and 6.14 MPa were recorded for CCSR20. It can be seen from these results that incorporating various sized rubber particles does not significantly affect the splitting tensile and flexural strengths of concrete compared to singlysized crumb rubber. In fact, the reduction effect for CCSR20 is between the bounds formed by the single rubber particle. Thus it can be inferred that incorporating well-graded rubber particles into the concrete does not affect the splitting tensile strength or the flexural strength significantly.

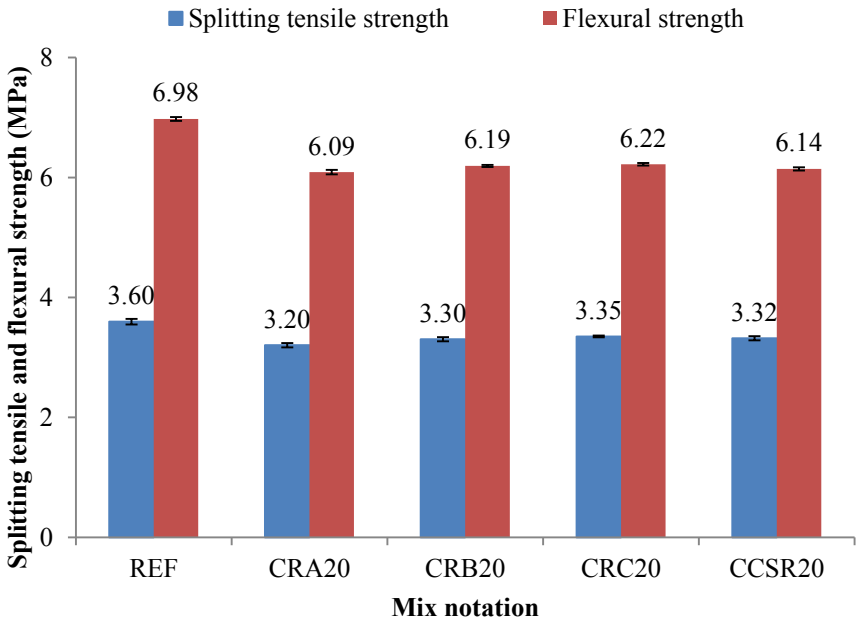

Figure 3-8. 28 days splitting tensile and flexural strengths of all the mixes.

3.3.5 Water permeability

A water permeability test was performed using the Autoclam test equipment as shown in Figure 3-9. This was performed as a modified version of BS 1881-208 [3.28]. 100 mm cube specimens were preconditioned (by being left in the lab for one week) to remove as much

moisture as possible before the water permeability test was undertaken. Prior to testing, it was ensured that the water reservoir was completely full. A metal ring with an internal diameter of 50 mm was attached (using an adhesive) to the surface of the specimen, and then the Autoclam was clamped onto the ring using bolts. The equipment was then switched on and the water was allowed to be drawn into the Autoclam. Finally, the cumulative flow of water into the concrete at a pressure of 500 mbar was recorded every minute for duration of 15 min.

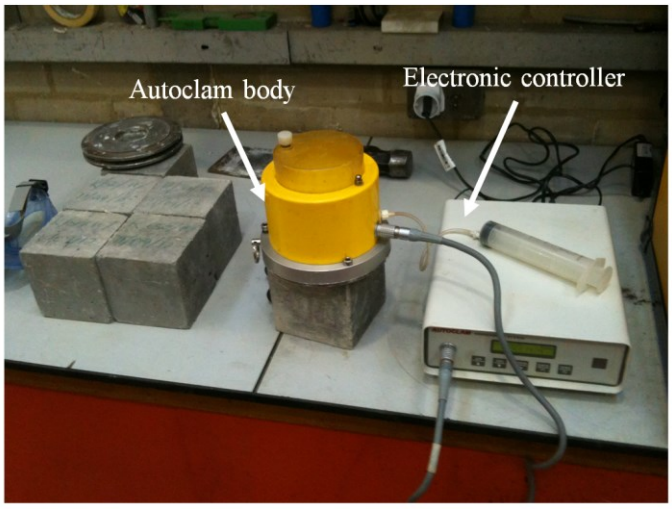

Figure 3-9. Apparatus for water permeability test.

Figure 3-10 shows the volume of water plotted against the square root of time according to the recommendations of The Concrete Society [3.29]. A regression equation for each specimen was determined, and the gradients of the lines between the 5th and 15th reading, which is known as the water permeability index, are shown in Table 3-3. Another two repeated testing on two separate samples were conducted and the mean of the results are shown in Figure 3-11. It was found that the increase in the permeability index for CRA20, CRB20, CRC20 and CCSR20 were 3.09, 1.42, 1.39 and 1.25 times the permeability index of REF. This means that the water permeability resistance of concrete is generally weakened

when rubber is incorporated. This observed behaviour is similar to that reported by other researchers [3.9], [3.30], [3.31]. It can be directly attributed to the increased porosity of rubber concrete. Because the lightweight crumb rubber tends to float in the wet mixture, this, coupled with its elastic behaviour under the compact condition, leads to the poorly compacted concrete containing more voids [3.32].

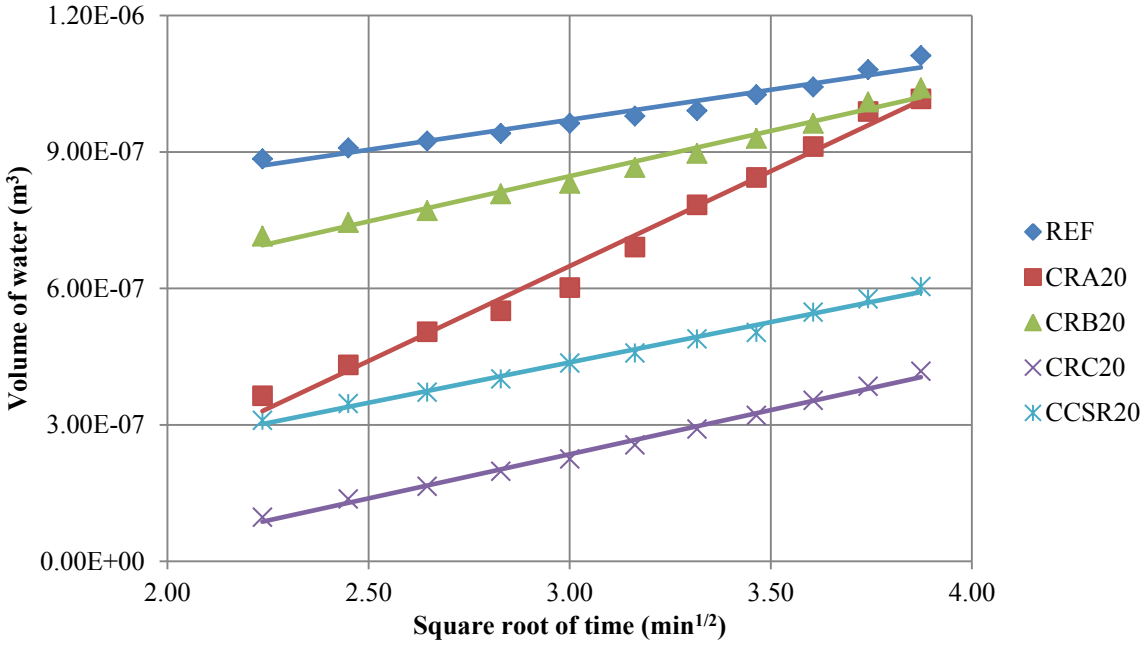

Figure 3-10. Volume of water flowing into specimen with time.

Table 3-3. Regression equations and index of water permeability of the tested mixes.

Samples	Regression equation	R-squared	Water permeability index ($\times 10^{-7}$ $m^3/\sqrt{min}$)
REF	$y = 1.32 \times 10^{-7}\chi + 5.76 \times 10^{-7}$	0.9614	1.32
CRA20	$y = 4.17 \times 10^{-7}\chi - 6.03 \times 10^{-7}$	0.9884	4.17
CRB20	$y = 1.99 \times 10^{-7}\chi + 2.50 \times 10^{-7}$	0.9840	1.99
CRC20	$y = 1.94 \times 10^{-7}\chi - 3.46 \times 10^{-7}$	0.9939	1.94
CCSR20	$y = 1.77 \times 10^{-7}\chi - 9.43 \times 10^{-8}$	0.9919	1.77

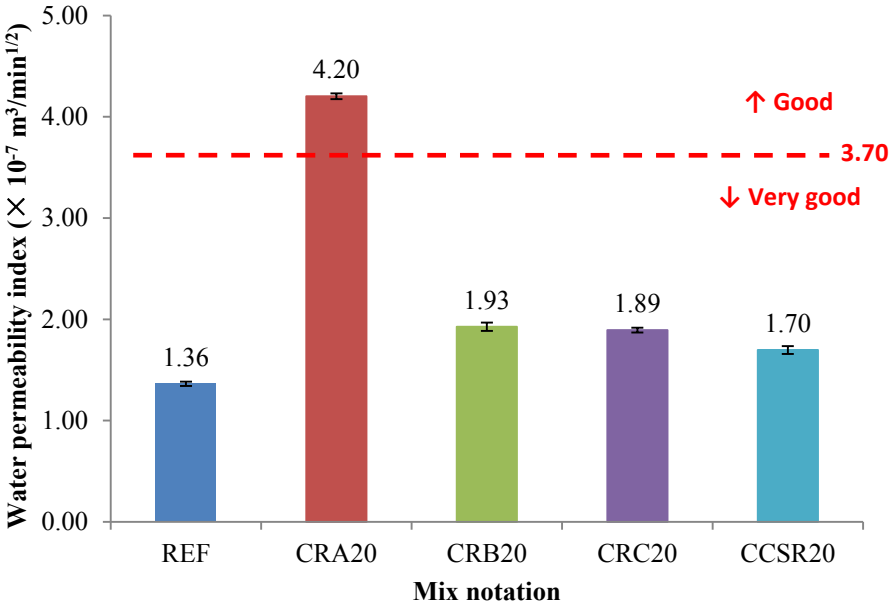

Figure 3-11. Water permeability indices of the mixes.

Two observations can be made from the test results presented in this section. Firstly, water permeability decreases with a decrease in rubber particle size. This may be due to the fact that when sand is partly replaced by large rubber particles (3 mm in this study), the resulting concrete (CRA20) cannot be as dense as concretes containing smaller or well-graded rubber particles (CRB20, CRC20 and CCSR20), resulting in more micro-conduits for water to travel through. Secondly, the resistance to water permeability of the concrete with CSR aggregate is higher than those with RA, RB and RC aggregates. This phenomenon is attributable to the PSD of CSR. Aggregate grading has a considerable effect on the voids structure of a concrete mixture [3.20]. Rubber particles with different sizes make the concrete more compact because the finer rubber particles fill the gaps formed by the larger ones. As a result, the number of conduits through which the water can transport is reduced. In comparison with the established values of the water permeability index classification shown in Table 3-4, it was found that, except for CRA20, all other mixes attained a 'very good' protective quality. Of all the concrete samples with rubber, the index of CCSR20 is the lowest, with a value of 1.70 ×

10^{-7} $m^3/\sqrt{min}$, which is less than the recommended value of 3.7×10^{-7} $m^3/\sqrt{min}$. Therefore, it can be concluded that CSR is preferred with respect to the performance of water permeability.

Table 3-4. Water permeability index of protective quality [3.29].

Protective quality	Water permeability index ($\times 10^{-7}$ $m^3/\sqrt{min}$)
Very good	≤3.70
Good	3.70 – 9.40
Poor	9.40 – 13.80
Very poor	>13.80

3.4 Summary

Workability, fresh density, compressive strength, splitting tensile strength, flexural strength and water permeability of concrete with different rubber particle sizes were studied and compared in this chapter. From the results of the experimental study, the main conclusions can be summarised that using different sizes of rubber particles in concrete as part of the fine aggregates affects the workability and water permeability considerably more than the fresh density and concrete strengths. Concrete specimens prepared with the larger rubber particles show a better workability than those with finer ones. Conversely, concrete with the finer rubber particles has a better performance in strengths and water permeability than those with the larger rubber particles. Varying sized rubber aggregates with continuous grading offer better workability and resistance to water permeability compared to the singly-sized rubber particles. In terms of the strength of concrete, the varying sized rubber performed similar to the finer rubber particles in the tests when added to the concrete mix.

The findings of this chapter can potentially be beneficial to the tyre recycling industry in designing the particle size distribution of rubber particles used for recycled aggregates. For example, rubber particles with well-graded sizes are preferred when high workability and water permeability resistance in rubber concrete are required. In engineering practice, the desired grading of rubber particles can be prepared at the waste tyre recycling and processing plant, which may save some time and capital cost. Furthermore, the dynamic performance of rubber concrete products is likely to be important. With a highly resilient nature, rubber particles of different sizes have a more positive effect on the dynamic performance when included in concrete. Research into the fatigue property and the ductility behaviour of concrete with rubber particles of combined sizes is studied in Chapter 6.

References

[3.1] M. Nehdi, A. Khan, Cementitious composites containing recycled tire rubber: an overview of engineering properties and potential application, Cem. Concr. Aggr. 23 (2001) 3-10.

[3.2] D.S.V. Prasad, G.V.R.P. Raju, M.A. Kumar, Utilization of industrial waste in flexible pavement construction, E. J. Geotec. Eng. 13 (2001) 1-12.

[3.3] D. Raghavan, H. Huynh, C.F. Ferraris, Workability, mechanical properties, and chemical stability of a recycled tyre rubber-filled cementitious composite, J. Mater. Sci. 33 (1998) 1745-1752.

[3.4] I. Marie, H. Quiasrawi, Closed-loop recycling of recycled concrete aggregate, J. Clean. Prod. 37 (2012) 243-248.

[3.5] J. Yang, Q. Du, Y.W. Bao, Concrete with recycled concrete aggregate and crushed clay bricks, Constr. Build. Mater. 25 (2011) 1935-1945.

[3.6] T.C. Ling, C.H. Poon, Use of recycled CRT funnel glass as fine aggregate in dry-mixed concrete paving blocks, J. Clean. Prod. 68 (2014) 209-215.

[3.7] S. Castro, J. Brito, Evaluation of durability of concrete made with crushed glass aggregates, J. Clean. Prod. 41 (2013) 7-14.

[3.8] N.N. Eldin, A.B. Senouci, Rubber-tire particles as concrete aggregate, J. Mater. Civil Eng. 5 (1993) 478-496.

[3.9] M.C. Bignozzi, F. Sandrolini, Tyre rubber waste recycling in self-compacting concrete, Cem. Concr. Res. 36 (2006) 735-736.

[3.10] C. Albano, N. Camacho, J. Reyes, J.L. Feliu, M. Hernández, Influence of scrap rubber addition to Portland I concrete composites: destructive and non-destructive testing, Compos. Struct. 71 (2005) 439-446.

[3.11] D.G. Goulias, A.H. Ali, Non-destructive evaluation of rubber modified concrete, Proceedings of a special conference, ASCE, New York, USA, 1997, pp. 111-120.

[3.12] N.I. Fattuhi, L.A. Clark, Cement-based materials containing shredded scrap truck tyre rubber, Constr. Build. Mater. 10 (1996) 229-236.

[3.13] D. Fedroff, S. Ahmad, B.Z. Savas, Mechanical properties of concrete with ground waste tire rubber, Transport. Res. Rec. 1532 (1996) 66-72.

[3.14] G. Li, M.A. Stubblefield, G. Garrick, J. Eggers, C. Abadie, B. Huang, Development of waste tire modified concrete, Cem. Concr. Res. 34 (2004) 2283-2289.

[3.15] İ.B. Topçu, The properties of rubberized concretes, Cem. Concr. Res. 25 (1995) 304-310.

[3.16] BS EN 197-1, Cement. Composition, Specifications and Conformity Criteria for Common Cements, British Standards Institution, 2011.

[3.17] BS EN 933-1, Tests for Geometrical Properties of Aggregates. Determination of Particle Size Distribution – Sieving Method, British Standards Institution, 2012.

[3.18] D.C. Teychenné, J.C. Nicholls, R.E. Franklin, D.W. Hobbs, Design of normal concrete mixes, second ed., Construction Research and Communications Limited, Watford, 1997.

[3.19] BS EN 12350-2, Testing Fresh Concrete. Slump-test, British Standards Institution, 2009.

[3.20] P.K. Mehta, P.J.M. Monteiro, Microstructures, Properties, and Materials. McGraw-Hill, USA, 2013.

[3.21] BS EN 12350-6, Testing Fresh Concrete. Density, British Standards Institution, 2009.

[3.22] R. Siddique, T.R. Naik, Properties of concrete containing scrap-tire rubber – an overview, Waste Manage. 24 (2004) 563-569.

[3.23] BS EN 12390-3, Testing Hardened Concrete. Compressive Strength of Test Specimens, British Standards Institution, 2009.

[3.24] Y. Guo, J. Zhang, G. Chen, Z. Xie, Compressive behaviour of concrete structures incorporating recycled aggregates, rubber crumb and reinforced with steel fibre, subjected to elevated temperatures, J. Clean. Prod. 72 (2014) 193-203.

[3.25] BS EN 12390-6, Testing Hardened Concrete. Tensile Splitting Strength of Test Specimens, British Standards Institution, 2009.

[3.26] BS EN 12390-5, Testing Hardened Concrete. Flexural Strength of Test Specimens, British Standards Institution, 2009.

[3.27] H.A. Toutanji, The use of rubber tire particles in concrete to replace mineral aggregates, Cem. Concr. Comp. 18 (1996) 135-139.

[3.28] BS 1881-208, Testing Concrete. Recommendations for the Determination of the Initial Surface Absorption of Concrete, British Standards Institution, 1996.

[3.29] Technical report No. 31 – Permeability Testing of Site Concrete, The Concrete Society, 2008.

[3.30] M. Bravo, J. Brito, Concrete made with used tyre aggregate: durability-related performance, J. Clean. Prod. 25 (2012) 42-50.

[3.31] E. Ganjian, M. Khorami, A.A. Maghsoudi, Scrap-tyre-rubber replacement for aggregate and filler in concrete, Constr. Build. Mater. 23 (2009) 1828-1836.

[3.32] O. Onuaguluchi, D.K. Panesar, Hardened properties of concrete mixtures containing pre-coated crumb rubber and silica fume, J. Clean. Prod. 82 (2014) 125-131.

CHAPTER 4

ANALYSIS AND PREDICTION OF CUBE COMPRESSIVE STRENGTH FOR CONCRETE WITH VARYING CONTENT OF RECYCLED AGGREGATE AS COARSE AGGREGATE AND RUBBER PARTICLES AS FINE AGGREGATE

4.1 Introduction

Demolished building concrete and waste tyres are two types of common wastes in construction and automobile industry, respectively. From the viewpoint of sustainability, recycled aggregate and scrap tyre rubber have been reused to replace aggregates in concrete with the purpose of lessening their negative influence on the environment. So far, numerous researches have been carried out and well developed on the properties of RAC [4.1]-[4.6] and RRC [4.7]-[4.12]. In the field of RAC, it is widely accepted that the compressive strength of RAC gradually decreases as the amount of recycled aggregate increases. Some researchers pointed out up to a certain ratio of substitution, this influence might be insignificant. For instance, Limbachiya et al. [4.1] selected rejected structural precast concrete elements to produce recycled aggregate which were used as substitutions of aggregates in concrete. They found that there was no effect on ceiling strength of concrete cube specimens with the replacement of recycled aggregate by up to 30%. Thereafter, the strength reduced gradually as the recycled aggregate content increased. Soares et al. [4.2] also used coarse recycled aggregates crushed from precast concrete rejects as part of natural coarse aggregate to evaluate the effect of various replacement ratios on mechanical and durability performance of concrete. They concluded that the concrete mixes with 100% recycled aggregates have an equivalent performance to that of the reference concrete in most of the properties. Similar

conclusion was reported by Rao et al. [4.3] that the strength of RAC and control concrete were comparable at full replacement, provided that the w/c was higher than 0.55. If the w/c was reduced to 0.4, the strength of RAC was about 75% of the control mix. On the contrary, Mukharjee and Barai [4.4] tested compressive strength at 7, 28, 90 and 365 days for fully natural and recycled aggregate concrete mixes made with or without nano-silica. The results of their study showed that full replacement of natural coarse aggregates with recycled ones have significant effect on compressive strength and interfacial transition zone characteristics of concrete. They also stated that compressive strength and microstructure of concrete mixes improves with the incorporation of nano-silica.

Many researchers have explained that the decrease in mechanical strength of RAC was primarily due to the existence of cement paste and/or mortar in recycled aggregates. Sanchez and Alaejos [4.5] further pointed out that the main properties unfavourably affected by mortar content were water absorption, density and Los Angeles abrasion. Duan and Poon [4.6] studied the mechanical and durability properties of RAC with varying amounts of old adhered mortars. They stated that the presence of residual mortar in recycled aggregates led to their poorer aggregate properties, including lower density and crushing strength values. Their experimental results on compressive strength, splitting tensile strength, elastic modulus, resistance to chloride ion penetration and drying shrinkage indicated that recycled aggregate of good quality, namely, low attached mortar content can be used to fully replace natural aggregate to produce concrete with mechanical properties and durability properties comparable to the concrete with natural aggregate.

In the area of RRC, a general consensus is that the strength decreases and ductility, impact resistance and dynamic energy dissipation capacity increase with a rising proportion of rubber phase in the mixture [4.7]. In an early study, the results obtained by Eldin and Senouci [4.8] indicated that there was approximately an 85% reduction in compressive strength and a 50% reduction in tensile strength when the coarse aggregate was fully replaced by coarse rubber chips. If fine aggregate was fully replaced by fine crumb rubber, specimens lost up to 65% of their compressive strength and up to 50% of their tensile strength. Rahman et al. [4.9] investigated some fundamental properties of rubber modified self-compacting concrete using 1-4 mm size rubber particles to replace natural fine aggregate with different dosage of super plasticizer. Their results showed that compared to the conventional self-compacting concrete, 28% fine aggregate replacement with rubber significantly reduced the compressive strength by about 35% while modestly reduced 10-20% dynamic modulus of rubber modified self-compacting concrete. They suggested if the durability issues are tackled properly, rubberized self-compacting concrete would have a high potential to be used as a vibration attenuation material where better dynamic properties are desirable. Yang et al. [4.10] carried out an experimental study on compressive, flexural, and splitting tensile strengths of crumb rubber concrete at both ambient temperature 20°C and low temperature -25°C. They found that not only the strengths increased as temperature decreased from 20°C to -25°C, but crumb rubber concrete still maintained its ductility. Based on these conclusions, they suggested that crumb rubber concrete might have more advantages in its application in cold climate regions than in warm climate region, and 50 kg/m^3 might be an optimized content for achieving overall satisfactory performance of crumb rubber concrete at low temperature.

The reduction of compressive strength is attributed to the low stiffness and poor surface texture of the rubber particles that resulted in an inconsistency of the concrete mix as well as the lack of bonding between the rubber particles and the surrounding cement paste, leading to a loss of compression resistance [4.8]. Given this fact, Segre and Joekes [4.11] immersed rubber particles in sodium hydroxide saturated aqueous solution for 20 minutes at room temperature before the particles were filtered, and the rubber was then washed with tap water and dried at the ambient temperature prior to using. They demonstrated that the surface modification enhanced the adhesion of tyre rubber particles to the surrounding paste, leading to an improvement in mechanical properties such as compressive strength, flexural strength and fracture energy. Su et al. [4.12] conducted surface treatment on rubber using SCA to improve the bond strength between rubber and matrix. Rubber particles were immersed in SCA until the entire surface was coated by the agent before being added into the mixture. The results showed that pre-treatment by SCA which acts as an adhesion promoter lead to an improvement in the compressive strength of hardened rubber concrete by 19.3% at 1 day, 9.3% at 7days, and 6.8% at 28 days, respectively.

The studies have been widely reported on replacement of coarse aggregate by recycled aggregate and replacement of fine aggregate by waste tyre rubber in separate concrete. However, investigation on replacing aggregates by both recycled aggregate and rubber simultaneously in concrete is rather scarce in the literature. Therefore, recycled aggregate and waste tyre rubber were used to replace coarse aggregate and fine aggregate simultaneously, with some PFA as well as some additional polypropylene fibre in this study. The aims of designing this concrete material are (a) to recycle waste concrete, scrap tyres and PFA for environmental sustainability; (b) to reduce the cost of raw materials for concrete production;

(c) to control early-age cracking of concrete by adding polypropylene fibre and; (d) to potentially use for fatigue and vibration control in structures due to high toughness and dynamic energy dissipation capacity of rubber material. Overall, this innovative concrete material is designed to be used in ways that are environmentally responsible, commercially competitive, technically sound, and supportive of a more sustainable society. Guo et al. [4.13], [4.14] presented a similar concrete material which is named RSRAC. They used ordinary Portland cement, recycled coarse aggregate with 0 and 100% natural coarse aggregate volume replacement ratios, crumb rubber with different volume replacement ratios of 0, 4%, 8%, 12% and 16% for fine aggregate, and steel fibre with 1% of concrete volume to prepare a series of concrete mixes. Effects of rubber content on the compressive and fracture behaviour of the RSRAC subjected to different temperatures were analyzed. Their results generally indicated that (a) compressive strength and stiffness of concrete mixes decreased after exposure to elevated temperature, with higher replacement of fine aggregate by rubber leading to lower compressive strength and stiffness magnitude; (b) rubber crumbs significantly enhanced the energy absorption capacity and explosive spalling resistance of concrete; (c) both the fracture toughness and fracture energy first increased and then decreased with increase of the rubber content; (d) the thermal damage because of heating from 25°C to 600°C obviously increased the fracture energy and critical crack mouth opening displacement, which did not apply to the fracture toughness; (e) exposure to high temperature made all cementitious materials tested in their studies significantly more ductile and less resistant to crack propagation.

Compressive strength is one of the most important and basic parameters for its proper application. Concrete mix design is also based on determining the material proportions

according to the designed compressive strength [4.15]. Therefore, the objectives of this study are to analyse the effect of recycled aggregate and rubber particles replacement ratios on concrete cube compressive strength, followed by establishing equations derived from the results obtained from experimental testing to predict cube compressive strength of this innovative concrete material.

4.2 Experiment details

4.2.1 Materials

The materials used in this study comprised cement with PFA, water, natural gravels, recycled aggregate, sand, waste tyre rubber particles and polypropylene fibre.

4.2.1.1 Cement

Portland siliceous fly ash (30% by weight) cement with a characteristic strength of 32.5 MPa (referred to CEM II/B-V 32.5) was used in accordance with BS EN 197-1 [4.16]. Fly ash and pure cement were mixed without grinding. They were stored in airtight packages before using.

4.2.1.2 Water

Tap water which is reasonably free from contamination in the laboratory was used to hydrate the cement in the mixtures, which in turn binds the aggregates together to make concrete hard and strong.

4.2.1.3 Coarse aggregate

Crushed gravels and recycled aggregate (shown in Figure 4-1) with a nominal maximum size of 10 mm were used as coarse aggregate. Tests of sieve analysis were carried out according to BS EN 933-1 [4.17] with some additional sieves required and the results are shown in Figure 4-2. It indicates that the PSD of crushed gravels and recycled aggregate used in this experiment were not much different from each other. Figure 4-3 shows the typical composition of recycled aggregate from a local demolition plant in Birmingham. Tests of aggregate crushing value were conducted on both crushed gravel and recycled aggregate according to BS 812-110 [4.18], with the results tabulated listing in Table 4-1. Water absorption of them in SSD condition was measured by immersion in water for 24 hours, followed by removing excess surface water with wet cloth after they were moved out. At the time when there was no free water on the surface, aggregates were assumed as SSD condition. The mass of sampled aggregates with saturated water in surface-dried condition was weighed and recorded as m_{SSD}. After 24 hours in the oven at the temperature of 105°C, the mass of the aggregates in oven-dried condition was re-weighed and recorded as m_{OD}. The SSD water absorption was calculated by the formula of $(m_{SSD}-m_{OD})/m_{OD}$. Volume of the sampled aggregates in SSD condition was measured in accordance with the principle of drainage and recorded as v_{SSD}. The SSD density of aggregates was calculated by the formula of m_{SSD}/v_{SSD}. Results of SSD water absorption and SSD density of crushed gravels and recycled aggregate are presented in Table 4-1.

Figure 4-1. Raw materials in oven-dried condition.

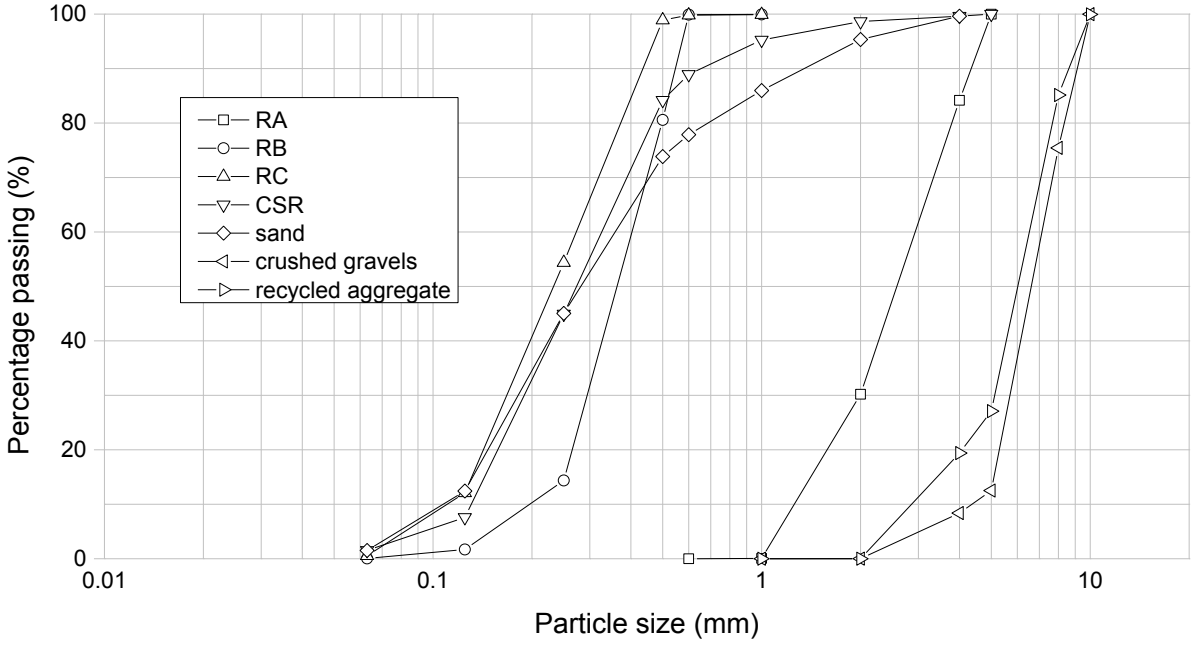

Figure 4-2. Grading curves of aggregates in oven-dried condition.

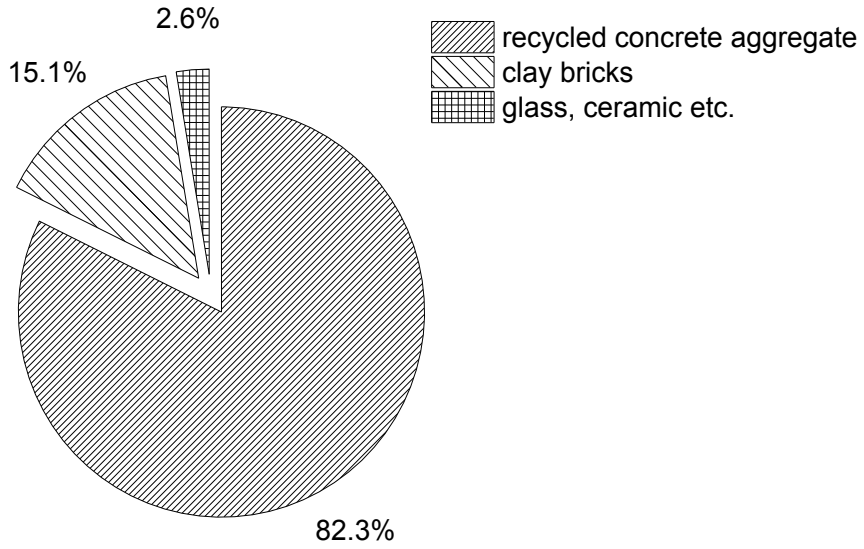

Figure 4-3. Composition of recycled aggregate in oven-dried condition.

Table 4-1. Related information of different kinds of aggregates.

Item	Crushed gravels	Recycled aggregate	River sand	Tyre rubber
Aggregate crushing value	20	23	N/A	N/A
SSD water absorption (%)	1.26	7.09	1.37	8.46
SSD density (kg/m^3)	2581	2539	2512	973

4.2.1.4 Fine aggregate

Natural river sand having a maximum particle size of 5 mm was used as the fine aggregate. Test of sieve analysis was conducted according to BS EN 933-1 [4.17]. As shown in Figure 4-2, the sand used in this experiment presented continuous granularity. Procedures of the sand SSD water absorption and SSD density measurements are the same as those of coarse aggregate and the results are presented in Table 4-1.

Waste tyre rubber was used as part of fine aggregate. CSR particles with continuous grading like sand were sorted out artificially by blending three different uniform size rubber particles, RA (cut to 3 mm), RB (ground to 0.5 mm) and RC (ground to 0.3 mm). They are sourced from a local waste tyre recycling plant in Manchester, without any pre-treatment, contaminant or tyre bead wire. Sieve analysis tests were carried out and the grading curve of each rubber sample is shown in Figure 4-2. SSD water absorption and SSD density of rubber particles were also measured. However, it should be noted that some rubber particles were found to float in water. To this end of immersion, a piece of tightly woven fabric was used to wrap rubber particles. The wrapped rubber particles were submerged in a water filled bucket, followed by gently shaking within the water to release as much trapped air as possible until it easily sank to the bottom of the bucket. Other procedures of measurements are the same as those of measuring coarse aggregates. Results of SSD water absorption and SSD density of rubber particles are shown in Table 4-1.

4.2.1.5 Polypropylene fibre

The polypropylene fibre shown in Figure 4-1 is non-hazardous. It is a polymeric fibre designed to impart reinforcement to a variety of concrete mixes. It is designed not only for use in structural concretes such as large section precast units, parking areas and industrial flooring, but also for reducing the possibility of early-age cracking of concrete. The properties of this fibre from the specification are listed in Table 4-2.

Table 4-2. Properties of the used polypropylene fibre.

Name	Polypropylene fibre
Acid and salt resistance	Excellent
Colour	Grey
Density	910 kg/m^3
Fibre length	54.0 mm
Melting point	160°C
Nature	Synthetic
Tensile strength	600 MPa
Water absorption	Nil

4.2.2 Mix design considerations

4.2.2.1 Method of substituting aggregates

Different researchers use different manners to replace aggregates. Guo et al. [4.13], [4.14] and Eguchi et al. [4.19] replaced natural coarse aggregate with recycled aggregate by volume while Tuyan et al. [4.20] and Yang et al. [4.21] did so by weight. Bravo and Brito [4.22] and Aiello and Leuzzi [4.23] used rubber to volumetrically substitute part of fine aggregate whereas Topçu and Bilir [4.24] and Albano et al. [4.25] adopted gravimetric manner. In this study, fine aggregate was replaced by rubber by volume while coarse aggregate was replaced by recycled aggregate by weight. The reason for volume replacement of fine aggregate rather than mass replacement is mainly because of the distinction between the densities of different materials. SSD density of sand is over twice as much as that of rubber materials (see Table 4-1). It means that if the sand is substituted by rubber in the manner of mass replacement, the

volume of resulted mixture would be much higher compared with the original one. Consequently, content of other aggregates and cement paste in unit volume would be decreased, resulting in severe strength reduction of concrete. It would potentially cause safety problems when this innovative concrete material is used in structural engineering applications. Besides, the changing volume would lead to incorrect concrete demand in the mix design. This is also applicable to industrial situations, as a change in volume of a mixture would cause either quantity issues for the purchaser, or cost issues for the supplier. However, this issue is not obvious in the case of substituting coarse aggregate since the values of SSD density of the crushed gravels and recycled aggregate used in this study were quite close to each other (see Table 1). The difference of them is 42 kg/m^3, approximately 1.64% of their density, allowing the substitution by weight to be conducted.

4.2.2.2 Use of a constant w/c ratio

It is well known that w/c ratio is intrinsically linked to the strength of concrete. A little variation of w/c ratio would cause profound influence on concrete strength when other parameters are kept constant, especially for high strength concrete [4.26]. Moreover, in accordance with the design method used in this study, the w/c ratio was firstly determined according to the designed cube compressive strength and some other auxiliary factors. Therefore, the same w/c ratio was strictly adhered to in each batch of mix to provide more comparable results.

4.2.3 Mix proportioning

Concrete mix proportioning was undertaken using the second edition of Design of Normal Concrete Mixes [4.15] published by the British Research Establishment. This design method is based on determining the material proportions. Using known or assumed parameters, the w/c ratio required to achieve the compressive strength was determined, culminating in mass quantities for individual material proportions.

The mix design of reference concrete in this chapter aimed to achieve a target mean strength of 43 MPa at 28 days with a slump value of 60-180 mm. Twenty-five batches of concrete mixtures, with each batch including three 100 mm cube specimens were prepared. The w/c ratio of 0.39, determined according to target mean strength, cement strength class and type of aggregates, was kept constant throughout the experiment programme. The amount of free water used to achieve the designed w/c ratio was determined according to the desired slump, maximum size of aggregate and type of aggregate. Cement content was calculated by the values of w/c ratio and the amount of free water. Recycled aggregate was used to replace 0, 25%, 50%, 75% and 100% of crushed gravels by weight while waste tyre rubber was used to replace 0, 10%, 20%, 30% and 40% of sand by volume. The amount of each kind of aggregate in different concrete mixture was figured out in compliance with the formulas provided by the second edition of Design of Normal Concrete Mixes [4.15]. Dosage rate of polypropylene fibre was 1.0 kg/m^3 recommended from the specification. All the concrete mix proportions are presented in Table 4-3.

Table 4-3. Mix proportions, experimental testing results and strength attenuation factors of the designed concrete material.

Notation	Recycled aggregate content (wt%)	Rubber content (vol%)	Water (kg/m^3)	Cement with PFA (kg/m^3)	Gravels (kg/m^3)	Recycled aggregate (kg/m^3)	Sand (kg/m^3)	Rubber (kg/m^3)	Fibre (kg/m^3)	1dCCS (MPa)	I_{1dCCS}	7dCCS (MPa)	I_{7dCCS}	28dCCS (MPa)	I_{28dCCS}
RA0R0	0	0	230	589	996	0	572	0	1.0	10.2	0.0000	37.5	0.0000	50.9	0.0000
RA25R0	25	0	230	589	747	249	572	0	1.0	10.0	0.0956	37.2	0.0967	50.1	0.0960
RA50R0	50	0	230	589	498	498	572	0	1.0	9.9	0.1893	35.9	0.1867	49.1	0.1881
RA75R0	75	0	230	589	249	747	572	0	1.0	9.7	0.2782	35.1	0.2738	47.8	0.2747
RA100R0	100	0	230	589	0	996	572	0	1.0	9.3	0.3556	33.6	0.3494	46.2	0.3540
RA0R10	0	10	230	589	996	0	515	22.2	1.0	9.8	0.0375	36.2	0.0376	49.3	0.0378
RA25R10	25	10	230	589	747	249	515	22.2	1.0	9.8	0.1311	35.9	0.1307	48.6	0.1303
RA50R10	50	10	230	589	498	498	515	22.2	1.0	9.5	0.2179	35.1	0.2190	47.5	0.2184
RA75R10	75	10	230	589	249	747	515	22.2	1.0	9.3	0.3023	33.8	0.2988	46.5	0.3028
RA100R10	100	10	230	589	0	996	515	22.2	1.0	9.0	0.3785	32.7	0.3741	44.8	0.3776
RA0R20	0	20	230	589	996	0	458	44.3	1.0	9.3	0.0711	34.8	0.0724	46.8	0.0717
RA25R20	25	20	230	589	747	249	458	44.3	1.0	9.2	0.1583	33.9	0.1587	46.0	0.1586
RA50R20	50	20	230	589	498	498	458	44.3	1.0	9.0	0.2409	33.1	0.2410	45.4	0.2435
RA75R20	75	20	230	589	249	747	458	44.3	1.0	8.8	0.3196	32.6	0.3221	44.1	0.3210
RA100R20	100	20	230	589	0	996	458	44.3	1.0	8.5	0.3900	31.3	0.3906	42.5	0.3908
RA0R30	0	30	230	589	996	0	400	66.5	1.0	8.4	0.0964	31.0	0.0967	42.6	0.0979
RA25R30	25	30	230	589	747	249	400	66.5	1.0	8.3	0.1745	30.7	0.1756	41.6	0.1753
RA50R30	50	30	230	589	498	498	400	66.5	1.0	8.3	0.2539	29.9	0.2488	40.9	0.2507
RA75R30	75	30	230	589	249	747	400	66.5	1.0	7.9	0.3172	29.1	0.3178	39.8	0.3202
RA100R30	100	30	230	589	0	996	400	66.5	1.0	7.7	0.3827	28.4	0.3840	38.3	0.3815
RA0R40	0	40	230	589	996	0	343	88.6	1.0	7.2	0.1101	26.6	0.1107	36.1	0.1106
RA25R40	25	40	230	589	747	249	343	88.6	1.0	7.1	0.1765	26.1	0.1764	35.4	0.1763
RA50R40	50	40	230	589	498	498	343	88.6	1.0	7.0	0.2409	25.7	0.2406	34.8	0.2400
RA75R40	75	40	230	589	249	747	343	88.6	1.0	6.8	0.2990	24.9	0.2978	33.9	0.2987
RA100R40	100	40	230	589	0	996	343	88.6	1.0	6.6	0.3533	24.2	0.3524	32.8	0.3518

Note: Gravels, recycled aggregate, sand and rubber are in SSD condition.

4.2.4 Preparation of concrete specimens

4.2.4.1 Mixing

All kinds of aggregates were prepared to be in SSD condition before mixing. The desired quantities of each item was accurately measured out and put in order of crushed gravels, sand, cement, fibre, rubber particles, and recycled aggregate in a mechanical mixer which had been inter-surface wetted. Prior to the addition of water, the mixer was turned on and the placed materials were mixed for 5 minutes to ensure homogenisation. Then half water was put in to mix for another 5 minutes, followed by adding the other half in. The mixer was stopped until there were no visual discrepancies in the mixture.

4.2.4.2 Sampling

Dimension of the moulds are 100 mm cube. Prior to filling, the inner surface of the moulds were brushed with a thin film oil to prevent concrete from adhering to the mould. All moulds were filled with fresh concrete in two equal layers, each of which was compacted using the vibrating table to remove air. Vibration was allowed for 30 seconds to ensure a smooth and even surface film, followed by trowelling the exposed surface to a clean finish.

4.2.4.3 Curing

Polythene sheet was placed over the samples after casting to prevent moisture loss. After 24 hours at a Civil Engineering laboratory temperature of 20°C, the samples were carefully

removed from the moulds, with each sample having mix notation and curing time written by marker pen clearly on its surface. Samples were then transferred to the curing water tank at a temperature of 20°C where they were immersed until the required age.

4.2.5 Testing method

1, 7 and 28 days cube compressive strength of hardened concrete were tested in accordance with BS EN 12390-3 [4.27]. The excess moisture from the surface of the cube specimen was wiped before testing. Then the specimen was positioned on the centre of the plate in a Denison digital pressure testing machine of a 2000 KN capacity, with non-trowelled faces placed in contact with the loading platen to prevent eccentric loading. Once the test was started, the uniaxial compression was applied continuously at a constant rate of 0.6 MPa/s. The value indicated was recorded when the sample failed and mean of the three specimens was set as the final result.

4.3 Results and discussion

Results of cube compressive strength and the corresponding intermediate variable P calculated at different ages are listed in Table 4-3.

4.3.1 Analysis of cube compressive strength

Correlation tests and linear models were used to test the association 28dCCS with recycled aggregate and rubber replacement ratio. All the statistical analyses below were performed

using software RStudio 0.98.1028 with the statistical significant level of 0.05. It is obviously observed from Figure 4-4 that there is a negative correlation between 28dCCS with the two factors. 28dCCS and rubber replacement ratio are highly correlated with each other, with a negative correlation coefficient of -0.928 (p-value < 0.001) shown in Table 4-4. On the contrary, the correlation between 28dCCS and recycled aggregate replacement ratio is -0.274, which is not statistically significant (p-value = 0.186). To further proof that rubber replacement ratio has more significant influence on strength, linear models were built with 28dCCS as dependent variable, recycled aggregate and/or rubber replacement ratio as independent variable (s). The results summarized in Table 4-5 show that Model 4-1 with recycled aggregate and rubber replacement ratio simultaneously produced an R^2 of 0.936. When rubber replacement ratio was excluded from the model, R^2 of Model 2 dropped by about 0.86, while removing recycled aggregate replacement ratio from the model (Model 4-3) only caused a minor drop of approximately 0.08 in R^2. This implies that rubber replacement ratio is of major contribution to the model, i.e. replacement ratio of rubber has much more significant impact than recycled aggregate on the strength of this concrete material.

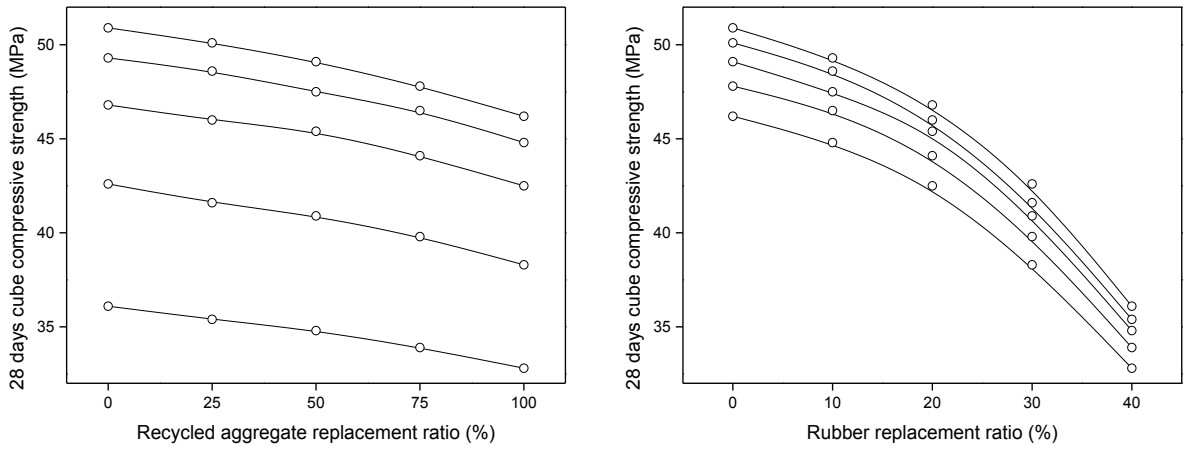

Figure 4-4. Trend of the 28 days cube compressive strength affected by different aggregate under different replacement ratios.

Table 4-4. Correlation of between-subjects.

Correlation test (variable *x*, variable *y*)	Pearson's correlation coefficient	95% confidence interval	p-value
28 days cube compressive strength, recycled aggregate replacement ratio	-0.274	(-0.603, 0.136)	0.186
28 days cube compressive strength, rubber replacement ratio	-0.928	(-0.968, -0.841)	< 0.001 (2.50e-11)

Note: correlation coefficient measures the linear association between two variables *x* and *y*, giving a value between -1 and 1 inclusive, where -1 stands for the strongest negative correlation, 0 stands for the weakest correlation, and 1 stands for the strongest positive correlation.

Table 4-5. Linear models of between-subjects.

	Estimate coefficient	Standard error	t-value	p-value
Model 4-1				
(Intercept)	52.372	0.648	80.850	< 0.001
Recycled aggregate replacement ratio	-4.144	0.819	-5.058	< 0.001 (4.58e-05)
Rubber replacement ratio	-35.140	2.048	-17.155	< 0.001 (3.21e-14)
Multiple R-squared: 0.936, Adjusted R-squared: 0.930				
Model 4-2				
(Intercept)	45.344	1.861	24.370	< 0.001
Recycled aggregate replacement ratio	-4.144	3.038	-1.364	0.186
Rubber replacement ratio	-	-	-	-
Multiple R-squared: 0.0748, Adjusted R-squared: 0.0346				
Model 4-3				
(Intercept)	50.300	0.722	69.700	< 0.001
Recycled aggregate replacement ratio	-	-	-	-
Rubber replacement ratio	-35.140	2.946	-11.930	< 0.001 (2.50e-11)
Multiple R-squared: 0.861, Adjusted R-squared: 0.855				

Note: Model 4-1 is 28 days cube compressive strength vs. recycled aggregate and rubber replacement ratio; Model 4-2 is 28 days cube compressive strength vs. recycled aggregate replacement ratio; Model 4-3 is 28 days cube compressive strength vs. rubber replacement ratio; R-squared, also known as the coefficient of determination, is the proportion of the variation in the response variable that is explained by the regression model.

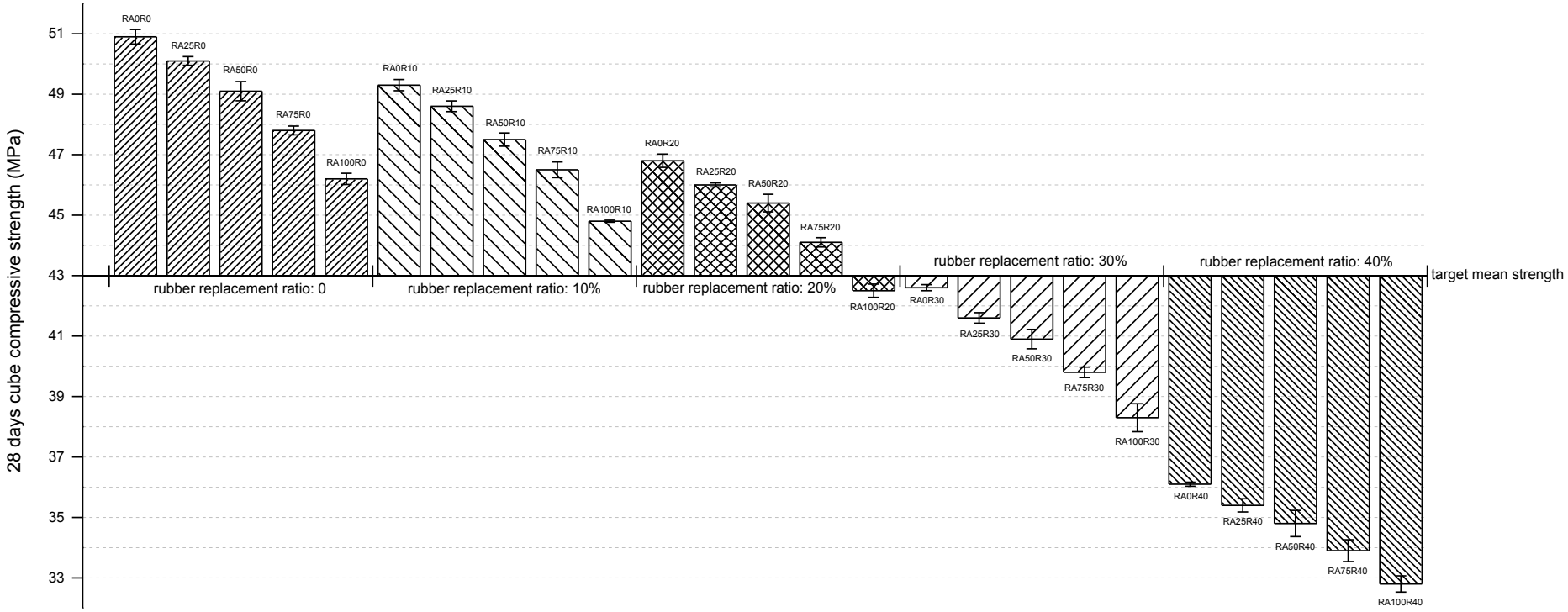

Figure 4-5. 28 days cube compressive strength of different specimens.

Results of the 28dCCS are diagrammed in a column graph shown in Figure 4-5 for a more evident comparison of changes. As expected, the compressive strength of all the specimens exhibited a decreasing tendency with increasing either recycled aggregate or rubber content. When the replacement ratio of rubber was no more than 20% by volume, the specimens have a 28dCCS of over 43 MPa which was the target mean strength of this designed concrete material regardless of the recycled aggregate replacement ratio, apart from RA100R20. However, all the samples with more than 20% rubber replacement ratio failed to reach the target mean strength. Value of RA100R40 was 32.8 MPa, about 35% lower than the reference specimen of 50.9 MPa. Therefore, rubber aggregate for replacing over 20% of sand by volume should be used carefully, especially for structural application. This is in line with the similar recommendation of Khaloo et al. [4.28].

The above arguments were supported by microscopic inspections and analysis of the crushed specimen particles. Interfaces of rubber-cement paste and recycled aggregate-cement paste were inspected using Keyence VHX-700F series scanning optical microscopy. Detailed investigations on 10 particles of each crushed specimen were performed and micrographs of typical fracture surfaces are shown in Figures 4-6 and 4-7. As shown in Figure 4-6(a), it is quite clear that there is a distinct crack highlighted by the curve in Zone I. In addition, from its 3D image shown in Figure 4-6(b), noticeable discontinuity in Zone II was found. Faults and cracks observed at the rubber-cement paste boundaries indicated that the adhesion between them was poor, leading to the increase of volume of the weakest phase and interfacial transition zone [4.29]. Besides, rubber particles can be deemed as voids in concrete due to its lower stiffness compared to other aggregates or cement paste. Stress concentration usually arises at the interface between rubber particles and the cement paste under

compression, resulting in the degradation of concrete strength. In contrast, a well-developed adhesive joint area Zone III was observed between recycled aggregate and cement paste in the micrograph of Figure 4-7(a). From its 3D image shown in Figure 4-7(b), the transition zone between recycled aggregate and cement paste was smooth in contrast to the counterpart shown in Figure 4-6(b). The modest reduction of compressive strength caused by recycled aggregate could be attributed to its higher ACV compared to crushed gravels. From the micrograph of recycled aggregate-cement paste shown in Figure 4-7(a), it could be observed that a crack initialised in the recycled aggregate rather than along the interface, suggesting that there was a relatively stronger bond in the interfacial transition zone. The mechanism about the bond strength illustrated above demonstrated that replacing sand by rubber has a more considerable effect on the 28dCCS of concrete than replacing crushed gravels by recycled aggregate.

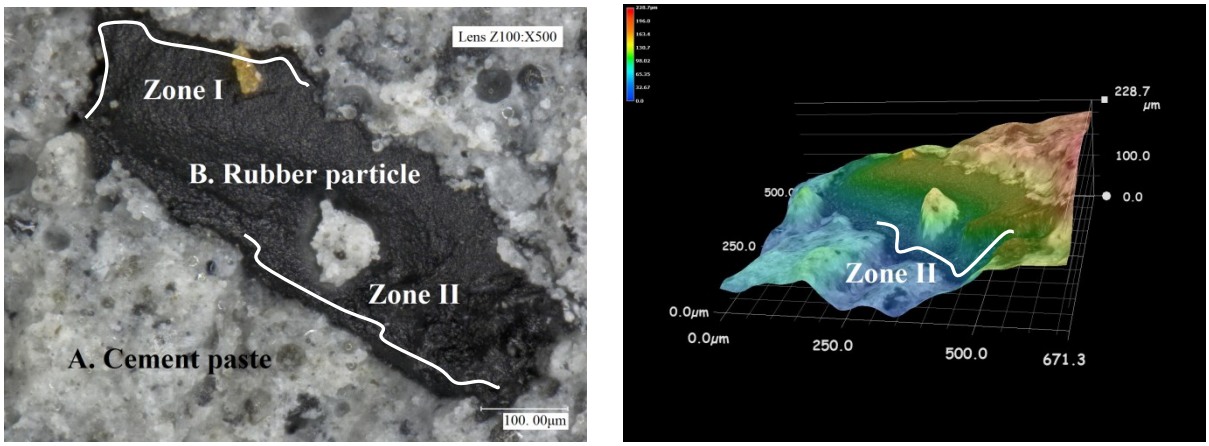

(a). Micrograph of rubber-cement paste interface.

(b). Three-dimensional image of rubber-cement paste interface.

Figure 4-6. Interface of rubber-cement paste, (a) micrograph and (b) three-dimensional image.

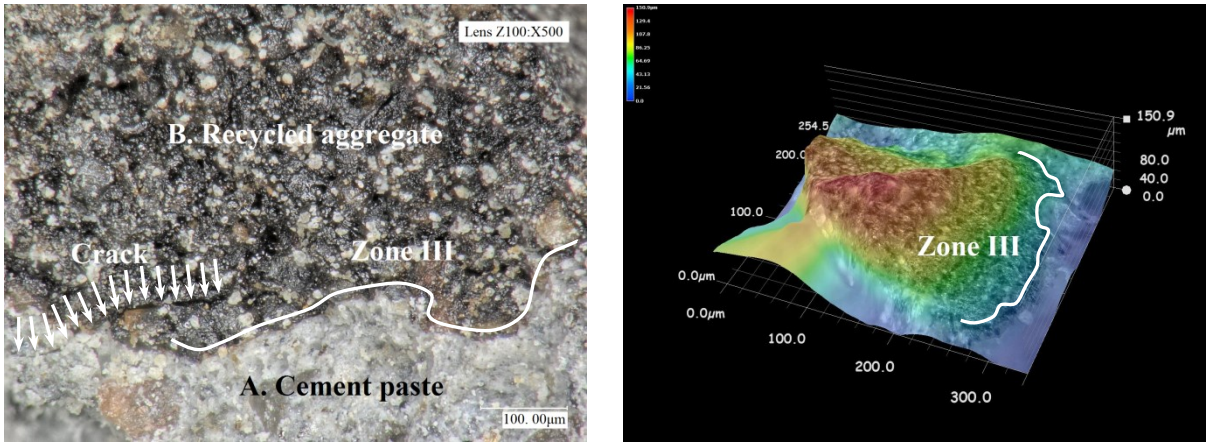

(a) Micrograph of recycled aggregate-cement paste interface. (b) Three-dimensional image of recycled aggregate-cement paste interface.

Figure 4-7. Interface of recycled aggregate-cement paste, (a) micrograph and (b) three-dimensional image.

4.3.2 Prediction of cube compressive strength

An intermediate variable I as shown in Equation (4-1) was established with independent variables of recycled aggregate and rubber replacement ratio for calculation of the predicted equation. It should be noted that I does not stand for the real reduction level of compressive strength. The results of I at different ages were plotted in different 3D scatter diagrams. By means of least square method, three fitting 3D surfaces were plotted in Figure 4-8 with separate function expression of I on m and n shown in Equations (4-2, 4-3 and 4-4) respectively to indicate the relationship among intermediate variable, recycled aggregate replacement ratio and rubber replacement ratio. The coefficients of determination, R-squared of the three surfaces were all 0.9999, indicating that Equations (4-2, 4-3 and 4-4) show a strong correlation among I, m and n. The compressive strength of this concrete material at 1, 7 and 28 days can be predicted by Equations (4-1, 4-2, 4-3 and 4-4), provided that the replacement ratio of rubber used is within the tested range.

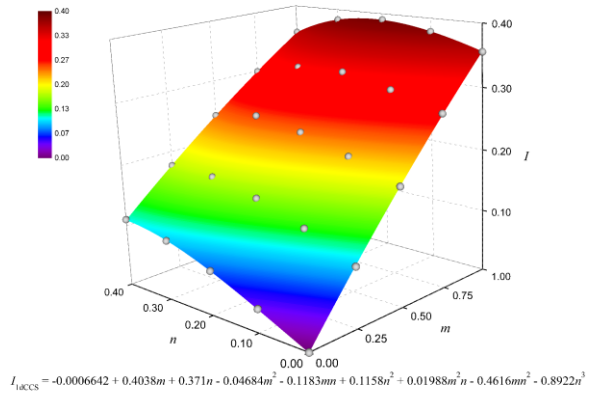

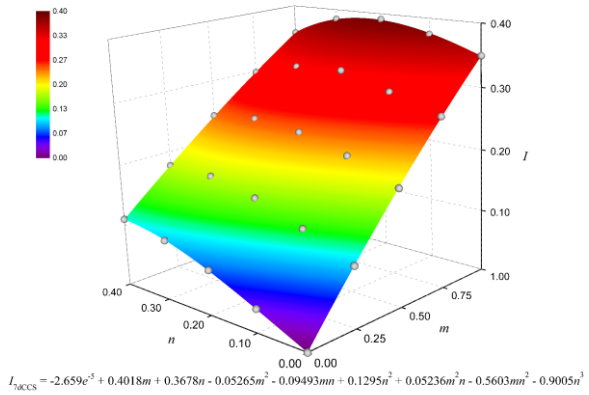

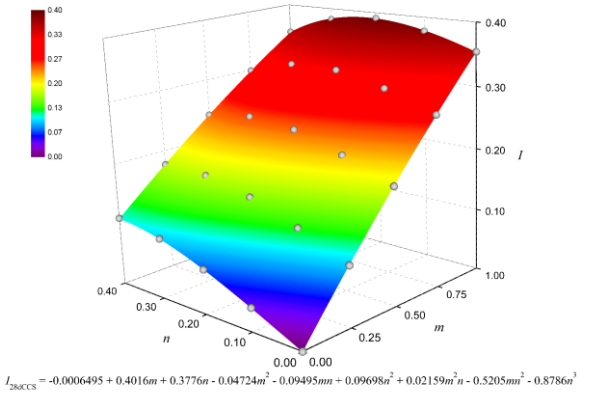

Figure 4-8. Fitting three-dimensional surfaces and function expressions of I on m and n with coefficients of determination at different ages of concrete specimens.

$$I = \left(\frac{f}{f_r}\right)\left(\frac{w}{c}\right)(m+n) \tag{4-1}$$

where $f =$ compressive strength of concrete specimen (MPa),

$f_r =$ compressive strength of reference concrete specimen (MPa),

$m =$ recycled aggregate replacement ratio,

$n =$ rubber replacement ratio.

$$I_{1dCCS} = -0.0006642 + 0.4038m + 0.371n - 0.04684m^2 - 0.1183mn + 0.1158n^2 + 0.01988m^2n - 0.4616mn^2 - 0.8922n^3 \tag{4-2}$$

$$I_{7dCCS} = -2.659e^{-5} + 0.4018m + 0.3678n - 0.05265m^2 - 0.09493mn + 0.1295n^2 + 0.05236m^2n - 0.5603mn^2 - 0.9005n^3 \tag{4-3}$$

$$I_{28dCCS} = -0.0006495 + 0.4016m + 0.3776n - 0.04724m^2 - 0.09495mn + 0.09698n^2 + 0.02159m^2n - 0.5205mn^2 - 0.8786n^3 \quad (4\text{-}4)$$

$$f_n = f_{28}\frac{\lg n}{\lg 28} \quad (4\text{-}5)$$

where $f_n =$ n days compressive strength of concrete specimen (MPa), $n \geq 3$,

$f_{28} =$ 28 days compressive strength of concrete specimen (MPa).

The proposed Equation (4-4) was used to predict the experimental data of compressive strength from the study of Guo et al. [4.14]. Prior to the prediction, two of their values were adjusted: the 89 days compressive strength was converted to the 28 days compressive strength according to the empirical equations shown in Equation (4-5), and the cylinder compressive strength was converted to the cube compressive strength by interpolation method according to BS EN 206 [4.30]. The results and the predicted values with error are listed in Table 4-6 and plotted in Figure 4-9. As can be seen, the predicted values are higher than the adjusted ones. The higher the rubber content is, the greater the error will be. This is understandable in view of different type of cement, PSD of aggregates, nature of fibre materials used, variety of preparation technology as well as calculation error of strength conversion. So far, experimental results reported on this kind of concrete material are too limited to sufficiently validate the equations. Thus, more work is needed before this proposed prediction approach could be used in concrete industry.

However, when rubber replacement ratio falls outside the tested range, the equations should be used with care. Due to the non-polar nature of rubber particles and their tendency to entrap air, when rubber is added to a concrete mixture, it may attract air adhered to the rough surface of rubber particles [4.31]. Increasing rubber content would result in higher air content in the

mixture, thereby increasing voids contents to degrade the hardened concrete. The increase of the attracted air would be non-linear with the increase of rubber content. This phenomenon is more obvious when the content of rubber is high [4.32]. Therefore, the proposed equations may not be applicable when rubber replacement ratio is over 40% by volume. They should be used prudently before further research is carried out on high volume replacement ratio of rubber for this concrete material.

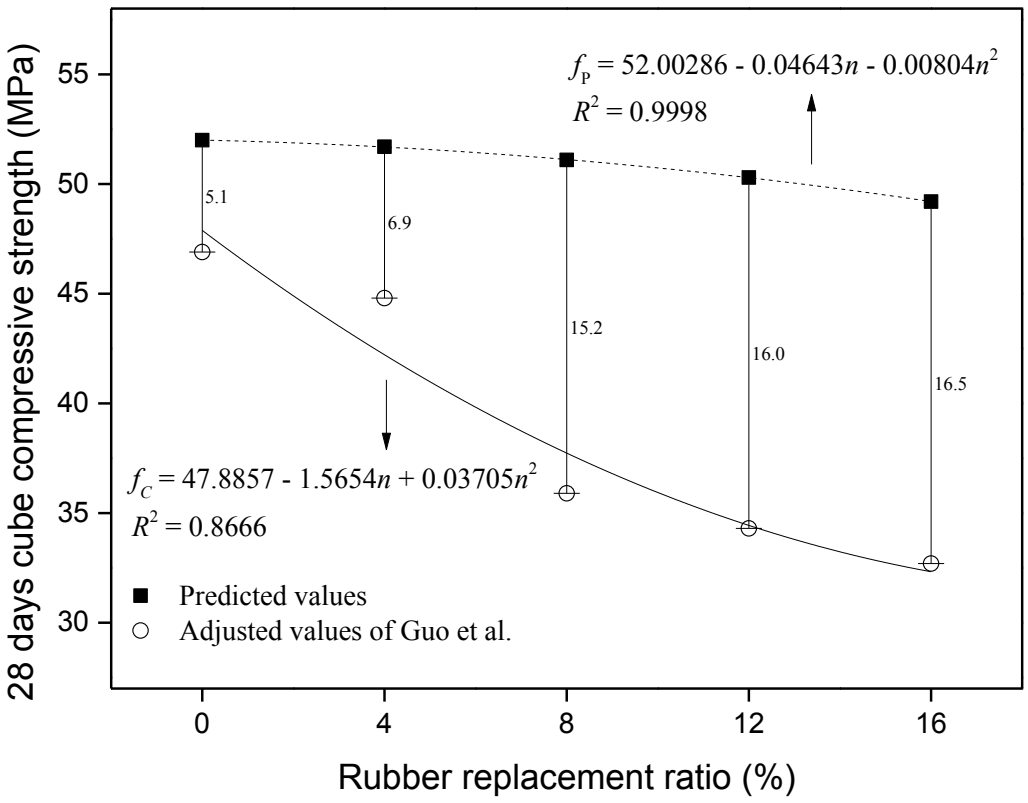

Figure 4-9. Comparison of the predicted and adjusted 28 days cube compressive strength.

Table 4-6. Adjusted and predicted 28 days cube compressive strength with error.

Mix	w/c	Tested 89 days cylinder compressive strength (MPa)	Adjusted 89 days cube compressive strength (MPa)	Adjusted 28 days cylinder compressive strength (MPa)	Adjusted 28 days cube compressive strength (MPa)	Predicted 28 days cube compressive strength (MPa)	Error between adjusted and predicted values (%)
NC-R0	0.35	56.5	69.4	41.9	51.5	N/A	N/A
RC-R0	0.35	51.4	63.1	38.2	46.9	52.0	9.8
RC-R4	0.35	49.1	60.3	36.5	44.8	51.7	13.3
RC-R8	0.35	39.4	48.2	29.2	35.9	51.1	29.7
RC-R12	0.35	37.6	46.2	27.9	34.3	50.3	31.8
RC-R16	0.35	35.9	44.1	26.7	32.7	49.2	33.5

Note: NC = concrete with 100% natural coarse aggregate, RC = concrete with 100% recycled aggregate replacing natural coarse aggregate by volume, R0, R4, R8, R12 and R16 for volume replacement ratio of rubber is 0, 4%, 8%, 12% and 16%, respectively [4.14].

4.4 Summary

Analysis and prediction of cube compressive strength for concrete with recycled aggregate and scrap tyre rubber particles as substitution of natural coarse and fine aggregate with varying replacement ratio respectively were conducted. Basing on the results of uniaxial compression tests on standard cube specimens of this concrete material in accordance with relevant standard, the following conclusions can be drawn from the experimental investigation:

- Concrete strength is affected by both the content of recycled aggregate and rubber particles. It decreases gradually with the simultaneous increase of recycled aggregate and rubber replacement ratio.

- Different substitution has a different effect on the reduction level of this concrete material. From the statistical analyses of experiment results and failure mechanism investigations of tested specimens, it can be concluded that rubber has a much more significant impact than recycled aggregate.

- When natural coarse aggregate was fully substituted by recycled aggregate by weight, the concrete still reached the target mean strength. However, rubber replacement ratio over 20% for fine aggregate by volume caused the strength of this concrete material lower than the designed compressive strength. Therefore, rubber aggregate for replacing over 20% of sand by volume is not recommended, especially for structural application.

- Polynomial fitting surfaces were proposed from the experiment testing results. Equations

$$I_{1dCCS} = -0.0006642 + 0.4038m + 0.371n - 0.04684m^2 - 0.1183mn + 0.1158n^2 + 0.01988m^2n - 0.4616mn^2 - 0.8922n^3$$
$$I_{7dCCS} = -2.659e^{-5} + 0.4018m + 0.3678n - 0.05265m^2 - 0.09493mn + 0.1295n^2 + 0.05236m^2n - 0.5603mn^2 - 0.9005n^3$$
$$I_{28dCCS} = -0.0006495 + 0.4016m + 0.3776n - 0.04724m^2 - 0.09495mn + 0.09698n^2 + 0.02159m^2n - 0.5205mn^2 - 0.8786n^3$$

  are valid to predict the compressive strength of this concrete material at different ages if the replacement ratio of rubber used is within the tested range of 0-40%.

- More research is needed before the fitting equation can be sufficiently validated and the proposed approach can be used for designing concrete material in practice. Influencing factors such as the type of cement, composition of waste materials, particle size distribution of aggregates as well as high volume replacement ratio of rubber for this concrete material should be considered in the equation so as to improve the overall prediction performance.

References

[4.1] M.C. Limbachiya, T. Leelawat, R.K. Dhir, Use of recycled concrete aggregate in high-strength concrete, Mater. Struct. 33 (2000) 574-580.

[4.2] D. Soares, J. Brito, J. Ferreira, J. Pacheco, Use of coarse recycled aggregates from precast concrete rejects: Mechanical and durability performance, Constr. Build. Mater, 71 (2014) 263-272.

[4.3] A. Rao, K.N. Jha, S. Misra, Use of aggregates from recycled construction and demolition waste in concrete, Resour. Conserv. Recy. 50 (2007) 71-81.

[4.4] B.B. Mukharjee, S.V. Barai, Influence of incorporation of nano-silica and recycled aggregates on compressive strength and microstructure of concrete, Constr. Build. Mater. 71 (2014) 570-578.

[4.5] J.M. Sanchez, G.P. Alaejos, Influence of attached mortar content on the properties of recycled concrete aggregate. In: Proceeding of international RILEM conference on the use of recycled materials in buildings and structures, Barcelona, Spain, November 8-11, 2004.

[4.6] Z.H. Duan, C.S. Poon, Properties of recycled aggregate concrete made with recycled aggregates with different amounts of old adhered mortars, Mater. Design. 58 (2014) 19-29.

[4.7] M.C. Bignozzi, F. Sandrolini, Tyre rubber waste recycling in self-compacting concrete, Cem. Concr. Res. 36 (2006) 735-739.

[4.8] N.N. Eldin, A.B. Senouci, Rubber-tire particles as concrete aggregate. J. Mater. Civil. Eng. 5 (1993) 478-496.

[4.9] M.M. Rahman, M. Usman, A.A. Al-Ghalib, Fundamental properties of rubber modified self-compacting concrete (RMSCC), Constr. Build. Mater. 36 (2012) 630-637.

[4.10] L. Yang, Z. Han, C. Li, Strength and flexural strain of CRC specimens at low temperature, Constr. Build. Mater. 25 (2011) 906-910.

[4.11] N. Segre, I. Joekes, Use of tire rubber particles as addition to cement paste, Cem. Concr. Res. 30 (2000) 1421-1425.

[4.12] H. Su, J. Yang, G.S. Ghataora, S. Dirar, Surface modified used rubber tyre aggregates: effect on recycled concrete performance, Mag. Concr. Res. 67 (2015) 680-691.

[4.13] Y.C. Guo, J.H. Zhang, G. Chen, G.M. Chen, Z.H. Xie, Fracture behaviors of a new steel fiber reinforced recycled aggregate concrete with crumb rubber, Constr. Build. Mater. 53 (2014) 32-39.

[4.14] Y. Guo, J. Zhang, G. Chen, Z. Xie, Compressive behaviour of concrete structures incorporating recycled aggregates, rubber crumb and reinforced with steel fibre, subjected to elevated temperatures, J. Clean. Prod. 72 (2014) 193-203.

[4.15] D.C. Teychenné, J.C. Nicholls, R.E. Franklin, D.W. Hobbs, Design of normal concrete mixes, second ed., Construction Research and Communications Limited, Watford, 1997.

[4.16] BS EN 197-1, Cement. Composition, Specifications and Conformity Criteria for Common Cements, British Standards Institution, 2011.

[4.17] BS EN 933-1, Tests for Geometrical Properties of Aggregates. Determination of Particle Size Distribution – Sieving Method, British Standards Institution, 2012.

[4.18] BS 812-110, Testing Aggregates. Methods for Determination of Aggregate Crushing Value (ACV), British Standards Institution, 1990.

[4.19] K. Eguchi, K. Teranishi, A. Nakagome, H. Kishimoto, K. Shinozaki, M. Narikawa, Application of recycled coarse aggregate by mixture to concrete construction, Constr. Build. Mater. 21 (2007) 1542-1551.

[4.20] M. Tuyan, A. Mardani-Aghabaglou, K. Ramyar, Freeze-thaw resistance, mechanical and transport properties of self-consolidating concrete incorporating coarse recycled concrete aggregate, Mater. Design. 53 (2014) 983-991.

[4.21] J. Yang, Q. Du, Y.W. Bao, Concrete with recycled concrete aggregate and crushed clay bricks, Constr. Build. Mater. 25 (2011) 1935-1945.

[4.22] M. Bravo, J. Brito, Concrete made with used tyre aggregate: durability-related performance, J. Clean. Prod. 25 (2012) 42-50.

[4.23] M.A. Aiello, F. Leuzzi, Waste tyre rubberized concrete: properties at fresh and hardened state, Waste Manage. 30 (2010) 1696-1704.

[4.24] İ.B. Topçu, T. Bilir, Experimental investigation of some fresh and hardened properties of rubberized self-compacting concrete, Mater. Design 30 (2009) 3056-3065.

[4.25] C. Albano, N. Camacho, J. Reyes, J.L. Feliu, M. Hernández, Influence of scrap rubber addition to Portland I concrete composites: destructive and non-destructive testing, Compos. Struct. 71 (2005) 439-446.

[4.26] P.K. Mehta, P.J.M. Monteiro, Microstructures, Properties, and Materials. McGraw-Hill, USA, 2013.

[4.27] BS EN 12390-3, Testing Hardened Concrete. Compressive Strength of Test Specimens, British Standards Institution, 2009.

[4.28] A.R. Khaloo, M. Dehestani, P. Rahmatabadi, Mechanical properties of concrete containing a high volume of tire-rubber particles, Waste Manage. 28 (2008) 2472-2482.

[4.29] C.S. Poon, Z.H. Shui, L. Lam, Effect of microstructure of ITZ on compressive strength of concrete prepared with recycled aggregates, Constr. Build. Mater. 18 (2004) 461-468.

[4.30] BS EN 206, Concrete. Specification, Performance, Production and Conformity, British Standards Institution, 2013.

[4.31] R. Siddique, T.R. Naik, Properties of concrete containing scrap-tire rubber – an overview, Waste Manage. 24 (2004) 563-569.

[4.32] A. Benazzouk, O. Douzane, T. Langlet, K. Mezreb, J.M. Roucoult, M. Quéneudec, Physico-mechanical properties and water absorption of cement composite containing shredded rubber wastes, Cem. Concr. Comp. 29 (2007) 732-740.

CHAPTER 5

SURFACE MODIFIED USED RUBBER TYRE AGGREGATES: EFFECT ON RECYCLED CONCRETE PERFORMANCE

5.1 Introduction

The rapid growth of vehicle use has resulted in a huge increase in waste tyres. This has created a pressing problem known as 'black pollution', which poses a potential threat to the environment and human health [5.1]. These waste tyres may create fire hazards, and they occupy a large volume of decreasing landfill sites with components that are non-biodegradable [5.2]. Several methods of recycling or reusing waste tyres have been proposed, including their use as lightweight aggregates in asphalt pavements, as fuel for cement kilns, as feedstock for making carbon black, and as artificial reefs in marine environments [5.2], [5.3]. However, some of these proposals are economically and environmentally unviable.

Many studies have been carried out on the use of waste tyre rubber as aggregate substitutes for making concrete [5.5]-[5.13] . Like recycled construction or demolition aggregate [5.25]-[5.31], recycled waste tyre rubber within concrete can be a feasible option for sustainable and eco-friendly construction. Although the existing literature has considered different aspects with regards to the properties of rubber concrete, the general consensus is that the use of crumb rubber as aggregate in concrete will reduce its workability and strength, but will improve its ductility, impact resistance and dynamic energy dissipation capacity, and this is attributed to the rubber aggregate's own properties of high resilience and low density. One of the most important influencing factors on the properties of rubber concrete is the rubber

replacement percentage, which has been widely studied and reported [5.5]-[5.18]. The decrease in concrete compressive strength with an increase of rubber content has been consistently reported, and how to reduce the loss of strength of rubber concrete is constantly being investigated. There has been some research studying the effect of rubber surface modification on the properties of concrete, but this area of investigation is limited. Segre and Joekes [5.21] carried out surface-treatment on the rubber particles by stirring with saturated NaOH solution for 20 minutes at room temperature before the mixture was filtered, and the rubber was then washed with tap water and dried at the ambient temperature before using. The results showed that the NaOH treatment enhanced the adhesion of tyre rubber particles to the surrounding paste, leading to an improvement in mechanical properties such as compressive strength, flexural strength and fracture energy. In contrast, Albano et al. [5.4] pointed out that prior treatment of rubber with NaOH did not produce obvious changes in compressive and splitting tensile strength of the resulting concrete when compared to untreated rubber concrete.

In order to address the negative results of reduced strength that the rubber concrete has often led to, this chapter aims to explore the potential treatments of crumb rubber and the resulting effects on the concrete properties. To this end, five groups of rubber concrete samples were devised and a series of concrete properties tests were carried out to reveal the differences resulted from the various methods of surface treatment of rubber parties before they are added into the concrete mix. All studied concrete samples include recycled rough aggregate, in addition to the crumb rubber partially replacing the fine natural aggregate particles. Saturated NaOH solution and SCA were both used to modify the surface of rubber particles. Tests on workability at the fresh stage, cube compressive strength, Young's modulus and

water permeability at the hardened stage were conducted. The results obtained are expected to provide a method to reduce the loss of strength and to improve the water permeability resistance of rubber concrete.

5.2 Experiment details

5.2.1 Materials

The materials used in this chapter comprised cement, tap water, sand, natural gravels, recycled aggregates and waste tyre rubber. Cement (CEM II/B-V 32.5) with 30% PFA was used as a binder for the concrete mixture. Natural river sand having a NMPS of 5 mm was used as fine aggregate. Washed crushed gravels with a NMPS of 10 mm were used as coarse aggregate. Recycled aggregates from a local demolition plant, with the same NMPS, were used to replace 50% of natural coarse aggregates by mass for all five concrete mixes. Figure 5-1 shows the typical composition of recycled concrete aggregates. CSR with continuous grading (blending different sized rubber particles artificially), similar to natural sand (shown in Figure 5-2), was sourced from the local recycling industry to replace 20% of sand by volume. Saturated NaOH solution and SCA were prepared to modify the surface of the rubber particles. Two batches of rubber particles were soaked in saturated NaOH solution for 2 hours and 24 hours, respectively, under ambient conditions. They were then washed with tap water and kept in laboratory condition for 24 hours before using. Another batch was soaked in SCA until the entire surface was coated by the agent before being added into the mixture.

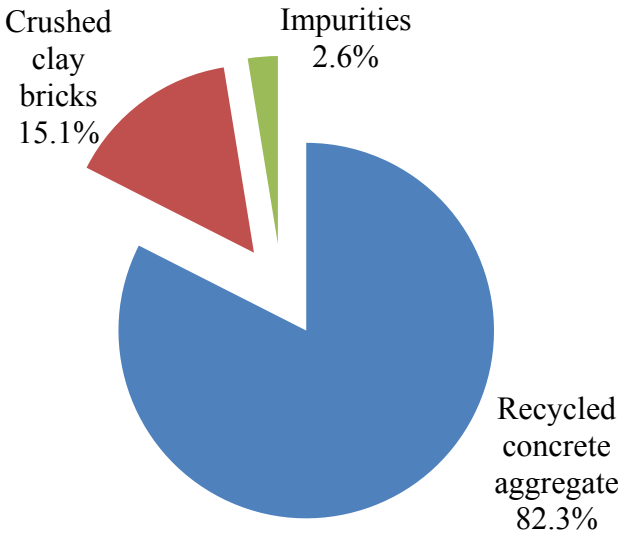

Figure 5-1. Composition of recycled aggregate.

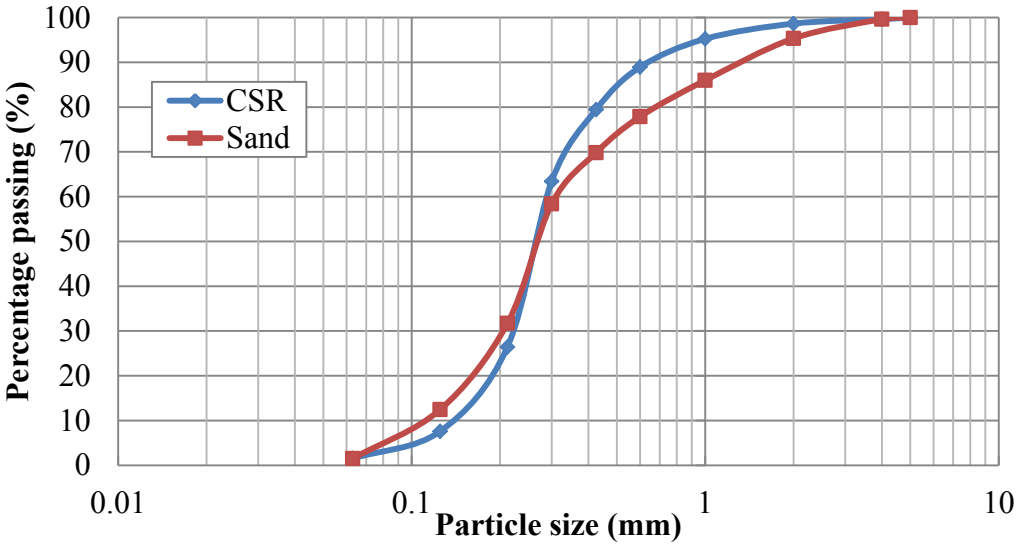

Figure 5-2. Grading curves of sand and rubber particles.

5.2.2 Mix design

The British DoE method widely used for concrete mix design in the UK was adopted in this chapter. The SSD density and SSD water absorption of the aggregates and crumb rubber are shown in Table 5-1. The mix design of the control concrete aimed to achieve a target mean strength (grade C30/37) of 43 MPa at 28 days with a slump value of 60-180 mm. A total of

five concrete mixes were prepared: REF, CCSR-AR, CCSR-N2h, CCSR-N24h and CCSR-SCA. There is no rubber aggregate or recycled aggregate in REF mix. 20% by volume of the sand was replaced with CSR, and 50% by mass of the natural gravels was replaced with recycled aggregate in the other four mixes. The mass ratio of water: binder: sand: natural gravel: recycled aggregate: rubber under the SSD condition is 0.37: 1: 0.66: 0.80: 0.80: 0.064 and all parameters were kept constant throughout the entire experiment programme.

Table 5-1. SSD density and SSD water absorption of natural and rubber aggregates.

Item	Sand	Natural aggregate	Recycled aggregate	CSR
SSD density (kg/m^3)	2512	2581	2539	973
SSD water absorption (%)	1.37	1.26	7.09	8.46

5.2.3 Casting and curing

The required quantity of each item was accurately measured out and placed in a mechanical mixer, which had been wetted on the internal surface. Prior to adding the water, the dry materials were blended for 5 minutes to produce an even distribution. The mixer was then allowed to run after the addition of water for several minutes until there were no visual discrepancies. All of the moulds used, including cube, cylinders and prisms, complied with BS EN 12390-1 [5.32]. Prior to moulding, the moulds were treated with oil to allow smooth specimen faces and free removal of the moulds when de-moulding. All moulds were then filled with fresh concrete in two equal layers, each of which was compacted by using the vibration table. The exposed surface was troughed off to a clean finish, after which polythene sheets were placed over the samples to prevent the moisture loss and early cracking, which

were left for 24 hours in Civil Engineering Laboratory. After 24 hours, the samples were carefully de-moulded and then transferred to the curing water tank where they were immersed in water at the room temperature until they were tested.

5.2.4 Testing

To evaluate the workability of fresh concrete, slump tests were carried out in accordance with BS EN 12350-2 [5.33]. For hardened concrete, cube and cylinder specimens were used to determine the cube compressive strength, and Young's modulus in accordance with BS EN 12390-3 [5.34] and 12390-13 [5.35], respectively. The water permeability index was evaluated to assess the water resistance of each mix. An XRD test was carried out to analyse the crystals and phases of the composites. Scanning optical microscopy was performed to observe the interface between the rubber and the matrix. Finally, the mercury intrusion method was adopted to characterise the pore structures of concrete with various surface modified crumb rubber particles.

5.3 Results and discussion

5.3.1 Rubber surface

Crumb rubber particles were observed by scanning optical microscopy as shown in Figure 5-3. A micrograph of the untreated rubber surface (Figure 5-3(a)) shows that the particle has a rough surface with irregular dents and cracks which were caused during the cutting and grinding of waste tyres. Figures 5-3(b) and 5-3(c) show that, apart from some NaOH crystals

which are loosely attached to the surface of rubber particles, no significant visual differences in the rubber particle surfaces were found compared to untreated rubber. This indicates that NaOH treatment does not markedly alter the surface roughness of the rubber particles. Regarding the SCA-treated rubber, it is quite clear from the micro-image (Figure 5-3(d)) that a coating of gel-like silicone was found on the surface of the rubber particles. A hydrolysis reaction, which is the chemical characteristic of SCA and the primary mechanism of the coupling effect, happens when SCA encounters water. The product of the hydrolysis reaction is silanol, which can not only polymerise with hydroxyls of inorganic material, but can also self-polymerise, generating the silane polymer-silicones [5.36].

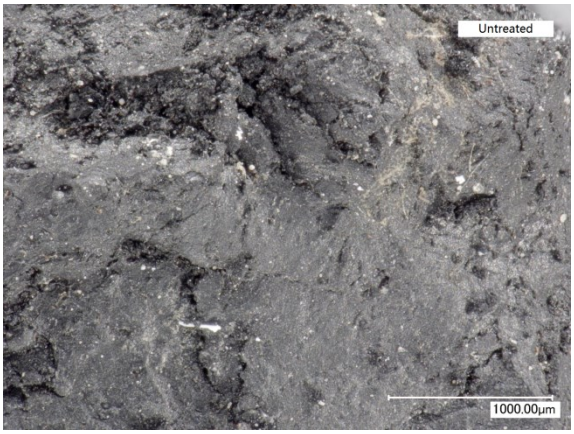

(a). Untreated rubber surface.

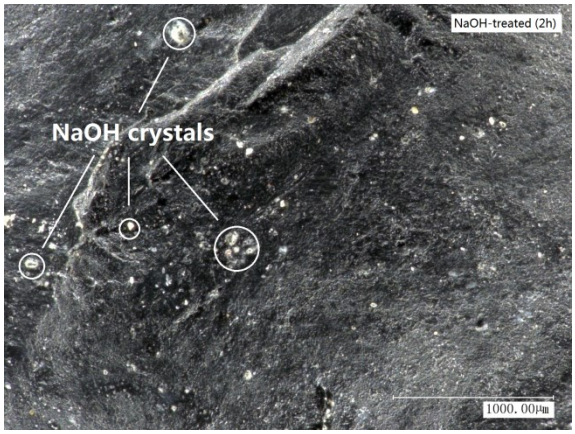

(b). NaOH-treated rubber surface (2h).

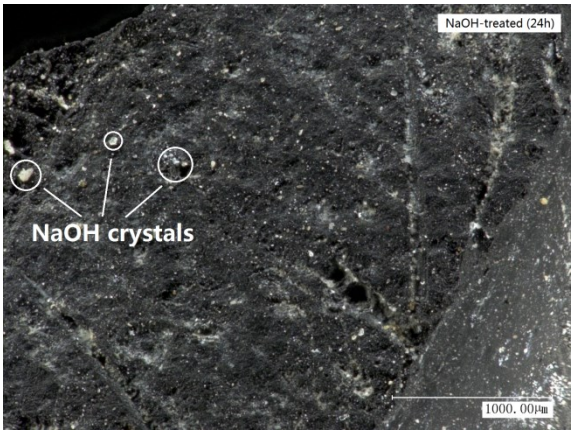

(c). NaOH-treated rubber surface (24h).

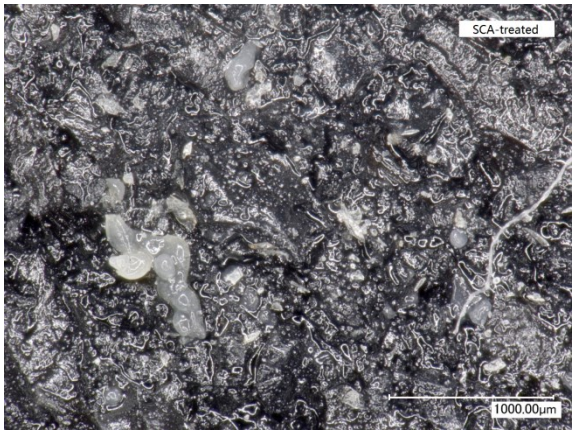

(d) SCA-treated rubber surface.

Figure 5-3. Micrographs of rubber particle surface.

5.3.2 Workability

All the concrete mixes were observed (by visual inspection) to be cohesive with no segregation during the mixing, placing or compaction. Figure 5-4 shows the slump for all five concrete mixes. A slump of 66 mm was recorded for the CCSR-AR. The slump values of the CCSR-N2h, CCSR-N24h and CCSR-SCA concrete mixes were 4.5% (3 mm) higher, 3.0% (2 mm) higher and 13.6% (9 mm) lower than the CCSR-AR mix respectively. This result indicates that the pre-treatment with saturated NaOH solution affects the workability of concrete very slightly, as the slumps with and without pre-treated rubber are quite similar. In contrast, the pre-treatment with SCA decreased the workability noticeably. This is mainly ascribed to the sticky nature of an SCA-treated rubber surface which tends to bond the rubber particles with the matrix, thus making the overall concrete mixture less workable. SCA is an organosilicon compound containing two different reactive groups. One functional group is organophilic, whilst the other polymerises and reacts with the surface of inorganic material. The formula of SCA is $YSi(OR)_3$, where Y is a non-hydrolytic group which tends to bond well the synthetic resin, rubber etc. in organic materials; and OR is a hydrolysable group that will hydrolyse in water to generate an SiOH group which will chemically react with hydroxyl on the surface of inorganic materials (such as silicate) to form a hydrogen bond. A further condensation reaction (dehydration synthesis) will then take place to form an oxygen covalent bond, and finally the surface of the inorganic material will be covered by the reaction products, thereby enhancing the cohesiveness [5.36]. The reaction process is shown in Figure 5-5. Because of the special molecular structure of SCA which can react with both organic and inorganic materials to form chemical bonds, two kinds of materials with different types of chemical structures can be well connected on their interface, thus decreasing the

workability. In practical production, this can be easily corrected by adding a commonly available admixture such as a super-plasticiser.

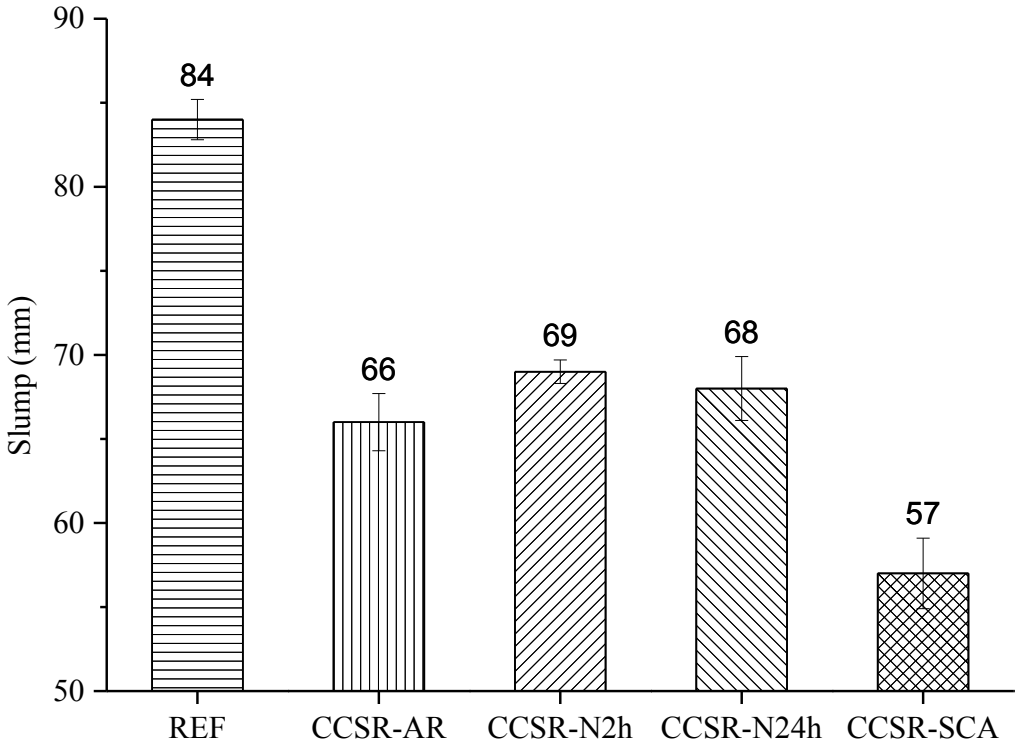

Figure 5-4. Slump test results of all the mixes.

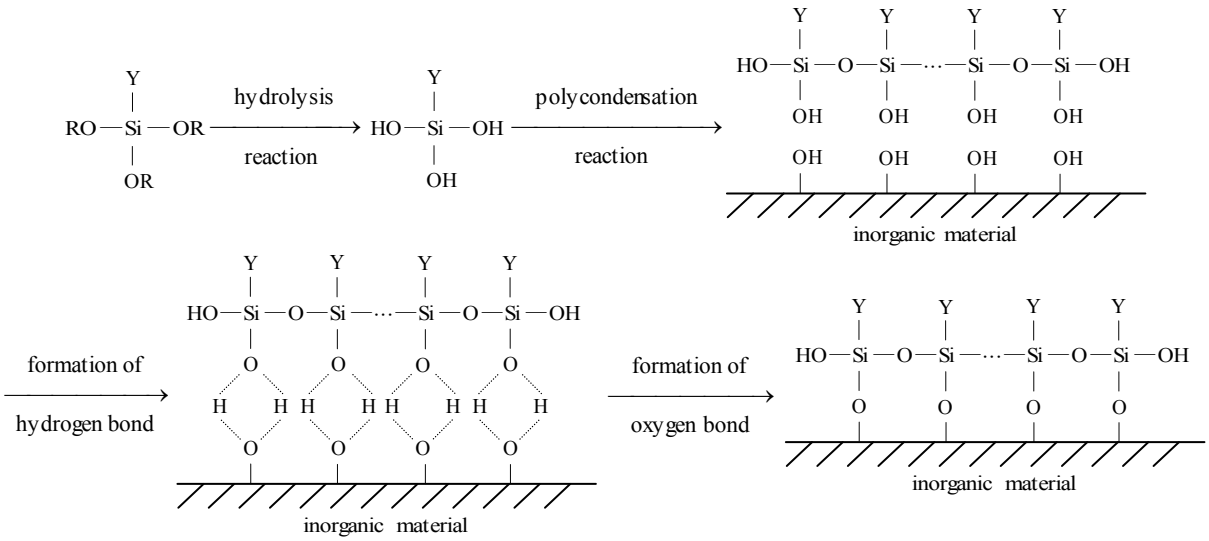

Figure 5-5. Reaction process of SCA with inorganic materials.

5.3.3 Compressive strength and Young's modulus

Compressive strength tests for different mixes were carried out at 1 day, 7 days and 28 days. The results are shown in Figure 5-6. The 1 day compressive strengths of CCSR-N2h and CCSR-N24h were 2.4% (0.2 MPa) lower and 1.2% (0.1 MPa) higher than CCSR-AR, respectively. However, the value of CCSR-SCA was 1.6 MPa, which is 19.3% higher than that of CCSR-AR. The 7 days compressive strengths of CCSR-N2h, CCSR-N24h and CCSR-SCA were 5.2% (1 MPa) lower, 2.6% (0.5 MPa) higher and 9.3% (1.8 MPa) higher than CCSR-AR, respectively. The 28 days compressive strengths of CCSR-N2h, CCSR-N24h and CCSR-SCA were 2.2% (0.8 MPa) lower, 0.8% (0.3 MPa) higher and 6.8% (2.5 MPa) higher than CCSR-AR, respectively. These results indicate that the improvement in compressive strength of the mixes containing NaOH pre-treated (2 hours and 24 hours) rubber is modest compared to the mix with untreated rubber. It can be further deduced that the surface modification of rubber particles by SCA has a better effect on the compressive strength enhancement than that treated with saturated NaOH solution (less than 24 hours). This conclusion is also applicable to the properties of the Young's modulus. The Young's moduli of CCSR-AR, CCSR-N2h and CCSR-N24h at 28 days were 22.1, 22.3 and 22.4 GPa, respectively, as shown in Figure 5-7. The difference between them is rather modest. The result of CCSR-SCA in terms of the Young's modulus was 23.8 GPa, which is 7.7% higher than that of CCSR-AR.

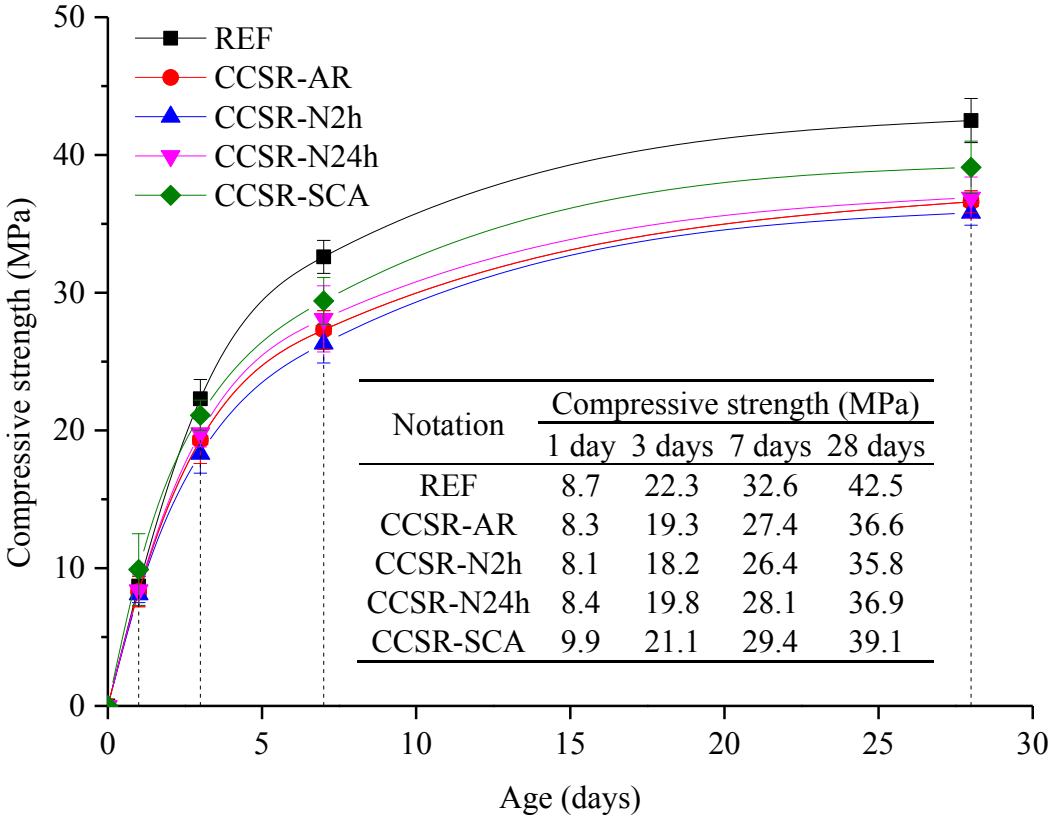

Notation	Compressive strength (MPa)			
	1 day	3 days	7 days	28 days
REF	8.7	22.3	32.6	42.5
CCSR-AR	8.3	19.3	27.4	36.6
CCSR-N2h	8.1	18.2	26.4	35.8
CCSR-N24h	8.4	19.8	28.1	36.9
CCSR-SCA	9.9	21.1	29.4	39.1

Figure 5-6. Cube compressive strength test results of all mixes.

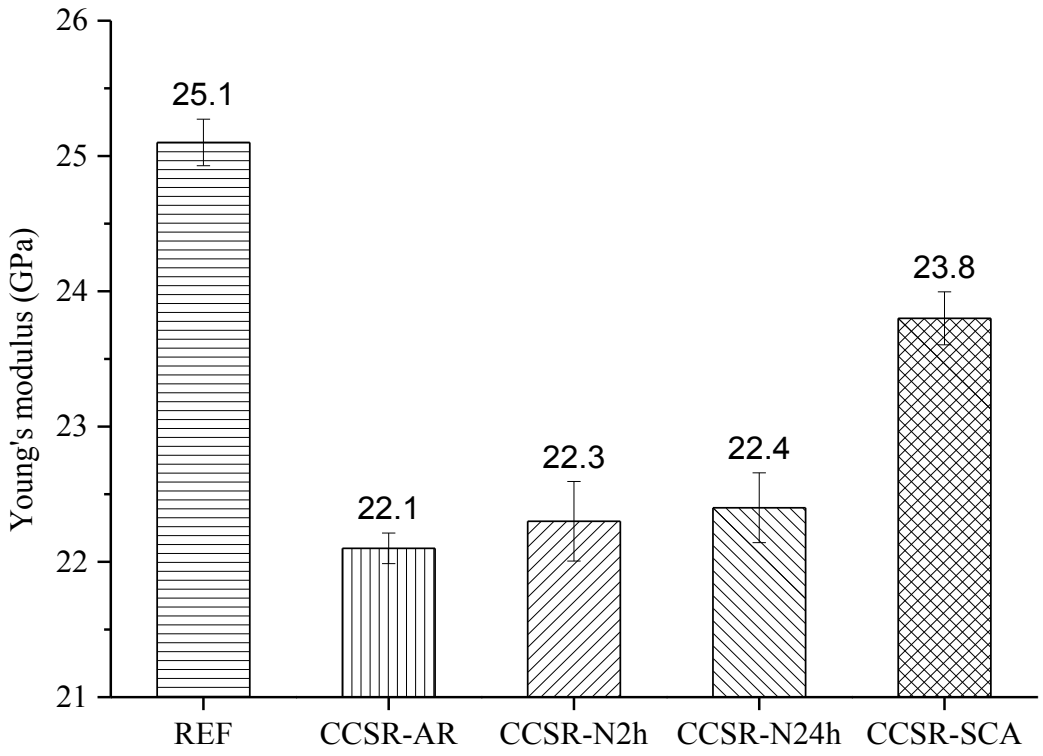

Figure 5-7. Young's modulus test results of all the mixes.

The above conclusions were supported by the microscopic inspections and analysis of the crushed sample particles at 28 days. The rubber-matrix interface was inspected by scanning optical microscopy, which was performed by using Keyence VHX-700F series optical microscope, shown in Figure 5-8. Detailed investigations on 10 rubber particles of each specimen were performed. Micrographs of typical fracture surfaces are shown in Figures 5-9 to 5-11. As shown in Figure 5-9(a), it is quite clear that there is a distinct crack highlighted by the curve in Zone I. From the 3D image (Figure 5-9(b)), significant discontinuity in Zone II was found. Faults and cracks observed at the rubber-matrix interface indicate that the untreated rubber-concrete matrix adhesion is poor. Similar phenomena are also found in concrete samples CCSR-N2h and CCSR-N24h, as shown in Figure 5-10. No obvious difference was revealed after the rubber was treated with NaOH. The modest effect of NaOH treatment may be attributed to the limited roughness gained from the surface treatment of rubber particles by being soaked in saturated NaOH solution for less than 24 hours. From the micrograph of CCSR-N24h (Figure 5-10(b)), it can be seen that two cracks initialised from the surface of the rubber particle. This may be ascribed to the fact that the stiffness of rubber is low compared to the mineral aggregates. Rubber particles can be deemed as voids, and stress concentration usually arises at the interface between a rubber particle and the matrix. In the micrograph of CCSR-SCA (Figure 5-11(a)), a well-developed adhesive joint area is observed between the SCA-treated rubber particles and the matrix, where the adhesion promoter has diffused to both substrate materials. From its 3D image shown in Figure 5-11(b), it can be seen that the transition zone between the rubber particle and the concrete matrix is very smooth, in contrast to the counterpart of CCSR-AR as shown in Figure 5-9(b) where a clear trough can be observed in Zone II. The observation for the CCSR-SCA specimen suggests that there is a relatively stronger bond at the interface. The mechanism of this

increase in bond strength, as illustrated above, is that the nature of SCA plays an enhanced role in developing bonding between organic and inorganic materials, leading to the improvements in strength.

Figure 5-8. Keyence VHX-700F series optical microscope.

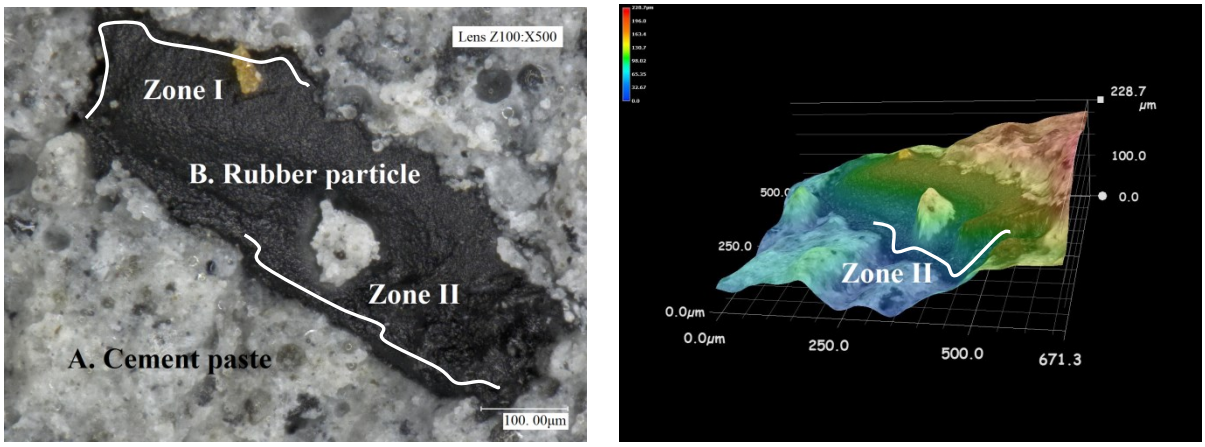

(a) (b)

Figure 5-9. Rubber-cement paste interface of CCSR-AR, (a) micrograph and (b) 3D image.

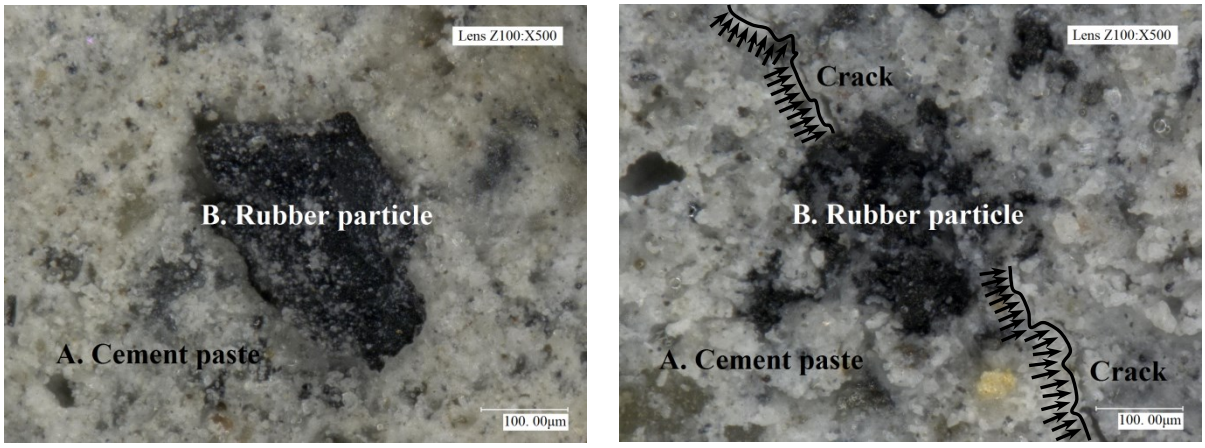

(a) (b)

Figure 5-10. Micrographs of rubber-cement paste interface of (a) CCSR-N2h and (b) CCSR-N24h.

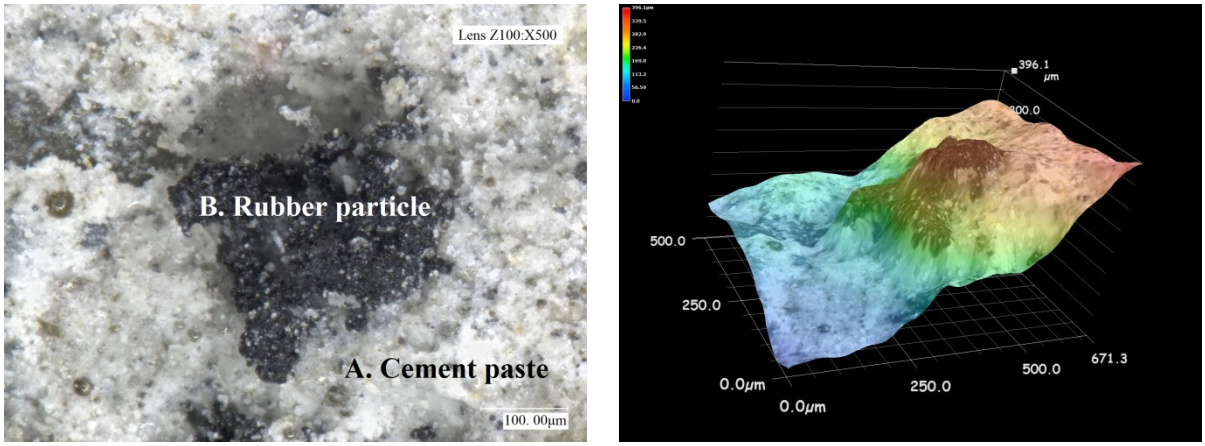

(a) (b)

Figure 5-11. Rubber-cement paste interface of CCSR-SCA, (a) micrograph and (b) 3D image.

XRD analysis for the CCSR-AR, CCSR-N2h, CCSR-N24h and CCSR-SCA mixes were also carried out. Crushed sample particle was placed in a rubber container, followed by filling with liquid resin. After solidification, the sample was demoulded and ground until the surface of concrete particle can be tested by X-ray (Figure 5-12). The device used for this test is D8 Discover from Bruker Corporation shown in Figure 5-13, with the testing results shown in

Figure 5-14. The diffraction pattern reveals a very intense diffraction peak A around 27 degrees which means that the major crystalline phase was quartz (SiO_2). Another major crystalline phase was calcite ($CaCO_3$) which is identified from the analysis of diffraction peak B. Apart from these two primary phases, the formation of germanium iron (Fe_3Ge), and Gismondine ($CaAl_2Si_2O_8 \cdot 4H_2O$) were observed, as well as a small quantity of sabinaite ($Na_4Zr_2TiO_4(CO_3)_4$), tacharanite ($Ca_{12}Al_2Si_{18}O_{51} \cdot 18H_2O$) and retgersite ($NiSO_4 \cdot 6H_2O$). The angles and intensities of the diffraction peaks of the four samples are quite similar to each other, indicating hardly any difference, which means that the compositions are almost the same among these four samples. In other words, the pre-treatment by NaOH solution or by SCA does not change the phase of rubber concrete significantly.

Figure 5-12. Concrete particle sample for XRD test.

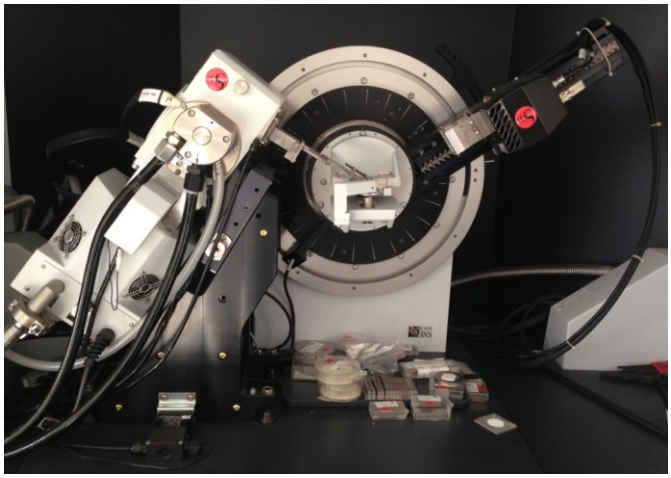

Figure 5-13. XRD test device.

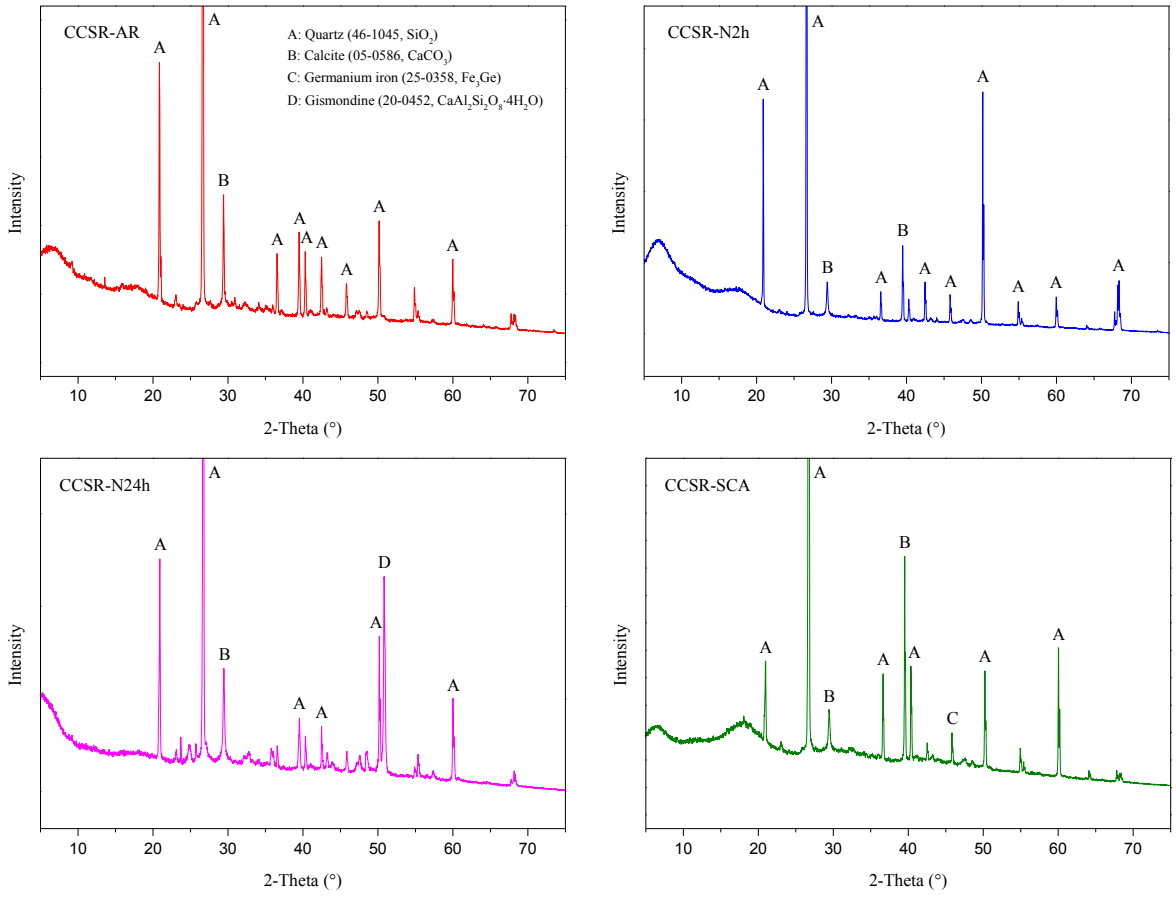

Figure 5-14. X-ray diffraction pattern of different samples.

5.3.4 Water permeability

A water permeability test was performed using the Autoclam test equipment shown in Figure 3-9. The test was performed as a modified version of the ISAT. 100 mm cube specimens were preconditioned (by being sheltered for one week) before the water permeability test was undertaken. The cumulative flow of water into the concrete cube at a pressure of 500 mbar was recorded every minute for 15 minutes. Figure 5-15 shows the volume of water flowing plotted against the square root of time, in accordance with the recommendations of The Concrete Society [5.37]. A regression equation for each specimen can be determined, and the

gradient of the line between the 5th and the 15th reading is known as the water permeability index. From the results of the graph, it was found that the water permeability indices of CCSR-AR, CCSR-N2h, CCSR-N24h and CCSR-SCA were 2.51, 2.43, 2.41 and 2.18 $m^3 \times 10^{-7}/\sqrt{min}$ respectively. The indices of the CCSR-N2h and CCSR-N24h mixes were approximately 96.4% of the CCSR-AR mix, while that of CCSR-SCA was 86.9%. This means that the surface modified rubber will improve the water permeability resistance compared to the as-received rubber. However, the effect of NaOH treated rubber (for less than 24 hours) is not as significant as SCA-treated rubber. The pre-treatment by SCA improves the adhesion between the rubber and the matrix and hence reduces the void or micro-crack size, and consequently reduces the micro-conduits through which water can penetrate.

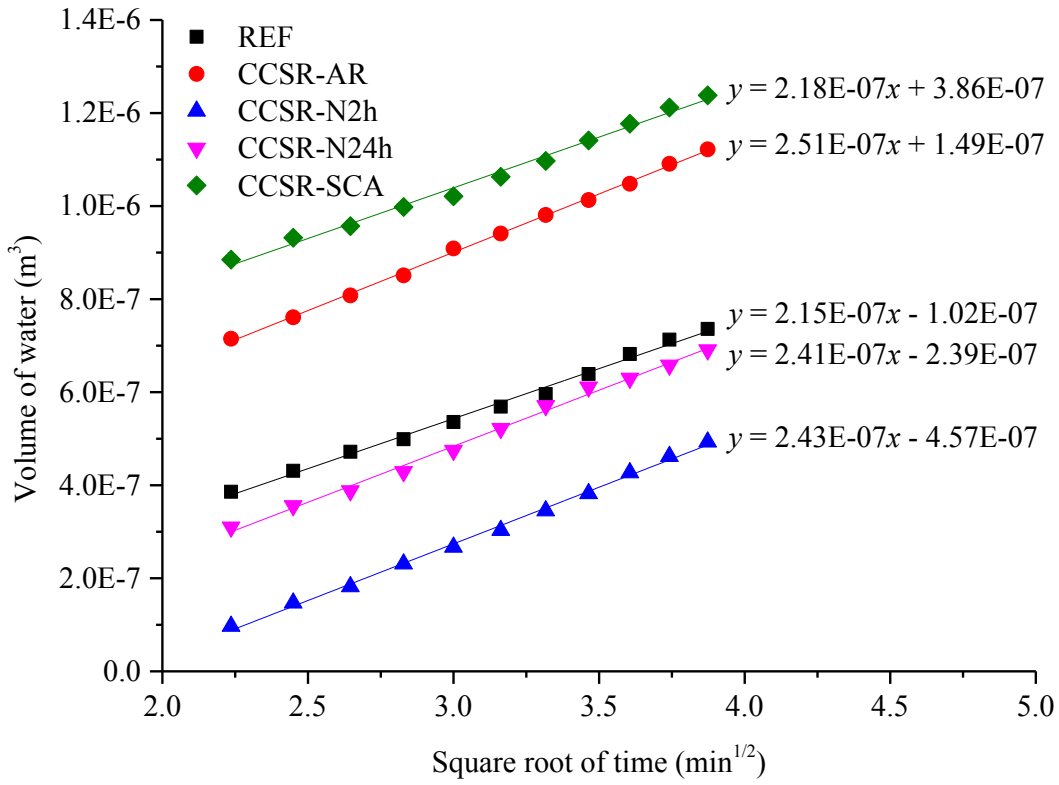

Figure 5-15. Volume of water flowing into specimen with time.

The above phenomenalistic observations are supported by the results of the mercury intrusion porosimetry test. The device used is AutoPore IV 9500 from Micromeritics Instrument Corporation, shown in Figure 5-16. The samples used were 5 mm cubes which were mechanically cut from untested concrete and they were oven dried at 105ºC for 24 hours before the test to remove water attached. Table 5-2 shows the porosity and tortuosity of the different mixes. The porosity of CCSR-SCA was the lowest one, which was 6.5% less than CCSR-AR. CCSR-N2h and CCSR-N24h were 4.3% and 3.9% lower than CCSR-AR, respectively. The difference between CCSR-N2h and CCSR-N24h was insignificant. The values of tortuosity for CCSR-N2h and CCSR-N24h were 4 and 10 higher than CCSR-AR, respectively. The value of CCSR-SCA was the highest, and this was 47 higher than CCSR-AR. This can be explained by the effect of SCA, causing the bonding between the rubber particles and the concrete matrix to be enhanced. The concrete mixture of CCSR-SCA was denser than CCSR-AR, leading to the lower porosity. Besides, because the conduits through which water can flow were reduced, water needs to find a longer path to travel from one pore to another, which means that the water permeability resistance was improved. Figures 5-17 and 5-18 show the pore size distribution of the different mixes. It can be seen that the four mixes have a similar trend in terms of pore size distribution. The range of the pore size is from 6 nm to 5×10^5 nm, with most being between 6 nm and 11 nm. The volume of intruded mercury increased sharply when the pore size was below 100 nm for each mix. It is quite clear from Figure 5-18 that when the pore diameter is greater than 11 nm, the mercury intrusion of the four samples is almost the same. When the pore diameter is around 7 nm or 9 nm, the mercury intrusion of CCSR-AR is much higher than that of the other three samples. CCSR-N2h and CCSR-N24h are much closer to each other in terms of mercury intrusion.

CCSR-SCA shows the lowest volume of intruded mercury in general, which confirms that it has the lowest porosity, leading to the best water permeability resistance of the four samples.

Figure 5-16. AutoPore IV 9500 from Micromeritics Instrument Corporation.

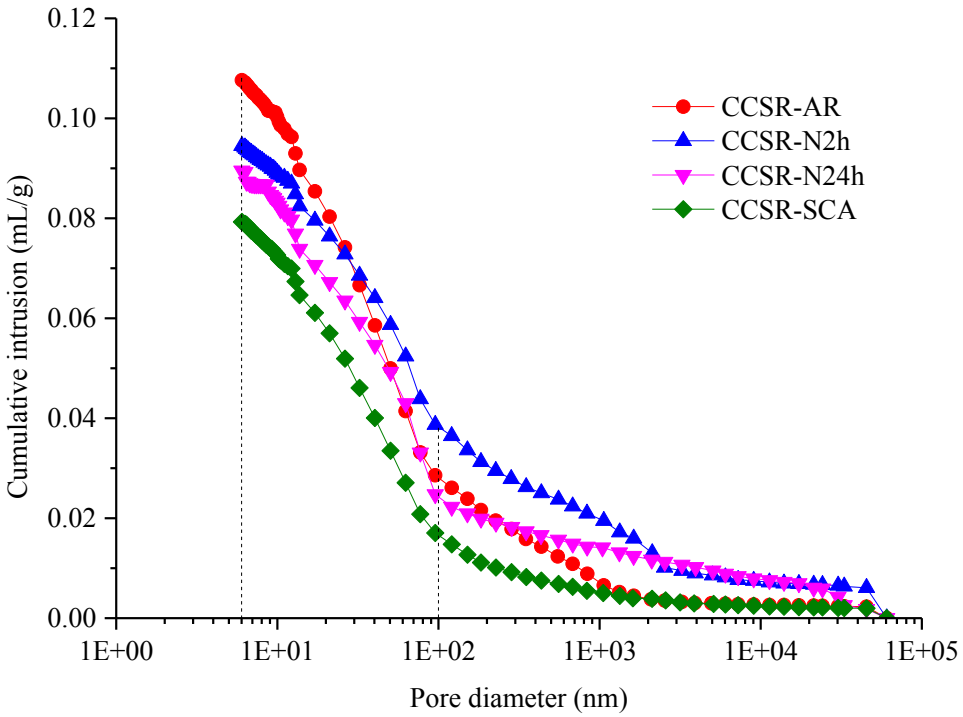

Figure 5-17. Pore size distribution of different mixes (cumulative intrusion vs pore diameter).

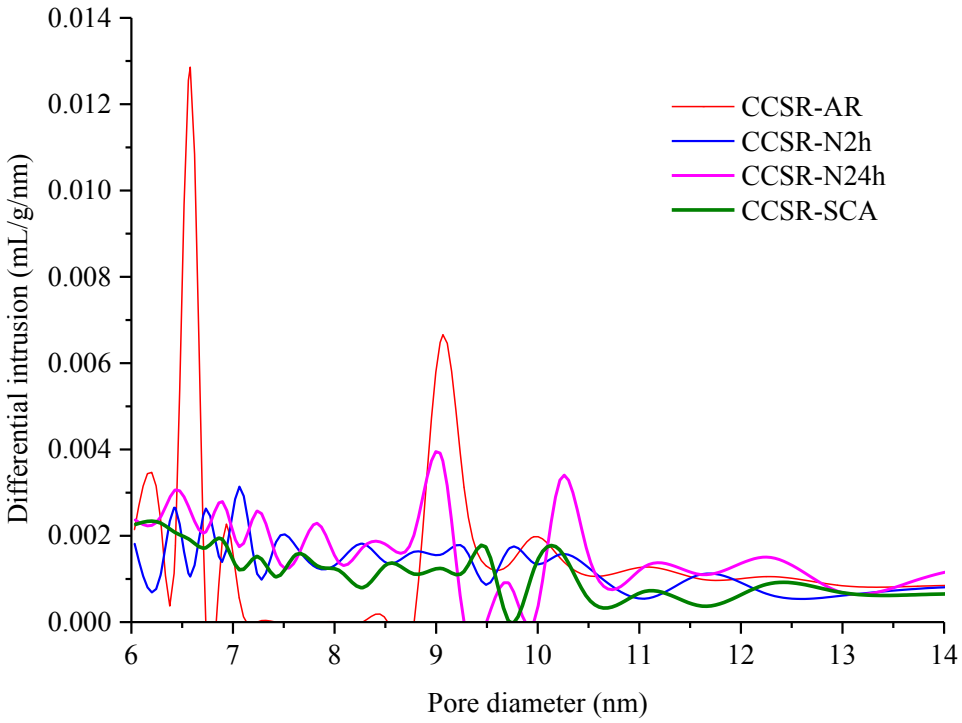

Figure 5-18. Pore size distribution of different mixes (differential intrusion vs pore diameter).

Table 5-2. Porosity and tortuosity of different mixes.

Notation	Porosity (%)	Tortuosity
CCSR-AR	20.5	116
CCSR-N2h	16.2	120
CCSR-N24h	16.6	126
CCSR-SCA	14.0	163

5.4 Effect of SCA usage on the loss of compressive strength of rubber concrete

It can be deduced from the above conclusions that SCA has a positive effect on reducing the loss of strength of rubber concrete. Therefore, further study in the influence of SCA usage on the loss of compressive strength of rubber concrete was also carried out.

5.4.1 Materials and experimental details

Raw materials of concrete used in this section are totally the same as those described in Section 5.2.1. The mix design of normal concrete in this section aimed to achieve a target mean strength of 43 MPa at 28 days with a slump value of 60-180 mm. Recycled aggregate was used to replace 50 wt% of gravel while CSR was used to replace 20 vol% of sand. Five batches of concrete with SCA-modified rubber (abbreviated as SCA-*x*, where *x* represents 0, 5%, 10%, 15% and 20% mass fraction of SCA) were prepared. The content of water, cement, gravel, recycled aggregate, sand and rubber was 232, 627, 501, 501, 414 and 40 kg/m^3, respectively.

Chemically pure SCA was diluted to certain mass fraction and rubber particles were soaked in SCA solution until the entire surface was coated. The raw materials were mixed and the resulting mixture was cast into 100 mm cube specimens. They were cured in a water tank maintained at a temperature of 20°C until the required age. The 1, 7 and 28 days cube compressive strength of hardened concrete were tested according to BS EN 12390-3 [5.34]. Three repeated experiments on duplicates were conducted and mean of the values was set as the final result for each test.

5.4.2 Compressive strength

Results of compressive strength at different ages are shown in Figure 5-19. Although none of them reached the target mean strength of 43 MPa at 28 days due to the existence of rubber,

concrete with SCA-modified rubber had an obviously higher compressive strength than with as-received rubber, and the strength increased with the increase of mass fraction of SCA solution. This is mainly ascribed to the nature of SCA. In section 5.3.2, it has been explained that SCA is an organosilicon compound containing two different reactive groups. One is organophilic whilst the other readily polymerises and reacts with inorganic material. The chemical formula of SCA is $YSi(OR)_3$, where Y is a non-hydrolytic group which tends to well bond synthetic resin, rubber etc. and OR is a hydrolysable group which will hydrolyse in water to generate a silanol group which will chemically react with hydroxyl on the surface of inorganic materials (such as silicate) to form a hydrogen bond. A further condensation reaction (dehydration synthesis) will happen to form an oxygen covalent bond, and finally the surface of the inorganic material will be covered by the reaction products, thereby enhancing the cohesiveness [5.36]. The reaction process of SCA and inorganic materials is shown in Figure 5-5. Overall, the mechanism of this enhanced adhesion is that because of the special molecular structure of SCA, organic rubber particles and inorganic concrete mixture can be well connected on their surface, thus increasing bond strength of interface. Besides, the increment at 1 day was up to 32.5%, which was much higher than 17.6% and 12.3% at 7 and 28 days. It means the effect of reduction caused by SCA on loss of strength is more significant at early age when concrete is weak.

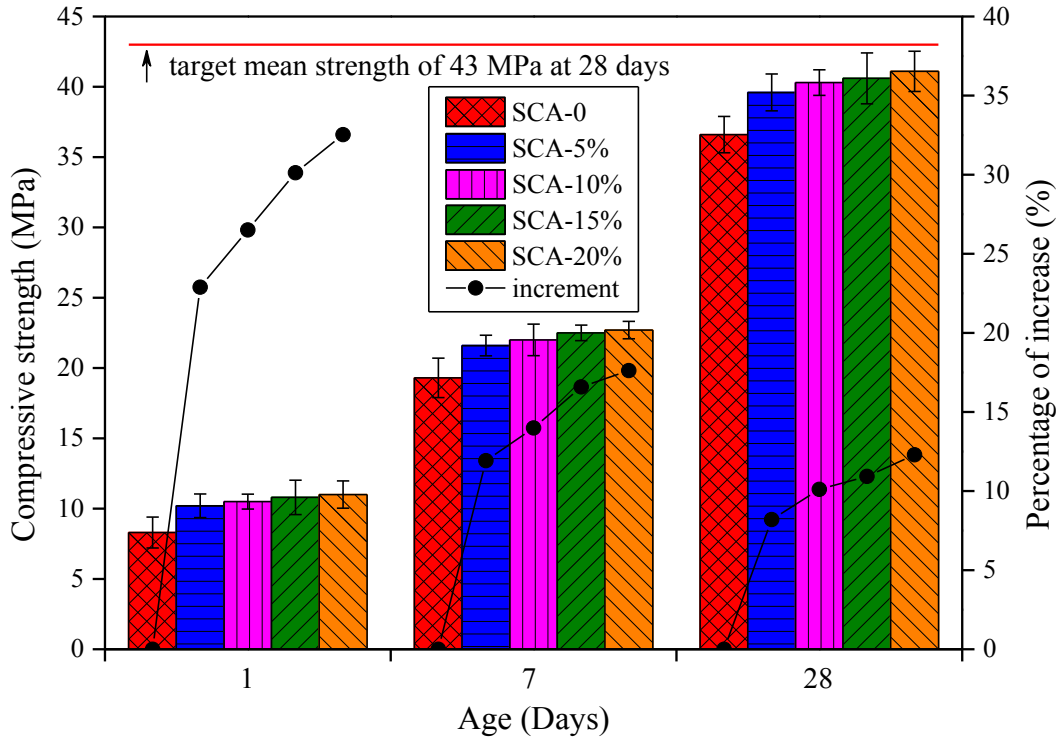

Figure 5-19. Compressive strength of different batches of concrete mixture at 1, 7 and 28 days.

5.4.3 XRD analysis

Comparison of XRD for the concrete with as-received and SCA-modified rubber was conducted. Figure 5-20 reveals some very intense diffraction peaks which were identified to be quartz and calcite of the major crystalline phases. The angles and intensities of the diffraction peaks of the two diffraction patterns are quite similar, indicating almost the same composition. In other words, modification on rubber surface by SCA does not change the phase of cement-based rubber concrete significantly. Therefore, it can be further deduced that the nature of cohesion of SCA plays an important role in enhancing the bond strength.

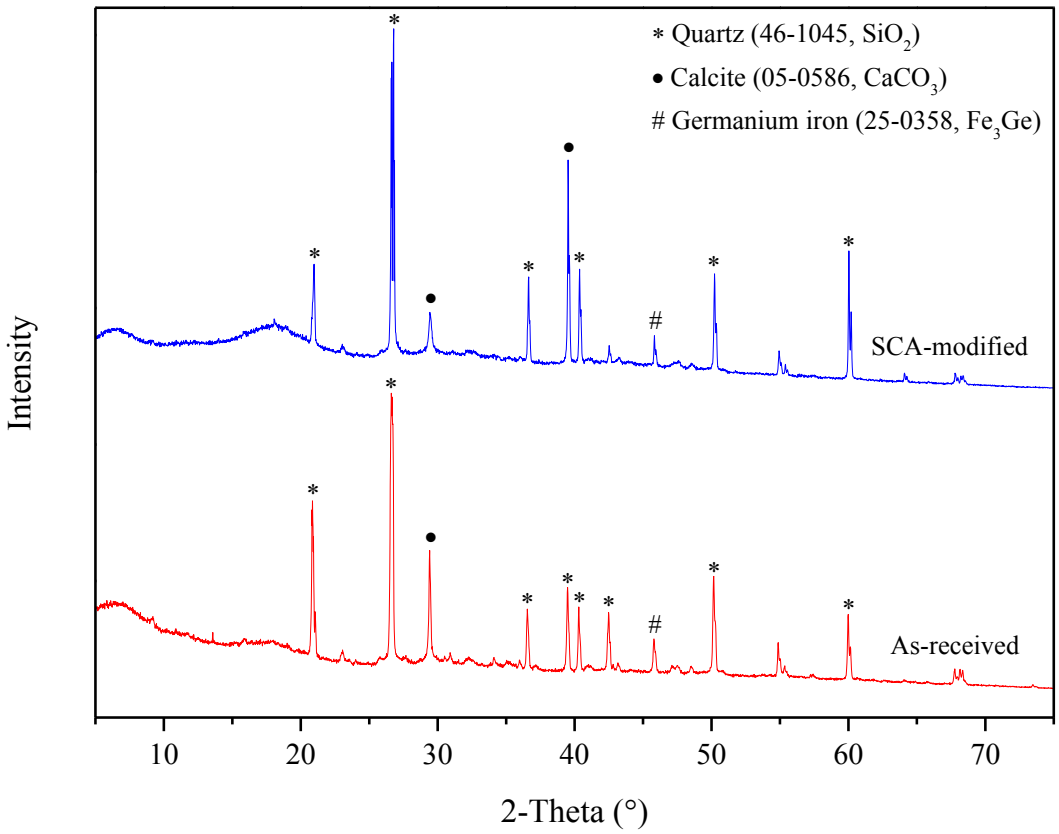

Figure 5-20. X-ray diffraction patterns of concrete with as-received and SCA-modified rubber.

5.5 Cost analysis

The price of rubber crumb used in this study is £240 per ton, higher than the price of natural river sand which is around £35 per ton. However, based on the mix design, if 20% of natural river sand is replaced by rubber crumbs by volume, a batch of 24 m^3 rubber concrete roughly needs 1 ton rubber crumb. The price ratio of crumb rubber to concrete can be calculated as £240 / (£100/m^3 × 24 m^3), equal to 1/10. So the cost of rubber accounts for approximately one tenth of the total cost of resulting cost, which is rather limited.

The price of chemically pure SCA and solid NaOH powders is about £20 and £2 per kilo, respectively. The SCA powder needs to be diluted to 1% of mass fraction before using for treating crumb rubber. The solid NaOH power is dissolved in water to prepare saturated NaOH solution. Solubility of NaOH under laboratory temperature 20°C is 109 g / (100g water). Table 5-3 shows the details on the capital cost. It can be found that the cost of SCA solution is around £8 per cubic concrete which is much cheaper than the cost of NaOH solution, i.e. £44 per cubic concrete. In practice, the solution can be reused for many times. As such, the extra cost of the treatment solution is reasonably low. Besides, tax will be levied for disposing waste tyres. The saved expense of tax by reusing the waste tyre can almost offset the additional costs introduced by the crumb rubber and its surface treatment, which makes this application economically viable.

Besides, a more important sustainability credential from the rubber concrete using waste tyres lies on the environmental aspect, where it not only can reduce the production of wastes but also alleviate the diminishing of natural resources. The improved performance of resulting concrete such as enhanced ductility and energy absorption is another positive driver of utilizing this type of concrete.

Table 5-3. Cost of different treatment solutions.

Item	Cost of chemically pure material (£/kg)	Cost of solution (£/kg)	Cost per unit concrete (£/m^3)
SCA	20	0.20	8.54
NaOH	2	1.04	44.41

5.6 Summary

In this chapter, the effect of rubber surface modifications by saturated NaOH solution and SCA on the concrete properties of workability, compressive strength, Young's modulus and water permeability, was investigated. The main findings include that the surface modified rubber pre-treated with SCA has a more positive effect on the concrete properties than that treated with saturated NaOH solution. Pre-treatment with saturated NaOH solution for less than 24 hours does not produce significant changes in the properties of concrete compared to concrete containing as-received rubber. However, compared to the control mix, the pre-treatment with SCA that acts as an adhesion promoter enhances the adhesion of tyre rubber particles to the matrix, resulting in (1) a reduction in the slump values of fresh concrete by 13.6%; (2) an improvement in the compressive strength of hardened concrete by 19.3% at 1 day, 9.3% at 7 days, and 6.8% at 28 days; (3) an increase in the Young's modulus of hardened concrete by 7.7% at 28 days; and (4) a decrease of the water permeability index of hardened concrete by 13.1%. The scanning optical microscopic inspection of test specimens showed that the rubber-matrix adhesion was enhanced with the use of SCA. The XRD data of the different mixes shows similar diffraction patterns, which means that pre-treatment by saturated NaOH solution or by SCA does not change the crystalline phase of rubber concrete significantly. The mercury intrusion porosimetry test showed that concrete with SCA-treated rubber has a similar pore size distribution to the control mix and to the concrete with NaOH-treated rubber, but it achieved the lowest porosity and the highest tortuosity, which results in the best water permeability resistance. In addition, it is experimentally shown that SCA has a positive effect on improving strength of cement-based rubber concrete containing recycled aggregate, especially when concrete is weak. This effect becomes more significant with the

increase of mass fraction of SCA solution. The nature of cohesion of SCA has been demonstrated to play an important role in improving the adhesion in interfacial transition zone, leading to an enhancement of bond strength of interface between rubber and cement paste. It offers an approach to reduce the loss of strength for cement-based rubber concrete, which is potential for practical application. A brief cost analysis was also carried out, demonstrating the economical viability of this type of rubber concrete that uses waste tyres. This feature, together with the well accepted sustainable attractiveness and technical benefits, reinforce the potential prospects of this concrete material.

References

[5.1] M. Nehdi, A. Khan, Cementitious composites containing recycled tire rubber: an overview of engineering properties and potential application, Cem. Concr. Aggr. 23 (2001) 3-10.

[5.2] D. Raghavan, H. Huynh, C.F. Ferraris, Workability, mechanical properties, and chemical stability of a recycled tyre rubber-filled cementitious composite, J. Mater. Sci. 33 (1998) 1745-1752.

[5.3] D.S.V. Prasad, G.V.R.P. Raju, M.A. Kumar, Utilization of industrial waste in flexible pavement construction, E. J. Geotec. Eng. 13 (2001) 1-12.

[5.4] C. Albano, N. Camacho, J. Reyes, J.L. Feliu, M. Hernández, Influence of scrap rubber addition to Portland I concrete composites: destructive and non-destructive testing, Compos. Struct. 71 (2005) 439-446.

[5.5] M.A. Aiello, F. Leuzzi, Waste tyre rubberized concrete: properties at fresh and hardened state, Waste Manage. 30 (2010) 1696-1704.

[5.6] A. Benazzouk, O. Douzane, T. Langlet, K. Mezreb, J.M. Roucoult, M. Quéneudec, Physico-mechanical properties and water absorption of cement composite containing shredded rubber wastes, Cem. Concr. Comp. 29 (2007) 732-740.

[5.7] M.C. Bignozzi, F. Sandrolini, Tyre rubber waste recycling in self-compacting concrete, Cem. Concr. Res. 36 (2006) 735-736.

[5.8] N.N. Eldin, A.B. Senouci, Observations on rubberized concrete behavior, Cem. Concr. Aggr. 15 (1993) 74-84.

[5.9] E. Ganjian, M. Khorami, A.A. Maghsoudi, Scrap-tyre-rubber replacement for aggregate and filler in concrete, Constr. Build. Mater. 23 (2009) 1828-1836.

[5.10] E. Guneyisi, M. Gesoglu, T. Ozturan, Properties of rubberized concretes containing silica fume, Cem. Concr. Res. 34 (2004) 2309-2317.

[5.11] A.R. Khaloo, M. Dehestani, P. Rahmatabadi, Mechanical properties of concrete containing a high volume of tire-rubber particles, Waste Manage. 28 (2008) 2472-2482.

[5.12] Z.K. Khatib, F.M. Bayomy, Rubberized Portland cement concrete, J. Mater. Civil Eng. 11 (1999) 206-213.

[5.13] L. Yang, Z. Han, C. Li, Strength and flexural strain of CRC specimens at low temperature, Constr. Build. Mater. 25 (2011) 906-910.

[5.14] L.-J. Li, Z.-Z. Chen, W.-F. Xie, F. Liu, Experimental study of recycled rubber-filled high-strength concrete, Mag. Concr. Res. 61 (2009) 549-556.

[5.15] H.A. Toutanji, The use of rubber tire particles in concrete to replace mineral aggregates, Cem. Concr. Comp. 18 (1996) 135-139.

[5.16] B.Z. Savas, S. Ahmad, D. Fedroff, Freeze-thaw durability of concrete with ground waste tire rubber, Transport. Res. Rec. 1574 (1997) 80-88.

[5.17] İ.B. Topçu, The properties of rubberized concretes, Cem. Concr. Res. 25 (1995) 304-310.

[5.18] D.G. Snelson, J.M. Kinuthia, P.A. Davies, S.R. Chang, Sustainable construction: composite use of tyres and ash in concrete, Waste Manage. 29 (2009) 360-367.

[5.19] R. Siddique, T.R. Naik, Properties of concrete containing scrap-tire rubber – an overview, Waste Manage. 24 (2004) 563-569.

[5.20] M.W. Tantala, J.A. Lepore, I. Zandi, Quasi-elastic behavior of rubber included concrete (RIC) using waste rubber tires, Proceedings of the 12th International Conference on Solid Waste Technology and Management, Philadelphia, USA, 1996.

[5.21] N. Segre, I. Joekes, Use of tire rubber particles as addition to cement paste, Cem. Concr. Res. 30 (2000) 1421-1425.

[5.22] İ.B. Topçu, N. Avcular, Analysis of rubberized concrete as a composite material, Cem. Concr. Res. 27 (1997) 1135-1139.

[5.23] T. Ling, Prediction of density and compressive strength for rubberized concrete blocks, Constr. Build. Mater. 25 (2011) 4303-4306.

[5.24] G. Li, M.A. Stubblefield, G. Garrick, J. Eggers, C. Abadie, B. Huang, Development of waste tire modified concrete, Cem. Concr. Res. 34 (2004) 2283-2289.

[5.25] H.S. Gokce, O. Simsek, The effects of waste concrete properties on recycled aggregate concrete properties, Mag. Concr. Res. 65 (2013) 844-854.

[5.26] T.C. Hansen, H. Narud, Strength of recycled concrete made from crushed concrete coarse aggregate, Concr. Int. Design. Constr. 5 (1983) 79-83.

[5.27] C.S. Poon, Z.H. Shui, L. Lam, Effect of microstructure of ITZ on compressive strength of concrete prepared with recycled aggregates, Constr. Build. Mater. 18 (2004) 461-468.

[5.28] R.S. Ravindrajah, Y.H. Loo, C.T. Tam, Strength evaluation of recycled aggregate concrete by in-situ tests, Mater. Struct. 21 (2006) 289-295.

[5.29] P. Saravanakumar, G. Dhinakaran, Durability aspects of HVFA-based recycled aggregate concrete, Mag. Concr. Res. 66 (2014) 186-195.

[5.30] B. Singh, D.K. Sahoo, N.M. Jacob, Efficiency factors of recycled aggregate concrete bottle shaped struts, Mag. Concr. Res. 65 (2013) 878-887.

[5.31] J. Yang, Q. Du, Y.W. Bao, Concrete with recycled concrete aggregate and crushed clay bricks, Constr. Build. Mater. 25 (2011) 1935-1945.

[5.32] BS EN 12390-1, Testing Hardened Concrete. Shape, Dimensions and Other Requirements for Specimens and Moulds, British Standards Institution, 2009.

[5.33] BS EN 12350-2, Testing Fresh Concrete. Slump-test, British Standards Institution, 2009.

[5.34] BS EN 12390-3, Testing Hardened Concrete. Compressive Strength of Test Specimens, British Standards Institution, 2009.

[5.35] BS EN 12390-13, Testing Hardened Concrete. Determination of Secant Modulus of Elasticity in Compression, British Standards Institution, 2009.

[5.36] M. Xanthos, Functional Fillers for Plastics. Wiley-VCH, Germany, 59-83, 2005.

[5.37] Technical report No. 31 – Permeability Testing of Site Concrete, The Concrete Society, 2008.

CHAPTER 6

EFFECT OF SURFACE-MODIFIED WASTE TYRE RUBBER AGGREGATE ON FLEXURAL PROPERTIES AND FATIGUE PERFORMANCE OF RECYCLED AGGREGATE CONCRETE

6.1 Introduction

Demolished building concrete and waste tyres are two types of common wastes in construction and automobile industry, respectively. Construction and demolition wastes not only occupy a large volume of decreasing land, but also cause much dust during transportation and landfill, resulting in soil, water and air pollution. Waste tyres have presented a pressing global issue which is known as 'black pollution' because they are not readily degradable and may create fire hazards, posing a potential threat to the environment and human health [6.1], [6.2]. From the viewpoint of sustainability, they have been reused to replace aggregates in concrete with the purpose of lessening their negative influence on the environment. So far, numerous researches have been carried out and well developed on the properties of recycled aggregate concrete and rubber concrete. In the field of recycled aggregate concrete, most researchers agree that the strength gradually decreases as the amount of recycled aggregate increases [6.3]-[6.7]. When up to a certain percentage of substitution, the influence may be insignificant [6.8], [6.9]. In the area of rubber concrete, a general census is that the strength decreases and ductility, impact resistance and dynamic energy dissipation capacity increase with a rising proportion of rubber phase in the mixture [6.10]-[6.13].

The studies have been widely reported on the use of recycled aggregate and waste tyre rubber in separate concrete. However, investigation on replacing aggregates by both recycled aggregate and rubber material simultaneously in concrete is rather scarce in the literature. Therefore, an innovative concrete material containing recycled aggregate, scrap tyre rubber, and pulverized fuel ash simultaneously was designed by the authors [6.14] with the aims to use it in ways that are environmentally responsible, commercially competitive, technically sound, and supportive of a more sustainable society. It was found that the reduction of compressive strength was mainly attributed to the low stiffness and poor surface texture of the rubber particles that resulted in an inconsistency of the concrete mix as well as the lack of bonding between the rubber particles and the surrounding cement paste, leading to a loss of compression resistance. The decrease in strength of rubber concrete compared to normal concrete has been consistently reported, and how to reduce the loss of strength is still being investigated. Segre and Joekes [6.15] immersed rubber particles in sodium hydroxide saturated aqueous solution for 20 minutes at room temperature before the particles were filtered, and the rubber was then washed with tap water and dried at the ambient temperature prior to using. They demonstrated that the surface modification enhanced the adhesion of tyre rubber particles to the surrounding paste, leading to an improvement in mechanical properties such as compressive strength, flexural strength and fracture energy. In contrast, Albano et al. [6.16] pointed out that prior treatment of rubber with NaOH did not produce obvious changes in the compressive and splitting tensile strength of the resulting concrete when compared to untreated rubber concrete. In the previous chapter, surface modification on rubber particles using SCA was conducted to improve the bond strength between rubber and matrix. Rubber particles were immersed in SCA until the entire surface was coated by the agent before being added into the mixture. It was demonstrated that surface modification by SCA which acts as

an adhesion promoter lead to an increase in compressive strength and Young's modulus compared to concrete with as-received rubber particles. Meanwhile, the results shown in Table 6-1 also indicated a lower slump, water permeability index and porosity of CCSR-SCA in contrast with CCSR-AR.

Table 6-1. Experimental results of a previous study in Chapter 5.

Notation	Slump (mm)	Compressive strength (MPa)	Young's modulus (GPa)	Water permeability index ($\times 10^{-7}$ $m^3/\sqrt{min}$)	Porosity (%)	Tortuosity
CCSR-AR	66	36.6	22.1	2.51	20.5	116
CCSR-N2h	69	35.8	22.3	2.43	16.2	120
CCSR-N24h	68	36.9	22.4	2.41	16.6	126
CCSR-SCA	57	39.1	23.8	2.18	14.0	163

Note: They were tested at the age of 28 days.

Rubber concrete is potentially to be used for fatigue control in structures. Wöhler [6.18] presented a general law which states that rupture may be caused, not only by a steady load which exceeds the ultimate strength, but also by repeated application of stresses, none of which are equal to this ultimate strength [6.19]. Fatigue failure of concrete refers to the phenomenon of rupture under repeated loadings each of which is smaller than a single static load that exceeds the strength of the material. Rubber can help improve the fatigue resistance of concrete due to the high toughness, energy-dissipative and damping capacity of rubber material. Liu et al. [6.20] studied the fatigue performance of rubber concrete containing 0, 5%, 10% and 15% tyre rubber as volumetric substitution of fine aggregate through central-point bending test with a constant amplitude repeated loading. They found that the fatigue life of rubber concrete was longer than normal concrete at the same stress level, and the fatigue life became even longer with the increase of proportion of rubber. They stated that the ratio of flexural strength to compressive strength of rubber concrete was higher than normal concrete,

indicating a better anti-cracking performance rubber concrete. Flexural fatigue behaviour of self compacting rubberized concrete was researched by Ganesan et al. [6.21]. Fatigue loadings at four different stress levels, the maximum of which ranged from 0.9 to 0.6, were applied to prism specimens with shredded rubber used to replace fine aggregate by volume. Their results showed an improvement of 15% in fatigue performance of self compacting rubberized concrete compared to normal self compacting concrete. Xiao et al., [6.22] investigated the fatigue life of rubberized asphalt concrete mixtures using a traditional fatigue analysis method. They pointed out that the addition of crumb rubber in the mixtures effectively extended the fatigue life and enhanced the energy dissipation capacity of rubber concrete compared to the control mixtures with no rubber. Their statistical analysis results indicated that there were no significant differences in stiffness and cumulative dissipated energy values for control and rubberized mixtures while fatigue life values of control mixtures were different from rubberized mixtures. Hernández-Olivares et al. [6.23] conducted fatigue bending tests on prismatic samples which were cut off from recycled tyre rubber-fill concrete slabs after one year exposition to natural weathering to study its fatigue behaviour and applications in design of rigid pavements. Their experimental results illustrated that the failure tension stress decreased while the dynamic Young's modulus increased with the increase of number of cycles when rubber was added into the concrete. Meanwhile, an analytical model was developed to calculate the minimum thickness of recycles tyre rubber-fill concrete and it was demonstrated based on their test results that the model is a powerful tool for designing rigid pavements subjected to high density traffic.

The aim of this chapter is to investigate the effect of surface-modified rubber particles on flexural properties and fatigue performance of concrete under cyclic loading with a constant

amplitude. To this end, four batches of rubber concrete specimens with recycled aggregate, coupled with one batch of control mix without rubber particles or recycles aggregate were designed. Flexural strength and mid-span deflection were tested by means of central-point flexural test, followed by carrying out a series of fatigue tests. Experimental results were analyzed and discussed to reveal the differences resulted from the various ways of surface modification on rubber parties before they were added into the concrete mixture. The results obtained were expected to provide a method to reduce the loss of flexural strength and to improve the fatigue performance of the described concrete material.

6.2 Preparation of concrete beams

6.2.1 Materials

The materials used in this chapter comprised cement, water, gravels, recycled aggregate, sand, waste tyre rubber particles, NaOH solid particles and SCA (analytical reagent).

6.2.1.1 Cement

Portland siliceous fly ash (30% by weight) cement with a characteristic strength of 32.5 MPa (often referred to CEM II/B-V 32.5) was used in accordance with BS EN 197-1 [6.24]. They were stored in airtight packages before using.

6.2.1.2 Water

Tap water which is reasonably free from contamination in the laboratory was used to hydrate the cement in the mixtures, which in turn binds the aggregates together to make concrete hard and strong.

6.2.1.3 Coarse aggregate

Crushed gravels and recycled aggregate (shown in Figure 6-1) with a nominal maximum size of 10 mm were used as coarse aggregate. Tests of sieve analysis were carried out according to BS EN 933-1 [6.25] with some additional sieves required and the results are shown in Figure 6-2. It indicates that the particle size distribution of crushed gravels and recycled aggregate used in this experiment were not much different from each other. Figure 6-3 shows the typical composition of recycled aggregate from a local demolition plant in Birmingham. Tests of aggregate crushing value were conducted on both crushed gravel and recycled aggregate according to BS 812-110 [6.26], with the results tabulated listing in Table 6-2. Water absorption of them in SSD condition was measured by immersion in water for 24 hours, followed by removing excess surface water with wet cloth after they were moved out. At the time when there was no free water on the surface, aggregates were assumed as SSD condition. The mass of sampled aggregates with saturated water in surface-dried condition was weighed and recorded as m_{SSD}. After 24 hours in the oven at the temperature of 105°C, the mass of the aggregates in oven-dried condition was re-weighed and recorded as m_{OD}. The SSD water absorption was calculated by the formula of $(m_{SSD}-m_{OD})/m_{OD}$. Volume of the sampled aggregates in SSD condition was measured in accordance with the principle of drainage and

recorded as v_{SSD}. The SSD density of aggregates was calculated by the formula of m_{SSD}/v_{SSD}. Results of SSD water absorption and SSD density of crushed gravels and recycled aggregate are presented in Table 6-2.

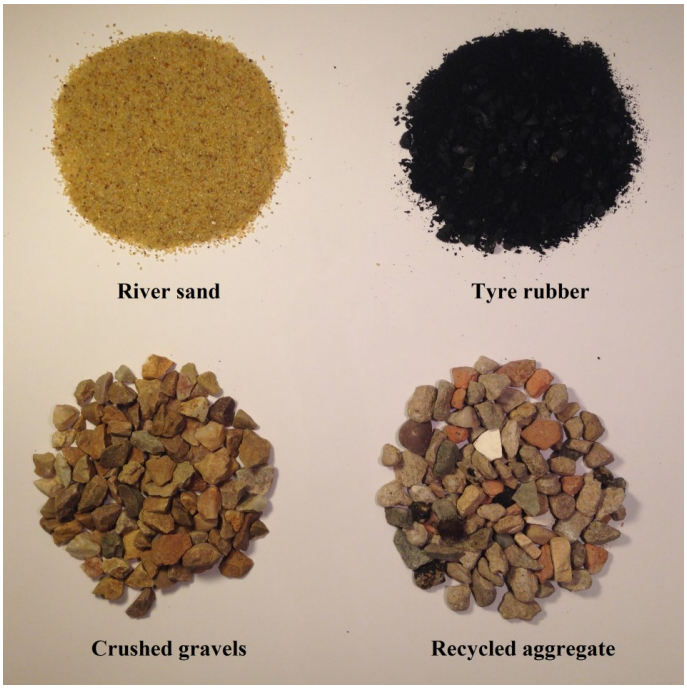

Figure 6-1. Raw materials in oven-dried condition.

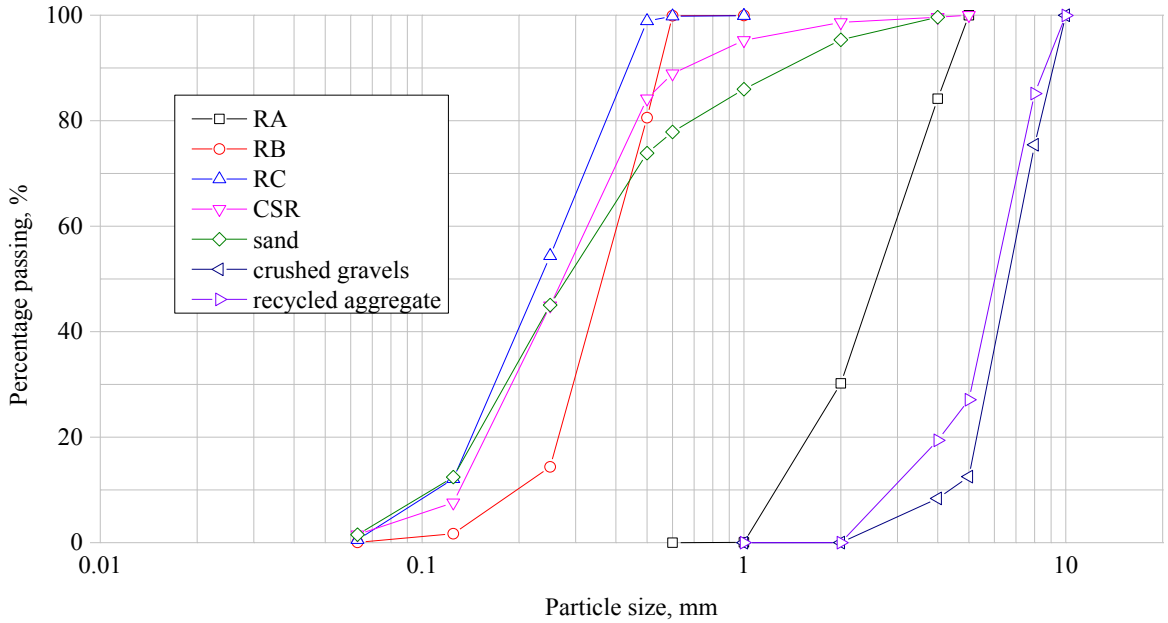

Figure 6-2. Grading curves of aggregates in oven-dried condition.

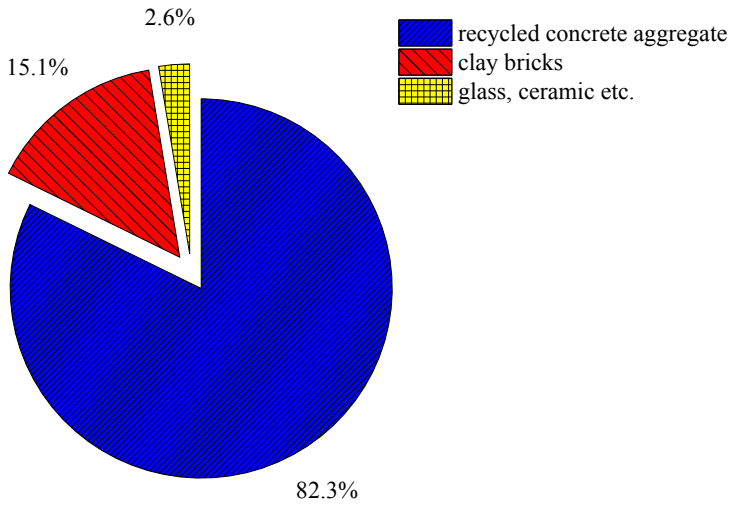

Figure 6-3. Composition of recycled aggregate in oven-dried condition.

Table 6-2. Related information of different kinds of aggregates.

Item	Crushed gravels	Recycled aggregate	River sand	Tyre rubber
Aggregate crushing value	20	23	N/A	N/A
SSD water absorption (%)	1.26	7.09	1.37	8.46
SSD density (kg/m^3)	2581	2539	2512	973

6.2.1.4 Fine aggregate

Natural river sand having a maximum particle size of 5 mm was used as the fine aggregate. Test of sieve analysis was conducted according to BS EN 933-1 [6.25]. As shown in Figure 6-2, the sand used in this experiment presented continuous granularity. Procedures of the sand SSD water absorption and SSD density measurements are the same as those of coarse aggregate and the results are presented in Table 6-2.

Waste tyre rubber was used as part of fine aggregate. CSR particles with continuous grading like sand were sorted out artificially by blending three different uniform size rubber particles,

i.e. RA (cut to 3 mm), RB (ground to 0.5 mm), and RC (ground to 0.3 mm). They are sourced from a local waste tyre recycling plant in Manchester, without any pre-treatment, contaminant or tyre bead wire. Sieve analysis tests were carried out and the grading curve of each rubber sample is shown in Figure 6-2. SSD water absorption and SSD density of rubber particles were also measured. However, some rubber particles of small sizes were found to float in water. To this end of immersion, a piece of tightly woven fabric was used to wrap rubber particles. The wrapped rubber particles were submerged in a water filled bucket, followed by gently shaking within the water to release as much trapped air as possible until it easily sank to the bottom of the bucket. Other procedures of measurements are the same as those of measuring coarse aggregates. Results of SSD water absorption and SSD density of rubber particles are shown in Table 6-2.

6.2.1.5 Solution for surface modification on rubber particles

NaOH saturated aqueous solution and SCA solution were used as the solution for rubber surface modification. NaOH solid particles with purity of 99% were used to prepare NaOH saturated aqueous solution according to its solubility under laboratory temperature. Chemically pure SCA was diluted to 1% of mass fraction to prepare SCA solution. Once the solution was ready, surface modification on rubber particles was carried out immediately.

6.2.2 Mix design considerations

6.2.2.1 Manner of substitution

Different researchers use different manners to replace aggregates. Galvín et al. [6.27] and Eguchi et al. [6.28] replaced natural coarse aggregate with recycled aggregate by volume

while Erdem and Blankson [6.29] and Tuyan et al. [6.30] did so by weight. Bravo and Brito [6.31] and Aiello and Leuzzi [6.32] used rubber to volumetrically substitute part of fine aggregate whereas Albano et al. [6.16] and Topçu and Bilir [6.33] adopted gravimetric manner. In this chapter, fine aggregate was replaced by rubber by volume while coarse aggregate was replaced by recycled aggregate by weight. The reason for volume replacement of fine aggregate rather than mass replacement is mainly because of the distinction between the densities of different materials. SSD density of sand is over twice as much as that of rubber materials (see Table 6-1). It means that if the sand is substituted by rubber in the manner of mass replacement, the volume of resulted mixture would be much higher compared with the original one. Consequently, content of other aggregates and cement paste in unit volume would be decreased, resulting in severe strength reduction of concrete. It would probably cause safety problem when this innovative concrete material is used in structural engineering. Besides, the changing volume would lead to incorrect concrete demand in the mix design. This is also applicable to industrial situations, as a change in volume of a mixture would cause either quantity issues for the purchaser, or cost issues for the supplier. However, this issue is not obvious in the case of substituting coarse aggregate since the values of SSD density of the crushed gravels and recycled aggregate used in this study are quite close to each other (see Table 6-1). The difference of them is 42 kg/m^3, approximately 1.64% of their density, allowing the substitution by weight to be conducted.

6.2.2.2 Use of a constant w/c ratio

It is well known that w/c ratio is intrinsically linked to the strength of concrete. A little variation of w/c ratio would cause profound influence on concrete strength when other

parameters are kept constant, especially for high strength concrete [6.34]. Moreover, in accordance with the design method used in this study, the w/c ratio was firstly determined according to the designed cube compressive strength and some other auxiliary factors. Therefore, the same w/c ratio was strictly adhered to in each batch of mix to provide more comparable results.

6.2.3 Mix proportioning

Concrete mix proportioning was undertaken using the second edition of Design of Normal Concrete Mixes [6.35] presented by the Building Research Establishment. This design method is based on determining the material proportions. Using known or assumed parameters, the w/c ratio required to achieve the compressive strength was determined, culminating in mass quantities for individual material proportions.

The mix design of reference concrete in this chapter aimed to achieve a target mean strength of 43 MPa at 28 days with a slump value of 60-180 mm. Five batches of concrete mixtures, i.e. REF, CCSR-AR, CCSR-N2h, CCSR-N24h, and CCSR-SCA, totally 75 beams were prepared. Each mix included 15 beams, 3 for flexural test and 12 for fatigue test under different stress level. The w/c ratio of 0.37, determined according to target mean strength, cement strength class and type of aggregates, was kept constant throughout the experiment programme. The amount of free water used to achieve the designed w/c ratio was determined according to the desired slump, maximum size of aggregate and type of aggregate. Cement content was calculated by the values of w/c ratio and the amount of free water. Recycled aggregate was used to replace 50% of crushed gravels by weight while waste tyre rubber was

used to replace 20% of river sand by volume. The amount of each kind of aggregate in different concrete mixes was figured out in compliance with the formulas provided by the second edition of Design of Normal Concrete Mixes [6.35]. Concrete mix proportions are presented in Table 6-3.

Table 6-3. Mix proportions of different concrete mixtures.

Notation	Recycled aggregate content (%)	Rubber content (%)	Tap water (kg/m^3)	Cement with PFA (kg/m^3)	Crushed gravels (kg/m^3)	Recycled aggregate (kg/m^3)	River sand (kg/m^3)	Tyre rubber (kg/m^3)
REF	0	0	234	632	1013	0	519	0
CCSR-*X*	50	20	232	627	501	501	414	40

Note: 1. Crushed gravels, recycled aggregate, river sand, and tyre rubber were in SSD condition.
2. *X* stands for AR, N2h, N24h, and SCA, respectively.

6.2.4 Preparation of concrete specimens

6.2.4.1 Surface modification on rubber particles

Two batches of rubber particles were soaked in NaOH saturated aqueous solution in ambient condition for 2 hours and 24 hours, respectively, with some occasional stirring. They were then washed with tap water and kept in airtight container in laboratory condition for another 24 hours before using. Another batch of rubber particles were soaked in SCA solution until the entire surface was coated by the agent before being added into the mixture.

6.2.4.2 Mixing

All kinds of aggregates were prepared to SSD condition before mixing. The desired quantities of each item was accurately measured out and put in order of crushed gravels, sand, cement,

rubber particles, and recycled aggregate in a mechanical mixer which had been inter-surface wetted. Prior to the addition of water, the mixer was turned on and the placed materials were mixed for 5 minutes to ensure homogenisation. Then half water was put in to mix for another 5 minutes, followed by adding the other half in. The mixer was stopped until there were no visual discrepancies in the mixture.

6.2.4.3 Sampling

Dimension of the moulds are 100 × 100 × 500 mm beam. Prior to filling, the inner surface of the moulds were brushed with a thin film oil to prevent the concrete from adhering to the mould. All moulds were filled with fresh concrete in two equal layers, each of which was compacted using the vibrating table to remove as many air voids as possible. Vibration was allowed for 30 seconds to ensure a smooth and even surface film, followed by trowelling the exposed surface to a clean finish.

6.2.4.4 Curing

Polythene sheet was placed over the samples after casting to prevent moisture loss. After 24 hours at a Civil Engineering laboratory temperature of 20°C, the samples were carefully removed from the moulds, with each sample having mix notation and curing time written by marker pen clearly on its surface. Samples were then transferred to the curing water tank at a temperature of 20°C where they were immersed until the required age of 28 days.

6.3 Experiment details and results discussion

6.3.1 Flexural properties

6.3.1.1 Test procedure

Tests on flexural strength of hardened concrete beams at 28 days after casting were conducted in conformity with BS EN 12390-5 [6.36]. The excess moisture from the surface of the beam was wiped off before placing in an electro-hydraulic servo testing machine of a 50 KN capacity. Figure 6-4 shows a centre-point flexural test used in this study. A specimen was simply supported by two lower rollers at a spacing of 300 mm. Gradiometer was used to make the longitudinal axis of the specimen perpendicular to the direction of the loading. Continuous loading was applied to a rectangular prism platen which was positioned horizontally on the centre of a non-trowelled face at a constant rate of 0.05 MPa/s. Value of peak load was recorded when the specimen failed. Another two repeated tests on duplicates were conducted and mean of the three values were calculated. Results are listed in Table 6-4, with corresponding mid-span peak deflection, as well as the calculated peak stress and strain.

Table 6-4. Results of centre-point flexural test.

Notation	Peak load (KN)	Peak stress (MPa)	Peak deflection (mm)	Peak strain ($\times 10^{-3}$)
REF	11.387	5.1	0.467	3.113
CCSR-AR	7.735	3.5	0.523	3.487
CCSR-N2h	8.219	3.7	0.518	3.453
CCSR-N24h	8.268	3.7	0.531	3.540
CCSR-SCA	9.135	4.1	0.559	3.727

Note: peak stress = $3PL/2bd^2$ and peak strain = $6Dd/L^2$, where P is peak load, L is support span, b is width of tested beam, d is depth of tested beam, and D is peak deflection.

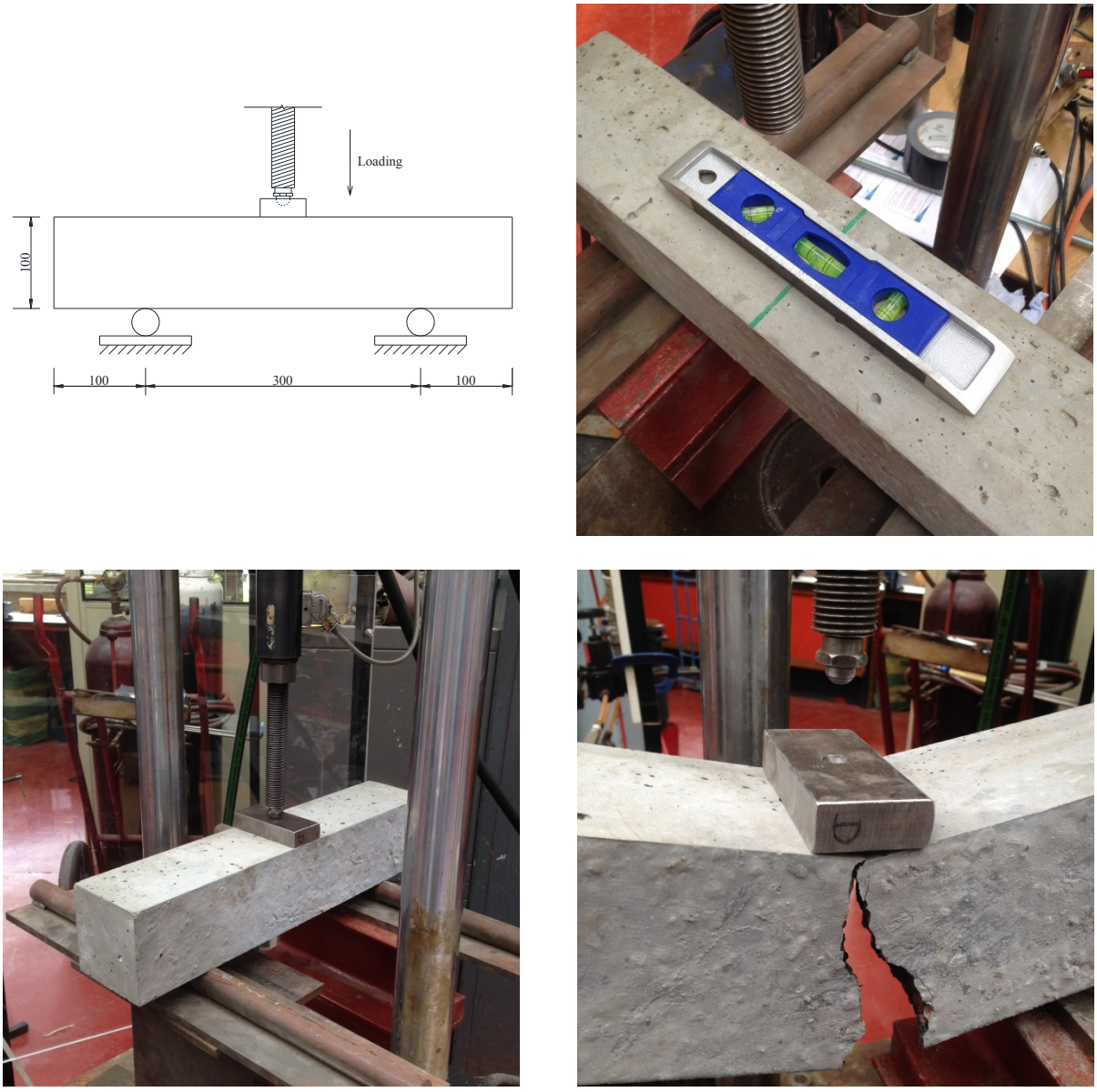

Figure 6-4. Centre-point flexural test.

6.3.1.2 Flexural strength and deformation

There was a general reduction in peak load when aggregates were partially replaced by waste materials, regardless of rubber surface modification. The 28 days peak stress, often referred to flexural strength of CCSR-AR, CCSR-N2h, CCSR-N24h, and CCSR-SCA was 31.4% (1.6 MPa), 27.5% (1.4 MPa), 27.5% (1.4 MPa), and 19.6% (1.0 MPa) lower than REF,

respectively. This is due to poor surface structure and lower stiffness of rubber particles. Non-polar natural of organic rubber particles results in an inconsistency of concrete mixture as well as lack of bonding between rubber particles and the surrounding cement paste, leading to a loss of strength [6.37]. Besides, rubber particles can be deemed as voids in concrete due to its lower stiffness compared to other aggregates or cement paste. Stress concentration usually arises at the interface between rubber particles and the cement paste under compression, resulting in the degradation of concrete strength [6.17]. Recycled aggregate also impaired the strength of concrete to some extent. However, because all aggregates used in this study were prepared to be in SSD condition before mixing, effect of strength reduction caused by recycled aggregate is much less significant than rubber particles [6.14].

Mid-span peak deflection of REF was 0.467 mm, which is the lowest in the five mixes. It is understandable in view of high ductility of rubber which decreased the stiffness magnitude of concrete. As is known, concrete is a kind of brittle material which is of much better compression resistance than tension resistance. However, because of the increased ductility caused by rubber, nature of the concrete changed from brittle to quasi-brittle/ductile material, leading to a larger deformation before reaching peak load [6.38]. Stress-strain curves of the five mixes are shown in Figure 6-5. It is clear that concrete without rubber, i.e. REF exhibited high stress but low strain performance compared to the other four mixes. In contrast, concrete with rubber particles showed higher deformability than REF, which is in line with the above argument.

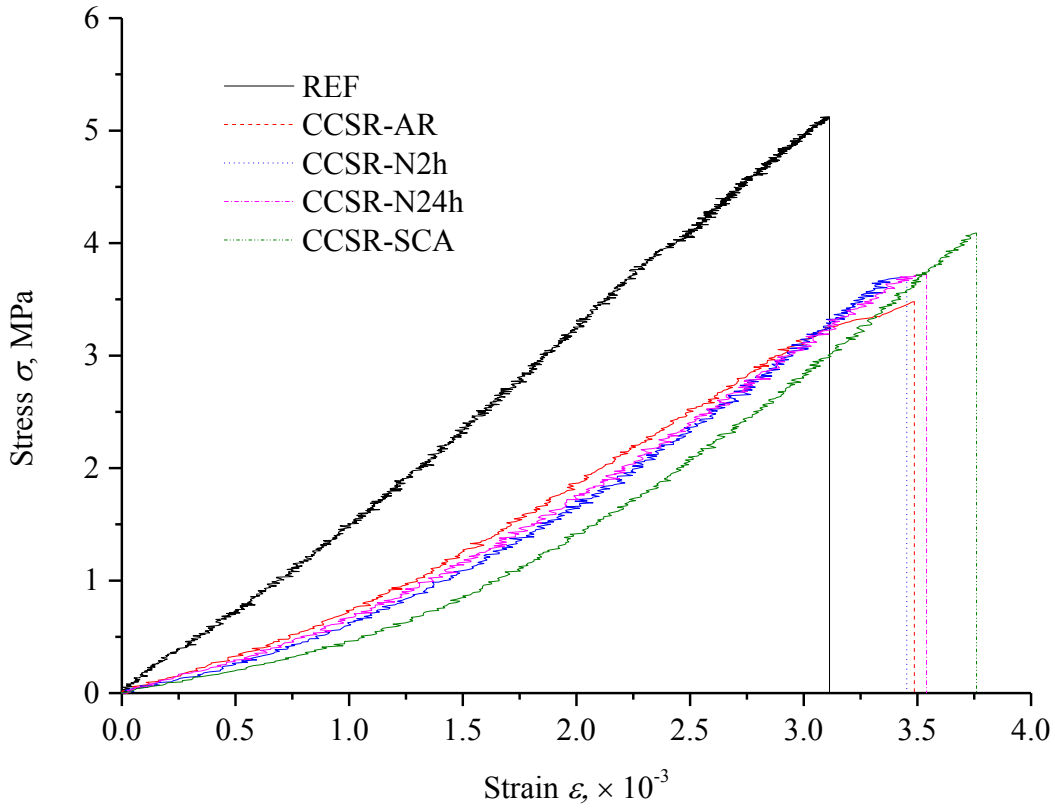

Figure 6-5. Stress-strain curves.

6.3.1.3 Mechanism and microstructure of strength enhancement

Flexural strength of concrete with as-received rubber particles (CCSR-AR) was 3.5 MPa, which is the lowest of the five mixes. When rubber particles were soaked in NaOH saturated aqueous solution for 2 and 24 hours, flexural strength of CCSR-N2h and CCSR-N24h both increased to 3.7 MPa, 5.7% higher than that of CCSR-AR. The results indicate that surface modification on rubber particles by NaOH improves concrete flexural strength compared to concrete with untreated rubber particles. It can be further deduced that time of soaking (less than 24 hours) in NaOH saturated aqueous solution to modify rubber particle surface does not affect flexural strength of concrete obviously, as the values are the same. If rubber particles were coated with SCA, flexural strength of CCSR-SCA was 4.1 MPa, 17.1% higher than that

of CCSR-AR. It implies that effect of surface modification by SCA is more noticeable than NaOH on concrete strength improvement. This is mainly ascribed to the sticky nature of an SCA-coated rubber surface which tends to bond the rubber particles with the matrix, thus enhancing the strength of interfacial transition zone. Please see Section 5.4.2 for the details. The above arguments were also supported by microscopic inspections and analysis of fractured specimen particles. Please refer to Section 5.3.3 for the details.

6.3.2 Fatigue performance

6.3.2.1 Test setup and procedure

A fatigue testing program consists of applying repeated loading of different magnitudes or stress levels to the specimen and observing the number of cycles of loading which is necessary for fracture at each stress level. In this study, fatigue tests by centre-point flexural loading were conducted in a mode of load control using the same electro-hydraulic servo testing machine. Stress level S was adopted and taken as 0.95, 0.90, 0.85, and 0.80, i.e. upper load f_u was 95%, 90%, 85%, and 80% of peak load f_{max}, respectively. Ratio of lower load f_l to f_u was set to 0.2 which was maintained constant in all tests. Table 6-5 presents the loading parameters of different mixes at four stress levels. After the platen and supporting rollers rested evenly against the test specimen, the beam was loaded up to f_m, the median of f_l and f_u at a constant rate of 0.05 MPa/s. After 10 seconds holding time under f_m, a continuously sinusoidal pulsation loading with a constant amplitude f_a at a frequency of 3 Hz as shown in Figure 6-6 was applied until the specimen fractured. Three beams of each mix were tested at

each stress level and number of cyclic loading was recorded and tabulated in Table 6-6, with corresponding mean, standard deviation and standard error.

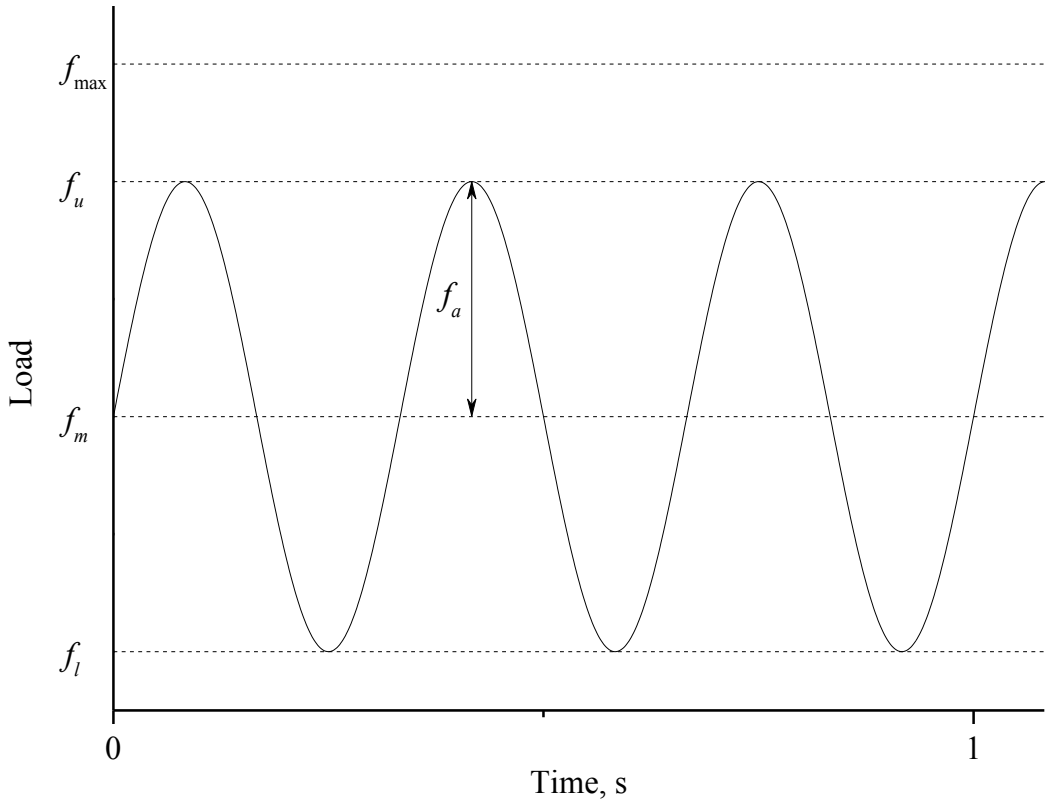

Figure 6-6. Sinusoidal pulsation loading adopted in the fatigue test.

Table 6-5. Loading parameters in the fatigue test.

S	f_l / f_u	REF				CCSR-AR				CCSR-N2h				CCSR-N24h				CCSR-SCA			
		f_{max}	f_u	f_m	f_l	f_{max}	f_u	f_m	f_l	f_{max}	f_u	f_m	f_l	f_{max}	f_u	f_m	f_l	f_{max}	f_u	f_m	f_l
0.95	0.2	11.387	10.818	6.491	2.164	7.735	7.348	4.409	1.470	8.219	7.808	4.685	1.562	8.268	7.855	4.713	1.571	9.135	8.678	5.207	1.736
0.90	0.2	11.387	10.248	6.149	2.050	7.735	6.962	4.177	1.392	8.219	7.397	4.438	1.479	8.268	7.441	4.465	1.488	9.135	8.222	4.933	1.644
0.85	0.2	11.387	9.679	5.807	1.936	7.735	6.575	3.945	1.315	8.219	6.986	4.192	1.397	8.268	7.028	4.217	1.406	9.135	7.765	4.659	1.553
0.80	0.2	11.387	9.110	5.466	1.822	7.735	6.188	3.713	1.238	8.219	6.575	3.945	1.315	8.268	6.614	3.969	1.323	9.135	7.308	4.385	1.462

Note: 1. Loading frequency was 3 Hz.

2. Unit is KN.

Table 6-6. Fatigue life of each specimen.

Notation	S = 0.95			Mean	SD	SE	S = 0.90			Mean	SD	SE	S = 0.85			Mean	SD	SE	S = 0.80			Mean	SD	SE
REF	4	3	6	4	2	1	145	79	101	108	34	19	1684	1481	1471	1545	120	69	28951	29530	29026	29169	315	182
CCSR-AR	11	19	10	13	5	3	236	261	196	231	33	19	2368	2334	1998	2233	205	118	35621	35545	35537	35568	46	27
CCSR-N2h	41	36	35	37	3	2	303	368	351	341	34	19	3411	3017	3228	3219	197	114	44352	44598	43506	44152	573	331
CCSR-N24h	30	22	22	25	5	3	411	281	268	320	79	46	3121	3301	3134	3185	100	58	43195	43791	43101	43362	374	216
CCSR-SCA	49	38	41	43	6	3	432	399	419	417	17	10	4285	4304	4189	4259	62	36	51311	51882	51575	51589	286	165

Note: 1. SD is standard deviation which reflects variation or dispersion amount of a single test result from the sample mean and measures precision of the data.

2. SE is standard error which reflects variation or dispersion amount of a sample mean from the population mean and measures precision of the results.

6.3.2.2 Fatigue life analysis

In this study, Weibull distribution function was used to evaluate fatigue life of the specimens. Weibull distribution is often used to describe the characteristics of fatigue life because safety life or minimum safety life it provided is very realistic and has a reliability of as high as 99.99 – 100% [6.20]. Probability density function $f(N)$ and cumulative density function $F(N)$ of specimen fatigue life N based on Weibull probability law [6.39] can be expressed by the forms as shown in Equations (6-1 and 6-2),

$$f(N) = \frac{k}{N_c - N_0}\left(\frac{N - N_0}{N_\alpha - N_0}\right)^{k-1} \exp\left[-\left(\frac{N - N_0}{N_c - N_0}\right)^k\right], \left(N \geq N_0\right) \tag{6-1}$$

$$F(N) = 1 - \exp\left[-\left(\frac{N - N_0}{N_c - N_0}\right)^k\right], \left(N \geq N_0\right) \tag{6-2}$$

where N_c is characteristic life, N_0 is minimum safety life, k = Weibull shape parameter. A survival function $L(N)$ can be obtained from Equation (6-2) and is shown in Equation (6-3).

$$L(N) = 1 - F(N) = \exp\left[-\left(\frac{N - N_0}{N_c - N_0}\right)^k\right], \left(N \geq N_0\right) \tag{6-3}$$

It is widely accepted that two-parameter Weibull distribution is better suited for describing the fatigue behaviour of engineering materials, since it usually gives more simplicity and safe reliability [6.40]. Therefore, N_0 is set as zero and the survival function can be simplified as shown in Equation (6-4).

$$L(N) = \exp\left[-\left(\frac{N}{N_c}\right)^k\right] \tag{6-4}$$

Taking the logarithm on both sides of Equation (6-4) gives Equation (6-5).

$$\ln[L(N)] = -\left(\frac{N}{N_c}\right)^k \tag{6-5}$$

Take the logarithm again for Equation (6-5) to obtain Equation (6-6).

$$\ln\left\{\ln\left[\frac{1}{L(N)}\right]\right\} = k\ln(N) - k\ln(N_c) \tag{6-6}$$

Define $y = \ln\left\{\ln\left[\frac{1}{L(N)}\right]\right\}$, $x = \ln(N)$, $b = -k\ln(N_c)$, then Equation (6-6) can be written as a form of Equation (6-7).

$$y = kx + b \tag{6-7}$$

Equation (6-7) is a linear equation, which could be used to examine whether experimental data comply with a two-parameter Weibull distribution or not. In addition, an empirical survival function $L(N)$ can also be expressed in Equation (6-8),

$$L(N) = 1 - \frac{i}{j+1} \tag{6-8}$$

where i and j are ordinal number and total number of specimens within one group, respectively.

Table 6-7 presents the data for carrying out an analysis based on Weibull distribution theory. Linear regression equations of $\ln\{\ln[1 / L(N)]\}$ versus $\ln(N)$ were fitted and the fitting lines were plotted with corresponding correlation coefficient r as shown in Figure 6-7. It can be seen that the experimental results at different stress levels were approximately in linear distribution. Due to the error caused by the testing system and the variation of concrete strength, there was some discreteness which is usual in laboratory tests of fatigue life of concrete. However, all the correlation coefficients were over 0.8, indicating a highly linear correlation between $\ln\{\ln[1 / L(N)]\}$ and $\ln(N)$. Therefore, it can be deduced that fatigue life

of both normal concrete and rubber concrete with as-received, NaOH-treated, and SCA-coated rubber particles followed a two-parameter Weibull distribution.

Table 6-7. Data for analysis of fatigue life based on Weibull distribution theory.

S	Notation	*N*	ln(*N*)	*i*	*j*	*L(N)*	ln{ln[1 / *L*(*N*)]}
0.95	REF-1	3	1.099	1	3	0.750	-1.246
	REF-2	4	1.386	2	3	0.500	-0.367
	REF-3	6	1.792	3	3	0.250	0.327
	CCSR-AR-1	10	2.303	1	3	0.750	-1.246
	CCSR-AR-2	11	2.398	2	3	0.500	-0.367
	CCSR-AR-3	19	2.944	3	3	0.250	0.327
	CCSR-N2h-1	35	3.555	1	3	0.750	-1.246
	CCSR-N2h-2	36	3.584	2	3	0.500	-0.367
	CCSR-N2h-3	41	3.714	3	3	0.250	0.327
	CCSR-N24h-1	22	3.091	1	3	0.750	-1.246
	CCSR-N24h-2	22	3.091	2	3	0.500	-0.367
	CCSR-N24h-3	30	3.401	3	3	0.250	0.327
	CCSR-SCA-1	38	3.638	1	3	0.750	-1.246
	CCSR-SCA-2	41	3.714	2	3	0.500	-0.367
	CCSR-SCA-3	49	3.892	3	3	0.250	0.327
0.90	REF-1	79	4.369	1	3	0.750	-1.246
	REF-2	101	4.615	2	3	0.500	-0.367
	REF-3	145	4.977	3	3	0.250	0.327
	CCSR-AR-1	196	5.278	1	3	0.750	-1.246
	CCSR-AR-2	236	5.464	2	3	0.500	-0.367
	CCSR-AR-3	261	5.565	3	3	0.250	0.327
	CCSR-N2h-1	303	5.714	1	3	0.750	-1.246
	CCSR-N2h-2	351	5.861	2	3	0.500	-0.367
	CCSR-N2h-3	368	5.908	3	3	0.250	0.327
	CCSR-N24h-1	268	5.591	1	3	0.750	-1.246
	CCSR-N24h-2	281	5.638	2	3	0.500	-0.367
	CCSR-N24h-3	411	6.019	3	3	0.250	0.327

	CCSR-SCA-1	399	5.989	1	3	0.750	-1.246
	CCSR-SCA-2	419	6.038	2	3	0.500	-0.367
	CCSR-SCA-3	432	6.068	3	3	0.250	0.327
0.85	REF-1	1471	7.294	1	3	0.750	-1.246
	REF-2	1481	7.300	2	3	0.500	-0.367
	REF-3	1684	7.429	3	3	0.250	0.327
	CCSR-AR-1	1998	7.600	1	3	0.750	-1.246
	CCSR-AR-2	2334	7.755	2	3	0.500	-0.367
	CCSR-AR-3	2368	7.770	3	3	0.250	0.327
	CCSR-N2h-1	3017	8.012	1	3	0.750	-1.246
	CCSR-N2h-2	3228	8.080	2	3	0.500	-0.367
	CCSR-N2h-3	3411	8.135	3	3	0.250	0.327
	CCSR-N24h-1	3121	8.046	1	3	0.750	-1.246
	CCSR-N24h-2	3134	8.050	2	3	0.500	-0.367
	CCSR-N24h-3	3301	8.102	3	3	0.250	0.327
	CCSR-SCA-1	4189	8.340	1	3	0.750	-1.246
	CCSR-SCA-2	4285	8.363	2	3	0.500	-0.367
	CCSR-SCA-3	4304	8.367	3	3	0.250	0.327
0.80	REF-1	28951	10.273	1	3	0.750	-1.246
	REF-2	29026	10.276	2	3	0.500	-0.367
	REF-3	29530	10.293	3	3	0.250	0.327
	CCSR-AR-1	35537	10.478	1	3	0.750	-1.246
	CCSR-AR-2	35545	10.479	2	3	0.500	-0.367
	CCSR-AR-3	35621	10.481	3	3	0.250	0.327
	CCSR-N2h-1	43506	10.681	1	3	0.750	-1.246
	CCSR-N2h-2	44352	10.700	2	3	0.500	-0.367
	CCSR-N2h-3	44598	10.705	3	3	0.250	0.327
	CCSR-N24h-1	43101	10.671	1	3	0.750	-1.246
	CCSR-N24h-2	43195	10.673	2	3	0.500	-0.367
	CCSR-N24h-3	43791	10.687	3	3	0.250	0.327
	CCSR-SCA-1	51311	10.846	1	3	0.750	-1.246
	CCSR-SCA-2	51575	10.851	2	3	0.500	-0.367
	CCSR-SCA-3	51882	10.857	3	3	0.250	0.327

Note: *N* was ranked in an ascending order of number of cycles in each group at different levels.

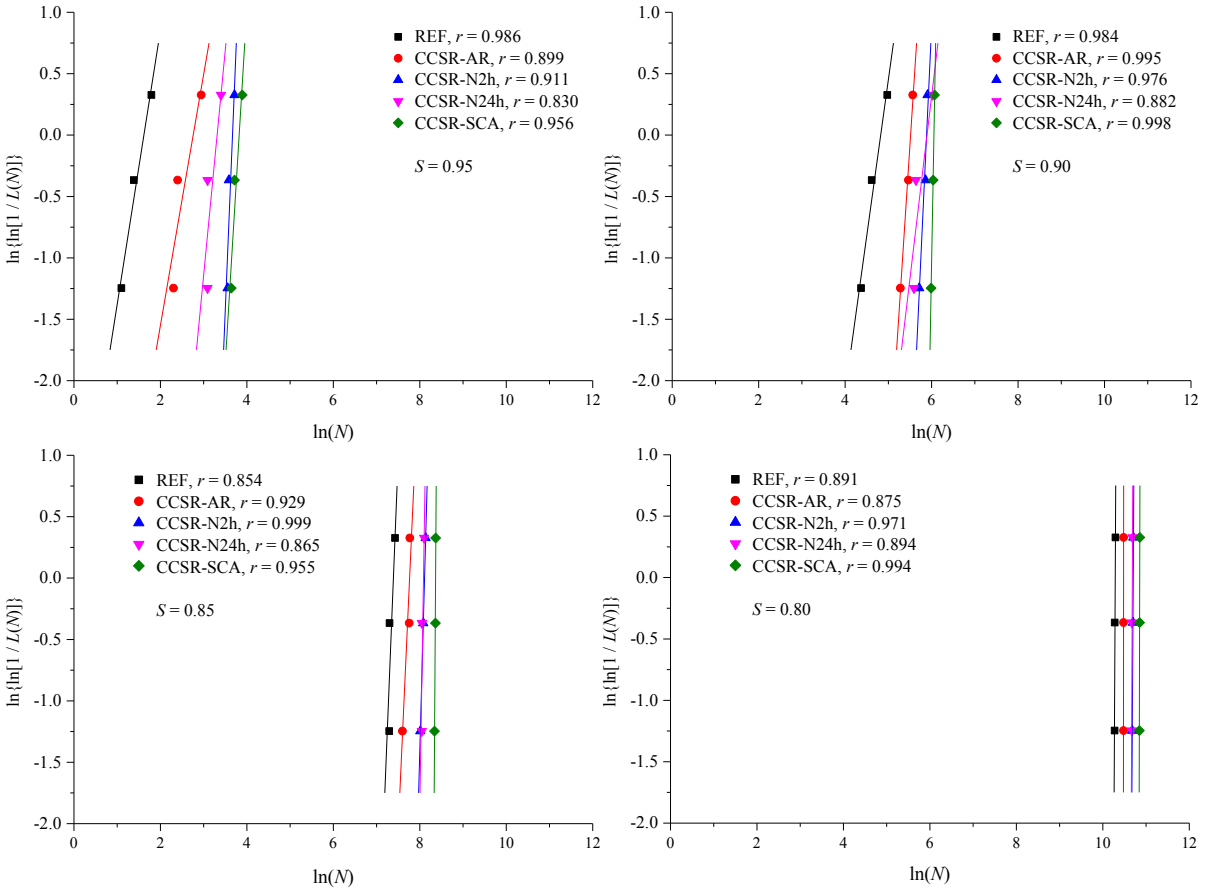

Figure 6-7. Linear fitting lines and correlation coefficients of different mixes at different stress levels.

It is very common to show fatigue test results of concrete by plotting the test data in an $S - N$ coordinate system where S represents testing stress level and N represents number of cycles for failure. $S - N$ curve comes from Wöhler curve which sets out a relationship between applied maximum stress and number of loading which causes fatigue failure. Since the susceptibility to fatigue is independent of concrete strength, stress coordinate of Wöhler curve is usually given in a non-dimensional form as f_u / f_{max}. Furthermore, if N is plotted in a in a logarithmic scale and S remains in a linear scale, fatigue curves for concrete is found to be approximately linear. Therefore, $S - N$ curve for concrete is usually expressed in Equation (6-9),

$$\frac{f_u}{f_{\max}} = \alpha \log_{10}(N) + \beta \tag{6-9}$$

where α and β are regression coefficients.

Linear fitting lines of stress level versus number of cycles in a logarithmic scale were plotted in Figure 6-8(a). The $S - N$ curves clearly shows that with the decrease of stress level, number of cycles when specimen fractured has an increasing trend. Rubber concrete has a longer fatigue life than normal concrete if stress level is over 0.80. Concrete with surface-modified rubber particles had a longer fatigue life than with as-received rubber particles, and CCSR-SCA exhibited the longest fatigue life in the five mixes. It indicates that SCA-treatment on rubber particles has a positive effect on improving fatigue life of rubber concrete due to the sticky nature of SCA.

It should be noted that some materials have infinite life and some have endurance limit at a certain stress level. The upper curve shown in Figure 6-8(b) is typical of fatigue tests of ferrous metals. The ordinate to the horizontal asymptote of this curve is the stress level at which the specimen will withstand an infinite number of cycles and is called the fatigue limit. Figure 6-8(b) also shows a typical $S - N$ curve for nonferrous metals. This curve does not become asymptotic to the horizontal, which means that no fatigue limit exists. For a material having this type of curve, it is customary to specify a fatigue strength of the material for any given life or number of cycles. Concrete belongs to the kind of material which has a fatigue limit at a certain stress level. Nevertheless, that stress level has not come to a general consensus which is understandable in view of different nature of raw materials of concrete, testing machine, and parameters set in the fatigue testing program. Majority of researchers

reported the stress level in a range of approximately 0.50 to 0.64 under flexural stress. Therefore, the linear regression equations in the form of Equation (6-9) may not apply to lower stress levels since it is not able to reflect a true tendency of fatigue life at lower stress levels. Another diagram, Figure 6-8(c) shows the fatigue life of concrete in a form of polynomial fitting curve which can come close to a true trend. However, more studies at different levels are needed before a function expression can be given to predict the fatigue life of concrete.

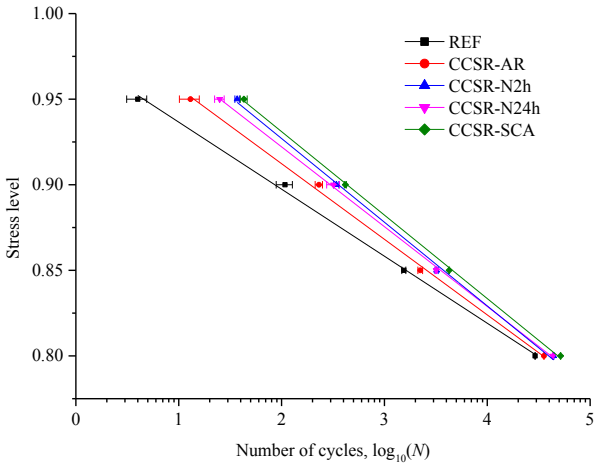

(a) Linear fitting lines

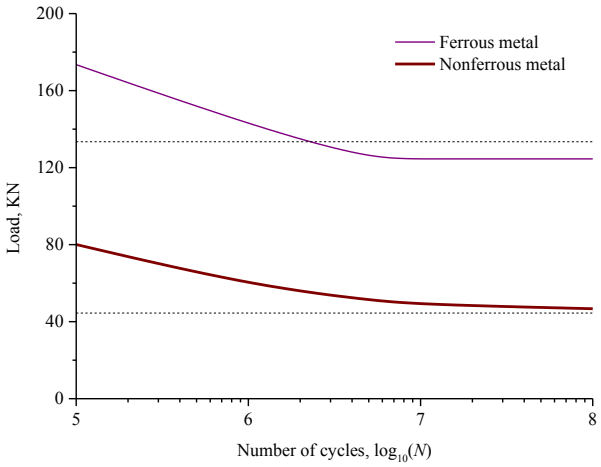

(b) Typical $S - N$ curves of ferrous and nonferrous metal

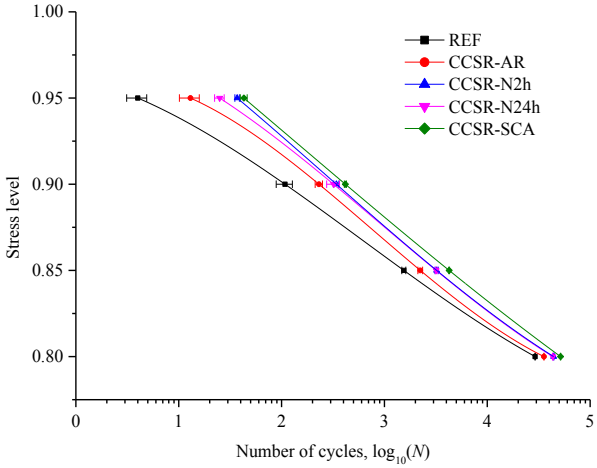

(c) Polynomial fitting curves

Figure 6-8. Curves of stress level versus number of cycles.

6.3.2.3 Ductility and damping capacity

Curves of deflection versus number of cycles of each mix at different stress level were plotted in Figure 6-9. It can be found from Figures 6-9(a) to 6-9(e) that deflection of rubber concrete specimens, regardless of surface modification on rubber particles, were all over 0.5 mm which is more than around 0.47 mm of REF, indicating a better deformability of rubber concrete than normal concrete. Rubber material has a good ability in absorbing energy by deformation because of its high ductility. When rubber concrete is subjected to external forces, rubber particles play a role in absorbing strain energy to improve impact resistance, resulting in a higher ductility and better fatigue performance than normal concrete [6.20]. δ – N curves of different mix at each of the same stress level are presented in Figure 6-9(f) to 6-9(i), respectively. It is distinct that REF had the smallest deflection whereas CCSR-SCA had the largest deflection at each stress level. Difference between CCSR-N2h and CCSR-N24h was insignificant, both of which had a minor increase of deflection compared to CCSR-AR. They are supported by the specific data of deflection results. Figure 6-10 shows a typical relationship of load and deflection of a specimen in the fatigue test described in this study, where m is peak deformation when specimen failed, n is residual deformation under cyclic loading, and ΔW is the shaded area. Mean values of experimental results m, n and calculated results ΔW are listed in Table 6-8.

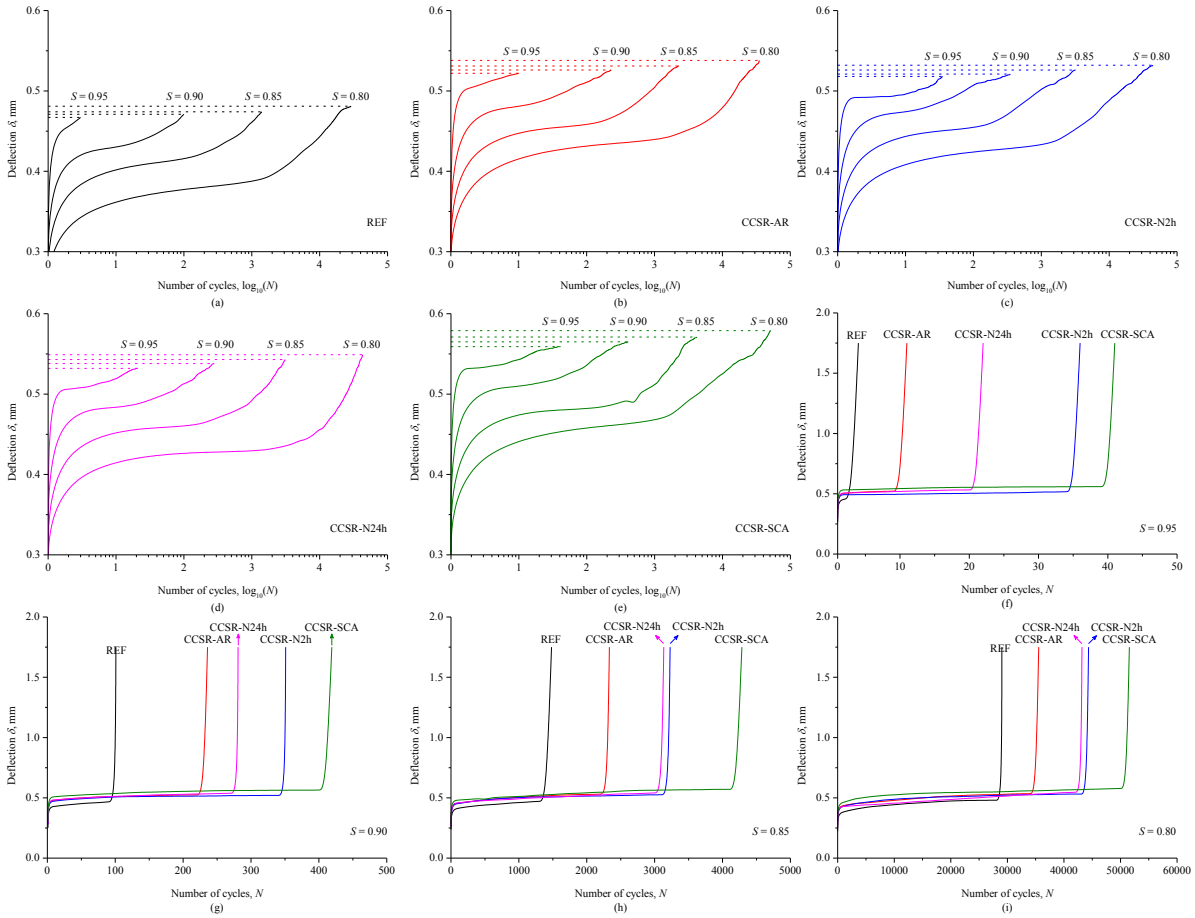

Figure 6-9. Curves of deflection versus number of cycles.

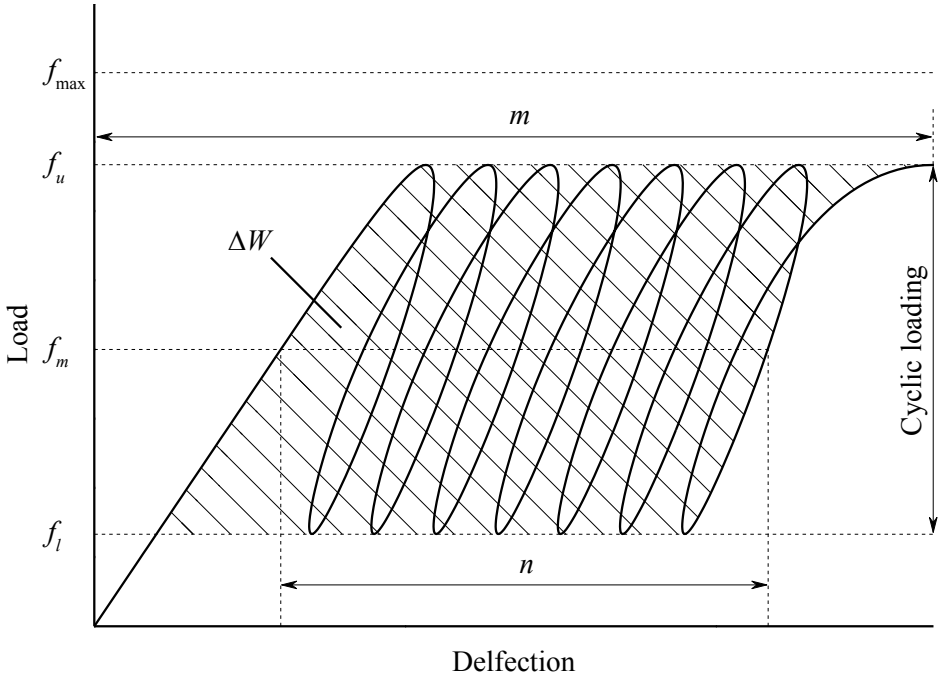

Figure 6-10. Typical curve of load and deflection versus number of cycles.

Table 6-8. Peak deformation, residual deformation and shaded area of different specimens.

S	Notation	m (mm)	n ($\times 10^{-3}$ mm)	ΔW ($\times 10^{-3}$ mm)
0.95	REF	0.467	0.19	0.144
	CCSR-AR	0.524	0.23	0.175
	CCSR-N2h	0.518	0.26	0.198
	CCSR-N24h	0.532	0.24	0.182
	CCSR-SCA	0.560	0.26	0.198
0.90	REF	0.471	0.94	0.677
	CCSR-AR	0.526	1.54	1.109
	CCSR-N2h	0.531	1.57	1.130
	CCSR-N24h	0.534	1.59	1.145
	CCSR-SCA	0.565	1.63	1.174
0.85	REF	0.474	3.84	2.611
	CCSR-AR	0.531	4.93	3.352
	CCSR-N2h	0.536	5.16	3.509
	CCSR-N24h	0.543	5.11	3.475
	CCSR-SCA	0.571	5.51	3.747
0.80	REF	0.481	6.88	4.403
	CCSR-AR	0.538	7.24	4.634
	CCSR-N2h	0.549	7.52	4.813
	CCSR-N24h	0.542	7.86	5.030
	CCSR-SCA	0.579	8.42	5.389

In the elastic range of concrete, all of the work done in deforming a specimen has been stored as strain energy. If the load is removed, the deformation will return to zero and the energy will be fully released. However, when a deformation exceeds the limit of elasticity, the

specimen then enters its plastic range. If the load is removed in this range, the deformation cannot be fully recovered, resulting in a permanent deformation in the specimen. In addition, the stored strain energy cannot be fully released because some structure of crystal lattice in the specimen are broken and realigned, resulting in some energy dissipation. The more energy it can dissipate, the higher damping capacity the material has. The shaded area ΔW shown in Figure 6-10 was used to represent the dissipated energy under cyclic loading for simplicity. It should be noted that the magnitude of the shaded area ΔW is not the true energy in this study. As is shown in Table 6-8, peak deformation m and residual deformation n of REF were the smallest whereas those of CCSR-SCA were the largest at each stress level. From the results of CCSR-N2h and CCSR-N24h, no clear trend of effect of soaking time on fatigue deformation can be obtained. However, both of them generally had a more deformation than concrete with as-received rubber particles, i.e. CCSR-AR. Shaded area ΔW of CCSR-SCA was also the biggest of all the mixes, indicating that concrete with SCA-coated rubber particles had a higher damping capacity than normal concrete, as-received and NaOH-treated rubber concrete.

6.3.2.4 Damage analysis of fatigue fracture

One of the noticeable features of concrete fatigue fracture is the gradual growth of internal micro-cracks with the increase of number of cycles, which results in an increase of irrecoverable deformation until it exceeds the overall deformability of the specimen. It can be observed from a typical diagram of deflection versus number of cycles as shown in Figure 6-11 that fatigue fracture of concrete subjected to cyclic loading went through three distinct stages. The first stage is characterized by a rapid increase of deflection with the increase of

number of cycles. Due to the initial flaws within concrete matrix, major energy absorbed by the specimen transferred to the flaw area, resulting in producing some micro-cracks fast in the early stage. Then the rate of crack formation in flaw area reduced gradually after most initial flaws had developed to micro-cracks. The cracks were restrained in micro scale because much more energy was needed for the development and propagation of the micro-cracks.

The second stage reflected a slow and progressive growth of the micro-cracks with the increase of a large number of cycles. During this process, energy played the role in enlarging deformation of the specimen, developing old micro-cracks and producing new micro-cracks. However, most energy were absorbed and stored in rubber particles. Therefore, energy to effectively develop old micro-cracks or produce new micro-cracks was reduced. Development and propagation rate of cracks within rubber concrete was lower than within normal concrete because of the damping nature of rubber material. This is why the duration of stage 2 of rubber concrete was longer than normal concrete.

In the final stage, with the increase of number of cycles, the cumulative energy exceeded the storage capacity of rubber particles. Some of the excessive energy applied was absorbed by the formed micro-cracks. The micro-cracks developed and propagated, followed by merging into each other to form some continuous networks of cracks and macro-cracks within the concrete. When the cracks reached a critical size, the specimen deformed rapidly, eventually leading to failure.

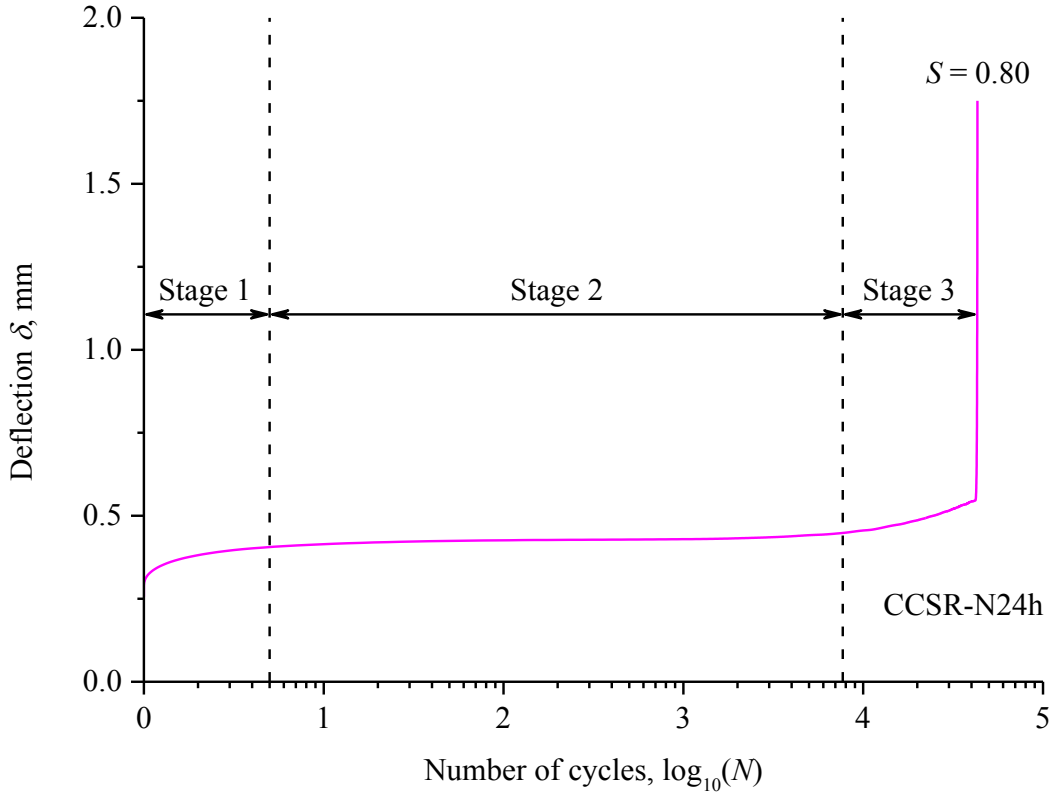

Figure 6-11. Typical curve of deflection versus number of cycles.

Fatigue loading can be divided into different categories. Hsu [6.41] presented a fatigue load spectrum based on number of cycles, including the range of low-cycle, high-cycle, and super-high cycle. Low-cycle fatigue refers to applying a few load cycles at high stress level whereas high-cycle fatigue is characterised by a very large number of cycles at low stress level. Figure 6-12 shows the classification of fatigue loading with relevant applications. Failure mechanisms of low-cycle and high-cycle fatigue within concrete are different. The dominant mechanism of low-cycle fatigue is the formation of internal cracks in mortar, leading to a continuous network of cracking. In contrast, high-cycle fatigue produces interface de-bonding in a slow and gradual process [6.42]. In this investigation, the objective of surface modification on rubber particles was to improve the bond strength along the interfacial

transition zone. Therefore, concrete with surface-modified rubber particles in this study has a promising application in high-cycle fatigue situation such as airport pavement and bridges.

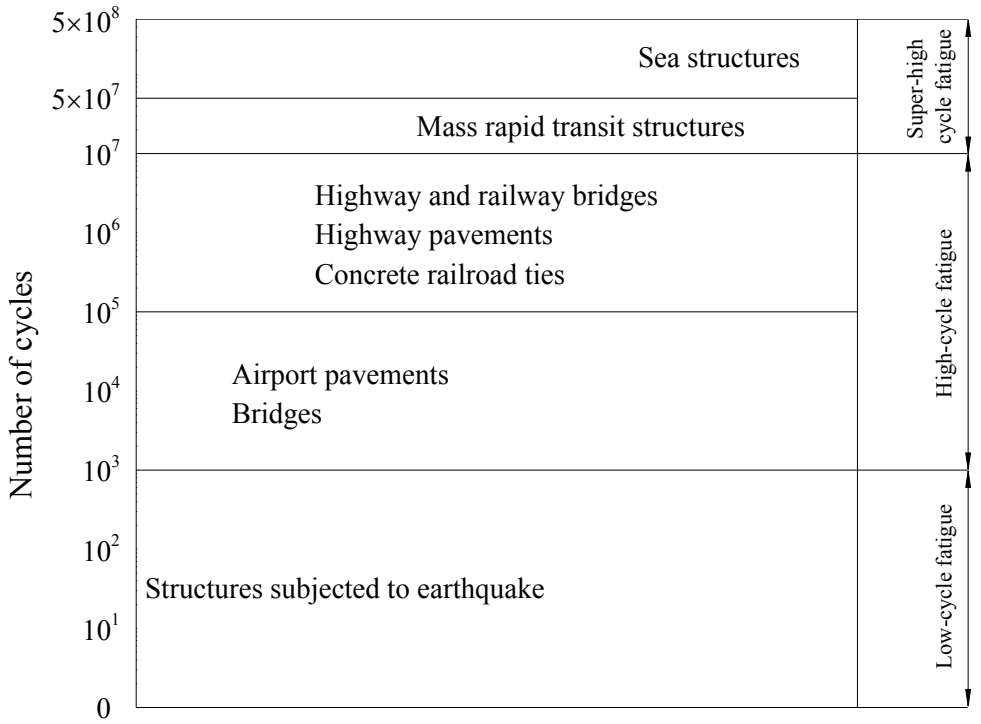

Figure 6-12. Fatigue loading spectrum [6.41].

6.4 Summary

This chapter explored the effect of surface-modified rubber particles on flexural properties and fatigue performance of concrete and the following conclusions can be experimentally drawn from this investigation:

- Comparing to normal concrete, loss of flexural strength of concrete with surface-modified rubber is less than with as-received rubber. Surface modification on rubber particles

enhances the bond strength of interfacial transition zone and this effect caused by SCA-coated rubber particles is more significant than NaOH-treated ones.

- Deformability of rubber concrete is better than normal concrete, irrespective of rubber surface modification. Peak strain of CCSR-SCA at mid-span is higher than CCSR-AR, CCSR-N2h and CCSR-N24h, all of which have a similar result.

- Scanning micrographs show a well-developed and smooth joint area between SCA-coated rubber particles and its surrounding matrix because of the sticky nature of SCA, leading to an improvement of adhesion between rubber particles and cement paste.

- Fatigue life of normal concrete and rubber concrete follows a two-parameter Weibull distribution with a highly statistical correlation coefficient. Waste tyre rubber particles as part substitution of fine aggregate results in an improvement in fatigue life of concrete and CCSR-SCA exhibits the longest fatigue life of the four rubber concrete at each stress level of 0.95, 0.90, 0.85 and 0.80.

- The addition of rubber particles increases the maximum deflection, residual deformation and stored strain energy of normal concrete subjected to cyclic loading. Despite the insignificant difference between CCSR-N2h and CCSR-N24h, surface modification on rubber particles indicates a positive effect on improving ductility and damping capacity of concrete with as-received rubber.

- Fatigue fracture process of both normal concrete and rubber concrete subjected to flexural loading can be divided into three stages. Basing on the provided fatigue load spectrum

and fatigue failure mechanism, the method of surface modification on rubber particles to improve the fatigue performance of concrete is potentially for high-cycle fatigue application such as airport pavement and bridges.

Stress level was restrained over 0.80 because number of cycles applied in this study was limited to 10^5 due to the restrictions of testing machine and laboratory condition. Further research on fatigue performance of this concrete material at lower stress level is needed before it could be reliably used in practice.

References

[6.1] D. Raghavan, H. Huynh, C.F. Ferraris, Workability, mechanical properties, and chemical stability of a recycled tyre rubber-filled cementitious composite, J. Mater. SCI. 33 (1998) 1745-1752.

[6.2] M. Nehdi, A. Khan, Cementitious composites containing recycled tire rubber: an overview of engineering properties and potential applications, Cement Concrete Aggr. 23 (2001) 3-10.

[6.3] K.H. Younis, K. Pilakoutas, Strength prediction model and method for improving recycled aggregate concrete, Constr. Build. Mater. 49 (2013) 688-701.

[6.4] J. Sim, C. Park, Compressive strength and resistance to chloride ion penetration and carbonation of recycled aggregate concrete with varying amount of fly ash and fine recycled aggregate, Waste Manage. 31 (2011) 2352-2360.

[6.5] C.S. Poon, S.C. Kou, L. Lam, Use of recycled aggregates in moulded concrete bricks and blocks, Constr. Build. Mater. 16 (2002) 281-289.

[6.6] X.S. Shi, F.G. Collins, X.L. Zhao, Q.Y. Wang, Mechanical properties and microstructure analysis of fly ash geopolymeric recycled concrete, J. Hazard. Mater. 237-238 (2012) 20-29.

[6.7] J. Yang, Q. Du, Y.W. Bao, Concrete with recycled concrete aggregate and crushed clay bricks, Constr. Build. Mater. 25 (2011) 1935-1945.

[6.8] D. Soares, J. Brito, J. Ferreira, J. Pacheco, Use of coarse recycled aggregates from precast concrete rejects: mechanical and durability performance, Constr. Build. Mater. 71 (2014) 263-272.

[6.9] M.C. Limbachiya, T. Leelawat, R.K. Dhir, Use of recycled concrete aggregate in high-strength concrete, Mater. Struct. 33 (2000) 574-580.

[6.10] Y. Guo, J. Zhang, G. Chen, Z. Xie, Compressive behaviour of concrete structures incorporating recycled concrete aggregates, rubber crumb and reinforced with steel fibre, subjected to elevated temperatures, J. Clean. Prod. 72 (2014) 193-203.

[6.11] D.G. Snelson, J.K. Kinuthia, P.A. Davies, S.R. Chang, Sustainable construction: composite use of tyres and ash in concrete, Waste Manage. 29 (2009) 360-367.

[6.12] A.R. Khaloo, M. Dehestani, P. Rahmatabadi, Mechanical properties of concrete containing a high volume of tire-rubber particles, Waste Manage. 28 (2008) 2472-2482.

[6.13] R. Siddique, T.R. Naik, Properties of concrete containing scrap-tire rubber – an overview, Waste Manage. 24 (2004) 563-569.

[6.14] H. Su, J. Yang, Analysis and prediction of cube compressive strength for concrete with varying content of recycled aggregate and rubber particles, Mater. Design. (Under review)

[6.15] N. Segre, I. Joekes, Use of tire rubber particles as addition to cement paste, Cement Concrete Res. 30 (2000) 1421-1425.

[6.16] C. Albano, N. Camacho, J. Reyes, J.L. Feliu, M. Hernandez, Influence of scrap rubber addition to Portland I concrete composites: destructive and non-destructive testing, Compos. Struct. 71 (2005) 439-446.

[6.17] H. Su, J. Yang, G.S. Ghataora, S. Dirar, Surface modified used rubber tyre aggregates: effect on recycled concrete performance, Mag. Concrete Res. 66 (2014) 1-12.

[6.18] A. Wöhler, Über die Festigkeits-Versuche mit Eisen und Stahl (On strength tests of iron and steel). Zeitschrift für Bauwesen (Journal for Construction) 20 (1870) 73-106.

[6.19] G.P. Sendeckjy, Constant life diagrams – a historical review. Int. J. Fatigue 23 (2001) 347-353.

[6.20] F. Liu, W. Zheng, L. Li, W. Feng, G. Ning, Mechanical and fatigue performance of rubber concrete, Constr. Build. Mater. 47 (2013) 711-719.

[6.21] N. Ganesan, J.B. Raj, A.P. Shashikala, Flexural fatigue behavior of self compacting rubberized concrete, Constr. Build. Mater. 44 (2013) 7-14.

[6.22] F. Xiao, P.E.W.Zhao, S.N. Amirkhanian, Fatigue behavior of rubberized asphalt concrete mixtures containing warm asphalt additives, Constr. Build. Mater. 23 (2009) 3144-3151.

[6.23] F. Hernández-Olivares, G. Barluenga, B. Parga-Landa, M. Bollati, B. Witoszek, Fatigue behaviour of recycled tyre rubber-filled concrete and its implications in design of rigid pavements, Constr. Build. Mater. 21 (2007) 1918-1927.

[6.24] BS EN 197-1, Cement. Composition, Specifications and Conformity Criteria for Common Cements, British Standards Institution, 2011.

[6.25] BS EN 933-1, Tests for Geometrical Properties of Aggregates. Determination of Particle Size Distribution – Sieving Method, British Standards Institution, 2012.

[6.26] BS 812-110, Testing Aggregates. Methods for Determination of Aggregate Crushing Value (ACV), British Standards Institution, 1990.

[6.27] A.P. Galvín, F. Agrela, J. Ayuso, M.G. Beltrán, A. Barbudo, Leaching assessment of concrete made of recycled coarse aggregate: physical and environmental characterisation of aggregates and hardened concrete, Waste Manage. 34 (2014) 1693-1704.

[6.28] K. Eguchi, K. Teranishi, A. Nakagome, H. Kishimoto, K. Shinozaki, M. Narikawa, Application of recycled coarse aggregate by mixture to concrete construction, Constr. Build. Mater. 21 (2007) 1542-1551.

[6.29] S. Erdem, M.A. Blankson, Environmental performance and mechanical analysis of concrete containing recycled asphalt pavement (RAP) and waste precast concrete as aggregate, J. Hazard. Mater. 264 (2014) 403-410.

[6.30] M. Tuyan, A. Mardani-Aghabaglou, K. Ramyar, Freeze-thaw resistance, mechanical and transport properties of self-consolidating concrete incorporating coarse recycled concrete aggregate, Mater. Design 53 (2014) 983-991.

[6.31] M. Bravo, J. Brito, Concrete made with used tyre aggregate: durability-related performance, J. Clean. Prod. 25 (2012) 42-50.

[6.32] M. Aiello, F. Leuzzi, Waste tyre rubberized concrete: properties at fresh and hardened state, Waste Manage. 30 (2010) 1696-1704.

[6.33] İ. Topçu, T. Bilir, Experimental investigation of some fresh and hardened properties of rubberized self-compacting concrete, Mater. Design 30 (2009) 3056-3065.

[6.34] P.K. Mehta, P.J.M. Monteiro, Microstructure, properties, and materials, fourth ed., McGraw-Hill, New York, 2013.

[6.35] D.C. Teychenné, J.C. Nicholls, R.E. Franklin, D.W. Hobbs, Design of normal concrete mixes, second ed., Construction Research and Communications Limited, Watford, 1997.

[6.36] BS EN 12390-5, Testing Hardened Concrete. Flexural Strength of Test Specimens, British Standards Institution, 2009.

[6.37] N.N. Eldin, A.B. Senouci, Rubber-tire particles as concrete aggregate, J. Mater. Civil Eng. 5 (1993) 478-496.

[6.38] M.M. Reda Taha, A.S. El-Diab, M.A. Abd El-Wahab, M.E. Abdel-Hameed, Mechanical, Fracture, and Microstructural Investigations of Rubber Concrete, J. Mater. Civil Eng. 20 (2008) 640-649.

[6.39] W. Weibull, Fatigue Testing and Analysis of Results. Pergamon Press, Oxford, 1961.

[6.40] B.H. Oh, Fatigue analysis of plain concrete in flexure, J. Struct. Eng. 112 (1986) 273-288.

[6.41] T.T.C. Hsu, Fatigue of plain concrete, ACI Journal Proceedings 78 (1981) 292-304.

[6.42] T.T.C. Hsu, Fatigue and microcracking of concrete, Mater. Struct. 17 (1984) 51-54.

CHAPTER 7

CONCLUSIONS AND FUTURE WORK

In this chapter, main conclusions derived from each experimental study and the corresponding analyses are listed. In addition, some recommendations for future work are also expressed.

7.1 Conclusions

7.1.1 Regarding the influence of rubber particle size on properties of rubber concrete

- Using different sizes of rubber particles in concrete as part of the fine aggregates affects the workability and water permeability considerably more than the fresh density and concrete strengths.

- Concrete prepared with the larger rubber particles shows a better workability than those with finer ones. Conversely, concrete with the finer rubber particles has a better performance in strengths and water permeability than those with the larger rubber particles.

- Varying sized rubber aggregates with continuous grading offer better workability and resistance to water permeability compared to the singly-sized rubber particles. In terms of the strength of concrete, the varying sized rubber performed similar to the finer rubber particles in the tests when added to the concrete mix.

7.1.2 Regarding the analysis and prediction of cube compressive strength for concrete with both recycled aggregate and scrap tyre rubber aggregate

- Concrete strength is affected by both the content of recycled aggregate and rubber particles. It decreases gradually with the simultaneous increase of recycled aggregate and rubber replacement ratio.

- Different substitution has a different effect on the reduction level of this concrete material. From the statistical analyses of experiment results and failure mechanism investigations of tested specimens, it can be concluded that rubber has a much more significant impact than recycled aggregate.

- When natural coarse aggregate was fully substituted by recycled aggregate by weight, the concrete still reached the target mean strength. However, rubber replacement ratio over 20% for fine aggregate by volume caused the strength of this concrete material lower than the designed compressive strength. Therefore, rubber aggregate for replacing over 20% of sand by volume is not recommended, especially for structural application.

- Polynomial fitting surfaces were proposed from the experiment testing results. Equations

$$I_{1dCCS} = -0.0006642 + 0.4038m + 0.371n - 0.04684m^2 - 0.1183mn + 0.1158n^2 + 0.01988m^2n - 0.4616mn^2 - 0.8922n^3$$
$$I_{7dCCS} = -2.659e^{-5} + 0.4018m + 0.3678n - 0.05265m^2 - 0.09493mn + 0.1295n^2 + 0.05236m^2n - 0.5603mn^2 - 0.9005n^3$$
$$I_{28dCCS} = -0.0006495 + 0.4016m + 0.3776n - 0.04724m^2 - 0.09495mn + 0.09698n^2 + 0.02159m^2n - 0.5205mn^2 - 0.8786n^3$$

  are valid to predict the compressive strength of this concrete material at different ages if the replacement ratio of rubber used is within the tested range of 0-40%.

7.1.3 Regarding the effect of surface modified rubber aggregate on the performance of rubber concrete

- Surface modified rubber pre-treated with silane coupling agent has a more positive effect on the concrete properties than that treated with saturated Sodium hydroxide solution. Pre-treatment with saturated sodium hydroxide solution for less than 24 hours does not produce significant changes in the properties of concrete compared to concrete containing as-received rubber. However, compared to the control mix, the pre-treatment with silane coupling agent that acts as an adhesion promoter enhances the adhesion of tyre rubber particles to the matrix, resulting in:

  (1) a reduction in the slump values of fresh concrete by 13.6%;

  (2) an improvement in the compressive strength of hardened concrete by 19.3% at 1 day, 9.3% at 7 days, and 6.8% at 28 days;

  (3) an increase in the Young's modulus of hardened concrete by 7.7% at 28 days;

  (4) an improvement in flexural strength of hardened concrete by 2.2% at 28 days and;

  (5) a decrease of the water permeability index of hardened concrete by 13.1%.

- Deformability of rubber concrete is better than normal concrete, irrespective of rubber surface modification. Peak strain of concrete with silane coupling agent-treated rubber aggregate at mid-span is higher than those of concrete with as-received or sodium hydroxide-treated, all of which have a similar result.

- Fatigue life of normal concrete and rubber concrete follows a two-parameter Weibull distribution with a high statistical correlation coefficient. Fatigue fracture process of both normal concrete and rubber concrete subjected to flexural loading can be divided into three distinct stages.

- Waste tyre rubber particles as part substitution of fine aggregate results in an improvement in fatigue life. Concrete with silane coupling agent-treated rubber aggregate exhibits longer fatigue life than concrete with as-received or sodium hydroxide rubber aggregate at each stress level of 0.95, 0.90, 0.85 and 0.80.

- The addition of rubber particles increases the maximum deflection, residual deformation and stored strain energy of normal concrete subjected to cyclic loading. Surface modification on rubber particles indicates a positive effect on improving ductility and damping capacity of concrete with as-received rubber.

- The scanning optical microscopic inspection of test specimens showed that the rubber-matrix adhesion was enhanced with the use of silane coupling agent. The X-ray diffraction data of different mixes shows similar diffraction patterns, which means that pre-treatment by saturated sodium hydroxide solution or by silane coupling agent does not change the crystalline phase of rubber concrete significantly. The mercury intrusion porosimetry test showed that concrete with silane coupling agent-treated rubber has a similar pore size distribution to the control mix and to the concrete with sodium hydroxide-treated rubber, but it achieved the lowest porosity and the highest tortuosity, which results in the best water permeability resistance.

- In addition, it is experimentally shown that silane coupling agent has a positive effect on improving strength of cement-based rubber concrete containing recycled aggregate, especially when concrete is weak. This effect becomes more significant with the increase of mass fraction of silane coupling agent solution.

- The nature of cohesion of silane coupling agent plays an important role in improving the adhesion in interfacial transition zone, leading to an enhancement of bond strength of interface between rubber and cement paste. It offers an approach to reduce the loss of strength for cement-based rubber concrete, which is potential for practical application.

- A brief cost analysis was also carried out, demonstrating the economical viability of this type of rubber concrete that uses waste tyres. This feature, together with the well accepted sustainable attractiveness and technical benefits, reinforce the potential prospects of this concrete material.

- Basing on the provided fatigue load spectrum and fatigue failure mechanism, the method of surface modification on rubber particles to improve the fatigue performance of concrete is potentially for high-cycle fatigue application such as airport pavement and bridges.

7.2 Future work

7.2.1 Regarding the analysis and prediction of cube compressive strength for concrete with both recycled aggregate and scrap tyre rubber aggregate

More research is needed before the fitting equation can be sufficiently validated and the proposed approach can be used for designing concrete material in practice. Influencing factors such as the type of cement, composition of waste materials, particle size distribution of aggregates as well as high volume replacement ratio of rubber for this concrete material should be considered in the equation so as to improve the overall prediction performance.

7.2.2 Regarding the fatigue performance for concrete with both recycled aggregate and surface modified scrap tyre rubber aggregate

Stress level was restrained over 0.80 because number of cycles applied in Chapter 6 was limited to 10^5 due to the restrictions of testing machine and laboratory condition. Further research on fatigue performance of this concrete material at lower stress level is needed before it could be reliably used in practice.

7.2.3 Regarding durability of concrete with both recycled aggregate and surface modified scrap tyre rubber aggregate

Concrete is usually designed to be used for tens of years. Durability is very important for concrete service life. Therefore, except water permeability resistance which has been studied

in this thesis, long-term durability such as freeze-thaw performance, carbonation, alkali silica reaction should be further studied.

7.2.4 Regarding other cement replacement materials for concrete with both recycled aggregate and surface modified scrap tyre rubber aggregate

PFA was used as 30% substitution of cement by mass in this research. However, some other cement replacement materials such as GGBS, silica fume are also helpful for different properties of concrete. More research should be carried out to try those industrial wastes in this type of concrete.

APPENDIX A

AN EXAMPLE OF MIX DESIGN CALCULATION

The mix design was undertaken using the second edition of Design of Normal Concrete Mixes presented by the Building Research Establishment in this thesis. This design method is based on determining the material proportions. Using known or assumed parameters, the water/cement ratio required to achieve the compressive strength was determined, culminating in mass quantities for individual material proportions. Process of mix design calculation for RA50R20 in Chapter 4 is given below as an example.

1. Confirm the mix design requirements. In Chapter 4, the desired concrete RA50R20 is:

- Concrete grade is C30/37.
- Slump value is between 60-180 mm.
- Rubber aggregate is used to replace 20% of fine aggregate by volume.
- Recycled aggregate is used to replace 50% of coarse aggregate by mass.
- Usage of fibre is 1 kg/m^3.

2. Test and get some data of raw materials. In Chapter, the following information is needed before the mix design calculation:

- Cement strength class is 32.5 MPa with pulverized fuel ash (PFA).
- Coarse aggregate is crushed limestone.
- Fine aggregate is crushed river sand.

- Maximum aggregate size is 10 mm.
- Proportion of PFA is 30%.
- Average density of combined aggregate saturated surface dry (SSD) basis is 2700 kg/m^3.
- Percentage of fine aggregate passing 600 μm sieve is 74%.
- SSD density of sand is 2512 kg/m^3.
- SSD density of rubber is 973 kg/m^3.

3. Tables, figures and equations used during the mix design process are given below.

Table A-1. Approximate free-water contents (kg/m^3) required to give various levels workability – Portland cement concrete.

Slump (mm)		0-10	10-30	30-60	60-180
Vebe time (s)		>12	6-12	3-6	0-3
Maximum size of aggregate (mm)	Type of aggregate				
10	Uncrushed	150	180	205	225
	Crushed	180	205	230	250
20	Uncrushed	135	160	180	195
	Crushed	170	190	210	225
40	Uncrushed	115	140	160	175
	Crushed	155	175	190	205

Table A-2. Approximate compressive strength (MPa) of Portland cement/pfa made with a W/(C+0.30F) ratio of 0.5.

Cement strength class	Type of coarse aggregate	Compressive strength at 28 days (MPa)
32.5	Uncrushed	36
	Crushed	43
42.5	Uncrushed	42
	Crushed	49
52.5	Uncrushed	48
	Crushed	55

Table A-3. Approximate free-water contents (kg/m^3) required to give various levels workability – Portland cement/PFA concrete.

Slump (mm)	0-10	10-30	30-60	60-180
Vebe time (s)	>12	6-12	3-6	0-3
Proportion, p, of PFA to cement plus PFA (%)	Reductions in water content (kg/m^3)			
10	5	5	5	10
20	10	10	10	15
30	15	15	20	20
40	20	20	25	25
50	25	25	30	30

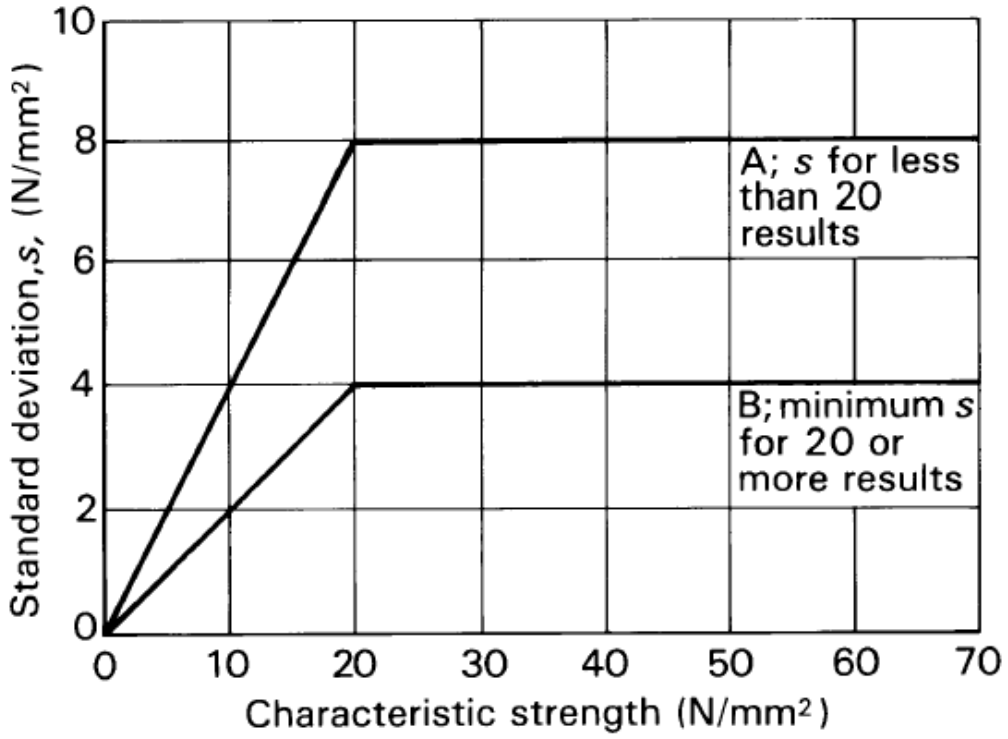

Figure A-1. Relationship between standard deviation and characteristic strength.

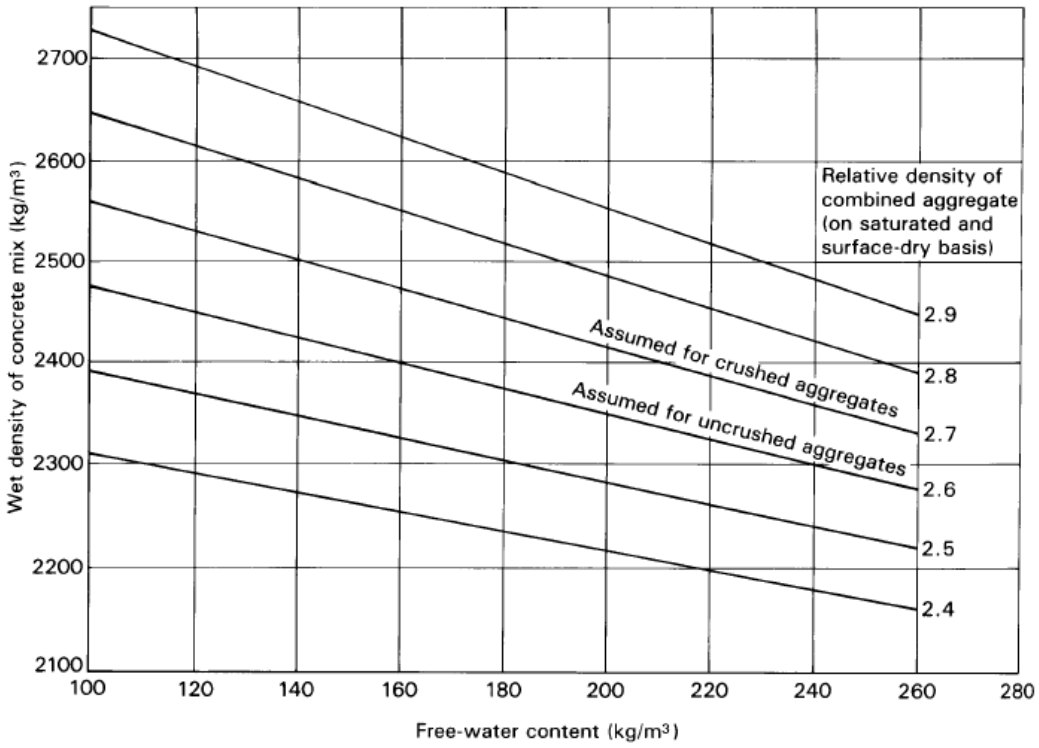

Figure A-2. Estimated wet density of fully compacted concrete.

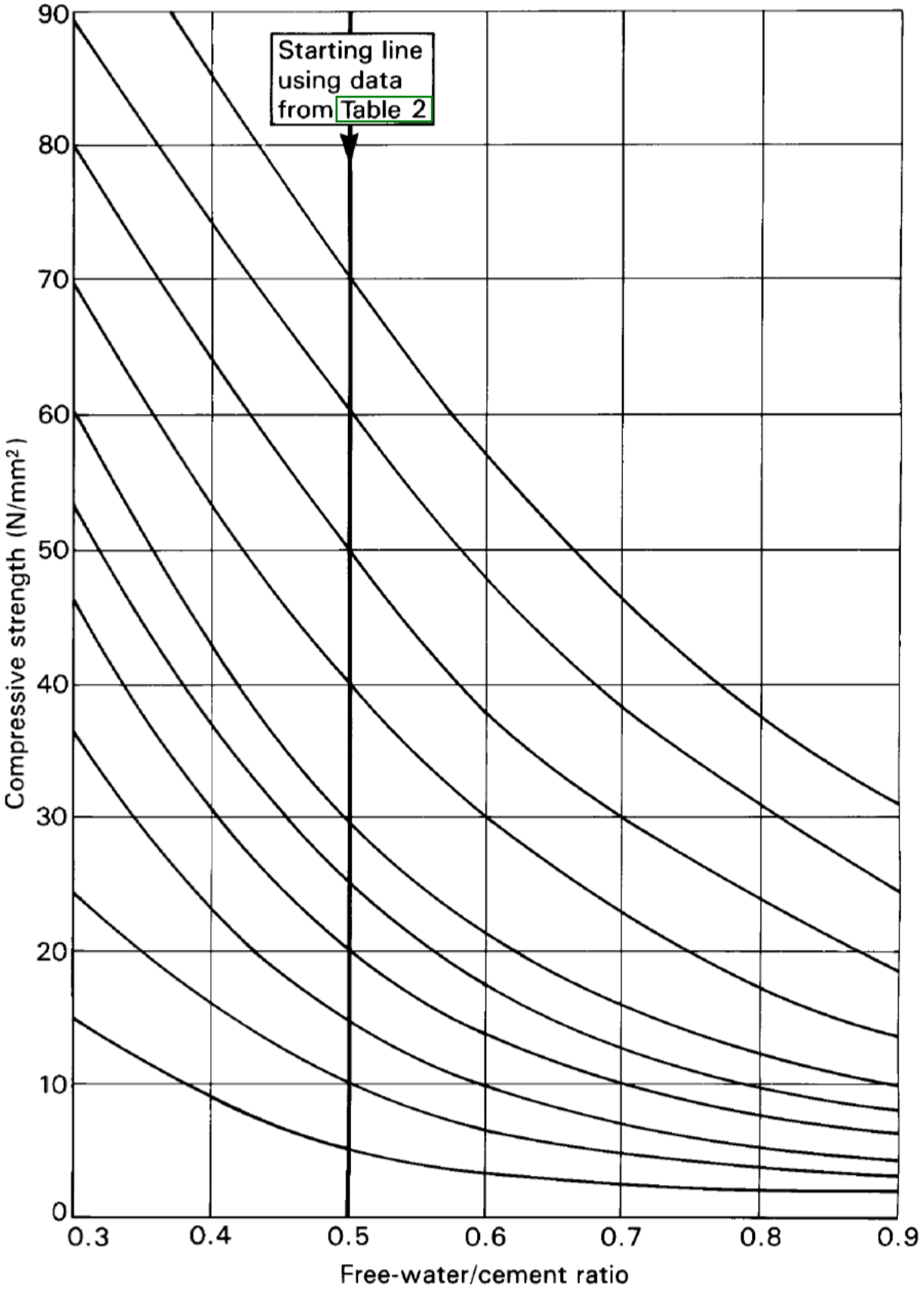

Figure A-3. Relationship between compressive strength and free-water/cement ratio.

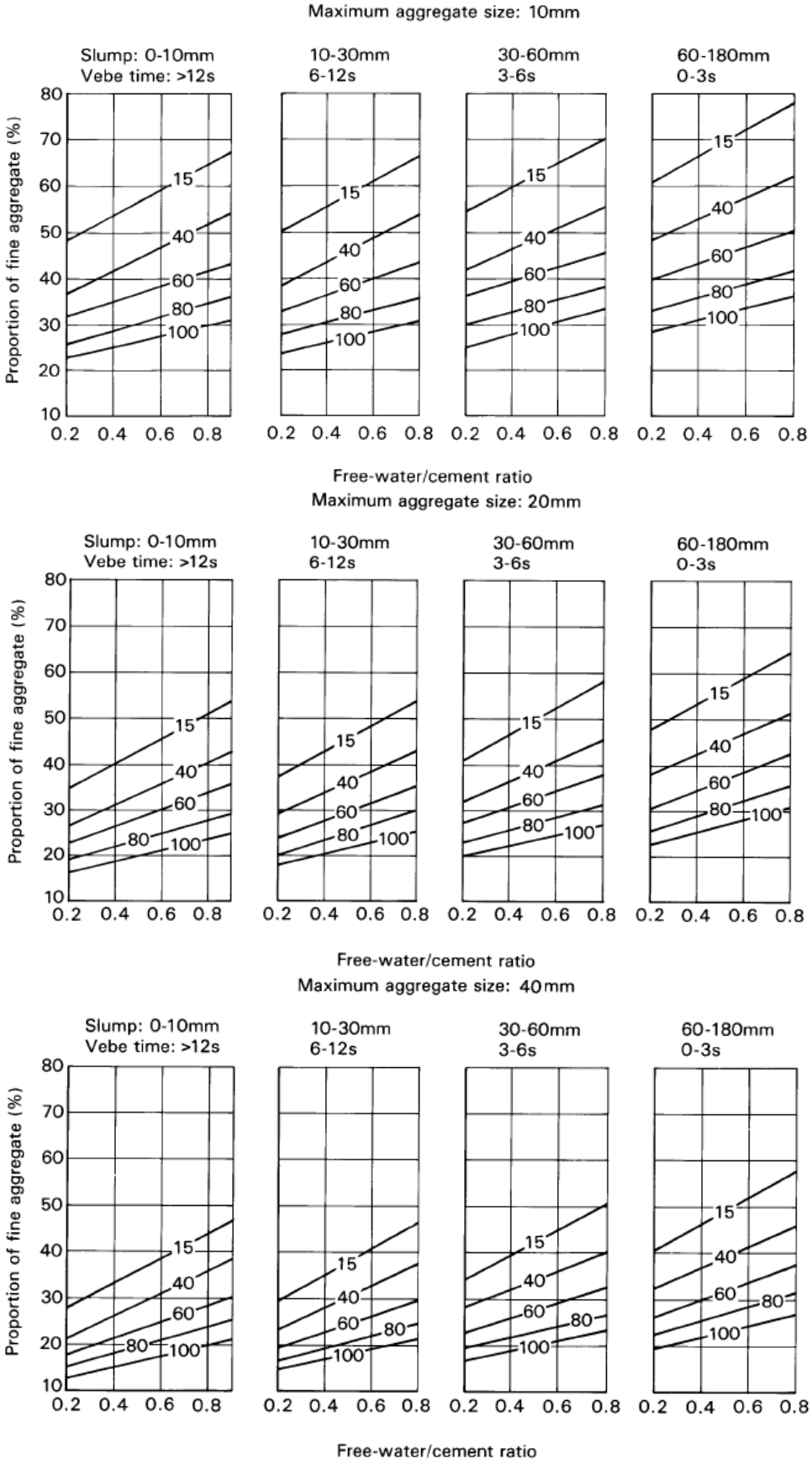

Figure A-4. Recommended proportions of fine aggregate according to percentage passing a 600μm sieve.

$$M = k \times s \tag{A-1}$$

where M is the margin;

k is a value appropriate to the 'percentage defectives' permitted blow the characteristic strength, usually taken as 1.64 when proportion defective is 5%;

s is the standard deviation.

$$f_m = f_c + M \tag{A-2}$$

where f_m is the target mean strength (MPa);

f_c is the specific characteristic strength (MPa);

M is the margin.

$$Portland\ cement\ content = \frac{(100 - p)W}{(100 - 0.7p)[W/(C + 0.30F)]} \tag{A-3}$$

where p is the proportion of PFA (%);

W is the content of free water (kg/m^3);

C is the content of Portland cement (kg/m^3);

F is the content of PFA (kg/m^3).

$$\text{PFA}\ content = \frac{pC}{100 - p} \tag{A-4}$$

where p is the proportion of PFA (%);

C is the content of Portland cement (kg/m^3).

$$Total\ aggregate\ content = D - (C + F) - W \quad \text{(A-5)}$$

where D is the wet density of concrete (kg/m^3);

C is the cement content (kg/m^3);

F is the PFA content (kg/m^3);

W is the free-water content (kg/m^3).

$$Fine\ aggregate\ content = Total\ aggregate\ content \times proportion\ of\ fines \quad \text{(A-6)}$$

$$Coarse\ aggregate\ content = Total\ aggregate\ content - fine\ aggregate\ content \quad \text{(A-7)}$$

4. Follow the stage in Table A-4 below and figure out the usage of each kind of raw material.

Regarding Stage 1.8: A value is obtained from Table A-2 for the strength of a mix made with a free-water/cement ratio of 0.5 according to the specified age, the strength class of the cement and the aggregate to be used. In this example, this value is equal to 43 MPa. This strength value 43 MPa is then plotted on Figure A-3 and a curve is drawn from this point and parallel to the printed curves until it intercepts a horizontal line passing through the ordinate representing the target mean strength of 43.12 MPa. The corresponding value for the free-water/cement ratio can then be read from the abscissa, i.e. 0.495 in this example. This should be compared with any maximum free-water/cement ratio that may be specified and the lower of these two values used.

Table A-4. Concrete mix design – RA50R20.

Stage	Item	Reference	Values
1	1.1 Characteristic strength	Specified	30 N/mm^2 at 28 days
	1.2 Proportion defective	Empirical	5%
	1.3 Standard deviation	Figure A-1	s = 8 N/mm^2
	1.4 Margin	Equation (A-1)	13.12 N/mm^2
	1.5 Target mean strength	Equation (A-2)	43.12 N/mm^2
	1.6 Cement strength class		32.5
	1.7 Aggregate type: coarse Aggregate type: fine		Crushed Crushed
	1.8 Free-water/cement ratio	Table A-2, Figure A-3	0.495
2	2.1 Slump	Specified	60-180 mm
	2.2 Maximum aggregate size	Tested	10 mm
	2.3 Proportion of PFA	Tested	p = 30%
	2.4 Free-water content	Table A-1, Table A-3	230 kg/m^3
3	3.1 Cement content	Equation (A-3)	412 kg/m^3
	3.2 PFA content	Equation (A-4)	177 kg/m^3
	3.3 Total		589 kg/m^3
	3.4 Modified free-water/cement ratio		0.39
4	4.1 Density of combined aggregate	Tested	2700 kg/m^3
	4.2 Concrete density	Figure A-2	2378 kg/m^3
	4.3 Total aggregate content	Equation (A-5)	1568 kg/m^3
5	5.1 Grading of fine aggregate	Percentage of passing 600 μm	74%
	5.2 Proportion of fine aggregate	Figure A-4	36.5%
	5.3 Fine aggregate content	Equation (A-6)	572
	5.4 Coarse aggregate content	Equation (A-7)	996

Since 20% of fine aggregate (by volume) is replaced by rubber aggregate and 50% of coarse aggregate (by mass) is substituted by recycled aggregate, the actual content of each aggregate is listed below:

Sand: $572 \times (1 - 20\%) = 458$ kg/m^3

Rubber: $(572 \times 20\%) \times 973 / 2512 = 44.3$ kg/m^3

Natural coarse aggregate: $996 \times 50\% = 498$ kg/m^3

Recycled aggregate: $996 \times 50\% = 498$ kg/m^3

Therefore, the content of each kind of raw materials are shown in Table A-5.

Table A-5. Proportions of each kind of raw materials for RA50R20.

Quantities (kg)	Water	Cement (including PFA)	Natural coarse aggregate	Recycled aggregate	Sand	Rubber aggregate	Fibre
per m^3	230	589	498	498	458	44.3	1

*Aggregate materials are in SSD condition.

Only the tables, figures and equations used for the mix design of RA50R20 in Chapter 4 are given in this appendix. Other information for the mix design of other mixes, please refer to the second edition of Design of Normal Concrete Mixes presented by the Building Research Establishment.

APPENDIX B

SOME PHOTOS DURING THE EXPERIMENTS AND TESTS

Figure B-1. Water content of rubber aggregate in saturated surface dry condition.

Figure B-2. Water content test.

Figure B-3. Weighing raw materials.

Figure B-4. Dry mix of raw materials.

Figure B-5. Ready fresh concrete.

Figure B-6. Casting and vibration.

Figure B-7. Trowel to a clean finish.

Figure B-8. Cover the samples.

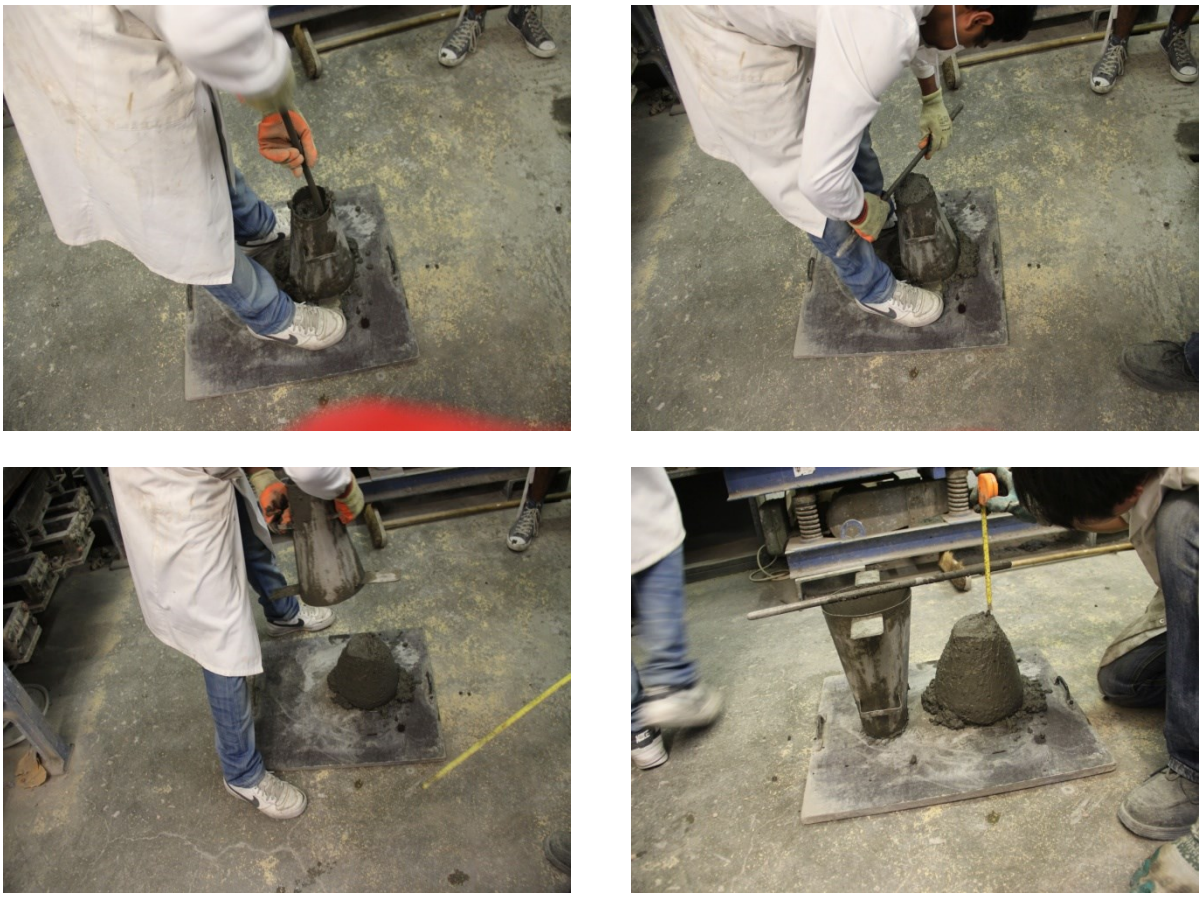

Figure B-9. Slump test.

Figure B-10. Demoulding the samples.

Figure B-11. Curing the samples in water tank.

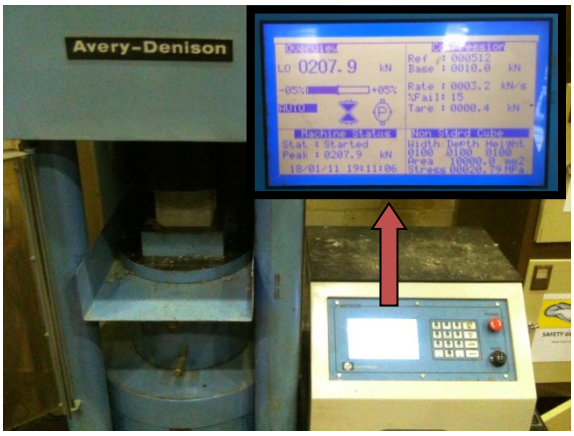

Figure B-12. Compressive strength test.

Figure B-13. Splitting tensile strength test.

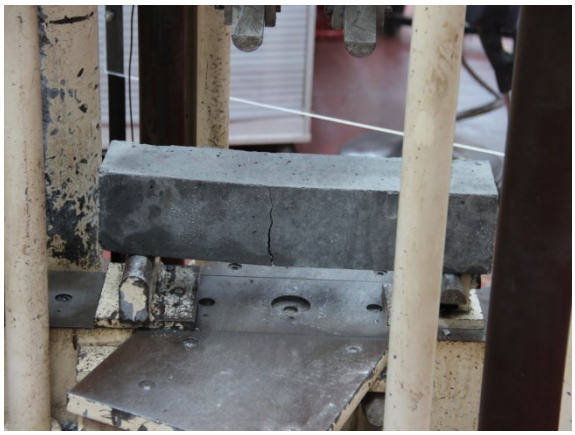

Figure B-14. Flexural strength test.

Figure B-15. Prepared samples for Young's modulus test.

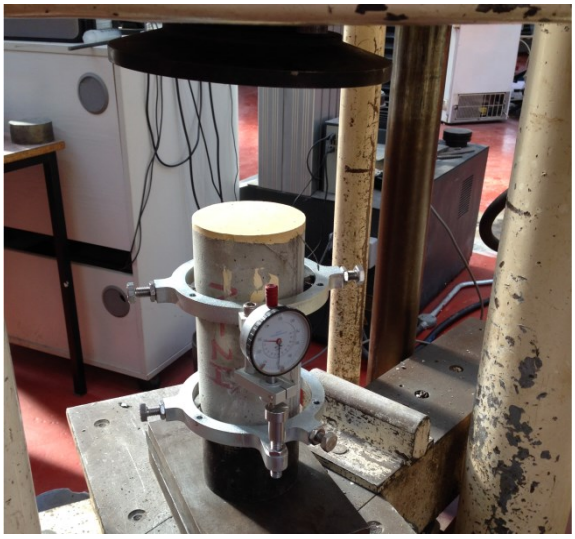


Figure B-16. Young's modulus test.


Figure B-17. Water permeability test.

Figure B-18. Fatigue life test.

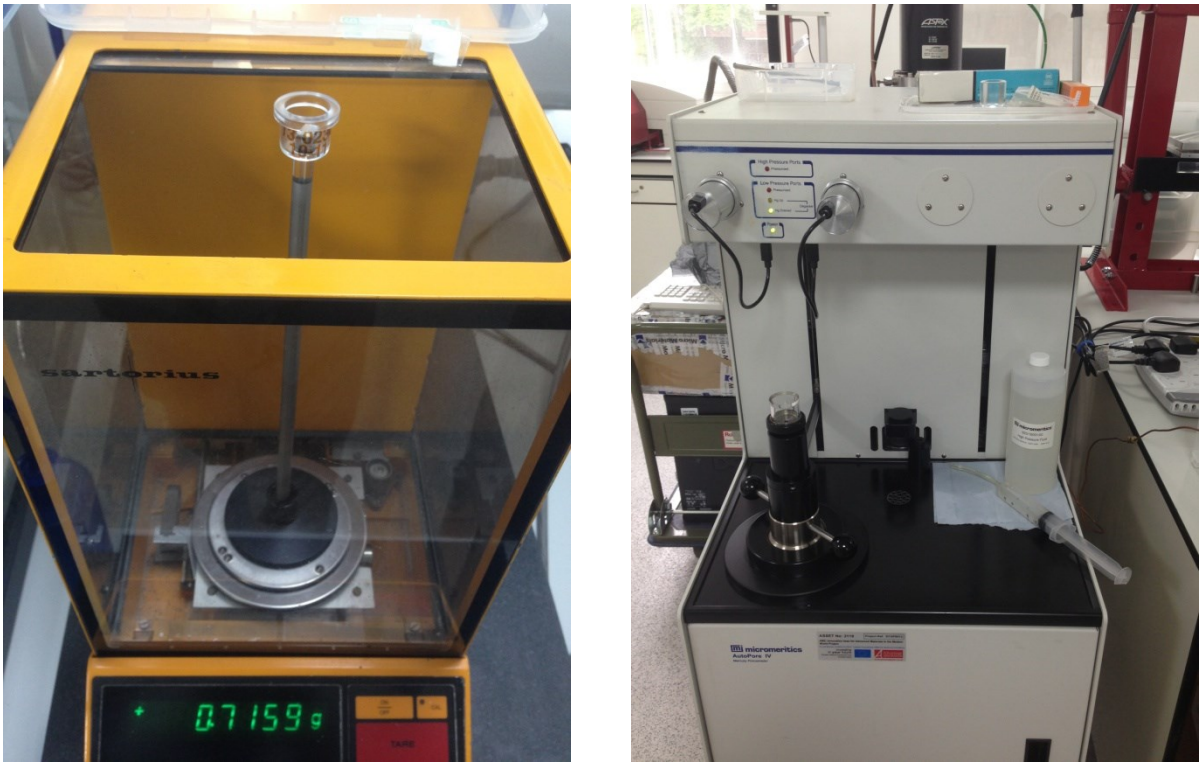

Figure B-19. Mercury intrusion porosimetry test.

APPENDIX C

PUBLICATIONS

[C.1] H. Su, J. Yang, G.S. Ghataora, S. Dirar, An overview of the properties of concrete containing rubber aggregate used to substitute aggregate by volume, Cem. Concr. Res. 2015 (under review). (**Chapter 2**)

[C.2] H. Su, J. Yang, T. Ling, G.S. Ghataora, S. Dirar, Properties of concrete prepared with waste tyre rubber particles of uniform and varying sized, J. Clean. Prod. 91 (2015) 288-296. (**Chapter 3**)

[C.3] H. Su, J. Yang, G.S. Ghataora, S. Dirar, Analysis and prediction of cube compressive strength for concrete with varying content of recycled aggregate and rubber particles, Mater. Design. 2014 (under review). (**Chapter 4**)

[C.4] H. Su, J. Yang, G.S. Ghataora, S. Dirar, Surface modified used rubber tyre aggregates: effect on recycled concrete performance, Mag. Concr. Res. 67 (2015) 680-691. (**Chapter 5**)

[C.5] H. Su, J. Yang, An approach to reduce the loss of strength of cement-based rubber concrete containing recycled aggregate, Mater. Lett. 2014 (under review). (**Chapter 5**)

[C.6] J. Yang, H. Su, G.S. Ghataora, S. Dirar, Effect of surface pre-treatment of waste tyre rubber aggregate on workability and compressive strength of concrete, Proceedings of Young Researchers' Forum II: Construction Materials, London, UK, 2014, pp. 177-182. (**Chapter 5**)

[C.7] H. Su, J. Yang, G.S. Ghataora, S. Dirar, Effect of surface-modified waste tyre rubber aggregate on flexural properties and fatigue performance of recycled aggregate concrete containing pulverized fuel ash, J. Hazard. Mater. 2015 (under review). (**Chapter 6**)